TANDEM MASS SPECTROMETRY AND DIFFERENTIAL ION MOBILITY SEPARATION OF SULFATED GLYCOSAMINOGLYCANS CARBOHYDRATES

by

John Kailemia Muchena

(Under the Direction of I. Jonathan Amster)

ABSTRACT

Glycosaminoglycans (GAGs) carbohydrates are biologically important molecules found in all the living organisms and efforts are made to identify their molecular structures in order to gain more understanding about their functions. Several tandem mass spectrometry (MS/MS) methods have been useful in structural characterization of GAGs. However, complete structural characterization of GAGs has remained elusive due to the inherent heterogeneity brought about by their non-template biosynthetic pathways. The highly sulfated and isomeric GAGs have remained relatively intractable to characterize. Highly sulfated GAGs have a tendency to lose SO_3 during ion activation thus producing few or no structurally informative fragment ions. On the other hand, isomeric oligosaccharides produce isobaric molecular ions in the MS stage and generally have identical MS/MS fragmentation patterns. This work will highlight some of the recent contributions made towards addressing these two issues. By controlling the ESI solvent conditions using a small amount of NaOH (1-2 mM), highly sulfated GAG molecules can be stabilized and location of SO_3 modifications identified using collision-induced dissociation (CID). Also, in some instances C_5 epimeric state of the uronic acid residues

can be obtained through the selection of the right molecular ions during CID activation. By use of field asymmetric-waveform ion mobility spectrometry (FAIMS), it is possible to separate isobaric ions and even diastereoisomers. The separated species can be fragmented using methods like electron detachment dissociation (EDD) to obtain useful structural information. Ion intensity spectral differences especially from isomeric compounds can be visualized using statistical methods like principal component analysis.

INDEX WORDS: Glycosaminoglycans, Carbohydrates, High field asymmetric-waveform ion mobility spectrometry, Fourier transform ion cyclotron resonance, Collision induced dissociation, Electron detachment dissociation, chemometrics.

TANDEM MASS SPECTROMETRY AND DIFFERENTIAL ION MOBILITY SEPARATION OF SULFATED GLYCOSAMINOGLYCANS CARBOHYDRATES

by

John Kailemia Muchena

B.Sc.Ed., Maseno University, Kenya, 2002

MS, East Tennessee State University, 2009

A Dissertation Submitted to the Graduate Faculty of The University of Georgia in Partial Fulfillment of the Requirements for the Degree

DOCTOR OF PHILOSOPHY

ATHENS, GEORGIA

2014

TANDEM MASS SPECTROMETRY AND DIFFERENTIAL ION MOBILITY SEPARATION OF SULFATED GLYCOSAMINOGLYCANS CARBOHYDRATES

by

JOHN KAILEMIA MUCHENA

Major Professor: I. Jonathan Amster

Committee: John L. Stickney
Ronald Orlando

Electronic Version Approved:

Maureen Grasso
Dean of the Graduate School
The University of Georgia
May 2014

DEDICATION

To my loving family, PAMOJA!.

ACKNOWLEDGEMENTS

First I would like to acknowledge my advisor Prof. I. Jonathan Amster for his continuous encouragement, guidance and support during my stay at UGA. Without him, this work could not have been done. I also want to acknowledge Prof. John L. Stickney and Prof. Ron Orlando for being part of my advisory committee and for the guidance they have offered me along the way. I would also like acknowledge Prof. Robert Linhardt, Dr. Ly, and Dr. Lingyun Li at Rensselaer Polytechnic Institute for the informative discussions we have had and also for allowing me to spend a week at their institute to learn about GAG sample separation and purification. This dissertation would not have been complete without the understanding and support from my family, especially my wife Mukami and my son Mutuma who although thousands of miles away have been constant motivators in my work. Last but not least, I acknowledge both former and current members of Prof. Amster lab for their support especially the GAGs team, Isaac Agyekum, Yuejie Zhao, Anish Patel and Dane Johnson.

TABLE OF CONTENTS

Page

LIST OF TABLES

Page

LIST OF FIGURES

Page

CHAPTER 1

OLIGOSACCHARIDE ANALYSIS BY MASS SPECTROMETRY: A REVIEW OF RECENT DEVELOPMENTS*

*Kailemia, M. J.; Ruhaak, R.; Lebrilla, C. B.; Amster, I. J. Oligosaccharide Analysis by Mass Spectrometry: A Review of Recent Development. *Anal. Chem.*, **2014**, 86 (1), pp 196–212. Reprinted here with permission of publisher.

ABSTRACT

This review covers developments in the application of mass spectrometry to the analysis of carbohydrates with more emphasis on glycosaminoglycans. These developments include approaches for improved ionization, new and improved methods of ion activation, advances in chromatographic separations of carbohydrates, the hybridization of ion mobility and mass spectrometry. The impacts of the developments are considered in terms of their ability to solve new problems or provide new capabilities for carbohydrate analysis, particularly for structure characterization by mass spectrometry and tandem mass spectrometry.

INTRODUCTION

Carbohydrates including glycosaminoglycans are central players in a number of important biological processes including cell signaling, cell adhesion, and the regulation of biochemical pathways. Unlike nucleic acids and proteins, the biosynthesis of carbohydrates is not template-driven. They occur in nature as heterogeneous mixtures, often of high complexity. There is no method for amplifying the amount of a carbohydrate analogous to overexpression for proteins or polymerase chain reaction for nucleic acids, and so carbohydrate analysis is typically limited to what can be obtained from natural sources, thus the researcher must cope with small quantities of heterogeneous material. Mass spectrometry has high sensitivity, is tolerant of mixtures, and is a natural choice for the analysis of this class of molecules.

Compared to advances in protein analysis, progress in the application of mass spectrometry to carbohydrates has evolved somewhat slowly, principally because carbohydrates are a more challenging set of targets for structural characterization. In contrast to proteins, there is no database containing an inclusive and closed set of sequences representing all possible carbohydrate structures. The characterization of carbohydrates relies upon obtaining the full details of structure from the mass spectrum. Subtle differences due to isomerism or chirality can produce molecules with very different biological activities, making complete structural analysis even more demanding. Mass spectrometry methodologies and technologies for biomolecule analysis continue to rapidly evolve and improve, and these developments have benefited Glycosaminoglycans (GAGs) carbohydrates analysis.

Glycosaminoglycans are negatively charged generally sulfated carbohydrates that can be divided into different classes depending on the disaccharide repeating unit compositions and the glycosidic linkages between them [1-3].

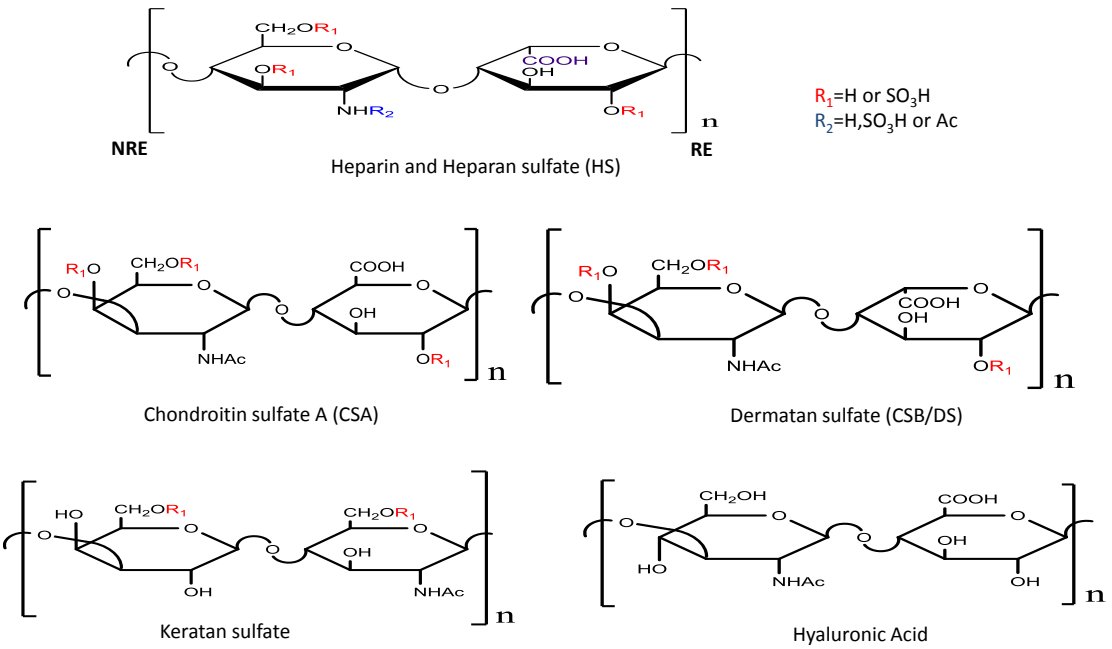

Figure 1. 1. Disaccharide units of different classes of GAGs. The hexuronic acid in heparin and heparan sulfate and chondroitin sulfates can either be glucuronic acid or iduronic acid residues.

As the Figure 1.1 shows, GAGs are highly heterogeneous compounds with variable modifications at different positions within the disaccharide unit. A key property of these biomolecules is the sulfate half ester bond which is very labile. Efforts to identify the exact location of the SO_3 groups within the chain are hindered by the lability of this bond as it breaks easily upon mild ion activation and sometimes during sample ionization process. The process for the analysis of GAGs generally starts with the extraction of the minute amount of sample molecules within a complex mixture from natural sources.

Upon extraction, the mixture is separated in terms of length and compositions using the existing analytical methods and then purified. The molecular level structural information involves identifying the exact locations of the SO_3, acetyl and assigning carbon-5 stereochemistry in uronic acid residues. All these structural features have profound effect on GAGs biological functions making their identification important in understanding how these they are involved in various biological activities [3]. As mentioned earlier in this chapter, mass spectrometry is a key tool for the analysis of carbohydrates including GAGs and important considerations for optimal use of this method will be discussed in the subsequent sections in this chapter.

Ionization Methods

The most widely used ionization method for carbohydrates are matrix assisted laser desorption/ionization (MALDI) [4, 5] and electrospray ionization (ESI) [6]. They impart little energy to the sample, producing less fragmentation during the ionization process compared to methods previously used for ionization of carbohydrates, such as fast atom bombardment (FAB).

To generate ions by MALDI, the sample is dissolved by an organic solvent, mixed with a solution of a matrix, dried and then spotted on a MALDI target. The dry mixture spot is then irradiated using a ultraviolet laser and the matrix absorbs and transfers some of the energy to the analyte which ionizes [7]. Detailed information about the application of MALDI to glycan analysis, including matrixes that are of particular use for carbohydrates, can be found in a comprehensive review by Harvey [7]. MALDI, compared to ESI, has higher sensitivity for N-glycans, ionizes well even at higher mass range, and it is more tolerant to contaminants. Spectra from this method are less complex

than ESI spectra because a majority of ions generated in both negative and positive mode are singly charged through protonation or deprotonation. Singly charged ions are also formed as adducts with alkali or alkaline earth metals, and these kind of ions have been found to generate useful fragment ions during tandem mass spectrometry analysis [8]. However, MALDI imparts more internal energy into the analyte than does ESI, and can cause in-source fragmentation of labile groups such as sulfates within GAGs molecules so it's not commonly used for GAGs analysis [9].

With ESI, analyte ions are generated by passing a dilute solution (1-10 μM) through a thin diameter needle placed near the MS inlet capillary, at a potential of 1-4 kV. The potential difference between the tip and the capillary generate fine charged droplets and then drying gas vaporizes the solvent from the ions as they are aspirated into the mass spectrometer [10]. Both positive and negative ions can be generated using this method, and multiple charging is generally observed. The pH of the sample and the presence of salts have a profound influence on the formation of molecular ions and their anionic or cationic adducts. ESI couples well with online liquid flow separation methods like HPLC or capillary electrophoresis (CE) techniques.

Generally, ESI sensitivity decreases as the mass of the glycan increases. Conventional ESI is known to be less effective for neutral oligosaccharides due to poor ionization efficiency but is useful for acidic molecules like GAGs that can readily form negative ions. Smaller sized droplets obtained in both static or flow nano-electrospray increase the sensitivity and show increased tolerance to salts and other contaminants compared to conventional electrospray [8, 11, 12]. Permethylation and reducing end modifications such as reductive amination and hydrazine tagging helps in LC separations

and improves the sensitivity for both neutral and acidic oligosaccharides. Permethylation also enables acidic oligosaccharides to be analyzed in positive mode [13-15].

ION ACTIVATION METHODS

Once the ions are formed, compositional information of GAGs can be derived from a single stage of MS, particularly with a high resolution, accurate mass measurement. The details of the structures of oligosaccharide molecules are obtained by tandem mass spectrometry (MS/MS or MS^n). In tandem mass spectrometry, a molecular ion is selected by a first stage of MS, undergoes activation and fragmentation, and the product ions are analyzed to provide information about the sequence, monosaccharide compositions, linkages and locations of various modifications [16-20].

Threshold Ion Activation

There are two broad categories of tandem mass spectrometry techniques that have been applied to oligosaccharide analysis [21-26]. The first category is comprised of threshold activation methods, including low energy collision induced dissociation (CID) [21] and infrared multiphoton dissociation (IRMPD) [22]. CID is the most commonly employed fragmentation method, and has been implemented on many different MS platforms. However, CID ruptures the weakest bonds (also true for IRMPD), which can be detrimental for the analysis of oligosaccharides with labile modifications especially GAGs. Recently, methods have been developed that can improve the utility of this method by modifying the ESI spray solutions, derivatization, for example, by methylation or acetylation, and also coupling the labile groups with metals [27-31].

Low energy CID fragmentation of positively charged ions, particularly native N-linked glycans, favor glycosidic fragmentation and may cause residue rearrangement

which can lead to the wrong structural assignment [32]. Metal adducted oligosaccharides ions do not undergo rearrangement and provide more fragment ions, including cross-ring fragments which provide more detailed information about the oligosaccharides [16, 32]. For gangliosides, both negative and positive precursor ions provide extensive fragmentation that complements each other [33-35]. Negative ionization and MS/MS has also been shown to produce informative fragment ions for acidic biomolecules especially glycosaminoglycans and other acidic glycans containing sialic acids [36]. For underivatized neutral oligosaccharides, fragment ions obtained from positive and negative mode may complement each other, enhancing structural assignment [37-40].

Electron Based Ion Activation

A second category of ion activation is electron based methods [23, 24]. These entail the transfer of an electron to or from the selected multiply charged molecular ion, yielding a radical ion which then undergoes fragmentation. These methods are gaining attention because they often result in backbone fragments that give detailed structural information about peptidoglycans and oligosaccharides, at the same time preserving labile modifications that would otherwise be lost using threshold methods. These methods include electron capture dissociation (ECD) [23], electron transfer dissociation (ETD) [25], electron detachment dissociation (EDD) [24], negative electron transfer dissociation (NETD) [26], and negative ion electron capture dissociation (niECD) [41]. EDD and NETD are suited for multiply charged negative ions especially from GAGs or glycopeptides [42-47]. ECD and ETD are used to fragment multiply positively charged ions and they have been useful for mapping sites of glycosylation from glycopeptides by producing backbone fragments while retaining the glycan within the peptide chain [48,

49]. niECD is a recently reported electron based fragmentation method in which negatively charged ions capture ~5 eV electrons and increase their charge state, in contrast to the aforementioned methods of EDD, NETD, ECD, and ETD, which lead to a reduction in charge state. The presence of charge-increased ions confirms electron capture, and these radical ions initiate fragmentation similar to the ones observed in ECD/ETD. This method requires a zwitterionic structure, presumably for electron capture by the positively charged region of the ion. niECD produces extensive backbone fragmentation and has been applied to characterize peptides [41] including O-sulfopeptides [50]. Although it has not yet been applied to carbohydrates, it would appear to have utility for negatively charged oligosaccharides, such as glycosaminoglycans.

The Domon and Costello nomenclature [51] is widely accepted as a convenient way to present the details of carbohydrate fragmentation. We have modified this nomenclature to include the loss of SO_3, sodium adducted fragments and EDD unique fragments (Figure 1.2). Two major types of product ions are produced by the fragmentation of oligosaccharides, those resulting from glycosidic fragmentation (B, Y, C and Z) and those from cross-ring fragmentation (A and X). The ions that retain charge on the reducing end are X, Y, and Z while the ones that retain the charge on the non-reducing end are A, B and C. Internal fragments may also be produced, but these are generally less informative regarding the structure. A complete set of glycosidic fragments give details about the sequence, monosaccharide compositions and branching while cross-ring fragments locate modifications and determine the position of glycosidic linkage within individual residues [16]. Several recent reviews address tandem mass spectrometry of oligosaccharides [16, 18, 19, 52, 53] and specific classes of

oligosaccharides, such as GAGs [54], glycopeptides [55, 56], O- and N-linked glycans [20, 31, 57, 58], and milk oligosaccharides [59].

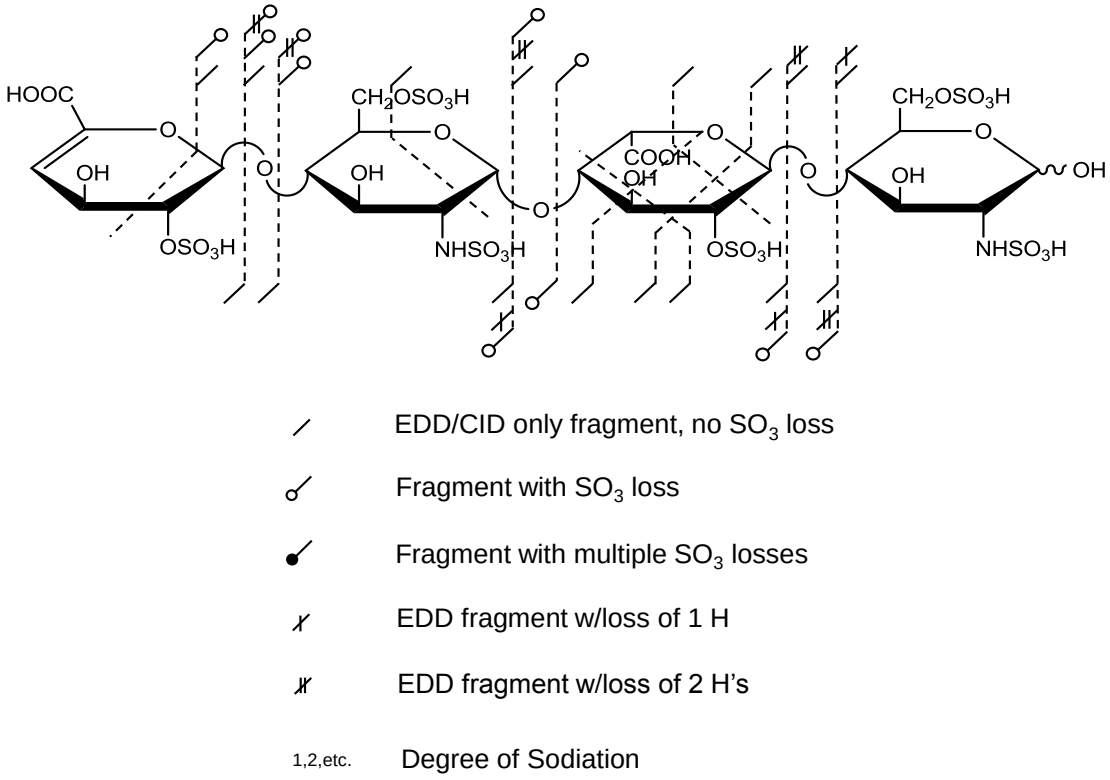

Figure 1.2. The structure showing different kinds of fragment assignment for the ions obtained in this dissertation. This method of assigning ions is modified from Domon-Costello nomenclature for hexose carbohydrates.

Glycosaminoglycan (GAG) sequencing has predominantly relied on tandem mass spectrometry of short GAG chains resulting from enzymatic or chemical depolymerization (bottom-up) [29, 45, 54, 60-77]. Recently, the first top-down MS/MS assignment of intact glycan chains from a GAG proteoglycan was obtained using Fourier transform ion cyclotron resonance (FTICR) and FT-orbitrap data (see Figure 1.3) [78]. The O-linked glycans were released from the proteoglycan, bikunin. These full-length glycans are a complex mixture, which have been characterized previously by mass

spectrometry and were known to have a modest degree of polymerization (dp20-dp45) and a low degree of sulfation [64, 79]. The glycan mixture was resolved partially by capillary gel electrophoresis, and the fractions were amenable to MS/MS analysis. One of the interesting observations was that CID yielded useful MS/MS data, contrary to the general observation for a GAG glycan.

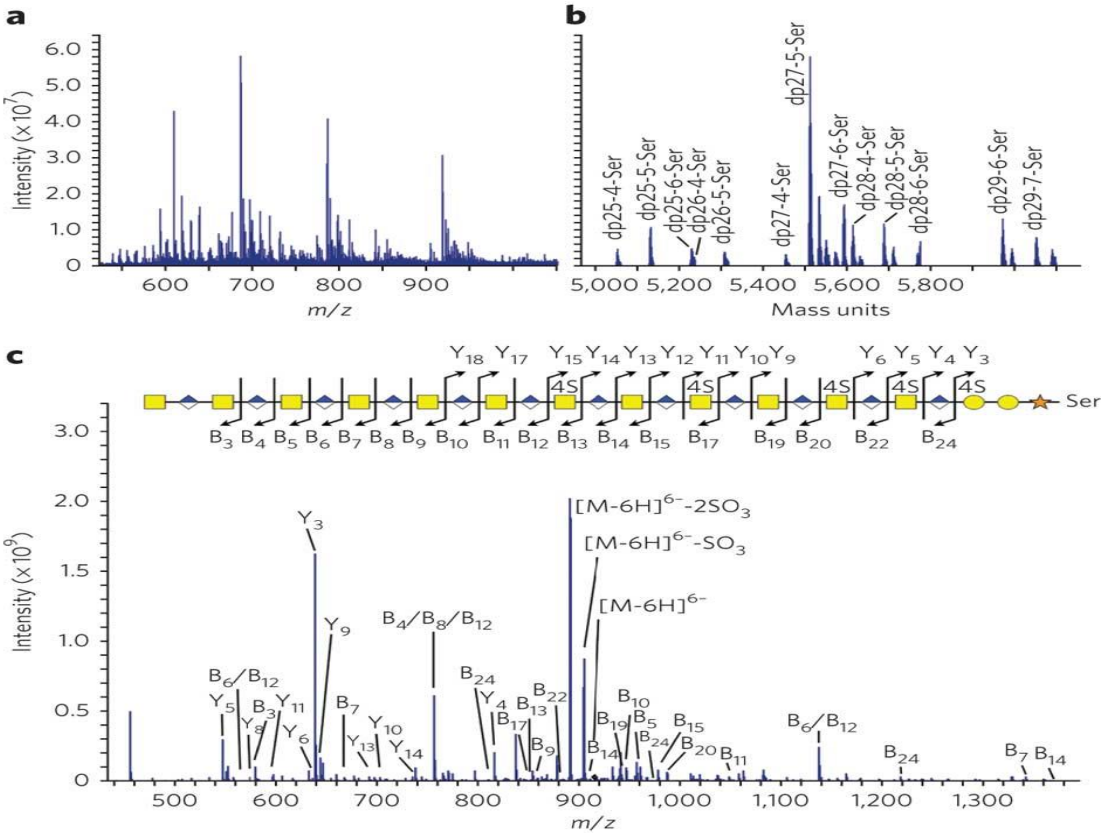

Figure 1.3. (a) FTICR negative-ion mass spectrum of 5.80-kDa MR fraction by PAGE with 18 isobars and 63 parent ions. (b) Deconvolution of spectrum in part a. (c) CID-FTICR-MS/MS spectra of parent-ion m/z = 917.38 (z = 6) and annotated fragment-ions providing sequence with dp27- 5-Ser fragmentation pattern assigned from spectrum. Reprinted with permission from Ly, M.; Leach, F. E., III; Laremore, T. N.; Toshihiko, T.; Amster, I. J.; Linhardt, R. J. Nat. Chem. Biol. 2011, 7, 827−833. Copyright 2011 Nature Publishing Group.

This was a result of the low degree of sulfation, which allowed the charge state of each precursor to be greater than the number of sulfo modifications within a chain. A particularly surprising result of this analysis is that each composition yielded a single sequence, and that there was a conserved pattern of sulfation modifications among all the glycan chains that were examined. This was unexpected since it was believed that GAGs modifications take place in a random manner during their biosynthesis. This important work provides scientists and medical researchers with a new understanding of these vital biomolecules [78].

It is believed that a similar approach may be applied to other more complex GAGs to learn whether they also exhibit a simple pattern of sulfate and acetyl modifications. However, more complex chains would pose challenges in separation and CID analysis due to the presence of a greater number of compositions, a higher degree of polymerization, a higher level of sulfation and more alkali metal-hydrogen heterogeneity. Having more compositions with close structural features will introduce separation issues, while higher sulfation often leads to unproductive SO_3 loss. Higher alkali metal-hydrogen heterogeneity will lead to reduction of signal and isolation issues due to overlap of multiple peaks within the spectrum. Previous reports have shown that having charge state equal or higher than the number of sulfates affords structural informative fragments and reduces SO_3 loss [44, 80].

Another biologically relevant aspect of GAG structure is the C_5 uronic acid stereochemistry. There have been a number of studies directed at determining uronic acid stereochemistry in different classes of GAGs from their MS/MS data. EDD was found to produce unique fragments for distinguishing glucuronic acid (GlcA) from iduronic acid

(IdoA) in heparan sulfate tetrasaccharides [43]. In a more recent work, EDD was combined with principal component analysis (PCA) and used to differentiate the uronic acid stereochemistry of four synthetic heparan sulfate GAG diastereomers, varying only in the uronic acid C_5 stereochemistry. The developed method explored the possibility of using PCA to quantitate the abundance of two epimers in a binary mixture [72]. CID has also been used for distinguishing chondroitin sulfate A (CS-A) and dermatan sulfate (DS), which differ only by their uronic acid stereochemistry [81]. More recent CID work utilizing MS^3 showed that glycosidic fragments were more diagnostic of uronic acid stereochemistry than the ones obtained by MS/MS [69]. EDD fragmentation in combination with statistical analysis has also been used to establish unique product ions for distinguishing GlcA from IdoA [74]. These analytical methods could potentially be utilized to assign uronic acid stereochemistry of CS or DS oligomers and to quantify the relative amount of each in the mixture.

EDD has been proven to be also very useful for analysis of N-glycans and other oligosaccharides [46]. EDD of chloride-adducted neutral and sialylated species was found to generate more cross-ring and glycosidic fragment ions compared to the ones obtained from EDD of deprotonated molecular ions [47]. Positive ion mode electron based methods can also be used for sulfated glycans. Recent work demonstrated the efficacy of ECD for sulfated carbohydrates complexed with divalent metal ions. When complexed with Ca^{2+}, kappa-carrageenan sulfated oligosaccharides containing one to four sulfate groups produced fragment ions that established the position of the sulfates within the chain residues [82].

SEPARATION METHODS

Chromatographic Methods

Although mass spectrometry is a powerful tool for GAGs analysis, the complexity of the mixture extracted from the natural sources including structural isomers, which do not produce any difference in mass demands a second mode of separation. Therefore, mass spectrometry is often combined with liquid chromatography (HPLC) or electrophoresis (e.g. capillary electrophoresis) depending on how the sample is prepared (e.g. types of enzyme or release procedure, native versus permethylation, and chromophore label). Reversed Phase (RP) chromatography is widely used for the derivatized glycans because they are retained in the column. Derivatization can be carried out by either permethylation or attaching a chromophoric tag for spectrophotometric detection [13]. A chemical derivatization method involving methylation of the –OH, –NH groups and replacement of the sulfite groups with acetyl or trideuteroacetyl groups followed by LC-MS^n was used for structural characterization of GAGs recently [15]. This method showed improved RPLC separation and the ions are detected in positive mode. The method is found to determine the structures of heparin and heparan sulfate GAGs [83] as well as distinguishing CS/DS isomers [15].

Reversed phase ion pairing (RPIP)-LC-MS has also been used for GAGs analysis [84-87], heparin-like glycosylaminoglycans (HLGAGs) [88] and glycol-split heparins [89]. RPIP separations strongly rely on the choice of ion pairing reagent as well as on the pH of the separation. Hydrophilic interaction chromatography (HILIC) has also been used for the analysis of glycosaminoglycans [66, 90]. Porous graphitized carbon (PGC) has also been GAG digests [62, 91]. These chromatographic methods are time consuming

and some require desalting or removal of ion pairing reagents before the samples are analyzed using mass spectrometry. Due to this, newer techniques including gas phase methods are being developed to increase selectivity and improve the speed of the method development.

Ion Mobility

Ion mobility (IM) is a gas phase separation technique that can be coupled to MS to provide more information about the biomolecules. IM is a pretty fast method that separate gas phase ions mixed with buffer gas in presence of alternating or constant electric field through the mobility region. Mass spec separates on the basis of M/Z while ion mobility discriminate ions in terms of charge state, gas phase conformations and shape [92, 93]. There are two main categories of ion mobility separations.

Time Dispersion IM

Methods based on separation through time-dispersion have been widely applied for glycomics. These methods can either be performed using drift tube ion mobility (DTIM), where ions are separated in an electrostatic field by collisions with a buffer gas, or traveling wave ion mobility (TWIM), where ions are separated using a buffer gas in an electrodynamic field [94].

Because of the homogeneous electric field in DTIM instruments, kinetic theory can be used to readily determine the collision cross section (CCS) of an analyte based on the drift time. Conversely, the electric field in the TWIMS instrument is not homogeneous, thereby limiting the use of this technology for obtaining gas-phase structure information [94]. To alleviate this limitation, external calibrants, for which the CCS has been determined using DTIM instrumentation and which are of similar

molecular identity, can be used to determine the CCS of analytes by TWIMS. TWIMS has been used to study the conformation changes that occur in heparins when they bind with metal cations [95]. TWIM has also been used to separate GAG hexasaccharides [65] and octasaccharides [96] due to their differences in conformation. Because this kind of ion mobility is time dependent, it is difficult to couple it with ion activation methods like EDD that require substantial amount of time during spectral acquisition or in cases where multiple ion activation methods are needed for the same molecular ion.

Spatial Dispersion IM

High field asymmetric-waveform ion mobility (FAIMS) also known as differential mobility spectrometry utilizes differences of ion mobility in alternating high and low electric field applied between two electrodes at atmospheric pressure. Ions are pushed through the FAIMS device by a carrier gas which could be pure or a mixture of gases. The applied field from an asymmetric, periodic waveform disperses the ions within the device toward one of the electrodes, depending on their differential mobility, and they end up neutralized. When a small dc potential (compensation voltage, CV) is applied, ions of a particular differential mobility assumes a stable trajectory through the device and are thus detected [97]. FAIMS- LTQ Orbitrap was recently used for the separation of isomeric O-linked glycopeptides differing only at the site of glycosylation (GalNAc), and that were difficult to separate using RPLC [98]. The site of glycosylation was determined from ETD fragment ions obtained from separated peaks at a given CV. Since FAIMS separate ions spatially rather than temporally, it is a useful tool particularly when coupled to mass spectrometers in which multiple ion activation methods can be used to fragment separated molecular ions.

In **Chapter 2,** the experimental procedure for the work described in this dissertation is presented. These include how synthetic, chemo-enzymatic and naturally depolymerized oligomers used in this work were produced. Both mass spectrometry and tandem mass spectrometry methods used will also be described in this section. The procedure of how FAIMS separation experiments were carried out and how this technique was coupled with FT-ICR for EDD fragmentation will also be discussed.

Chapter 3 deals with the application of a CID method on differentially ionized molecular ions of a highly sulfated pentasaccharide, Arixtra. Arixtra is a pharmaceutical drug used as an anticoagulant. Ionizing of the acidic groups was carried out either through charge or Na^+/ H^+ exchange. The nature of the fragment ions obtained from different ionized state of the molecule will be discussed and the quality of the precursor ion that generated complete sets of both glycosidic and cross-ring fragment ions which located SO_3 modifications will be discussed.

While chapter 3 details the method for stabilizing the acidic groups within highly sulfated chain, most of the GAG compounds involved in biological activities are longer than a pentasaccharide. **Chapter 4** explores the method described in chapter 3 on longer highly sulfated GAGs produced using different methods. The compounds chemically synthesized using enzymes and naturally occurring oligomers resulting from enzymatic depolymerization are studied here. Differences in fragments ions obtained from the free reducing end oligomers and the ones whose anomeric –OH is locked will also be discussed.

One of the key observations in the above mentioned work is the appearance of some ions in glucuronic containing GAG chains and generally absent or in low intensity

in iduronic containing counterparts. In **chapter 5** we explore diagnostic uronic acid cross-ring fragment ions in CSA and DS dp4, dp6, dp8 and dp10. The characteristics of the molecular ions that produce diagnostic ions will be discussed experimentally while the structural quality of the diagnostic ions will also be assessed and their relative intensity measured.

Chapter 6 describes a FAIMS-FTICR method used to separate ESI generated isobaric charge state ions resulting from different length of chondroitin sulfate A GAGs. Additionally, epimeric mixture of heparan sulfate tetrasaccharides differing only at one stereogenic center was separated and their ions activated using EDD to obtain structural information. The ability of FAIMS to separate anomers and how the multiplicity of peaks originating from this phenomenon can be reduced will be described.

REFERENCES

1. Chi, L.; Amster, J. and Linhardt, R. J., Mass Spectrometry for the Analysis of Highly Charged Sulfated Carbohydrates. *Curr. Anal. Chem.* **2005**, 1, 223-240.
2. Capila, I. and Linhardt, R. J., Heparin–Protein Interactions. *Angew. Chem. Int. Ed.* **2002**, 41, 390-412.
3. Gandhi, N. S. and Mancera, R. L., The Structure of Glycosaminoglycans and their Interactions with Proteins. *Chem. Biol. Drug Des.* **2008**, 72, 455-482.
4. Hillenkamp, F.; Karas, M.; Beavis, R. C. and Chait, B. T., Matrix-assisted laser desorption/ionization mass spectrometry of biopolymers. *Anal. Chem.* **1991**, 63, 1193A-1203A.
5. Tanaka, K.; Waki, H.; Ido, Y.; Akita, S.; Yoshida, Y.; Yoshida, T. and Matsuo, T., Protein and polymer analyses up to m/z 100 000 by laser ionization time? of? flight mass spectrometry. *Rapid Commun. Mass Spectrom.* **1988**, 2, 151-153.
6. Fenn, J.; Mann, M.; Meng, C.; Wong, S. and Whitehouse, C., Electrospray ionization for mass spectrometry of large biomolecules. *Science.* **1989**, 246, 64-71.
7. Harvey, D. J., Matrix-assisted laser desorption/ionization mass spectrometry of carbohydrates. *Mass Spectrom. Rev.* **1999**, 18, 349-450.
8. Zhou, W. and Hakansson, K., Structural Characterization of Carbohydrates by Fourier Transform Tandem Mass Spectrometry. *Curr. Proteomics.* **2011**, 8, 297-308.

9. Tissot, B.; Gasiunas, N.; Powell, A. K.; Ahmed, Y.; Zhi, Z.-l.; Haslam, S. M.; Morris, H. R.; Turnbull, J. E.; Gallagher, J. T. and Dell, A., Towards GAG glycomics: Analysis of highly sulfated heparins by MALDI-TOF mass spectrometry. *Glycobiology.* **2007**, 17, 972-982.

10. Karas, M.; Bahr, U. and Dülcks, T., Nano-electrospray ionization mass spectrometry: addressing analytical problems beyond routine. *Fresenius J. Anal. Chem.* **2000**, 366, 669-676.

11. Yang, B.; Solakyildirim, K.; Chang, Y. and Linhardt, R. J., Hyphenated techniques for the analysis of heparin and heparan sulfate. *Anal. Bioanal. Chem.* **2011**, 399, 541-557.

12. Fabrik, I.; Cmelik, R. and Bobalova, J., Analysis of free oligosaccharides by negative-ion electrospray ion trap tandem mass spectrometry in the presence of H2PO4- anions. *Int. J. Mass Spectrom.* **2012**, 309, 88-96.

13. Ruhaak, L. R.; Zauner, G.; Huhn, C.; Bruggink, C.; Deelder, A. M. and Wuhrer, M., Glycan labeling strategies and their use in identification and quantification. *Anal. Bioanal. Chem.* **2010**, 397, 3457-3481.

14. Wuhrer, M., Glycomics using mass spectrometry. *Glycoconj. J.* **2013**, 30, 11-22.

15. Huang, R.; Pomin, V. H. and Sharp, J. S., LC-MS (n) Analysis of Isomeric Chondroitin Sulfate Oligosaccharides Using a Chemical Derivatization Strategy. *J. Am. Soc. Mass Spectrom.* **2011**, 22, 1577-1587.

16. Harvey, D. J., Identification of protein-bound carbohydrates by mass spectrometry. *Proteomics* **2001**, 1, 311-328.

17. Zaia, J., Mass spectrometry of oligosaccharides. *Mass Spectrom. Rev.* **2004**, 23, 161-227.

18. Zaia, J., Mass spectrometry and glycomics. *Omics.* **2010**, 14, 401-418.

19. Zaia, J., Mass spectrometry and the emerging field of glycomics. *Chem. Biol.* **2008**, 15, 881-892.

20. An, H. J. and Lebrilla, C. B., Structure Elucidation of Native N- and O-Linked Glycans by Tandem Mass Spectrometry (Tutorial). *Mass Spectrom. Rev.* **2011**, 30, 560-578.

21. Cody, R.; Burnier, R. and Freiser, B., Collision-induced dissociation with Fourier transform mass spectrometry. *Anal. Chem.* **1982**, 54, 96-101.

22. Little, D. P.; Speir, J. P.; Senko, M. W.; O'Connor, P. B. and McLafferty, F. W., Infrared multiphoton dissociation of large multiply charged ions for biomolecule sequencing. *Anal. Chem.* **1994**, 66, 2809-2815.

23. Zubarev, R. A.; Kelleher, N. L. and McLafferty, F. W., Electron capture dissociation of multiply charged protein cations. A nonergodic process. *J. Am. Chem. Soc.* **1998**, 120, 3265-3266.

24. Budnik, B. A.; Haselmann, K. F. and Zubarev, R. A., Electron detachment dissociation of peptide di-anions: an electron–hole recombination phenomenon. *Chem. Phys. Lett.* **2001**, 342, 299-302.

25. Syka, J. E. P.; Coon, J. J.; Schroeder, M. J.; Shabanowitz, J. and Hunt, D. F., Peptide and protein sequence analysis by electron transfer dissociation mass spectrometry. *Proc. Natl. Acad. Sci. U. S. A.* **2004**, 101, 9528-9533.

26. Herron, W. J.; Goeringer, D. E. and McLuckey, S. A., Gas-Phase Electron Transfer Reactions from Multiply-Charged Anions to Rare Gas Cations. *J. Am. Chem. Soc.* **1995**, 117, 11555-11562.

27. Zaia, J.; Miller, M. J. C.; Seymour, J. L. and Costello, C. E., The Role of Mobile Protons in Negative Ion CID of Oligosaccharides. *J. Am. Soc. Mass Spectrom.* **2007**, 18, 952-960.

28. Zaia, J. and Costello, C. E., Tandem Mass Spectrometry of Sulfated Heparin-Like Glycosaminoglycan Oligosaccharides. *Anal. Chem.* **2003**, 75, 2445-2455.

29. Kailemia, M. J.; Li, L.; Ly, M.; Linhardt, R. J. and Amster, I. J., Complete mass spectral characterization of a synthetic ultralow-molecular-weight heparin using collision-induced dissociation. *Anal. Chem.* **2012**, 84, 5475-5478.

30. Xie, Y. and Lebrilla, C. B., Infrared Multiphoton Dissociation of Alkali Metal-Coordinated Oligosaccharides. *Anal. Chem.* **2003**, 75, 1590-1598.

31. Khoo, K.-H. and Yu, S.-Y., Mass Spectrometric Analysis of Sulfated N- and O-Glycans; In *Methods in Enzymology*, Vol 478: Glycomics;M. Fukuda; **2010**; pp. 3-26

32. Wuhrer, M.; Deelder, A. M. and van der Burgt, Y. E. M., Mass Spectrometric Glycan Rearrangements. *Mass Spectrom. Rev.* **2011**, 30, 664-680.

33. Lee, H.; An, H. J.; Lerno, L. A., Jr.; German, J. B. and Lebrilla, C. B., Rapid profiling of bovine and human milk gangliosides by matrix-assisted laser desorption/ionization Fourier transform ion cyclotron resonance mass spectrometry. *Int. J. Mass Spectrom.* **2011**, 305, 138-150.

34. Park, Y. and Lebrilla, C. B., Application of Fourier transform ion cyclotron resonance mass spectrometry to oligosaccharides. *Mass Spectrom. Rev.* **2005**, 24, 232-264.

35. McFarland, M.; Marshall, A.; Hendrickson, C.; Nilsson, C.; Fredman, P. and Månsson, J.-E., Structural characterization of the GM1 ganglioside by infrared multiphoton dissociation, electron capture dissociation, and electron detachment dissociation electrospray ionization FT-ICR MS/MS. *J. Am. Soc. Mass Spectrom.* **2005**, 16, 752-762.

36. Harvey, D. J. and Rudd, P. M., Fragmentation of negative ions from N-linked carbohydrates. Part 5: Anionic N-linked glycans. *Int. J. Mass Spectrom.* **2011**, 305, 120-130.

37. Rohmer, M.; Baeumlisberger, D.; Stahl, B.; Bahr, U. and Karas, M., Fragmentation of neutral oligosaccharides using the MALDI LTQ Orbitrap. *Int. J. Mass Spectrom.* **2011**, 305, 199-208.

38. Chai, W.; Piskarev, V. and Lawson, A. M., Negative-ion electrospray mass spectrometry of neutral underivatized oligosaccharides. *Anal. Chem.* **2001**, 73, 651-657.

39. Chai, W.; Lawson, A. and Piskarev, V., Branching pattern and sequence analysis of underivatized oligosaccharides by combined MS/MS of singly and doubly charged molecular ions in negative-ion electrospray mass spectrometry. *J. Am. Soc. Mass Spectrom.* **2002**, 13, 670-679.

40. Harvey, D. J.; Bateman, R. H. and Green, M. R., High-energy Collision-induced Fragmentation of Complex Oligosaccharides Ionized by Matrix-assisted Laser Desorption/Ionization Mass Spectrometry. *J. Mass Spectrom.* **1997**, 32, 167-187.

41. Yoo, H. J.; Wang, N.; Zhuang, S.; Song, H. and Håkansson, K., Negative-ion electron capture dissociation: Radical-driven fragmentation of charge-increased gaseous peptide anions. *J. Am. Chem. Soc.* **2011**, 133, 16790-16793.

42. Wolff, J. J.; Amster, I. J.; Chi, L. and Linhardt, R. J., Electron Detachment Dissociation of Glycosaminoglycan Tetrasaccharides. *J. Am. Soc. Mass Spectrom.* **2007**, 18, 234-244.

43. Wolff, J. J.; Chi, L.; Linhardt, R. J. and Amster, I. J., Distinguishing Glucuronic from Iduronic Acid in Glycosaminoglycan Tetrasaccharides by Using Electron Detachment Dissociation. *Anal. Chem.* **2007**, 79, 2015-2022.

44. Wolff, J. J.; Laremore, T. N.; Busch, A. M.; Linhardt, R. J. and Amster, I. J., Influence of Charge State and Sodium Cationization on the Electron Detachment Dissociation and Infrared Multiphoton Dissociation of Glycosaminoglycan Oligosaccharides. *J. Am. Soc. Mass Spectrom.* **2008**, 19, 790-798.

45. Wolff, J. J.; Leach, F. E.; Laremore, T. N.; Kaplan, D. A.; Easterling, M. L.; Linhardt, R. J. and Amster, I. J., Negative Electron Transfer Dissociation of Glycosaminoglycans. *Anal. Chem.* **2010**, 82, 3460-3466.

46. Adamson, J. T. and Håkansson, K., Electron Detachment Dissociation of Neutral and Sialylated Oligosaccharides. *J. Am. Soc. Mass Spectrom.* **2007**, 18, 2162-2172.

47. Kornacki, J. R.; Adamson, J. T. and Håkansson, K., Electron Detachment Dissociation of Underivatized Chloride-Adducted Oligosaccharides. *J. Am. Soc. Mass Spectrom.* **2012**, 23, 2031-2042.

48. Han, L. and Costello, C. E., Electron transfer dissociation of milk oligosaccharides. *J. Am. Soc. Mass Spectrom.* **2011**, 22, 997-1013.

49. Zhao, P.; Viner, R.; Teo, C. F.; Boons, G.-J.; Horn, D. and Wells, L., Combining High-Energy C-Trap Dissociation and Electron Transfer Dissociation for Protein O-GlcNAc Modification Site Assignment. *J. Proteome Res.* **2011**, 10, 4088-4104.

50. Hersberger, K. E. and Håkansson, K., Characterization of O-Sulfopeptides by Negative Ion Mode Tandem Mass Spectrometry: Superior Performance of Negative Ion Electron Capture Dissociation. *Anal. Chem.* **2012**, 84, 6370-6377.

51. Domon, B. and Costello, C. E., A Systematic Nomenclature for Carbohydrate Fragmentations in Fab-Ms Ms Spectra of Glycoconjugates. *Glycoconjugate J.* **1988**, 5, 397-409.

52. Sekiya, S. and Iida, T., Glycan analysis by mass spectrometry. *Trends Glycosci Glyc.* **2008**, 20, 51-65.

53. Han, L. and Costello, C., Mass spectrometry of glycans. *Biochemistry Moscow*. **2013**, 78, 710-720.

54. Laremore, T. N.; Leach, F. E., III; Solakyildirim, K.; Amster, I. J. and Linhardt, R. J., Glycosaminoglycan Characterization by Electrospray Ionization Mass Spectrometry Including Fourier Transform Mass Spectrometry; In *Methods in Enzymology*, Vol 478: Glycomics;M. Fukuda; 2010; pp. 79-108

55. Wuhrer, M.; Catalina, M. I.; Deelder, A. M. and Hokke, C. H., Glycoproteomics based on tandem mass spectrometry of glycopeptides. *J. Chromatogr. B.* **2007**, 849, 115-128.

56. Vékey, K.; Ozohanics, O.; Tóth, E.; Jekő, A.; Révész, Á.; Krenyácz, J. and Drahos, L., Fragmentation characteristics of glycopeptides. *Int. J. Mass Spectrom.* **2013**, 345–347, 71-79.

57. Jensen, P. H.; Karlsson, N. G.; Kolarich, D. and Packer, N. H., Structural analysis of N- and O-glycans released from glycoproteins. *Nat. Protoc.* **2012**, 7, 1299-1310.

58. Harvey, D. J., Structural determination of N-linked glycans by matrix-assisted laser desorption/ionization and electrospray ionization mass spectrometry. *Proteomics.* **2005**, 5, 1774-1786.

59. Bird, B.; Romeo, M. J.; Diem, M.; Bedrossian, K.; Laver, N. and Naber, S., Cytology by infrared micro-spectroscopy: Automatic distinction of cell types in urinary cytology. *Vib. Spectrosc.* **2008**, 48, 101-106.

60. Zaia, J. and Costello, C. E., Compositional Analysis of Glycosaminoglycans by Electrospray Mass Spectrometry. *Anal. Chem.* **2000**, 73, 233-239.

61. Naggar, E. F.; Costello, C. E. and Zaia, J., Competing fragmentation processes in tandem mass spectra of heparin-like glycosaminoglycans. *J. Am. Soc. Mass Spectrom.* **2004**, 15, 1534-1544.

62. Karlsson, N. G.; Schulz, B. L.; Packer, N. H. and Whitelock, J. M., Use of graphitised carbon negative ion LC-MS to analyse enzymatically digested

glycosaminoglycans. *J.Chromatogr.B Analyt.Technol.Biomed.Life Sci.* **2005**, 824, 139-147.

63. Saad, O. M.; Myers, R. A.; Castleton, D. L. and Leary, J. A., Analysis of hyaluronan content in chondroitin sulfate preparations by using selective enzymatic digestion and electrospray ionization mass spectrometry. *Anal. Biochem.* **2005**, 344, 232-239.

64. Chi, L.; Wolff, J. J.; Laremore, T. N.; Restaino, O. F.; Xie, J.; Schiraldi, C.; Toida, T.; Amster, I. J. and Linhardt, R. J., Structural analysis of bikunin glycosaminoglycan. *J. Am. Chem. Soc.* **2008**, 130, 2617-2625.

65. Schenauer, M. R.; Meissen, J. K.; Seo, Y.; Ames, J. B. and Leary, J. A., Heparan Sulfate Separation, Sequencing, and Isomeric Differentiation: Ion Mobility Spectrometry Reveals Specific Iduronic and Glucuronic Acid-Containing Hexasaccharides. *Anal. Chem.* **2009**, 81, 10179-10185.

66. Staples, G. O.; Bowman, M. J.; Costello, C. E.; Hitchcock, A. M.; Lau, J. M.; Leymarie, N.; Miller, C.; Naimy, H.; Shi, X. and Zaia, J., A chip-based amide-HILIC LC/MS platform for glycosaminoglycan glycomics profiling. *Proteomics.* **2009**, 9, 686-695.

67. Taylor, C. J.; Burke, R. M.; Wu, B.; Panja, S.; Nielsen, S. B. and Dessent, C. E. H., Structural characterization of negatively charged glycosaminoglycans using high-energy (50-150 keV) collisional activation. *Int. J. Mass Spectrom.* **2009**, 285, 70-77.

68. Auray-Blais, C.; Bherer, P.; Gagnon, R.; Young, S. P.; Zhang, H. H.; An, Y.; Clarke, J. T. R. and Millington, D. S., Efficient analysis of urinary

glycosaminoglycans by LC-MS/MS in mucopolysaccharidoses type I, II and VI. *Mol. Genet. Metab.* **2011**, 102, 49-56.

69. Bielik, A. M. and Zaia, J., Multistage tandem mass spectrometry of chondroitin sulfate and dermatan sulfate. *Int. J. Mass Spectrom.* **2011**, 305, 131-137.

70. Leach, F. E., III; Wolff, J. J.; Xiao, Z.; Ly, M.; Laremore, T. N.; Arungundram, S.; Al-Mafraji, K.; Venot, A.; Boons, G.-J.; Linhardt, R. J. and Amster, I. J., Negative electron transfer dissociation Fourier transform mass spectrometry of glycosaminoglycan carbohydrates. *Eur. J. Mass Spectrom.* **2011**, 17, 167-176.

71. Leach, F. E., III; Xiao, Z.; Laremore, T. N.; Linhardt, R. J. and Amster, I. J., Electron detachment dissociation and infrared multiphoton dissociation of heparin tetrasaccharides. *Int. J. Mass Spectrom.* **2011**, 308, 253-259.

72. Oh, H.; Leach, F., III; Arungundram, S.; Al-Mafraji, K.; Venot, A.; Boons, G.-J. and Amster, I. J., Multivariate Analysis of Electron Detachment Dissociation and Infrared Multiphoton Dissociation Mass Spectra of Heparan Sulfate Tetrasaccharides Differing Only in Hexuronic acid Stereochemistry. *J. Am. Soc. Mass Spectrom.* **2011**, 22, 582-590.

73. Flangea, C.; Sisu, E.; Seidler, D. G. and Zamfir, A. D., Analysis of oversulfation in biglycan chondroitin/dermatan sulfate oligosaccharides by chip-based nanoelectrospray ionization multistage mass spectrometry. *Anal. Biochem.* **2012**, 420, 155-162.

74. Leach, F., III; Ly, M.; Laremore, T.; Wolff, J.; Perlow, J.; Linhardt, R. and Amster, I. J., Hexuronic Acid Stereochemistry Determination in Chondroitin

Sulfate Glycosaminoglycan Oligosaccharides by Electron Detachment Dissociation. *J. Am. Soc. Mass Spectrom.* **2012**, 23, 1488-1497.

75. Leymarie, N.; McComb, M. E.; Naimy, H.; Staples, G. O. and Zaia, J., Differential characterization and classification of tissue specific glycosaminoglycans by tandem mass spectrometry and statistical methods. *Int. J. Mass Spectrom.* **2012**, 312, 144-154.

76. Li, L.; Ly, M. and Linhardt, R. J., Proteoglycan sequence. *Molecular Biosystems.* **2012**, 8, 1613-1625.

77. Li, L.; Zhang, F.; Zaia, J. and Linhardt, R. J., Top-down approach for the direct characterization of low molecular weight heparins using LC-FT-MS. *Anal. Chem.* **2012**, 84, 8822-8829.

78. Ly, M.; Leach III, F. E.; Laremore, T. N.; Toida, T.; Amster, I. J. and Linhardt, R. J., The proteoglycan bikunin has a defined sequence. *Nat. Chem. Biol.* **2011**, 7, 827-833.

79. Laremore, T. N.; Leach, F. E., 3rd; Amster, I. J. and Linhardt, R. J., Electrospray ionization Fourier transform mass spectrometric analysis of intact bikunin glycosaminoglycan from normal human plasma. *Int. J. Mass Spectrom.* **2011**, 305, 109-115.

80. McClellan, J. E.; Costello, C. E.; O'Conno, P. B. and Zaia, J., Influence of Charge State on Product Ion Mass Spectra and the Determination of 4S/6S Sulfation Sequence of Chondroitin Sulfate Oligosaccharides. *Anal. Chem.* **2002**, 74, 3760-3771.

81. Zaia, J.; Li, X.; Chan, S. and Costello, C., Tandem mass spectrometric strategies for determination of sulfation positions and uronic acid epimerization in chondroitin sulfate oligosaccharides. *J. Am. Soc. Mass Spectrom.* **2003**, 14, 1270-1281.

82. Liu, H. and Hakansson, K., Electron capture dissociation of divalent metal-adducted sulfated oligosaccharides. *Int. J. Mass Spectrom.* **2011**, 305, 170-177.

83. Huang, Y.; Mao, Y.; Shao, C. and Zaia, J., Development of structurally-defined heparan sulfate/heparin oligosaccharide libraries using 2D chromatography and mass spectrometry-based structural determination. *Glycobiology.* **2012**, 22, 1609-1609.

84. Langeslay, D. J.; Urso, E.; Gardini, C.; Naggi, A.; Torri, G. and Larive, C. K., Reversed-phase ion-pair ultra-high-performance-liquid chromatography-mass spectrometry for fingerprinting low-molecular-weight heparins. *J. Chromatogr. A* **2013**, 1292, 201-210.

85. Yang, B.; Weyers, A.; Baik, J. Y.; Sterner, E.; Sharfstein, S.; Mousa, S. A.; Zhang, F.; Dordick, J. S. and Linhardt, R. J., Ultra-performance ion-pairing liquid chromatography with on-line electrospray ion trap mass spectrometry for heparin disaccharide analysis. *Anal. Biochem.* **2011**, 415, 59-66.

86. Wang, B.; Buhse, L. F.; Al-Hakim, A.; Boyne Ii, M. T. and Keire, D. A., Characterization of currently marketed heparin products: analysis of heparin digests by RPIP-UHPLC-QTOF-MS. *J. Pharm. Biomed. Anal.* **2012**, 67-68, 42-50.

87. Jones, C. J.; Beni, S. and Larive, C. K., Understanding the Effect of the Counterion on the Reverse-Phase Ion-Pair High-Performance Liquid Chromatography (RPIP-HPLC) Resolution of Heparin-Related Saccharide Anomers. *Anal. Chem.* **2011**, 83, 6762-6769.

88. Xue, B.; Alves, S.; Desbans, C.; Souchaud, M.; Filali-Ansary, A.; Soubayrol, P. and Tabet, J.-C., Heparin-like glycosaminoglycan/amine salt-bridge interactions: A new potential tool for HLGAGs analysis using mass spectrometry. *J. Mass Spectrom.* **2011**, 46, 689-695.

89. Alekseeva, A.; Casu, B.; Torri, G.; Pierro, S. and Naggi, A., Profiling glycol-split heparins by high-performance liquid chromatography/mass spectrometry analysis of their heparinase-generated oligosaccharides. *Anal. Biochem.* **2013**, 434, 112-122.

90. Huang, Y.; Shi, X.; Yu, X.; Leymarie, N.; Staples, G. O.; Yin, H.; Killeen, K. and Zaia, J., Improved Liquid Chromatography-MS/MS of Heparan Sulfate Oligosaccharides via Chip-Based Pulsed Makeup Flow. *Anal. Chem.* **2011**, 83, 8222-8229.

91. Gill, V. L.; Wang, Q.; Shi, X. and Zaia, J., Mass Spectrometric Method for Determining the Uronic Acid Epimerization in Heparan Sulfate Disaccharides Generated Using Nitrous Acid. *Anal. Chem.* **2012**, 84, 7539-7546.

92. Harvey, S. R.; Macphee, C. E. and Barran, P. E., Ion mobility mass spectrometry for peptide analysis. *Methods.* **2011**, 54, 454-461.

93. Konijnenberg, A.; Butterer, A. and Sobott, F., Native ion mobility-mass spectrometry and related methods in structural biology. *Biochim. Biophys. Acta* **2013**, 1834, 1239-1256.

94. Kanu, A. B.; Dwivedi, P.; Tam, M.; Matz, L. and Hill, H. H., Ion mobility–mass spectrometry. *J. Mass Spectrom.* **2008**, 43, 1-22.

95. Seo, Y.; Schenauer, M. R. and Leary, J. A., Biologically relevant metal-cation binding induces conformational changes in heparin oligosaccharides as measured by ion mobility mass spectrometry. *Int. J. Mass Spectrom.* **2011**, 303, 191-198.

96. Seo, Y.; Andaya, A. and Leary, J. A., Preparation, Separation, and Conformational Analysis of Differentially Sulfated Heparin Octasaccharide Isomers Using Ion Mobility Mass Spectrometry. *Anal. Chem.* **2012**, 84, 2416-2423.

97. Purves, R. W.; Guevremont, R.; Day, S.; Pipich, C. W. and Matyjaszczyk, M. S., Mass spectrometric characterization of a high-field asymmetric waveform ion mobility spectrometer. *Rev. Sci. Instrum.* **1998**, 69, 4094-4105.

98. Creese, A. J. and Cooper, H. J., Separation and Identification of Isomeric Glycopeptides by High Field Asymmetric Waveform Ion Mobility Spectrometry. *Anal. Chem.* **2012**, 84, 2597-2601.

CHAPTER 2

EXPERIMENTAL METHODS

Natural heparin oligosaccharides preparation

Heparin sodium salt used was obtained from porcine intestinal mucosa (Celsius laboratories, Cincinnati, OH). Heparin (6 g) was digested by 10 U recombinant heparinase 1 (EC 4.2.2.7) in 250 mL volume at 30º C until 30% completion at which boiling water was used to quench the reaction [1]. Vacuum rotary evaporation was used to concentrate the reaction mixture before filtering with 0.22-μm Millipore membrane. Before loading the filtrate into the P-10 (BioRad, Hercules, CA) column, the column was equilibrated and eluted with 0.2 M NaCl solution. Uniform size oligosaccharide fractions were pooled together and then desalted using P-2 column. These uniformly sized oligosaccharides were lyophilized and then purified on a semi-preparative strong anion exchange–high performance liquid chromatography (SAX-HPLC) (Waters Spherisorb S5). Fractionation of various uniform-sized oligosaccharide mixtures were carried out using a gradient of water and 2 M NaCl and chromatographic profiles at 232 nm were used to combine fractions from repeated separations. Primary structure and the level of purity was performed using polyacrylamide gel electrophoresis (PAGE) analysis [2].

Chemo-enzymatically synthesized heparan sulfate preparation

A detailed procedure on the preparation of HS oligosaccharides used in this study can be found in Ref. [3]. Briefly, N-sulfonation or 6-O-sulfonation was performed by

incubating 6 μg of de-N-trifluoro-acetylated or de-6-O-sulfo N-trifluoro-acetylated oligosaccharide substrates with the appropriate enzymes and 3'-phosphoadenosine 5'-phosphosulfate (PAPS), overnight at 37^{o} C in mixture of 80 μM PAPS, 50 mM 2-(N-morpholino) ethanesulfonic acid (MES), pH 7.0, 1% Triton X-100 and 4 μg of N-sulfotransferase or 6-O-sulfotransferase-1 and 6-O-sulfotransferase-3 in a total volume of 300 μL. Purification was carried out using diethylaminoethyl (DEAE) column and dialyzed using 2500 molecular weight cut-off (MWCO) 3500 membrane and dried before further purification by a DEAE-NPR HPLC column (0.46 x 7.5 cm; Tosohaas) [3].

Chondroitin sulfate A and dermatan sulfate preparation

Chondroitin sulfate A (CSA) and dermatan sulfate (DS) oligosaccharides were independently prepared by partial enzymatic depolymerization. CSA was depolymerized from bovine trachea chondroitin sulfate A (Celsus Laboratories, Cincinnati, OH) while DS used in this work originated from porcine intestinal mucosa dermatan sulfate (Celsus Laboratories, Cincinnati, OH). Chondroitin ABC lyase from *proteus vulgaris*, EC 4.2.2.4 (Seikagaku, Japan) was used to incubate 20 mg/mL solution of each sample in 50 mM Tris HCL/60 mM sodium acetate buffer, pH 8 at 37^{o} C. When the UV absorbance at 232 nm indicated 50% complete, the digestion mixture was heated for 3 min at 100^{o} C. Ultra-filtration was carried out using a 5000 MWCO membrane to remove the enzyme and the high-molecular-weight oligosaccharide. Concentrate the remaining oligosaccharide mixture, rotary evaporation was used and then fractionated by low pressure GPC on a Bio-Gen p10 (Bio-Rad, Richmond, CA) column. The oligosaccharide fractions were desalted by GPC on a Bio-Gel P2 column and freeze dried [1]. Strong anion exchange high-pressure liquid chromatography (SAX-HPLC) on an semi-preparative SAX S5

Spherisorb column (Waters Corp, Milford, MA) was used for further purification of the oligosaccharides. The resulting SAX-HPLC with over 90% oligosaccharides fractions were collected, desalted by GPC and then freeze-died. The dried solid was reconstituted in water and purified one more time using SAX-HPLC. Only the oligosaccharides within the top 30% of the chromatogram peak was collected, desalted and freeze-dried. Oligomer concentration in the solution was determined by measuring the absorbance at 232 nm (e=3800 M^{-1} cm^{-1}). The final oligosaccharide fractions were characterized by PAGE, ESI-MS, and high-field NMR spectroscopy [2].

Heparan sulfate epimers synthesis

Heparan sulfate tetra-saccharides epimers (GlcA-GlcNAc6S-IdoA-GlcNAc6S (GI) and GlcA-GlcNAc6S-GlcA- GlcNAc6S (GG)) and GlcA-GlcNAc6S-GlcA-GlcNAc6S-(CH2)5-NH2 (GG2) and GlcA-GlcNAc6S-IdoA-GlcNAc6S-(CH2)5-NH2 (GI2),were synthesized by a modular approach and purified as described in Ref. [4]. Use of accurate mass measurement and ^{1}H NMR confirmed the structures of the tetrasaccharides.

Arixtra analysis

Arixtra was purchased from the hospital formulary and desalted on a BioGel P2 column BioRad (Hercules, CA, USA). Arixtra (1.3 μM) in 50:50 methanol: water with 1.0 mM NaOH was used for analysis. A Bruker 9.4 T FTICR (Billerica, MA, USA) with an Apollo II duo source or a Thermo Scientific LTQ Orbitrap XL FT mass spectrometer with a standard, factory-installed nanospray ion source (San Jose, CA, USA) was used in these experiments. The FT-ICR experimental conditions will be discussed in the subsequent paragraph. For orbitrap measurements, nitrogen was used as the collision gas.

Hydrogen/deuterium exchange

The Arixtra sample was lyophilized to dryness and then dissolved in D_2O to make 1mg/mL stock solution. A small amount of this solution was dissolved in 50:50 MeOD:D_2O to make 0.05mg/mL of the spray solution. Before the H/D exchange experiment the sample syringe and ESI lines were rinsed with a mixture of MeOD and D_2O.

Mass spectrometry analysis

A 9.4 Bruker Apex Ultra Qh-FTICR instrument (Billerica, MA, USA) was used in these experiments. Negative-mode ESI was used to ionize the samples using metal capillary (Agilent Technologies, Santa Clara, CA, #G2427A). The samples were introduced at a concentration 0.05-0.1 mg/mL in 50:50 methanol: H_2O unless otherwise stated. The degree of sodiation was controlled by the addition of 0.05-2 mM NaOH (Sigma, St. Louis, MO, USA) to the electrospray solution depending on the length and the level of sulfation of the analyte. All samples were infused at the rate of 120 μL/h. The precursor-ions were mass isolated in the external quadruple with 3 Da isolation window and CID was performed in the collision cell external to the high magnetic field region while ensuring the precursor ion intensity remained above the product ions intensity to minimize the production of internal fragments. Argon was used as the collision gas. 512 k to one mega points of data were acquired for each mass spectrum, padded with one zero-fill and apodized using a sinebell window. A 5 ppm mass accuracy was achieved through an external calibration while internal calibration using accurately

assigned glycosidic bond cleavage products yields a mass accuracy of < 1 ppm. Accurate mass measurement values were used to assign product-ions, whose m/z values were calculated using Glycoworkbench version 2.1 [5]. The product ions are reported using the annotation described previously [6], derived from the Domon and Costello nomenclature [7].

ESI FAIMS

Ions were generated using negative mode ESI. Solutions for given GAG samples were made at a concentration of 0.05- 0.1 mg/mL in 50:50:0.1 MeOH: H_2O: HCOOH (Sigma, St. Louis, MO, USA). All sample solutions were infused at a rate of 120 μL/h using ESI metal capillary (Agilent Technologies, Santa Clara, CA, #G2427A) tip placed about 2-3 mm from the FAIMS curtain gas cap. Generated ions were passed through Bruker Daltonics planar FAIMS analyzer (Billerica, MA, USA) with electrode gap width of 0.5 mm. The FAIMS device was held in place by a cylindrical peek that facilitates proper interfacing to a 9.4 T Bruker Apex IV QeFTMS (Billerica, MA, USA). Ions were separated in FAIMS using 2.4 MHz bi-sinusoidal waveform between dispersion voltages (DV) 1.50 - 1.95 kV and the carrier gas used was air. No modifiers were added to the carrier gas.

ESI-FAIMS-EDD

The positive CV scan (0-30 V) was carried out (negative CV scan did not yield any ions) and the specific CV at which the ion of interest appears in the MS was noted and subsequently used to selectively and continuously transmit one ion at a time for EDD experiments. Indirectly heated hollow cathode was used for generating electrons for EDD experiments. Isolation refinement of the precursor was done in the external quadrupole

where the ions were accumulated for 1–2.5 s before they enter the FTICR-MS analyzer cell. The isolation/cell fill was repeated up to 3 times. In-cell isolation with a coherent harmonic excitation frequency (CHEF) event was used for further ion selection. The precursor ions were irradiated with electrons for 1 s. For electron irradiation the cathode bias, ECD lens, and cathode heater were set at -19 V, -18.6 V, and 1.6 A respectively. 36 acquisitions per mass spectrum were averaged and for each mass spectrum 512 k points were acquired, padded with one zero fill, and apodized using a sinebell window. Background spectra were acquired by leaving all parameters the same but setting the cathode bias to 0 V to ensure that no electrons reached the analyzer cell.

Principal component analysis (PCA)

PLS toolbox (Eigenvector research, inc., Wenatchee, WA) was used for the principal component analysis (PCA). The intensity of 19 assigned fragment ions for each spectrum was used for PCA analysis. These fragment ions were selected based on relative intensity and then normalized using the intensity of the base peak from the background spectra. Each row of the data matrix consists of the mass spectra of each particular sample, while each column contained the normalized peak intensities for the selected fragment ions. During the PCA analysis, the data was mean-centered and cross-validated. For each sample peak, the spectra were acquired in quintuplicate starting with the same precursor intensity and using the same EDD experimental conditions.

REFERENCES

1. Pervin, A.; Gallo, C.; Jandik, K. A.; Han, X.-J. and Linhardt, R. J., Preparation and structural characterization of large heparin-derived oligosaccharides. *Glycobiology.* **1995**, 5, 83-95.
2. Muñoz, E.; Xu, D.; Avci, F.; Kemp, M.; Liu, J. and Linhardt, R. J., Enzymatic synthesis of heparin related polysaccharides on sensor chips: Rapid screening of heparin-protein interactions. *Biochem. Biophys. Res. Commun.* **2006**, 339, 597-602.
3. Liu, R.; Xu, Y.; Chen, M.; Weïwer, M.; Zhou, X.; Bridges, A. S.; DeAngelis, P. L.; Zhang, Q.; Linhardt, R. J. and Liu, J., Chemoenzymatic Design of Heparan Sulfate Oligosaccharides. *J. Biol. Chem.* **2010**, 285, 34240-34249.
4. Arungundram, S.; Al-Mafraji, K.; Asong, J.; Leach, F. E.; Amster, I. J.; Venot, A.; Turnbull, J. E. and Boons, G.-J., Modular Synthesis of Heparan Sulfate Oligosaccharides for Structure−Activity Relationship Studies. *J. Am. Chem. Soc.* **2009**, 131, 17394-17405.
5. Ceroni, A.; Maass, K.; Geyer, H.; Geyer, R.; Dell, A. and Haslam, S. M., GlycoWorkbench: A Tool for the Computer-Assisted Annotation of Mass Spectra of Glycans†. *J. Proteome Res.* **2008**, 7, 1650-1659.
6. Wolff, J. J.; Laremore, T. N.; Busch, A. M.; Linhardt, R. J. and Amster, I. J., Electron Detachment Dissociation of Dermatan Sulfate Oligosaccharides. *J. Am. Soc. Mass Spectrom.* **2008**, 19, 294-304.

7. Domon, B. and Costello, C. E., A Systematic Nomenclature for Carbohydrate Fragmentations in Fab-Ms Ms Spectra of Glycoconjugates. *Glycoconjugate J.* **1988**, 5, 397-409.

CHAPTER 3

COMPLETE MASS SPECTRAL CHARACTERIZATION OF A SYNTHETIC ULTRA-LOW MOLECULAR WEIGHT HEPARIN USING COLLISION INDUCED DISSOCIATION*

* Kailemia, M. J.; Li, L.; Ly, M.; Linhardt, R. J. and Amster, I. J., Complete Mass Spectral Characterization of a Synthetic Ultralow-Molecular-Weight Heparin Using Collision-Induced Dissociation. *Anal. Chem.* **2012**, 84, 5475-5478. Reprinted here with permission of publisher.

ABSTRACT

Glycosaminoglycans (GAGs) are a class of biologically important molecules and their structural analysis is the target of considerable research effort. Advances in tandem mass spectrometry (MS/MS) have recently enabled the structural characterization of several classes of GAGs. However, the highly sulfated GAGs, such as heparins, have remained a relatively intractable class due their tendency to lose SO_3 during MS/MS producing few sequence-informative fragment ions. The present work demonstrates for the first time the complete structural characterization of the highly sulfated heparin-based drug, Arixtra. This was achieved by Na^+/H^+ exchange, to create a more ionized species that was stable against SO_3 loss, and that produced complete sets of both glycosidic and cross-ring fragment ions. MS/MS enables the complete structural determination of Arixtra®, including the stereochemistry of its uronic acid residues and suggests an approach for solving the structure of more complex, highly sulfated heparin-based drugs.

INTRODUCTION

Heparin (Hp) and structurally related heparan sulfate (HS) are biopolymers comprised of highly sulfated uronic acid and glucosamine repeating units and are found intracellularly, in the extracellular matrix, and on the cell surface of a wide variety of species [1, 2]. To develop a deeper understanding of their biological function in angiogenesis [3], tumor metastasis [4], viral invasion [5], cell growth and proliferation [6] and anticoagulation [7], elucidation of their molecular level structures is of great interest but remains a challenge [8]. Unlike biopolymers such as proteins or nucleic acids, the biosynthetic pathways for GAGs are not based on a template mechanism; thus they are heterogeneous in composition, and highly polydisperse in molecular weight [9, 10]. While Hp is produced in large amounts as a drug, HS is often extracted from tissues in small quantities requiring sensitive analytical methods, such as MS [9]. Negative mode electrospray ionization (ESI) is commonly used due to the highly acidic nature of Hp and HS [11] and it provides multiply charged precursor ions which facilitates MS/MS of higher mass molecules.

The presence of a high number of labile sulfate groups renders many MS/MS techniques insufficient for the structural characterization of Hp and HS [12]. Previously, methods such as collision induced dissociation (CID) and infrared multi-photon dissociation (IRMPD) were found to lead to sulfate decomposition (loss of SO_3) and to provide few sequence-informative cleavages [10, 11, 13]. Electron detachment dissociation (EDD) and other electron based methods have been used to characterize HS oligosaccharides with a low level of sulfation as well as chondroitin sulfate GAGs [14-

16], but these methods become less efficient as the number of sulfo groups per disaccharide increases.

Research on MS/MS methods for Hp analysis has been directed at the retention of labile sulfate groups during ion activation but with limited success. Increasing the charge state to a level where all the sulfate groups are ionized reduces sulfate loss and increases structurally-informative cleavages [13, 17, 18], but as the number of sulfate groups per disaccharide increases, charge-charge repulsion limits the ability to produce molecular ions with higher charge states with sufficient intensities for MS/MS [10, 19]. Even when the right charge state is selected, most of the cleavages obtained are glycosidic bond fragmentation, which cannot be used for locating the position of the sulfate groups within a monosaccharide unit. Multistage CID (MS^n) has provided structural information on these molecules but requires substantial amounts of sample and still is inefficient in Hp oligosaccharides having more than one sulfo group per disaccharide unit [13].

Exchanging H^+ with metal cations such as Na^+ or Ca^{2+} has been show to stabilize sulfate groups and to increase the formation of sequence-informative fragment ions [13, 20], but these previous studies showed few glycosidic and cross-ring cleavages and failed to provide comprehensive structural identification of analytes [13], Here we show that use of NaOH as a component of electrospray (ESI) enables the production of a precursor in which all ionizable protons are removed or replaced by Na^+. This precursor is found to be uniquely suitable for MS/MS analysis, and leads to the production of abundant glycosidic and cross-ring fragments, enabling full characterization of a highly sulfated synthetic Hp oligosaccharide using a single CID spectrum.

RESULTS AND DISCUSSIONS

Arixtra® is a synthetic ultralow molecular weight heparin based on the pentasaccharide sequence that comprises the antithrombin III binding site present in both Hp and HS that is responsible for anticoagulant activity [21]. Arrangement of the monosaccharide units, the position of the sulfo group substitution, and the stereochemistry of the uronic acid within this pentasaccharide are critical for its anticoagulant activity [22, 23]. Arixtra® [$C_{31}H_{53}O_{49}S_8N_3$] has 8 sulfo groups and three carboxyl groups for a total of 10 acidic sites. Higher charge states lead to less sulfate loss [13, 17] but charge-charge repulsion limits the ability to achieve a charge state in which all the sulfo groups are deprotonated.

The most abundant charge state observed in the mass spectrum of Arixtra® was $[M-3H]^{3-}$ (Appendix A). In this case only three sulfo groups were deprotonated, leaving the remaining 7 acidic groups protonated. Mild CID activation of this molecular ion produces very intense SO_3 loss peaks, as shown in Figure 3.1a. As previously reported [13], increasing the deprotonation of sulfo and carboxyl groups through metal cation/H^+ exchange reduces SO_3 loss and affords structurally-informative cleavages. In Figure 3.1b, Na^+/H^+ exchange leads to de-protonation of 8 acidic groups, $[M-8H+5Na]^{3+}$, which equals the number of sulfo groups in Arixtra®. While the most intense peaks in the resulting spectrum are the SO_3 loss peaks, a few glycosidic fragments are observed that provide limited structural information. When all the acidic groups were deprotonated, a CID spectrum for $[M-10H+7Na]^{3-}$ was obtained, which had a uniform distribution of both glycosidic, cross-ring cleavages with few low intensity peaks resulting from neutral SO_3 loss (Figure 3.1c).

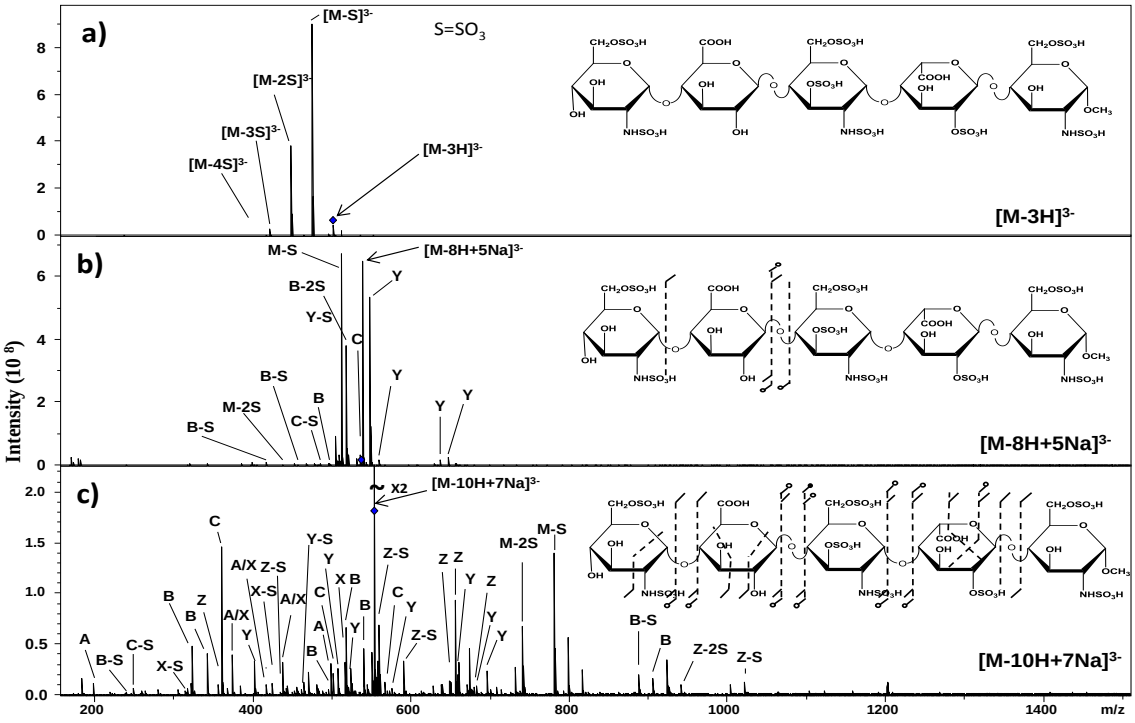

Figure 3.1. CID spectra for triply deprotonated molecular ions of Arixtra®. a) CID of $[M\text{-}3H]^{3-}$ showing that a low charge state leads to the loss of SO_3 and little useful structural information. b) Deprotonation of eight acidic groups, equal to the number of sulfo groups, through Na^+/H^+ exchange and charging, reduces SO_3 loss but provides few useful fragments. c) When all ten acidic groups are deprotonated, a large number of structurally informative glycosidic and cross-ring cleavages are observed.

Due to the high density of assignable peaks within this spectrum, a simple annotation is used that does not include the entire ion nomenclature. In this annotation, A is used to denote any cleavage corresponding to the actual A fragment while A-S is used to denote loss of SO_3 from the corresponding A fragment. A complete peak list is included in the Appendix A. Higher charge states of the fully deprotonated sample were examined and found to give complementary data. Annotated structures for $[M\text{-}10H+6Na]^{4-}$ and $[M\text{-}10H+5Na]^{5-}$ show the observed fragmentations, which include an

entire set of glycosidic bond cleavages and abundant cross-ring cleavages (Figure 3.2). For the molecular ion $[M\text{-}10H+6Na]^{4-}$, Z_1 places two sulfo groups on the reducing end residue, and the mass difference between $^{0,2}X_1$ and Y_1 places a sulfo group at the 2-position of the iduronic acid residue.

The mass difference between B_3 and C_2 show there are three sulfo groups in the central glucosamine residue occupying all available sites of modification, *i.e.*, 2-*N*-sulfo, 3-*O*-sulfo and 6-*O*-sulfo. The mass difference between Y_4 and the $^{2,4}X_4$ cleavage in the non-reducing end residue establishes sulfation on the 6-*O*- and 2-*N*- positions. The $^{2,4}X_4$ fragment is isobaric with a $^{1,5}A_5$ fragment, but 1,5 cleavage is unusual in the CID mass spectra of GAGs, while 2,4 cleavage is fairly common. Fragmentation of another fully deprotonated molecular ion of one higher charge state $[M\text{-}10H+5Na]^{5-}$ (Figure 3.2) produces similar cleavages to those observed for $[M\text{-}10H+6Na]^{4-}$ with additional fragments including $^{2,4}A_5$ that allow for the placement of the two sulfo groups on the 2-N and 6-O positions in the reducing end residue. The $^{2,4}A_5$ fragment is isobaric with a $^{1,5}X_4$ cleavage, but again, the former is common and abundant in CID spectra of GAGs, and can be confidently assigned as such. A full mass list can be found in the supporting information.

The effectiveness of this method using FTMS Orbitrap provided similar results, indicating that this approach can be applied using a wide variety of FT mass spectrometers. Moreover, the Orbitrap can afford additional low mass fragments such as $^{0,3}X_{0,}$ $^{3,5}X_{0,}$ $^{0,3}A_{1,}$ $^{0,4}A_{1,}$ and $^{1,3}A_1$ ions using a higher collision dissociation (HCD) fragmentation approach (Appendix A). An increase in SO_3 loss fragments is observed in the spectra as the charge state increases and the number of the sodium cations in the

molecular ion decreases. This suggests that stabilizing the sulfo groups is more readily achieved by increasing the degree of sodiation of the molecular ion rather than by increasing the molecular ion charge.

Uronic acid C_5-stereochemistry (glucuronic acid/ iduronic acid) is another important aspect of the Arixtra® structure that determines how it interacts antithrombin III and other proteins to influences their functions [21, 24]. Efforts to distinguish iduronic acid and glucuronic acid in Hp, HS and dermatan sulfate analytes is an ongoing challenge [15, 25, 26] for analytical chemists. In the attempt to determine whether the abundant cross-ring cleavages generated by CID can aid in elucidating uronic acid stereochemistry, we examined the cross-ring cleavages all of the uronic acid residues in a variety of GAG samples (chondroitin 4-sulfate, dermatan sulfate) dp4-dp10, Hp oligosaccharides dp4-dp8, and chemoenzymatically synthesized Hp (dp7) and HS dp10-dp12) oligosaccharides. These results will be a subject of a future publication, which establishes the diagnostic nature of $^{2,4}A_n$ ions in characterizing uronic acid stereochemistry.

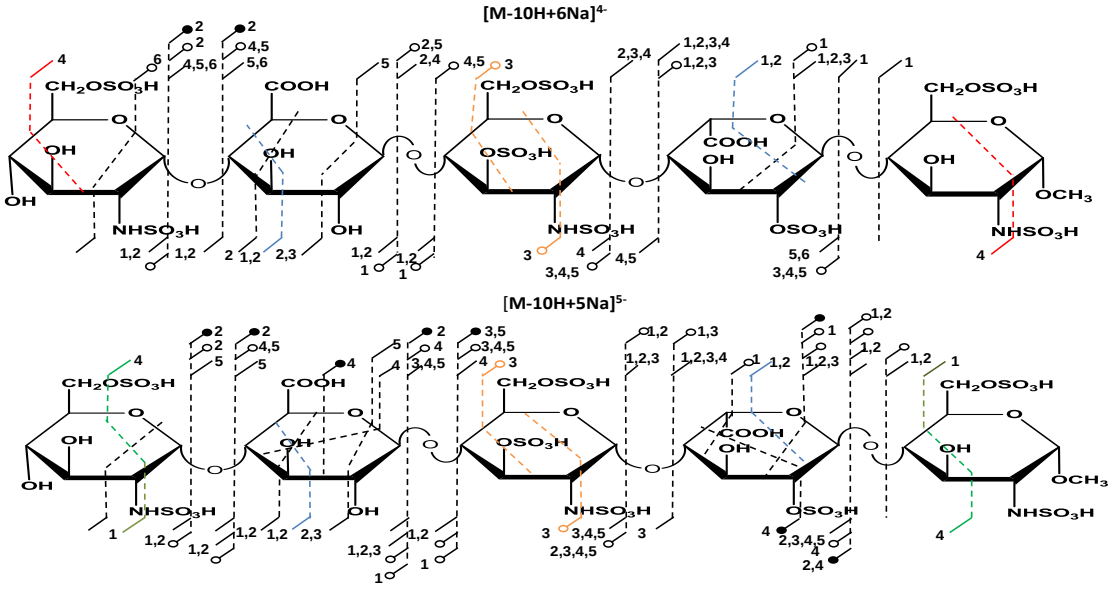

Figure 3.2. Annotated structures showing observed cleavages for Arixtra for two different charge states and levels of sodiation. Both $[M-10H+6Na]^{4-}$ and $[M-10H+5Na]^{5-}$ show similar fragmentation patterns affording more comprehensive structural information. The numbers adjacent to a cleavage indicate the number of sodium ions present in the fragment ion, open circles denotes SO_3 loss accompanying the indicated fragmentation, and filled circles denote loss of 2 or more SO_3 groups.

In all experiments, $^{2,4}A_n$ (where n is the uronic acid residue position in the analyte) cleavage(s) appeared in all glucuronic acid residues but is absent (or present at very low intensity) in iduronic acid residues as long as all the acidic groups in the ion are deprotonated. In Arixtra®, a $^{2,4}A_2$ fragment appears in the glucuronic acid residue but not in the iduronic acid residue. Although $^{2,4}A_2$ fragment is isobaric with $^{1,5}X_1$ fragments, H/D exchange experiments confirmed the assignment of the $^{2,4}A_2$ fragment (Appendix A).

Unlike the previously reported Q-TOF mass spectral data on Arixtra®,[13] our study fully assigns all the fragments required for the complete establishment of primary

structure. Additional studies are underway in the investigators' laboratories on longer oligosaccharides and even full-length Hp and HS chains to establish the effectiveness of this method on larger highly sulfated GAGs.

It is interesting to compare this approach to prior efforts on GAGs and other polyanionic biomolecules such as nucleic acids. Molecules with multiple acidic sites have a high propensity to pair with metal ions, which adversely impacts mass spectrometric analysis, by introducing heterogeneity from incomplete replacement of the ionizable protons by metal ions. For this reason, researchers usually take great care to rigorously desalt anionic samples prior to MS analysis [27-29]. During the ESI experiments, reagents such as formic acid or ammonium hydroxide have been used to reduce metal/proton exchange and the consequential splitting of peaks that reduces the efficiency of both MS and MS/MS analysis [17, 29]. In contrast to the standard approach for anionic biomolecules, the current work purposely introduces metal ions to exhaustively replace ionizable protons, which greatly improves the MS/MS analysis.

Prior investigations of the MS/MS behavior of highly sulfated GAGs have had limited success because they did not investigate the appropriate precursor species. When more than a single protonated acidic group remains in a precursor ion, MS/MS fragmentation is generally accompanied by the loss of SO_3. Since sulfo group loss effectively competes with glycosidic and through-ring cleavage, this results in a loss of sequence-informative fragmentation. In conclusion, MS/MS analysis can provide complete sequence coverage for highly sulfated GAG oligosaccharides if the precursor molecular ion has all, or all but one, of its acidic groups deprotonated through a combination of charging and Na^+/H^+ exchange.

REFERENCES

1. Blackhall, F. H.; Merry, C. L.; Davies, E. J. and Jayson, G. C., Heparan sulfate proteoglycans and cancer. *Br. J. Cancer.* **2001**, 85, 1094-1098.
2. Kjellen, L. and Lindahl, U., Proteoglycans: Structures and Interactions. *Annu. Rev. Biochem.* **1991**, 60, 443-475.
3. Vlodavsky, I. and Friedmann, Y., Molecular properties and involvement of heparanase in cancer metastasis and angiogenesis. *J. Clin. Invest.* **2001**, 108, 341-347.
4. Liu, D.; Shriver, Z.; Qi, Y.; Venkataraman, G. and Sasisekharan, R., Dynamic regulation of tumor growth and metastasis by heparan sulfate glycosaminoglycans. *Semin. Thromb. Hemost.* **2002**, 28, 67-78.
5. Hilgard, P. and Stockert, R., Heparan sulfate proteoglycans initiate dengue virus infection of hepatocytes. *Hepatology.* **2000**, 32, 1069-1077.
6. Higashiyama, S.; Abraham, J. A. and Klagsbrun, M., Heparin-Binding EGF-like Growth Factor Stimulation of Smooth Muscle Cell Migration: Dependence on Interactions with Cell Surface Heparan Sulfate. *J. Cell Biol.* **1993**, 122, 933-940.
7. Rabenstein, D. L., Heparin and heparan sulfate: structure and function. *Nat. Prod. Rep.* **2002**, 19, 312-331.
8. Thanawiroon, C.; Rice, K. G.; Toida, T. and Linhardt, R. J., Liquid Chromatography/Mass Spectrometry Sequencing Approach for Highly Sulfated Heparin-derived Oligosaccharides. *J. Biol. Chem.* **2004**, 279, 2608-2615.

9. Capila, I.; Gunay, N. S.; Shriver, Z. and Venkataraman, G., Methods for Structural Analysis of Heparin and Heparan Sulfate; In Chemistry and Biology of Heparin and Heparan Sulfate;H. G. Garg, R. J. Linhardt and C. A. Hales; Elsevier Science: Amsterdam, **2005**; pp. 55-77.

10. Chi, L.; Amster, J. and Linhardt, R. J., Mass Spectrometry for the Analysis of Highly Charged Sulfated Carbohydrates. *Curr. Anal.* **2005**, 1, 223-240.

11. Naggar, E. F.; Costello, C. E. and Zaia, J., Competing fragmentation processes in tandem mass spectra of heparin-like glycosaminoglycans. *J. Am. Soc. Mass. Spectrom.* **2004**, 15, 1534-1544.

12. Jones, C. J.; Beni, S.; Limtiaco, J. F. K.; Langeslay, D. J. and Larive, C. K., Heparin Characterization: Challenges and Solutions. *Annu. Rev. Anal. Chem.* **2011**, 4, 439-465.

13. Zaia, J. and Costello, C. E., Tandem Mass Spectrometry of Sulfated Heparin-Like Glycosaminoglycan Oligosaccharides. *Anal. Chem.* **2003**, 75, 2445-2455.

14. Wolff, J. J.; Amster, I. J.; Chi, L. and Linhardt, R. J., Electron Detachment Dissociation of Glycosaminoglycan Tetrasaccharides. *J. Am. Soc. Mass. Spectrom.* **2007**, 18, 234-244.

15. Wolff, J. J.; Chi, L.; Linhardt, R. J. and Amster, I. J., Distinguishing Glucuronic from Iduronic Acid in Glycosaminoglycan Tetrasaccharides by Using Electron Detachment Dissociation. *Anal. Chem.* **2007**, 79, 2015-2022.

16. Wolff, J. J.; Leach, F. E.; Laremore, T. N.; Kaplan, D. A.; Easterling, M. L.; Linhardt, R. J. and Amster, I. J., Negative Electron Transfer Dissociation of Glycosaminoglycans. *Anal. Chem.* **2010**, 82, 3460-3466.

17. Wolff, J. J.; Laremore, T. N.; Busch, A. M.; Linhardt, R. J. and Amster, I. J., Influence of Charge State and Sodium Cationization on the Electron Detachment Dissociation and Infrared Multiphoton Dissociation of Glycosaminoglycan Oligosaccharides. *J. Am. Soc. Mass. Spectrom.* **2008**, 19, 790-798.

18. McClellan, J. E.; Costello, C. E.; O'Conno, P. B. and Zaia, J., Influence of Charge State on Product Ion Mass Spectra and the Determination of 4S/6S Sulfation Sequence of Chondroitin Sulfate Oligosaccharides. *Anal. Chem.* **2002**, 74, 3760-3771.

19. Saad, O. M. and Leary, J. A., Compositional Analysis and Quantification of Heparin and Heparan Sulfate by Electrospray Ionization Ion Trap Mass Spectrometry. *Anal. Chem.* **2003**, 75, 2985-2995.

20. Taylor, C. J.; Burke, R. M.; Wu, B.; Panja, S.; Nielsen, S. B. and Dessent, C. E. H., Structural characterization of negatively charged glycosaminoglycans using high-energy (50–150 keV) collisional activation. *Int. J. Mass Spectrom.* **2009**, 285, 70-77.

21. Petitou, M. and van Boeckel, C. A. A., A Synthetic Antithrombin III Binding Pentasaccharide Is Now a Drug! What Comes Next? *Angew. Chem. Int. Ed.* **2004**, 43, 3118-3133.

22. Rosenberg, R. D. and Lam, L., Correlation between structure and function of heparin. *Proc. Nat. Acad. Sci.* **1979**, 76, 1218-1222.

23. Noti, C. and Seeberger, P. H., Chemical Approaches to Define the Structure-Activity Relationship of Heparin-like Glycosaminoglycans. *Chem. Biol.* **2005**, 12, 731-756.

24. Kuberan, B.; Lech, M. Z.; Beeler, D. L.; Wu, Z. L. and Rosenberg, R. D., Enzymatic synthesis of antithrombin III-binding heparan sulfate pentasaccharide. *Nat Biotech.* **2003**, 21, 1343-1346.

25. Zaia, J.; Li, X.; Chan, S. and Costello, C., Tandem mass spectrometric strategies for determination of sulfation positions and uronic acid epimerization in chondroitin sulfate oligosaccharides. *J. Am. Soc. Mass. Spectrom.* **2003**, 14, 1270-1281.

26. Hitchcock, A. M.; Costello, C. E. and Zaia, J., Glycoform Quantification of Chondroitin/Dermatan Sulfate Using a Liquid Chromatography−Tandem Mass Spectrometry Platform†. *Biochem.* **2006**, 45, 2350-2361.

27. Gilar, M.; Belenky, A. and Wang, B. H., High-throughput biopolymer desalting by solid-phase extraction prior to mass spectrometric analysis. *J. Chromatogr. A.* **2001**, 921, 3-13.

28. Fountain, K. J.; Gilar, M. and Gebler, J. C., Electrospray ionization mass spectrometric analysis of nucleic acids using high-throughput on-line desalting. *Rapid Commun. Mass Spectrom.* **2004**, 18, 1295-1302.

29. Laremore, T. N.; Leach III, F. E.; Solakyildirim, K.; Amster, I. J. and Linhardt, R. J., Glycosaminoglycan Characterization by Electrospray Ionization Mass Spectrometry Including Fourier Transform Mass Spectrometry; In *Methods Enzymol*.;F. Minoru; Academic Press: **2010**; pp. 79-108.

CHAPTER 4

STRUCTURALLY INFORMATIVE TANDEM MASS SPECTROMETRY OF HIGHLY SULFATED NATURAL AND CHEMO-ENZYMATICALLY SYNTHESIZED HEPARIN AND HEPARAN SULFATE GLYCOSAMINOGLYCANS*

* Kailemia, M. J.; Li, L.; Xu, Y.; Liu, J.; Linhardt, R. J. and Amster, I. J., Structurally Informative Tandem Mass Spectrometry of Highly Sulfated Natural and Chemoenzymatically Synthesized Heparin and Heparan Sulfate Glycosaminoglycans. *Mol. Cell. Proteomics*. **2013**, 12, 979-990. Reprinted with permission of publisher.

ABSTRACT

The highly sulfated glycosaminoglycan oligosaccharides derived from heparin and heparan sulfate have been a highly intractable class of molecules to analyze by tandem mass spectrometry. Under many methods of ion-activation, this class of molecules generally exhibit SO_3 loss as the most significant fragmentation pathway, interfering with the assignment of the location of sulfo groups in glycosaminoglycan chains. We report here a method that stabilizes sulfo groups, and facilitates the complete structural analysis of densely sulfated (2 or more sulfo groups per disaccharide repeat unit) heparin and heparan sulfate oligomers. This is achieved by complete removal of all ionizable protons, either by charging during electrospray ionization, or by Na^+/H^+ exchange. The addition of mM levels of NaOH to the sample solution facilitates the production of precursor ions that meet this criterion. This approach is found to work for a variety of heparin sulfate oligosaccharides derived from natural sources, or produced by chemoenzymatic synthesis, with up to twelve saccharide subunits and up to eleven sulfo groups.

INTRODUCTION

Heparin (Hp) and heparan sulfate (HS) are linear, poly-disperse and highly sulfated glycosaminoglycans (GAGs), with a repeating disaccharide building block composed of a 1-4 linked glucosamine and an uronic acid residue [1]. The saccharide residues may have a variety of modifications, and these are usually heterogeneous due to the non-template nature of their biosynthesis [2]. Glucosamine residues may be substituted with *N*-sulfo, or *N*-acetyl and 3- and/or 6-*O*-sulfo groups. Uronic acid residues can be either glucuronic or iduronic acid and substituted with 2-*O*-sulfo groups [3, 4]. These structural features are thought to control Hp and HS biological activity, for example, their interactions with proteins, and so the structural characterization of GAGs is an important target for chemical analysis [1, 5, 6]. A particularly well-known example of a GAG-protein interaction is the role of Hp as an antithrombin III (AT) activator. A pentasaccharide unit with a very specific pattern of modification interacts with AT causing it to undergo a conformational change that increases the anticoagulation activity of AT by more than three orders of magnitude [7, 8]. Contamination of pharmaceutical Hp was a major issue recently, associated with over 70 fatalities worldwide [9-12]. This problem highlights the need for rapid, robust and sensitive analytical methods for the analysis of heparin, and for identifying contaminants of similar composition [11]. While nuclear magnetic resonance spectroscopy is often the method of choice for determining the structure of GAGs, such as Hp and HS, it requires substantial sample preparation to obtain pure samples, relatively large amounts of sample, and time-consuming interpretation.

Mass spectrometry (MS) and tandem mass spectrometry (MS/MS) offer high sensitivity and specificity, and are often used for the analysis of complex mixtures. For these reasons, MS and MS/MS have been explored by a number of researchers as tools for the structural analysis of GAGs [13-31]. Recently, the sequence of intact, full length chondroitin sulfate GAG chains from bikunin were elucidated [32]. However, these were sparsely sulfated compared to typical HS/Hp GAGs, averaging less than 0.5 sulfate modifications per disaccharide repeat unit. Hp in particular is highly sulfated, making it extremely difficult to deduce composition and other structural details from intact samples. Controlled enzymatic digestion (heparin lyases I, II and III) [33] and chemical methods (using nitrous acid) [34] can depolymerize Hp and HS to oligosaccharides of sizes that can be analyzed using the current instrumentation. The resulting products occur as a mixture of different sizes, compositions, isomers and epimers, making their characterization extremely challenging.

Use of MS to analyze highly sulfated HS oligosaccharides, with two or more sulfo groups per disaccharide repeating unit, is difficult due to the loss of labile SO_3 with mild ion-activation [27]. Negative-mode electrospray ionization (ESI) is commonly used to analyze GAGs due to its ability to preserve the sulfo groups during the ionization process, and its propensity to form multiply-charged anions from these acidic molecules [35]. Information about the composition and the length of the molecule can be achieved by the first step MS but cannot provide structural details on the monosaccharide residue connectivity and locations of various GAG modifications, *i.e.*, sulfo groups, acetyl groups, and uronic acid C_5 stereochemistry. MS/MS is required to obtain these structural details. Fragmentation of glycosidic bonds produce ion products that determine the

composition of individual residues, while cross-ring cleavages are useful for assigning the sites of modification within a monosaccharide residue.

For Hp and HS oligosaccharides, previous studies have shown that threshold ion-activation methods such as low energy collision-induced dissociation (CID) or infrared multiphoton dissociation (IRMPD) produces a relatively low number of structurally useful fragments, due to the preference for loss of SO_3 rather than glycosidic bond fragmentation or cross-ring cleavage [13, 25, 36]. Nevertheless, CID has been used to differentiate 6-*O*-sulfo and 3-*O*-sulfo groups in Hp disaccharide units, due to differences in their multi-dimensional tandem mass spectrometry (MS^n) fragments [37]. Metal cationization has also been used for the MS/MS analysis of carbohydrates [38-42], and it has been found that increasing the charge-state and metal-hydrogen exchange in these biomolecules increases the density of fragments and reduces SO_3 loss [17, 25, 43, 44]. Hp and HS GAGs have been characterized by their MS^n with CID activation, for both multiply-charged ions cationized by Ca^{2+} (and Na^+ to a lesser extent), ranging from a trisaccharide with 4 sulfo groups to a pentasaccharide with 8 sulfo groups. Although this work resulted in more glycosidic and cross-ring cleavages, there were still too few fragment-ions to provide detailed structural information about the sites of sulfo group modifications [25]. However, this work established that the presence of metal cations in these molecules increased the stability of the sulfo groups, leading to more useful fragment-ions [45]. In recent years, electron-based methods, especially electron detachment dissociation (EDD), have proved to be very useful in both locating the sulfo groups and determining the uronic acid C-5 stereochemistry of undersulfated HS-derived

tetrasaccharides but the efficiency of EDD decreases as the number of sulfo groups per disaccharide unit increases [13-16, 18, 20, 22].

Sodium metal cation/proton exchange has been investigated for EDD and IRMPD of sparsely sulfated dermatan sulfate oligosaccharides (one sulfo group per disaccharide) [17]. This work showed that increasing sodium cationization so that all sulfo groups in the molecule are deprotonated greatly reduces the number of SO_3 loss peaks, but this approach also resulted in a reduction of the number of both glycosidic and cross-ring cleavages [17]. The current work demonstrates a new method to stabilize sulfo groups during MS/MS of Hp and HS oligosacchardies, while producing much more extensive and structurally informative fragmentation. This is achieved by the exhaustive deprotonation of all ionizable sites in Hp and HS oligomers, using sodium hydroxide to cationize or deprotonate every acidic group in the precursor-ion. This approach has recently been shown in our lab to be effective for the highly sulfated heparin-like pentasaccharide drug, Arixtra® [46]. Here we show that this approach is generally applicable to Hp and HS oligosaccharides from pentasulfated tetrasaccharides up to undecasulfated octasaccharide Hp, derived from natural sources, as well as chemoenzymatically synthesized HS oligomers up to twelve residues in length.

EXPERIMENTAL

GAG oligomers were produced from naturally occurring sources and by chemoenzymatic synthesis. Those produced by enzymatic digestion of naturally occuring GAGs range from a pentasulfated tetrasaccharide to undecasulfated octasaccharide. The chemoenzymatically synthesized oligosaccharides range from a decasaccharide with 8

sulfo groups to dodecasaccharide with 10 sulfo groups and under sulfated HS ranging from degree of polymerization (dp) 10-dp12.

Natural Hp oligosaccharides preparation

Heparin sodium salt used was obtained from porcine intestinal mucosa (Celsius laboratories, Cincinnati, OH). Heparin (6 g) of was digested by 10 U recombinant heparinase 1 (EC 4.2.2.7) in 250 mL volume at 30º C until 30% completion at which boiling water was used to quench the reaction. Vacuum rotary evaporation was used to concentrate the reaction mixture before filtering with 0.22-μm Millipore membrane. Before loading the filtrate into the P-10 (BioRad, Hercules, CA) column, the column was equilibrated and eluted with 0.2 M NaCl solution. Uniform size oligosaccharide fractions were pooled together and then desalted using P-2 column. These uniformly sized oligosaccharides were lyophilized and then purified on a semi-preparative strong anion exchange–high performance liquid chromatography (SAX-HPLC) (Waters Spherisorb S5). Fractionation of various uniform-sized oligosaccharide mixtures were carried out using a gradient of water and 2 M NaCl and chromatographic profiles at 232 nm were used to combine fractions from repeated separations. Primary structure and the level of purity was performed using polyacrylamide gel electrophoresis (PAGE) analysis [47].

Chemo-enzymatically Synthesized HS Preparation

A detailed procedure on the preparation of HS oligosaccharides used in this study can be found in the paper [48]. Briefly, *N*-sulfonation or 6-*O*-sulfonation was performed by incubating 6 μg of de-*N*-trifluoro-acetylated or de-6-*O*-sulfo *N*-trifluoro-acetylated oligosaccharide substrates with the appropriate enzymes and 3'-phosphoadenosine 5'-phosphosulfate (PAPS), overnight at 37^{o} C in mixture of 80 μM PAPS, 50 mM 2-(*N*-

morpholino) ethanesulfonic acid (MES), pH 7.0, 1% Triton X-100 and 4 μg of *N*-sulfotransferase or 6-*O*-sulfotransferase-1 and 6-*O*-sulfotransferase-3 in a total volume of 300 μL. Purification was carried out using diethylaminoethyl (DEAE) column and dialyzed using 2500 molecular weight cut-off (MWCO) 3500 membrane and dried before further purification by a DEAE-NPR HPLC column (0.46 x 7.5 cm; Tosohaas) [48].

Mass Spectrometry Analysis

A 9.4 Bruker Apex Ultra Qh-FTICR instrument (Billerica, MA, USA) was used in these experiments. Negative-mode ESI was used to ionize the samples using metal capillary (Agilent Technologies, Santa Clara, CA, #G2427A). The samples were introduced at a concentration 0.05-0.1 mg/mL in 50:50 methanol: H_2O. The degree of sodiation was controlled by the addition of 1-2 mM NaOH (Sigma, St. Louis, MO, USA) to the electrospray solution depending on the level of sulfation of the analyte. All samples were infused at the rate of 120 μL/h. The precursor-ions were mass isolated in the external quadruple with 3 Da isolation window and CID was performed in the collision cell external to the high magnetic field region while ensuring the precursor ion intensity remained above the product ions intensity to minimize the production of internal fragments. The effect of adding NaOH in the solution was studied by first introducing the sample in H_2O: MeOH only and then with NaOH to a hexasaccharide containing 8 sulfo groups. The MS of the hexasaccharide sample with and without NaOH is shown in Figure 4.1.

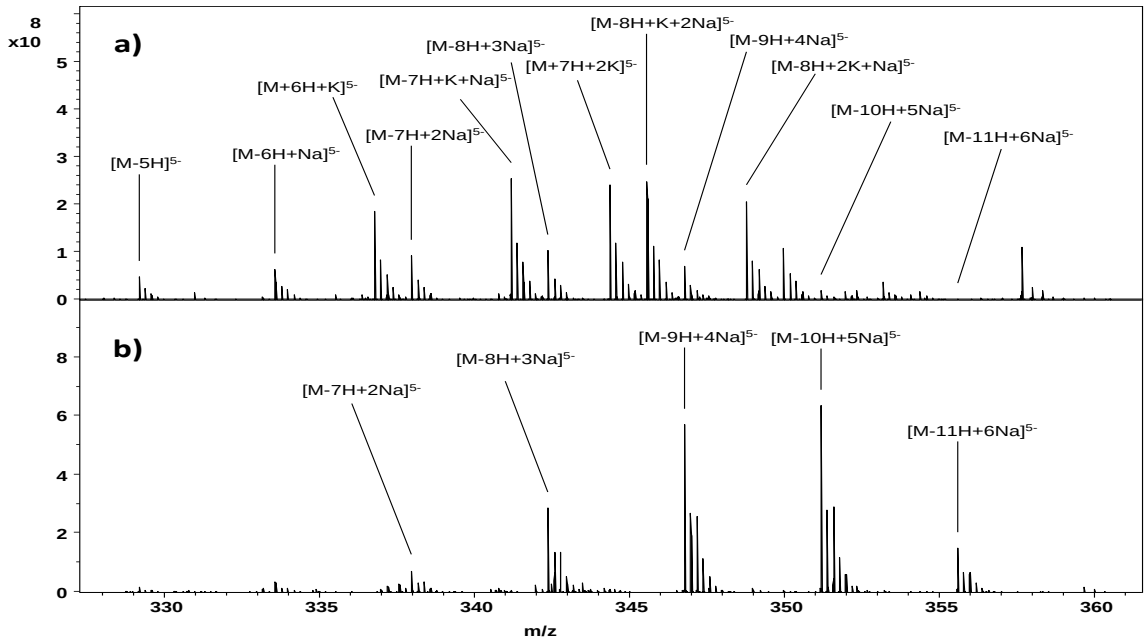

Figure 4.1. Showing the heterogeneity observed when there is no NaOH applied (a) and when 1mM NaOH is added to a hexasaccharide with 8S groups (b).

Molecular-ions of charge-state envelope for 3-, 4-, 5- and -6 were observed. Within the charge state envelop, there are numerous peaks resulting from metal/hydrogen exchange. These include the ones with Na^+ and K^+/H^+ individually and the ones with a combination of Na^+ and K^+ in a single peak. This phenomenon is clearly seen when we zoom in one charge-state envelop as shown in Figure 4.1. The zoom in of the 5^- charge state shows the distribution of metal cation/hydrogen exchange peaks. One striking observation from these data is the disappearance of K^+ and Na^+/K^+ peaks after the addition of 1 mM NaOH solution. The peak intensities of the remaining Na^+ peaks increase two-fold, enabling the isolation of the precursor in the quadruple mass filter without interfering peaks around that would otherwise be co-isolated with the precursor.

One mega points of data were acquired for each mass spectrum, padded with one zero-fill and apodized using a sinebell window. A 5 ppm mass accuracy was achieved

through an external calibration while internal calibration using accurately assigned glycosidic bond cleavage products yields a mass accuracy of < 1 ppm. Accurate mass measurement values were used to assign product-ions, whose m/z values were calculated using Glycoworkbench version 2.1 [49]. The product ions are reported using the annotation described previously [18], derived from the Domon and Costello nomenclature [50].

RESULTS AND DISCUSSION

Negative-mode ESI is a useful method for analyzing highly sulfated GAGs because the labile sulfo groups are retained and also because multiply charged anions are produced [5, 44]. Sulfo and carboxyl groups comprise the acidic groups in GAGs, which serve as charge-bearing residues in the ionized sample. Alkali ion/proton heterogeneity can be a significant issue for highly sulfated GAGs, because a substantial reduction in ion intensity results when the signal is divided into several different mass channels. Adding formic acid to the sample solution reduces both Na^+ and K^+ heterogeneity in less sulfated GAGs, but it is less efficient for longer and more highly sulfated Hp and HS oligosaccharides. Although formic acid reduces the intensity of the Na^+ and K^+ peaks, they are still present, leading to difficulties during the ion isolation step of a tandem mass spectrometry experiment; there can be many co-isolated peaks that complicate the resulting MS/MS spectrum. As shown in the 4.1, addition of 1 mM NaOH removes all the adduct peaks that contain K^+, retaining only Na^+ adducts. This increased the signal intensity of the remaining Na^+ containing peaks and allowed clean selection of the precursor ions by the mass selective quadrupole. The structures of all the GAGs molecules used in this work can be found in Figure 4.2. Also found in the Appendix B

are their mass spectra showing the molecular ions obtained and an inset of a zoom in of regions around the precursor ions used in the MS/MS analysis.

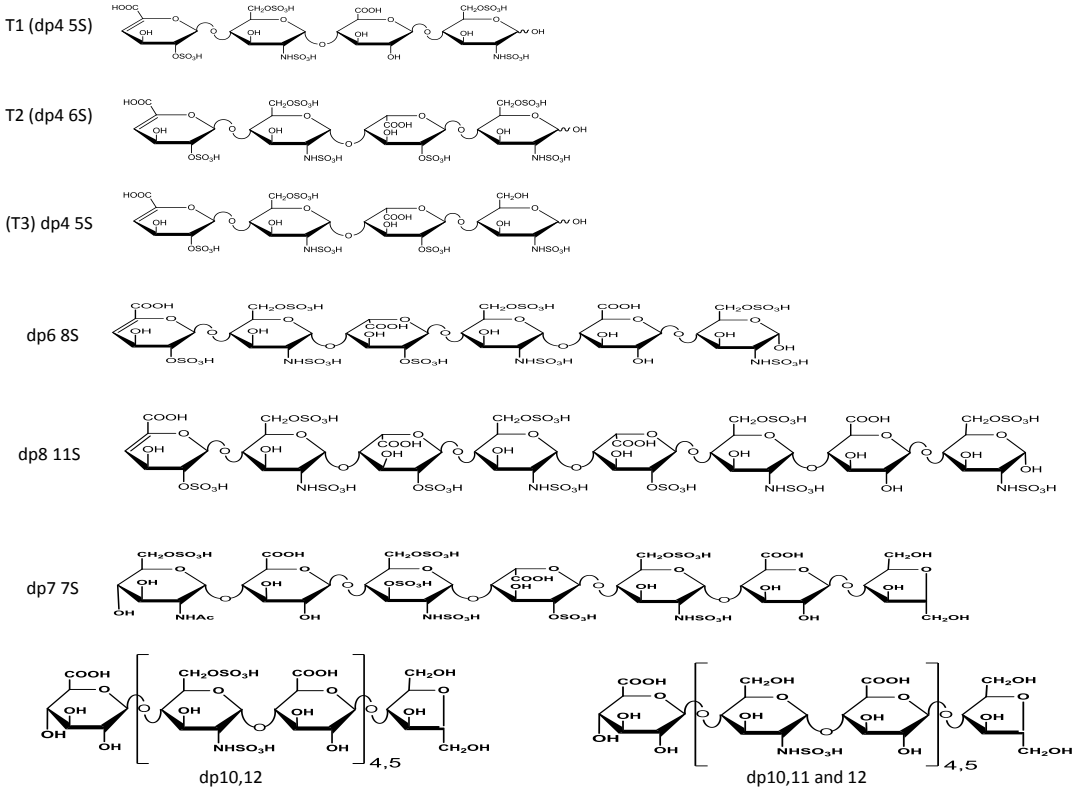

Figure 4.2. The structures of the samples investigated in this work including naturally occurring (T1, T2, T3, dp6 with $8SO_3$ and dp8 with 11 SO_3 groups) and chemo-enzymatically produced GAGs.

Naturally Depolymerized GAGs

A pentasulfated tetrasaccharide (ΔUA2S-GlcNS6S-GlcA-GlcNS6S) (T1) was examined using the procedures described above. The mass spectrum of this compound produced 2-, 3- and 4- charge state molecular ions as shown in the supporting information. One of the molecular ion $[M-7H+4Na]^{3-}$ that was selected for CID analysis has all the acidic groups ionized, including five sulfo and two carboxyl groups. A simple spectrum was obtained in which the fragment-ions permit the identification and location

of all the sulfo groups, Figure 4.3. All the observed fragment-ions are either singly- or doubly- charged. The three most intense peaks in the spectrum are cross-ring fragments $[^{0,2}A_4+4Na]^{2-}$, and a fragment from the same fragment with water loss, and $[^{2,4}A_4+4Na]^{-}$. The fragmentation pathway for these $^{0,2}A_n$ and $^{2,4}A_n$ fragments at the reducing end is highly favored and they are observed as the most intense fragments in all the highly sulfated compounds with two sulfo groups in the reducing end residues and from a precursor with all the acidic groups de-protonated. Abundant $^{0,2}A_n$ fragmentation on the reducing end has been observed for CID of heparin disaccharides before and the mechanism for its occurrence postulated by a reducing end retro-aldol rearrangement pathway [30, 51, 52]. $^{0.2}A_n$ formed at the reducing end can undergo further fragmentation forming $^{2,4}A_n$ product ion [53] and this may explain the appearance of intense $^{2,4}A_n$ fragments within the reducing end of the aldehyde terminated molecules studied here. CID fragmentation of the same fully deprotonated precursor ion $[M-7H+4Na]^{3-}$ from an isomeric tetrasaccharide (T3) (discussed below) without sulfation at the 6-O position on the reducing end preceded by 2-O-sulfated IdoA produced much less intense $[^{2,4}A_4+4Na]^{2-}$, an indication that the presence of 6-O sulfation at the reducing end amino sugar promotes the occurrence of this fragment. Additionally, the CID spectra for the T3 $[M-7H+4Na]^{3-}$ precursor had a markedly higher percentage of SO_3 loss (2% of the fragment ion intensity) compared to a much lower degree of SO_3 loss for the T1 (<1%) as indicated in Table 4.1. Other observable MS/MS spectral differences between these precursor ions for the two isomers can be obtained in the supporting information. The location of the two sulfo groups in the reducing end reside are identified by the $^{2,4}X_0$ peak, or by the mass difference between the $^{2,4}A_4$ and C_3 fragments. The location of the

two sulfo groups in the central glucosamine residue derive from the mass difference between $^{2,4}A_2$ and B_2, whereas the site of sulfo group substitution in the non-reducing end residue is ascertained through the mass difference of $^{0,2}X_3$ and Y_3 fragments.

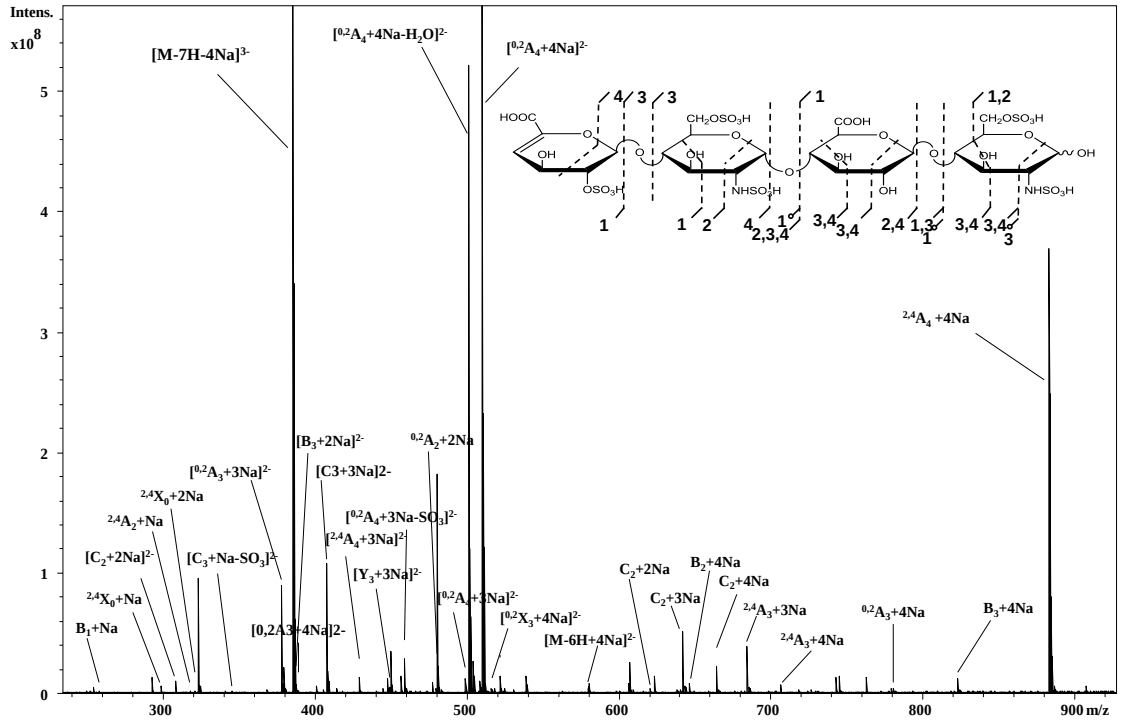

Figure 4.3. CID spectra of pentasulfated heparin tetramer, precursor $[M-7H+4Na]^{3-}$. The fragment ions observed are shown in the annotated structure (inset). The precursor used has all the sulfates and carboxyl groups ionized through charge or Na^+/H^+ exchange.

Compound, number of sulfates, precursor with its M/Z	% product ion yield	% of SO_3 loss product ions	Number of Free protons	Sulfate/ Disaccharide
dp4 (T1) 5S, $[M-7H+4Na]^{3-}$ M/Z 386.29	54	<1	0	2.5
dp4 (T3) 5S, $[M-7H+4Na]^{3-}$ M/Z 386.29	42	2	0	2.5
dp4 (T1) 5S, $[M-6H+2Na]^{4-}$ M/Z 278.48	41	10	1	2.5
dp4 (T3) 5S, $[M-6H+2Na]^{4-}$ M/Z 278.48	30	21	1	2.5
dp4 (T2) 6S, $[M-7H+3Na]^{4-}$ M/Z 303.96	43	12	1	3
dp6 8S, $[M-11H+7Na]^{4-}$ M/Z 450.20	55	1	0	2.7
dp8 11S, $[M-14H+7Na]^{7-}$ M/Z 339.25	56	23	1	2.8
dp10 8S, $[M-13H+7Na]^{6-}$ M/Z 412.66	44	11	0	1.6
dp7 7S, $[M-10H+5Na]^{5-}$ M/Z 376.39	50	15	0	2
dp12 10S, $[M-16H+9Na]^{7-}$ M/Z 430.85	41	14	0	1.7
dp12 5S, $[M-11H+4Na]^{7-}$ M/Z 358.03	62	7	0	0.8
dp11 5S, $[M-9H+3Na]^{6-}$ M/Z 384.87	62	7	1	0.9
dp 10 4S, $[M-9H+3Na]^{6-}$ M/Z 344.70	63	6	0	0.8

Table 4.1. Shows the compounds and the precursor ions used in this work. The product ion yield is given by (the sum of all assigned product ions divided by the sum of all the ions in the spectrum including the precursor)*100. The percent of SO_3 loss experienced during the CID of the given precursor is calculated by summing up all the intensities of the fragments resulting from SO_3 loss and dividing this value with the sum of the intensities of all assigned fragment ions excluding the precursor and then multiplying the result by 100. Number of free protons in this work is calculated using this formula ((number of SO_3 + carboxyl groups in the compound)-(precursor charge + number of Na^+ in it)).

The product yield from this precursor was 54% and most of the remaining ion abundance was from the precursor ion whose intensity was considerably larger than the product ions (commonly observed in most of the mass spectra reported in this work even

though product ion yields are 30-60%, as product ions are divided between my fragment channels). There were only three peaks exhibiting SO_3 loss (from C_2, C_3 and $^{0,2}A_4$ fragments) accounting for less than 1% of the product ions confirming that the Na^+ ions stabilize the sulfo groups during ion activation leading to backbone fragmentations. CID of a precursor-ion from the same compound, but with one ionizable proton present, $[M-6H+2Na]^{4-}$, also produced fragments that enabled the location of all sulfo groups in the molecule but with markedly increased SO_3 loss.

This approach was tested with two additional tetrasaccharides ΔUA2S-GlcNS6S-IdoA2S-GlcNS (T3) and ΔUA2S-GlcNS6S-IdoA2S-GlcNS6S (T2), with five and six sulfo groups, respectively. CID for singly protonated molecular-ions for T2 $[M-7H+3Na]^{4-}$ and T3 $[M-6H+2Na]^{4-}$ produced fragments that were able to locate all sites of sulfo group substitution. The structures for T2 and T3 with annotations denoting the sites of observed fragmentation as well as their MS/MS spectra and tables with the m/z values and assignment of the fragments can be found in the supplementary information. A lower charge state molecular-ion $[M-7H+4Na]^{3-}$ for T3 produced a product yield of 42% with only a total of 21 fragment ions in the spectrum with 2% of all the products resulting from SO_3 loss. CID of T2 molecular ion $[M-8H+5Na]^{3-}$ produced only 12 fragments (6 cross-ring and 6 glycosidic) with no loss of SO_3 fragments observed. Another observation is that the presence of an acidic proton in the selected precursor within these tetrasaccharide units leads to much higher SO_3 loss, as seen from Table 4.1. T1 precursor $[M-7H+4Na]^{3-}$ with no free proton show less than 1% SO_3 loss while a different precursor $[M-6H+2Na]^{4-}$of the same compound but with a free acidic group produced 10% SO_3 loss (the same is observed for T3).

An interesting observation from these data was the correlation of particular fragment ions with uronic acid stereochemistry. $^{2,4}A_n$ appear with significant abundance in the glucuronic acid residue and is absent or present at very low abundance in 2-O-sulfated iduronic acid residues. As will be seen in the data below, $^{2,4}A_n$ cleavages are absent in 2-O-sulfated iduronic acid residues for all the compounds that we have analyzed, except in these tetrasaccharides, where they may occur with low abundance. These suggest that these ions may be used to assign the stereochemistry of the uronic acid residues in Hp and HS oligosaccharides. Since the analyzed compounds do not contain desulfated uronic acid residues, further investigations is required to ascertain whether the observed fragmentation pattern is due to the presence of the sulfate group in the iduronic acid, and this is currently being done by exploring heparin and heparan sulfate analytes containing desulfated uronic acid residues. Ongoing work using this approach on epimeric chondroitin and dermatan sulfate dp4-10 oligosaccharides containing GlcA and IdoA which are not sulfated indicate that $^{2,4}A_n$ fragment often appears exclusively in GlcA and is absent in IdoA residues indicating that it may be useful in assigning the uronic acid stereochemistry in those kinds of GAGs (Chapter 5).

The octasulfated hexasaccharide (ΔUA2S-GlcNS6S-IdoA2S-GlcNS6S-GlcA-GlcNS6S) was examined by this method, and its CID spectrum is shown in Figure 4.2. The mass spectrum obtained from this compound contained charge states 3-, 4-, 5-, and 6- as can be seen in the Appendix B. Like the tetrasaccharides, the precursor-ion selected for analysis, $[M-11H+7Na]^{4-}$, had all eleven acidic groups deprotonated. The fragment-ions $[^{2,4}A_6+7Na]^{2-}$, $[^{0,2}A_6+7Na]^{3-}$ and its water loss are found to produce the three most intense peaks in this spectra, similar to the tetrasaccharide in Figure 4.3.

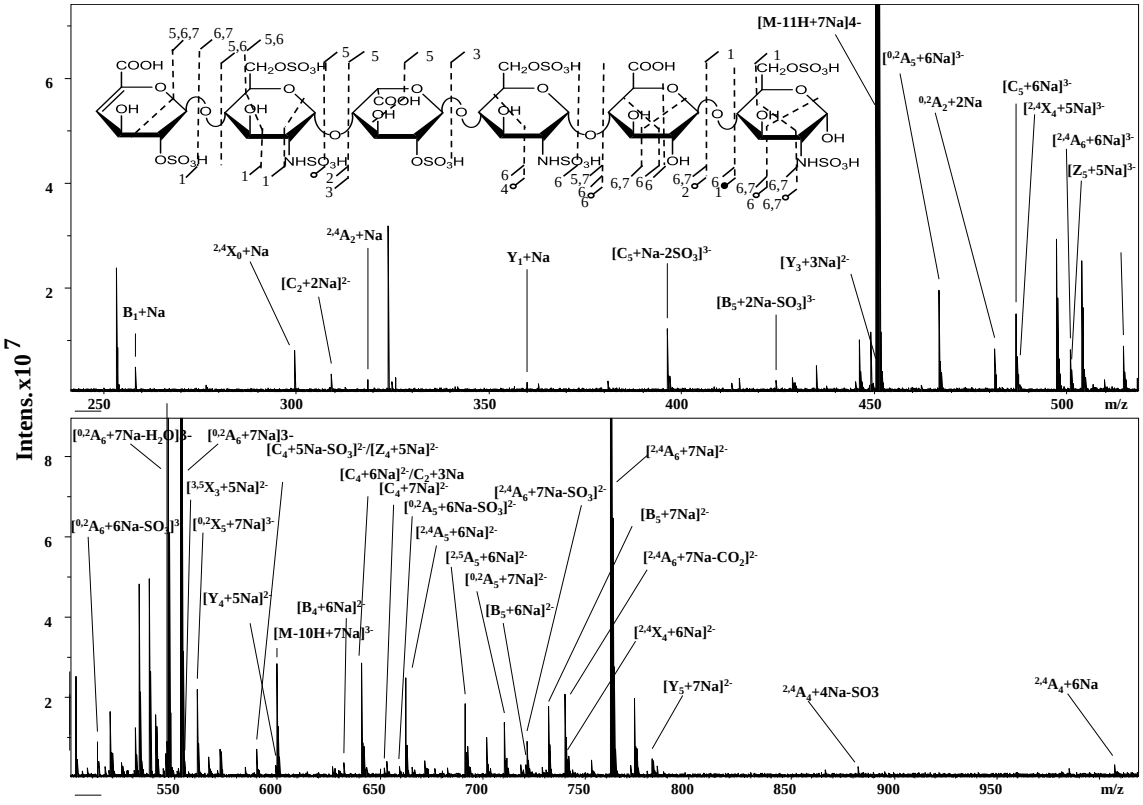

Figure 4.4. CID spectrum of the precursor $[M-11H+Na]^{4-}$ for the hexamer with 8 sulfate and 3 carboxylate groups. All the acidic groups in this precursor are ionized and the annotated structure is shown in the inset. Abundant glycosidic and cross-ring cleavages enable the location of the sulfate modifications in the structure.

Despite the density of the sulfates per disaccharide (2.7), total ion current of SO_3 loss fragments resulting from the CID of this fully deprotonated precursor was less than 2 % of the total ion abundance excluding the precursor intensity, Table 4.1. As it can be seen from Figure 4.4, there are more X, Y, and Z fragments on the non-reducing side of the molecule and more A, B, and C fragments on the reducing end side, while the middle residues of the molecule exhibit only a few fragments. However, the abundant glycosidic and cross-ring fragment-ions obtained unambiguously locate all the sulfo groups in the compound except for the one in the iduronic acid (third residue from the non-reducing

end). This modification could be located using a different precursor $[M-11H+6Na]^{5-}$ (data not shown).

The undecasulfated octasaccharide (ΔUA2S-GlcNS6S-IdoA2S-GlcNS6S-IdoA2S-GlcNS6S-GlcA-GlcNS6S) was successfully characterized by this method, Figure 4.5. There are 11 sulfo and 4 carboxyl groups in this octasaccharide, corresponding to fifteen ionizable protons.

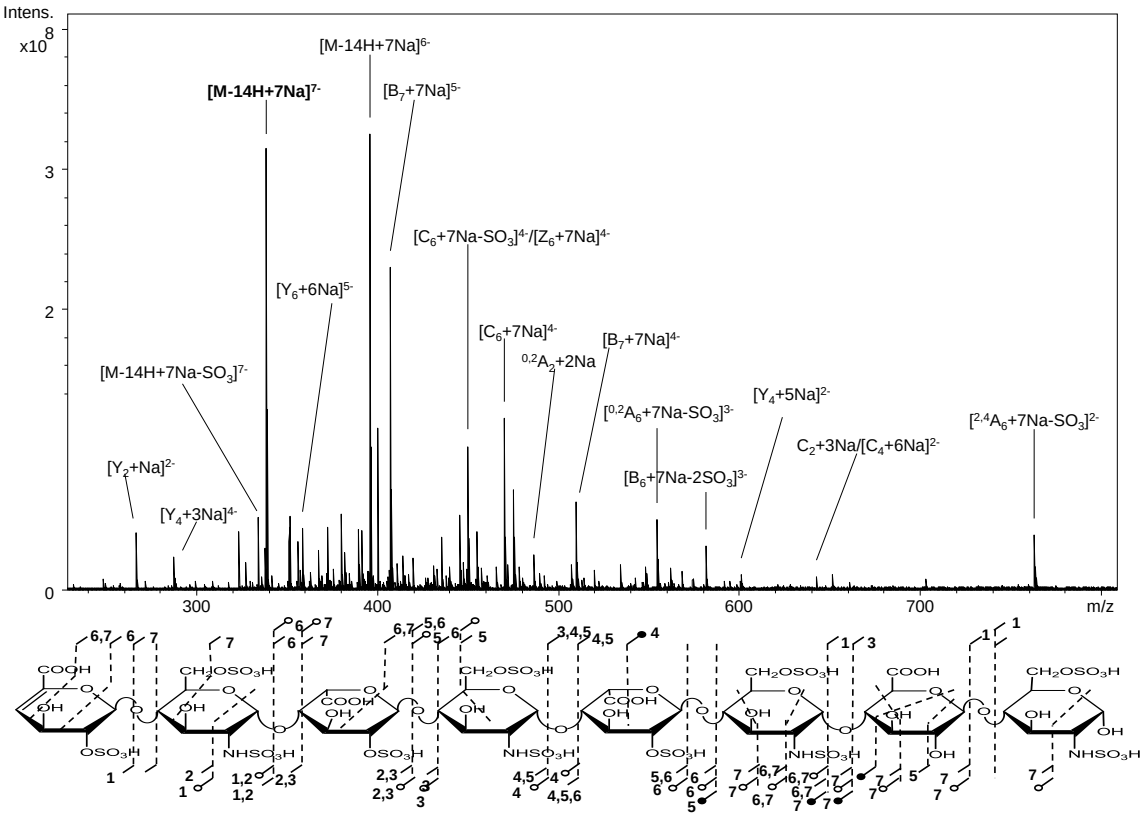

Figure 4.5. CID spectrum for an octamer with 11 sulfates. The precursor [M-14H+Na]7- used had only one acidic group uncharged. Due to the density of ions formed, only the most intense fragments are annotated. Full assignment of all the fragments is placed in the supporting information. The annotated structure showing the fragments obtained is located below the spectrum.

The $[M-14H+7Na]^{7-}$ ion with a single protonated acidic group was analyzed by MS/MS. Multiple molecular ions for charge states 4-, 5-, 6- and 7- were observed in the mass spectrum of this compound. Use of 2 mM NaOH for this long and densely sulfated oligomer led to the reduction of less sulfated molecular ions leaving only highly sodiated ones. The mass spectrum and the expanded regions of the precursor ion used for CID analysis can be obtained from the Appendix B. An interesting observation made during the application of this approach for highly sulfated compounds is that it gets harder to get fully deprotonated molecular ions at higher charge states. For this dp8, there was no fully deprotonated molecular ion $[M-15H+8Na]^{7-}$ observed in the MS spectrum but other fully deprotonated precursor ions appeared in all other charge states with increasing intensity as the charge state decreased. This observation was also partly true for the dp4 and dp 6 compounds analyzed as can be seen in the supporting materials.

The three most intense fragments observed in the tetrasaccharide and hexasaccharide samples above were absent or of low intensity. The reducing end $^{0,2}A_8$ fragment was observed but in low intensity and there was no $^{2,4}A_8$ product ion observed an indication that presence of a free acidic proton within the ion has a profound effect on the fragments observed at the reducing end residue especially the $^{2,4}A_n$ fragments. Increased loss of SO_3 was observed accounting for 23% of the total ion abundance, Table 4.1. We believe that the mobile acidic proton as well as the density of the sulfates (2.8 sulfates per disaccharide) within this dp 8 oligomer has a substantive contribution to the observed increase in SO_3 loss. Despite this increase SO_3 loss, the product yield was high (56%) and there were sufficient glycosidic and cross-ring fragments to locate all the sulfo groups except the one on the reducing end residue, which was established after

fragmenting the fully deprotonated precursor $[M-15H+9Na]^{6-}$, and one in the iduronic acid residue (4^{th} from the non-reducing end). As observed in those other heparin oligosaccharides analyzed above, the charge reduced precursor $[M-13H+7Na]^{6-}$ was present in high abundance in the CID spectra of the analyzed precursor.

Chemo-enzymatically Synthesized GAGs

Part of the challenge in structural elucidation of highly sulfated GAGs using mass spectrometry is lack of structurally defined oligosaccharides. A complementary method to chemical synthesis that generates well defined HS structures is the use of regioselective HS biosynthetic enzymes to synthesize structurally defined sulfated oligosaccharides. Tandem mass spectrometry of these compounds can help to build a library of well-defined fragments from specified structures that can be useful in identifying unknowns. This work shows the analysis of this type of oligosaccharide using CID and the result establish the capability of this approach to locate the sites of sulfo group substitution in most oligosaccharides.

Figure 4 shows the chemoenzymatically synthesized heptasaccharide, GlcNAc6S-GlcA-GlcNS3S6S-IdoA2S-GlcNS6S-GlcA-AnMan, with 7 sulfo groups and 3 carboxyl groups. This molecule is similar in structure to the drug, Arixtra®, examined recently using this approach [46]. The differences in structure from the chemoenzymatically produced compound are that the first two residues from the reducing end are replaced by a methyl group in Arixtra®, and the non-reducing end residue contains an N-sulfo group in Arixtra®, but an *N*-acetyl group in the chemoenzymatically prepared compound.

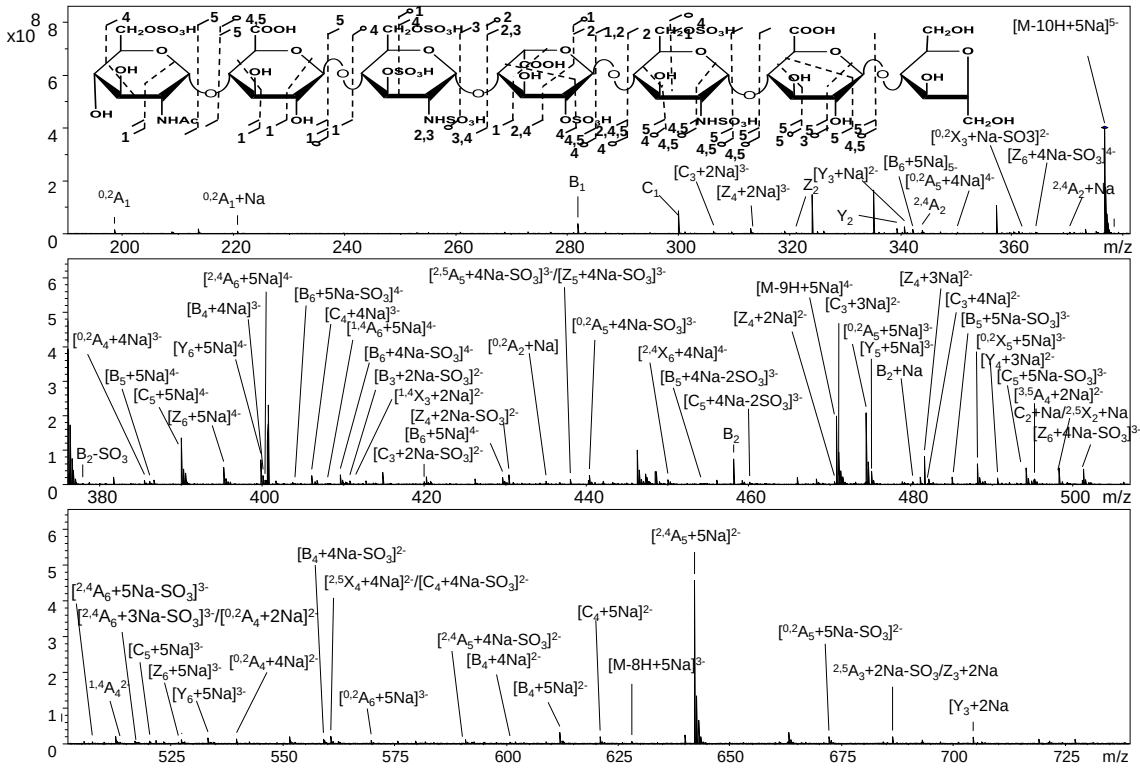

Figure 4.6. CID Spectrum of heparin heptasaccharide precursor $[M-10H+5Na]^{5-}$ with all the acidic groups deprotonated. Abundant glycosidic and cross-ring cleavages produced enable locate all the sites of sulfation. Inset is the annotated structure showing the obtained fragments.

The spectrum obtained from a fully deprotonated molecular-ion $[M-10H+5Na]^{5-}$ produced abundant glycosidic and cross-ring fragments that are able to locate all the sulfo groups in the molecule including the trisulfated saccharide residue (3rd from the non-reducing end). Since there are only three possible sulfo group locations in this residue, the mass-difference from glycosidic bond fragments Y_5 and Y_4 provides sufficient information to locate them. 15% of the product ions intensity was due to SO_3 loss. This is understandable considering the density of the SO_3 per disaccharide which is 2 and the presence of a trisulfated amino sugar within the chain, Table 4.1.

The presence of 3-O-sulfation in the trisulfated residue seems to affect its fragmentation patterns. Unlike most of the other amino sugar residues, $^{0,2}A$ and $^{2,4}A$ fragments are absent in the trisulfated sugar residue in the obtained CID spectra of this heptasaccharide and similar behavior was apparent during the analysis of Arixtra® which also contains a trisulfated amino residue. Researchers have postulated earlier that, a C_n glycosidic fragment can undergo further fragmentation to form $^{0,2}A$ ion which can in turn lead to the formation of $^{2,4}A$ ion within 1-4 linked glycans [52, 53]. The fragmentation mechanism for the formation of $^{0,2}A$ ion requires the 3-O hydrogen in the sugar ring [30] and since the 3-O hydrogen is substituted with SO_3 group within the trisulfated residue this fragmentation pathway may be less favored. As noted earlier, $^{2,4}A_n$ fragments are common in glucuronic acid residues and extremely rare in 2-O-sulfated iduronic acid monosaccharides. There are two glucuronic acid residues, and one 2-O-sulfated iduronic acid residue present in this oligosaccharide. The $^{2,4}A_n$ fragments are only present in the two glucuronic acid residues and none on the 2-O-sulfated iduronic acid residue.

The tandem mass spectrum of a chemoenzymatically produced decasaccharide with 8 sulfo groups (GlcA-(GlcNS6S-GlcA)$_4$-AnMan) is shown in Figure 4.7. Molecular ions having charge state 5-, 6- and 7- were obtained in the mass spectrum for this compound and molecular ion $[M-13H+7Na]^{6-}$ was used for CID analysis (Appendix B).

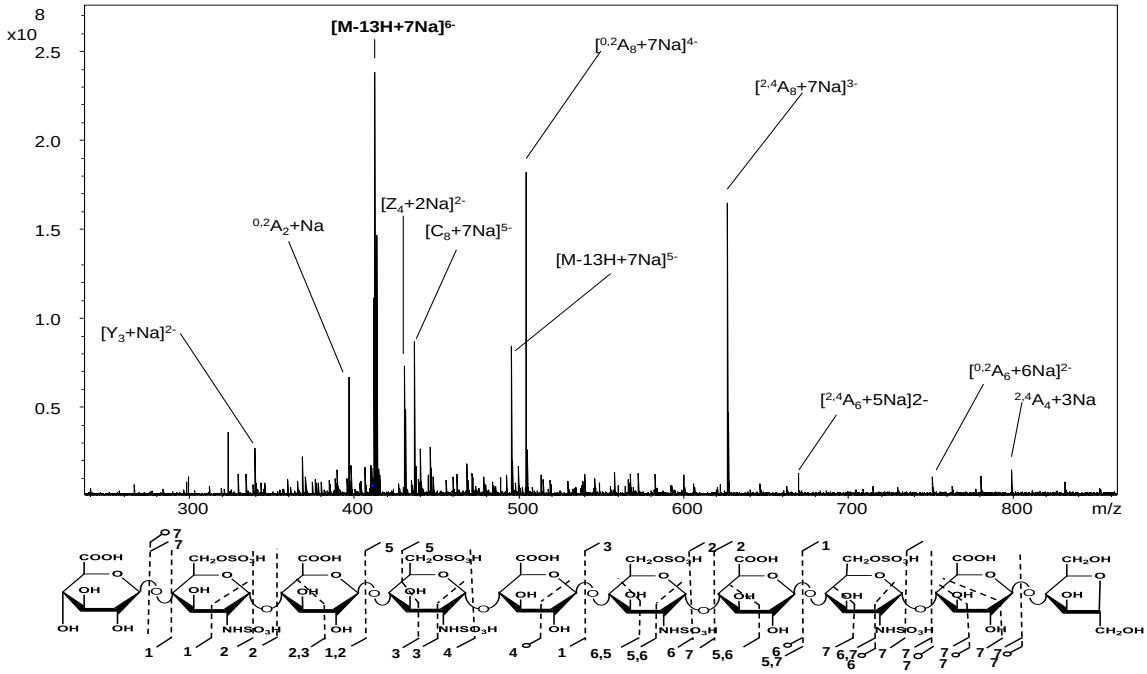

Figure 4.7. Shows $[M-13H+7Na]^{6-}$ CID spectrum and the annotated structure for highly sulfated HS decasaccharide. Only the most intense fragments are annotated but all the ion assignments can be found in the supporting materials. Below the spectrum is the annotated structure showing the fragments obtained.

All the sulfo groups in the decasaccharide can be unambiguously located except the one on the 2nd residue from the non-reducing end. Due to the large number of fragments obtained, only the most intense ones are annotated in the figure, but the entire annotations for this analyte can be found in the supporting materials. There are very few C and Z ions in the spectrum as compared to the B and Y ions. This is somewhat different for the highly sulfated oligosaccharides obtained from natural sources as discussed above. The most intense fragment ions from fully deprotonated molecular ions for the naturally occurring compounds analyzed here are the ^{0,2}A and ^{2,4}A ions, the same type of ions appear to dominate this spectrum and the one for dp 7 (discussed above) but this time they appear in the disulfated amino sugar, 3rd residue from the reducing end of

these molecules. One characteristic for these intense daughter ions for all the samples tested using this method is that they appear when a fully deprotonated precursor is fragmented and these daughter ions themselves contain fully deprotonated acidic groups. The result obtained for the dodecasaccharide with 10 sulfo groups (GlcA-(GlcNS6S-GlcA)$_5$-AnMan), whose MS/MS spectrum and annotated peak list are found in the supporting materials is similar to that of dp10 discussed above. Most of the sulfo groups were located after fragmenting the full deprotonated precursor, $[M-16H+9Na]^{7-}$. The fragmentation due to the SO_3 loss for the dp10-8S and dp12-10S accounted for 11 and 14% respectively, Table 4.1. This is consistent with the number of sulfate groups in the analyzed chain with the one with more SO_3 loss observed for the more highly sulfated oligomer.

Figure 6 shows a CID spectrum acquired from a fully deprotonated precursor-ion, $[M-11H+4Na]^{7-}$, of dodecasaccharide (GlcA-(GlcNS-GlcA)$_5$-AnMan) with 5 sulfo groups. In the MS spectra charge states 4-, 5-, 6-, and 7- were observed (Appendix B). Although only the most abundant fragment-ions are annotated in the figure, most of the low intensity fragments could be assigned, as can be seen in the inset, representing an expansion of the region m/z 460-500. All other annotations from this compound are listed in the supporting materials. It is noteworthy that the product yield was high (62%) and the most intense fragments were either glycosidic or cross-ring fragments and not fragments-ions resulting from SO_3 loss, which accounted for only 7% of the total product ion intensity. All the sulfo groups were located unambiguously.

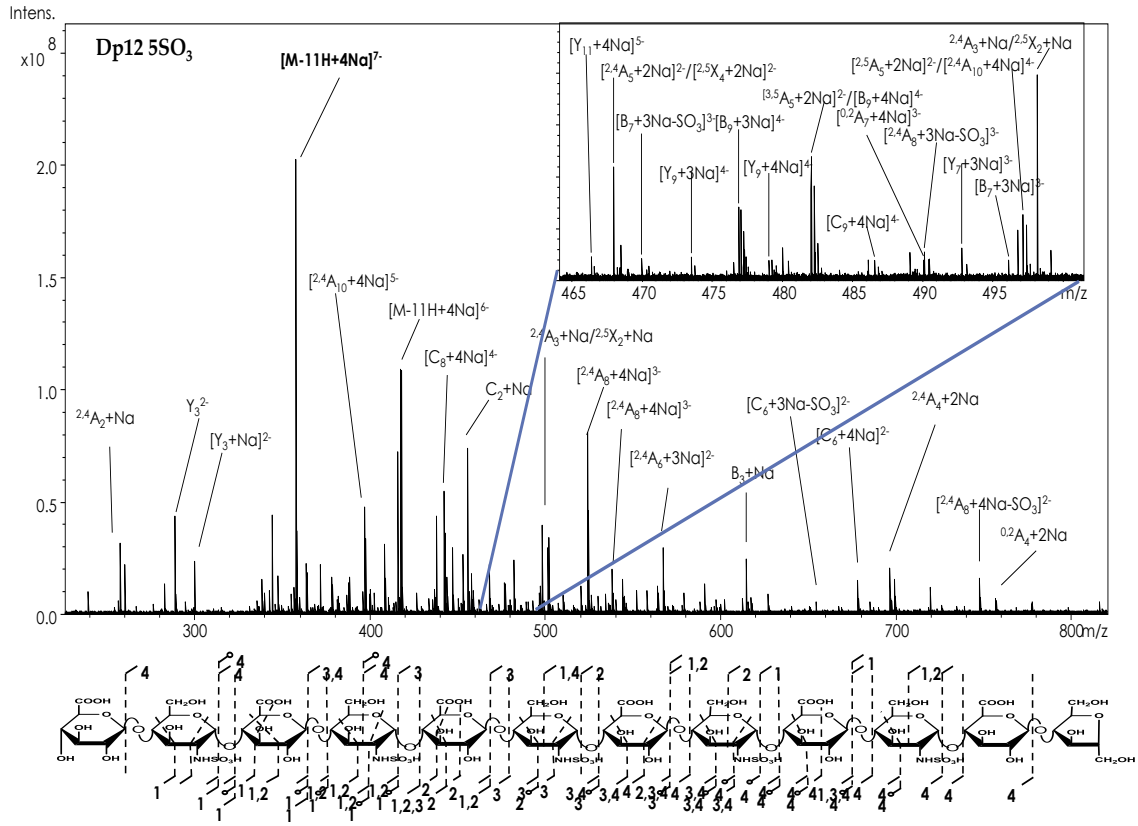

Figure 4.8. The CID spectrum of chemo-enzymatically produced dodecasaccharide precursor $[M-11H+4Na]^{7-}$ With the insert showing a small zoomed in region of the spectrum with the annotations. Only the intense peaks are annotated but all fragment assignments for this analyte can be found in the supporting materials.

The annotated structures for a decasaccharide (GlcA-(GlcNS-GlcA)$_4$-AnMan) and an undecasaccharide ((GlcNS-GlcA)$_5$-AnMan) with 4 and 5 sulfo groups respectively are shown in Figure 4.9. A fully deprotonated precursor was used to obtain the data that assigned the sulfo group positions for dp 10. Due to a low density of fragments obtained from the fully deprotonated precursor for dp11 (data not shown), a precursor with one protonated acidic group was used. A large number of both glycosidic and cross-ring fragments enabled the assignment of the location of all the sulfo groups for the

decasaccharide structure except the sulfo group in second residue from the non-reducing end, which can be easily identified after fragmenting a singly protonated acidic group precursor for the same charge state. The sites of sulfo group substitution in the dp 11 were all located except the one at the non-reducing end. Just like the more highly sulfated chemoenzymatically synthesized GAGs studied above, there were very few C and Z ions observed in these spectra. As expected, the less sulfated chemoenzymatically GAGs (0.8-0.9 sulfates/ disaccharide) had very low levels of SO_3 loss (6-7 %) and the level is half of that observe for the same length, but higher sulfated, counterparts (1.6-1.7 SO_3/disaccharide). The presence of a free acidic proton in the dp11 with 5 sulfates did not seem to affect this level as much as observed in the highly sulfated naturally produced GAGs, Table 4.1. Additionally, the product yield for the less sulfated chemo enzymatically produced compounds (62-63%) was higher than the highly sulfated counterparts (41-50%) partly due to relatively higher number of fragments that could not be assigned.

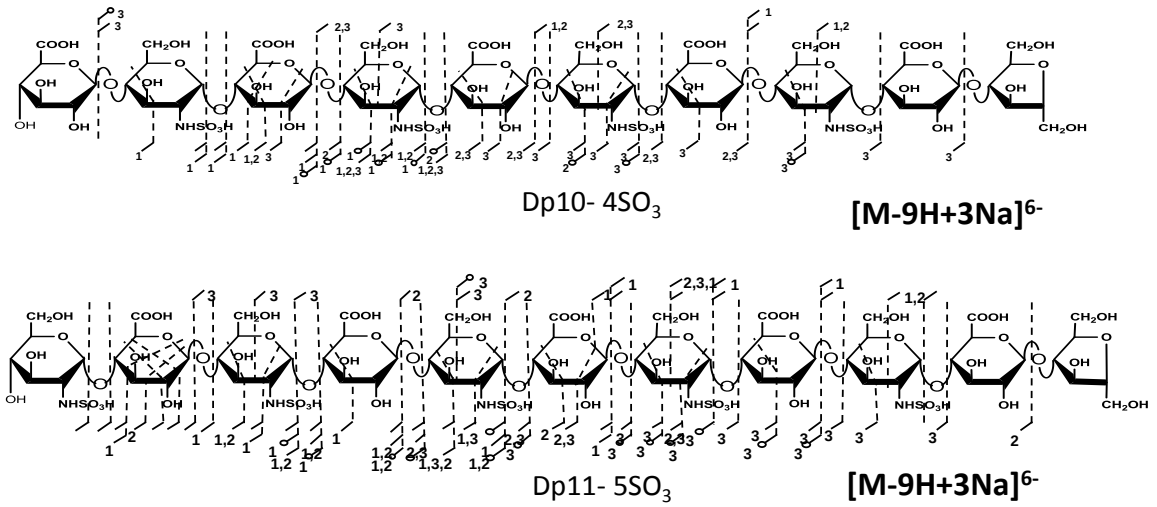

Figure 4.9. Shows the annotated structures for dp10 and 11 with 4 and 5 sulfates respectively, showing the fragments obtained from the tandem mass spectrometry experiments. The spectra for these compounds are placed in the supporting materials.

There were no cross-ring fragments obtained within the reducing end (AnMan) and the non-reducing end, as observed for all the chemo-enzymatically produced oligosaccharides. This could be due to the type of the residues in both the reducing end and the non-reducing end of these molecules. Unlike the chemo-enzymatically produced GAGs used in this work, the naturally occurring heparin oligosaccharides analyzed contains Δ^{4-5} –unsaturated uronic acid at the non-reducing end which promotes the formation of $^{0,2}X$ through the well-established retro-Diels Alder rearrangement of the non-reducing end [30]. The $^{0,2}X$ is within the non-reducing end residue is observed in all the naturally occurring heparin oligosaccharides analyzed (Figures 4.3-4.6) and not in any of the chemo-enzymatically ones (Figures 4.7-4.9). The disappearance of reducing end fragments observed in the naturally occurring heparins (Figure 4.3-4.6) within all the chemo-enzymatically produced GAGs (Figure 4.7-4.9) tested using this approach may be

due to lack of terminal aldehyde which could promote the formation of ^{0,2}A fragment through the retro-aldo rearrangement of the reducing end as noted above.

CONCLUSIONS

While mass spectral analysis is widely used in proteomics, the mass spectrometric analysis of sulfated oligosaccharides has proven much more challenging, slowing the development of glycomics. This work demonstrates that under proper spray conditions, and with selection of the proper precursor, MS/MS using CID will yield a complete set of cross-ring and glycosidic fragment-ions, which enables the characterization of highly sulfated Hp and HS oligosaccharides. The method is equally efficient for undersulfated and highly sulfated oligosaccharides as well as short and long Hp and HS chains. Useful structural information is produced when all the acidic groups are either deprotonated, or undergo Na^+/H^+ exchange. Previous MS/MS studies on Hp and HS suggested that the charge state should be equal or slightly more than the number of sulfo groups [21]. This normally works well for shorter or more sparsely sulfated GAGs (zero to two sulfo groups per disaccharide subunit) but fails for highly sulfated GAGs (two to three sulfo groups per disaccharide subunit). Although other work had suggested use of ammonium acetate to improve upon Na^+ cationization, we find a substantial advantage from the addition of 1-2 mM NaOH to the spray solution, specifically the elimination of other interfering metal adducts, improving isolation and producing cleaner, easier to assign, fragmentation spectra.

There is a difference between these results and those obtained previously with Ca^{2+} cationization, for which there were fewer useful fragments obtained for metal adducted highly sulfated GAGs [25]. In this previous study, Ca^{2+} adduction gave an

improvement in the production of structurally significant product ions compared to those from precursors lacking metal cations. However, the precursors in prior studies were not exhaustively deprotonated. In all the compounds studied in this work, the precursor ions used had all acidic groups deprotonated or with one proton present. In most cases, a single precursor provides all the structural information (monosaccharide composition and the sites of sulfo group substitutions) but in few cases, a combination of assignments from fully deprotonated and from a singly protonated acidic group provide the full structural characterization. The work here demonstrates that this approach, recently demonstrated in our laboratory for the pentasaccharide drug, Arixtra® [46] is generally applicable to Hp and HS oligomers of a broad range of lengths and degrees of sulfation.

ACNOWLEDGEMENTS

The authors gratefully acknowledge financial support from the National Institutes of Health grant #2R01-GM038060-20.

REFERENCES

1. Capila, I. and Linhardt, R. J., Heparin–Protein Interactions. *Angew. Chem. Int. Ed.* **2002**, 41, 390-412.
2. Benito, C., Structure and Biological Activity of Heparin; In Adv. Carbohydr. Chem. Biochem.;R. S. Tipson and H. Derek; Academic Press: **1985**; pp. 51-134
3. Ampofo, S. A.; Wang, H. M. and Linhardt, R. J., Disaccharide compositional analysis of heparin and heparan sulfate using capillary zone electrophoresis. *Anal. Biochem.* **1991**, 199, 249-255.
4. Velve-Casquillas, G.; Le Berre, M.; Piel, M. and Tran, P. T., Microfluidic tools for cell biological research. *Nano Today.* **2010**, 5, 28-47.
5. Chi, L.; Amster, J. and Linhardt, R. J., Mass Spectrometry for the Analysis of Highly Charged Sulfated Carbohydrates. *Curr. Anal. Chem.* **2005**, 1, 223-240.
6. Conrad H E. 1998. Heparin-binding proteins, San Diego: Academic
7. Vanboeckel, C. A. A. and Petitou, M., The Unique Antithrombin-III Binding Domain of Heparin - a Lead to New Synthetic Antithrombotics. *Angew. Chem. Int. Edit.* **1993**, 32, 1671-1690.
8. Petitou, M.; Mourey, L.; Samama, J. P. and Pascal, M., Molecular Interaction of Synthetic Oligosaccharides with Antithrombin-III. *J. Cell. Biochem.* **1993**, 369-369.
9. Hess, G., Congress investigates tainted heparin. *Chem. Eng. News.* **2008**, 86, 8-8.
10. Kemsley, J., Heparin undone. *Chem. Eng. News.* **2008**, 86, 38-40.

11. Liu, H.; Zhang, Z. and Linhardt, R. J., Lessons learned from the contamination of heparin. *Nat. Prod. Rep.* **2009**, 26,

12. Yang, B.; Solakyildirim, K.; Chang, Y. and Linhardt, R., Hyphenated techniques for the analysis of heparin and heparan sulfate. *Anal. Bioanal. Chem.* **2010**, 1-17.

13. Wolff, J. J.; Amster, I. J.; Chi, L. and Linhardt, R. J., Electron Detachment Dissociation of Glycosaminoglycan Tetrasaccharides. *J. Am. Soc. Mass. Spectrom.* **2007**, 18, 234-244.

14. Wolff, J. J.; Chi, L.; Linhardt, R. J. and Amster, I. J., Distinguishing Glucuronic from Iduronic Acid in Glycosaminoglycan Tetrasaccharides by Using Electron Detachment Dissociation. *Anal. Chem.* **2007**, 79, 2015-2022.

15. Leach III, F. E.; Wolff, J. J.; Laremore, T. N.; Linhardt, R. J. and Amster, I. J., Evaluation of the experimental parameters which control electron detachment dissociation, and their effect on the fragmentation efficiency of glycosaminoglycan carbohydrates. *Int. J. Mass Spectrom.* **2008**, 276, 110-115.

16. Wolff, J. J.; Laremore, T. N.; Aslam, H.; Linhardt, R. J. and Amster, I. J., Electron-Induced Dissociation of Glycosaminoglycan Tetrasaccharides. *J. Am. Soc. Mass. Spectrom.* **2008**, 19, 1449-1458.

17. Wolff, J. J.; Laremore, T. N.; Busch, A. M.; Linhardt, R. J. and Amster, I. J., Influence of Charge State and Sodium Cationization on the Electron Detachment Dissociation and Infrared Multiphoton Dissociation of Glycosaminoglycan Oligosaccharides. *J. Am. Soc. Mass. Spectrom.* **2008**, 19, 790-798.

18. Wolff, J. J.; Laremore, T. N.; Busch, A. M.; Linhardt, R. J. and Amster, I. J., Electron Detachment Dissociation of Dermatan Sulfate Oligosaccharides. *J. Am. Soc. Mass. Spectrom.* **2008**, 19, 294-304.

19. Wolff, J. J.; Leach, F. E.; Laremore, T. N.; Kaplan, D. A.; Easterling, M. L.; Linhardt, R. J. and Amster, I. J., Negative Electron Transfer Dissociation of Glycosaminoglycans. *Anal. Chem.* **2010**, 82, 3460-3466.

20. Leach, F. E.; Wolff, J. J.; Xiao, Z.; Ly, M.; Laremore, T. N.; Arungundram, S.; Al-Mafraji, K.; Venot, A.; Boons, G.-J.; Linhardt, R. J. and Amster, I. J. Negative electron transfer dissociation Fourier transform mass spectrometry of glycosaminoglycan carbohydrates. *Eur. J. Mass Spectrom.* **2011**, 17, 167.

21. Leach III, F. E.; Xiao, Z.; Laremore, T. N.; Linhardt, R. J. and Amster, I. J., Electron detachment dissociation and infrared multiphoton dissociation of heparin tetrasaccharides. *Int. J. Mass Spectrom.* **2011**, 308, 253-259.

22. Oh, H.; Leach, F.; Arungundram, S.; Al-Mafraji, K.; Venot, A.; Boons, G.-J. and Amster, I., Multivariate Analysis of Electron Detachment Dissociation and Infrared Multiphoton Dissociation Mass Spectra of Heparan Sulfate Tetrasaccharides Differing Only in Hexuronic acid Stereochemistry. *J. Am. Soc. Mass. Spectrom.* **2011**, 22, 582-590.

23. Zaia, J.; McClellan, J. E. and Costello, C. E., Tandem Mass Spectrometric Determination of the 4S/6S Sulfation Sequence in Chondroitin Sulfate Oligosaccharides. *Anal. Chem.* **2001**, 73, 6030-6039.

24. McClellan, J. E.; Costello, C. E.; O'Conno, P. B. and Zaia, J., Influence of Charge State on Product Ion Mass Spectra and the Determination of 4S/6S Sulfation

Sequence of Chondroitin Sulfate Oligosaccharides. *Anal. Chem.* **2002**, 74, 3760-3771.

25. Zaia, J. and Costello, C. E., Tandem Mass Spectrometry of Sulfated Heparin-Like Glycosaminoglycan Oligosaccharides. *Anal. Chem.* **2003**, 75, 2445-2455.

26. Zaia, J.; Li, X.; Chan, S. and Costello, C., Tandem mass spectrometric strategies for determination of sulfation positions and uronic acid epimerization in chondroitin sulfate oligosaccharides. *J. Am. Soc. Mass. Spectrom.* **2003**, 14, 1270-1281.

27. Naggar, E. F.; Costello, C. E. and Zaia, J., Competing fragmentation processes in tandem mass spectra of heparin-like glycosaminoglycans. *J. Am. Soc. Mass. Spectrom.* **2004**, 15, 1534-1544.

28. Miller, M. J. C.; Costello, C. E.; Malmström, A. and Zaia, J., A tandem mass spectrometric approach to determination of chondroitin/dermatan sulfate oligosaccharide glycoforms. *Glycobiology.* **2006**, 16, 502-513.

29. Bielik, A. M. and Zaia, J., Multistage Tandem Mass Spectrometry of Chondroitin Sulfate and Dermatan Sulfate. *Int. J. Mass Spectrom.* **2011**, 305, 131-137.

30. Saad, O. M. and Leary, J. A., Delineating mechanisms of dissociation for isomeric heparin disaccharides using isotope labeling and ion trap tandem mass spectrometry. *J. Am. Soc. Mass. Spectrom.* **2004**, 15, 1274-1286.

31. Saad, O. M. and Leary, J. A., Heparin Sequencing Using Enzymatic Digestion and ESI-MSn with HOST: A Heparin/HS Oligosaccharide Sequencing Tool. *Anal. Chem.* **2005**, 77, 5902-5911.

32. Ly, M.; Leach, F. E.; Laremore, T. N.; Toida, T.; Amster, I. J. and Linhardt, R. J., The proteoglycan bikunin has a defined sequence. *Nat. Chem. Biol.* **2011**, 7, 827-833.

33. Lohse, D. and Linhardt, R., Purification and characterization of heparin lyases from Flavobacterium heparinum. *J. Biol. Chem.* **1992**, 267, 24347-24355.

34. Conrad, H. E., Nitrous Acid Degradation of Glycosaminoglycans. *Curr. Protoc. Mol. Biol.* **2001**, 32:17.22.1–17.22.5.

35. Takagaki, K.; Kojima, K.; Majima, M.; Nakamura, T.; Kato, I. and Endo, M., Ion-Spray Mass-Spectrometric Analysis of Glycosaminoglycan Oligosaccharides. *Glycoconjugate J.* **1992**, 9, 174-179.

36. Jones, C. J.; Beni, S.; Limtiaco, J. F. K.; Langeslay, D. J. and Larive, C. K., Heparin Characterization: Challenges and Solutions. *Ann. Rev. Analyt. Chem.* **2011**, 4, 439-465.

37. Meissen, J.; Sweeney, M.; Girardi, M.; Lawrence, R.; Esko, J. and Leary, J., Differentiation of 3-O-sulfated heparin disaccharide isomers: Identification of structural aspects of the heparin CCL2 binding motif. *J. Am. Soc. Mass. Spectrom.* **2009**, 20, 652-657.

38. Orlando, R.; Allen Bush, C. and Fenselau, C., Structural analysis of oligosaccharides by tandem mass spectrometry: Collisional activation of sodium adduct ions. *Biol. Mass Spectrom.* **1990**, 19, 747-754.

39. Staempfli, A.; Zhou, Z. and Leary, J. A., Gas-phase dissociation mechanisms of dilithiated disaccharides: tandem mass spectrometry and semiempirical calculations. *J. Org. Chem.* **1992**, 57, 3590-3594.

40. Desaire, H. and Leary, J. A., The effects of coordination number and ligand size on the gas phase dissociation and stereochemical differentiation of cobalt-coordinated monosaccharides. *Int. J. Mass Spectrom.* **2001**, 209, 171-184.

41. Gaucher, S. P. and Leary, J. A., Determining anomericity of the glycosidic bond in Zn(II)-Diethylenetriamine-Disaccharide complexes using MSn in a quadrupole ion trap. *J. Am. Soc. Mass. Spectrom.* **1999**, 10, 269-272.

42. Harvey, D., Ionization and collision-induced fragmentation of N-linked and related carbohydrates using divalent cations. *J. Am. Soc. Mass. Spectrom.* **2001**, 12, 926-937.

43. Zhou, Z.; Ogden, S. and Leary, J. A., Linkage position determination in oligosaccharides: mass spectrometry (MS/MS) study of lithium-cationized carbohydrates. *J. Org. Chem.* **1990**, 55, 5444-5446.

44. Tissot, B.; Gasiunas, N.; Powell, A. K.; Ahmed, Y.; Zhi, Z.-l.; Haslam, S. M.; Morris, H. R.; Turnbull, J. E.; Gallagher, J. T. and Dell, A., Towards GAG glycomics: Analysis of highly sulfated heparins by MALDI-TOF mass spectrometry. *Glycobiology.* **2007**, 17, 972-982.

45. Zhang, Z. and Linhardt, R. J., Sequence Analysis of Native Oligosaccharides Using Negative ESI Tandem MS. *Curr. Anal. Chem.* **2009**, 5, 225-237.

46. Kailemia, M. J.; Li, L.; Ly, M.; Linhardt, R. J. and Amster, I. J., Complete mass spectral characterization of a synthetic ultralow-molecular-weight heparin using collision-induced dissociation. *Anal. Chem.* **2012**, 84, 5475-5478.

47. Xiao, Z.; Zhao, W.; Yang, B.; Zhang, Z.; Guan, H. and Linhardt, R. J., Heparinase 1 selectivity for the 3,6-di-O-sulfo-2-deoxy-2-sulfamido-α-D-glucopyranose (1,4)

2-O-sulfo-α-L-idopyranosyluronic acid (GlcNS3S6S-IdoA2S) linkages. *Glycobiology.* **2011**, 21, 13-22.

48. Liu, R.; Xu, Y.; Chen, M.; Weïwer, M.; Zhou, X.; Bridges, A. S.; DeAngelis, P. L.; Zhang, Q.; Linhardt, R. J. and Liu, J., Chemoenzymatic Design of Heparan Sulfate Oligosaccharides. *J. Biol. Chem.* **2010**, 285, 34240-34249.

49. Ceroni, A.; Maass, K.; Geyer, H.; Geyer, R.; Dell, A. and Haslam, S. M., GlycoWorkbench: A Tool for the Computer-Assisted Annotation of Mass Spectra of Glycans†. *J. Proteome Res.* **2008**, 7, 1650-1659.

50. Domon, B. and Costello, C. E., A Systematic Nomenclature for Carbohydrate Fragmentations in Fab-Ms Ms Spectra of Glycoconjugates. *Glycoconjugate J.* **1988**, 5, 397-409.

51. Hofmeister, G. E.; Zhou, Z. and Leary, J. A., Linkage position determination in lithium-cationized disaccharides: tandem mass spectrometry and semiempirical calculations. *J. Am. Chem. Soc.* **1991**, 113, 5964-5970.

52. Spengler, B.; Dolce, J. W. and Cotter, R. J., Infrared laser desorption mass spectrometry of oligosaccharides: fragmentation mechanisms and isomer analysis. *Anal. Chem.* **1990**, 62, 1731-1737.

53. Leymarie, N. and Zaia, J., Effective Use of Mass Spectrometry for Glycan and Glycopeptide Structural Analysis. *Anal. Chem.* **2012**, 84, 3040-3048.

CHAPTER 5

DIFFERENTIATING CHONDROITIN SULFATE GLYCOSAMINOGLYCANS USING CID URONIC ACID CROSS-RING DIAGNOSTIC FRAGMENTS IN A SINGLE STAGE OF MS/MS*

*Kailemia, M. J.; Patel, B. A.; Johnson, T. D.; Li, L.; Linhardt, R. J.; Amster, I. J. Differentiating Chondroitin Sulfate Glycosaminoglycans Using CID Uronic Acid Crossring Diagnostic Fragments in a Single Stage of MS/MS. To be submitted to *J. Am. Soc. Mass Spectrom.*

ABSTRACT

Stereochemistry of hexuronic acid residues of glycosaminoglycans (GAGs) structure is a key feature that determines their interactions with proteins and functions. Electron based tandem mass spectrometry methods especially electron detachment dissociation (EDD) have been able to differentiate between glucuronic (GlcA) and iduronic acid (IdoA) residues in heparan sulfate tetrasaccharides by producing epimeric unique fragments. Likewise, relative abundance of mostly glycosidic collision induced dissociation (CID) and EDD fragment ions have been shown to characterize hexuronic acid epimeric state of chondroitin sulfate (CS) GAGs. The present work examines the effect of charge state and the degree of sodium cationization on the CID fragmentation products for identifying glucuronic and iduronic acid containing CSA and DS chains. Interestingly, we find cross-ring fragments $^{2,4}A_n$ and $^{0,2}X_n$ formed within the hexuronic acid residues which in some cases are unique to a given CSA chain especially for long chains like dp8 and dp10. These diagnostic fragments are produced by specific molecular ions and they also have a particular charge state and sodium cationization characteristics. The identified ions with these characteristics displayed diagnostic properties for all the CS and DS chains (dp4-dp10) studied.

INTRODUCTION

Chondroitin sulfates (CS) are a class of GAGs responsible for various useful biological activities [1, 2]. During their biosynthesis enzymatic modifications take place on differentially elongated chains of CS thus producing highly heterogeneous products [3]. Unique sulfo-transferases place SO_3 modifications at various prior undefined positions of the disaccharide repeating unit especially in the amino sugar, while some of the GlcA residues are converted to IdoA residues in presence of C_5 epimerase enzymes. The extracted sample from natural sources is thus a mixture of different length of CS chains with different sets of modifications within these sequences. Differential SO_3 modifications and epimeric state of uronic acid leads to large number of compounds some having the same composition but differing in their structures.

CS can be divided into different sub-classes depending on the extent and positions of the sulfate modifications and the hexuronic acid C_5 stereochemistry. The basic repeating disaccharide unit of CS polysaccharides is N-acetyl-galactosamine (GalNAc) and a uronic acid (GlcA or IdoA). Chondroitin sulfate A (CSA) is O-sulfated at C_4 of GalNAc and the uronic acid is mainly GlcA while dermatan sulfate (CSB or DS) have the same composition as the CSA but most of the GlcA residues are epimerized to idoA [1, 4]. Chondroitin sulfate C (CSC) which is sulfated at the 6-O position and other forms CS with multiple SO_3 groups within the disaccharide unit including the ones with 2-O sulfation at the hexuronic acid also exists. Most single GAG chains can contain differentially modified disaccharide units with IdoA sometime appearing continuously within a given portion and intermittently in other portions of the intact chain [1, 5].

Structural identification of chondroitin sulfates at molecular level can have profound effects in medicine and could provide insight on structural motifs associated with protein binding and regulation which may lead to clinical applications [6]. Sulfation, epimerization, and extracellular matrix composition of CSA/DS have enormous effect on their binding activities: IdoA containing CSA/DS chains found in large amounts in some parts of the brain have been found to be critical in neuritogenesis during the brain development of mice and other organisms [7, 8]. DS is also implicated in connective tissue maintenance and embryonic development [9, 10] and has been found to induce antithrombotic effect by activating heparin cofactor II, a plasma protein which inhibits thrombin [9, 11]. Mutations in CSA/DS sulfotransferases lead to abnormal levels of CSA/DS in corneal tissue, causing macular corneal dystrophy [12]. CSA/DS chains play critical roles in the central nervous system, regulating both brain development and plasticity. Some pathogens use CS and DS to bind to host cells as well. Mutant CHO cells defective in CS cannot be bound by the malarial parasite *P. falciparum* [13]. Because of the many functions of GAGs like CSA/DS, most of them not mentioned here, their molecular structural elucidation and characterization in relation to protein binding can lead to important therapies.

Various analytical techniques including nuclear magnetic resonance (NMR) and mass spectrometry (MS) are being implemented in elucidating structures of GAGs including differentiation of hexuronic acid C_5 stereochemistry [14-16]. Low sample sizes obtained from complex GAGs extraction methods makes MS analysis more essential due to its high sensitivity. Presence of sufficient glycosidic and cross-ring fragments during tandem mass spectrometry provides detailed molecular level structural information of

GAGs. For the sulfated GAGs, unwanted neutral loss of sulfite (SO_3) is the most favorable mechanism pathway of fragmentation, leading to less informative MS/MS results but recent advancement in MS/MS methods has enabled more informative structural information from these biomolecules [15, 17-28]. Combination of glycosidic and cross-ring fragments enable the identification of the positions of the sulfo groups within the residue and in some cases the epimeric state of the hexuronic acid [13, 20, 22, 29-33]. Research has shown that epimerization of hexuronic acid and sulfate position along GalNAc residues can affect the number and the intensity of some glycosidic and cross-ring bond cleavages obtained in a given MS/MS experiment [20, 31, 32]. Thus, diagnostic ions that can distinguish differentially modified chains can be obtained.

CID is a novel approach for fragmentation; however, fragmentation through this technique often causes significant losses of labile SO_3 groups. SO_3 loss reduction could be accomplished through sufficient ionization of acidic groups through charge or metal cation/hydrogen ion exchanges [28, 30, 33]. CID has been used in the past to sequence intact chains of chondroitin sulfate from Bikunin proteoglycan [34]. Different conformers could be identified through the intensity of the glycosidic fragments obtained from CID spectra. Relative abundance of B, X and Y CID ions have been previously used for the characterization of hexuronic acid epimeric state of chondroitin sulfate (CS) GAGs.[31, 32, 35, 36] Recently, relative abundance of MS^n B and Y fragment ions was used to distinguish between CSA and DS [18].

Electron based ion activation methods are promising tandem mass spectrometry techniques for both determination of sulfate locations and the epimeric state of GAGs molecules [22, 29, 30]. EDD produces relatively high number of useful product ions with

minimal loss in SO_3 and it has been found to produce unique fragment ions that can distinguish between GlcA and IdoA in heparan sulfate tetrasaccharides [20]. EDD, electron induced dissociation (EID) and negative electron transfer dissociation (NETD) combined with multivariate analysis have also been applied in distinguishing chondroitin and dermatan sulfate GAGs in the past [37]. The effect of EDD fragmentation method for DS different chain length and also with increase in sodiation level has been investigated [22, 29, 30]. The mass difference between cross-ring fragments $^{0,2}A$ and $^{2,4}A$ fragments for N-glycan reducing end residue can be used to distinguish core-fucosylated (mass difference 206 Da) and the ones that are not (60 Da) [38]. $^{0,2}A_n$ fragments at the reducing end can also be combined with ions like B and Y for structural identification [39].

Most of the previous work investigated molecular ions in which the number of ionized acidic species was equal to the number of sulfate groups within the molecules [23, 35]. In most instances, CID of these precursor ions do not produce large number of cross-ring cleavages. Recently, we have shown that ionizing all the acidic groups within highly sulfated GAGs lead to more useful daughter ions including cross-ring fragments [17, 28]. In such cases, higher number of cross-ring fragments is obtained. This work investigates cross-ring fragment ions formed during this process. We find that CID of molecular ions of CSA and DS with a single free proton produces abundant glycosidic and cross-ring fragments (in hexuronic acid residues) ions. These cross-ring daughter ions were found to be useful in distinguishing GlcA and IdoA residues on a single MS/MS step. Release of these ions depends on the precursor charge state and the number of ionized species within the GAG chain.

METHODS

CSA and DS Preparation

CSA and DS oligosaccharides were independently prepared by partial enzymatic depolymerization. CSA was depolymerized from bovine trachea chondroitin sulfate A (Celsus Laboratories, Cincinnati, OH) while DS used in this work originated from porcine intestinal mucosa dermatan sulfate (Celsus Laboratories, Cincinnati, OH). Chondroitin ABC lyase from *proteus vulgaris*, EC 4.2.2.4 (Seikagaku, Japan) was used to incubate 20 mg/mL solution of each sample in 50 mM Tris HCL/60 mM sodium acetate buffer, pH 8 at 37^{o} C. When the UV absorbance at 232 nm indicated 50% complete, the digestion mixture was heated for 3 min at 100^{o} C. Ultra-filtration was carried out using a 5000 MWCO membrane to remove the enzyme and the high-molecular-weight oligosaccharide. Concentrate the remaining oligosaccharide mixture, rotary evaporation was used and then fractionated by low pressure GPC on a Bio-Gen p10 (Bio-Rad, Richmond, CA) column. The oligosaccharide fractions were desalted by GPC on a Bio-Gel P2 column and freeze dried [40]. Strong anion exchange high-pressure liquid chromatography (SAX-HPLC) on an semi-preparative SAX S5 Spherisorb column (Waters Corp, Milford, MA) was used for further purification of the oligosaccharides. The resulting SAX-HPLC with over 90% oligosaccharides fractions were collected, desalted by GPC and then freeze-died. The dried solid was reconstituted in water and purified one more time using SAX-HPLC. Only the oligosaccharides within the top 30% of the chromatogram peak was collected, desalted and freeze-dried. Oligomer concentration in the solution was determined by measuring the absorbance at 232 nm ($e=3800\ M^{-1}\ cm^{-1}$). The final oligosaccharide fractions were characterized by PAGE,

ESI-MS, and high-field NMR spectroscopy [41]. The general structures for the molecules used are shown in Figure 5.1.

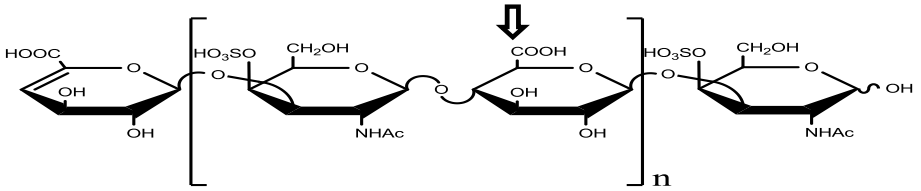

Chondroitin sulfate (CSA)

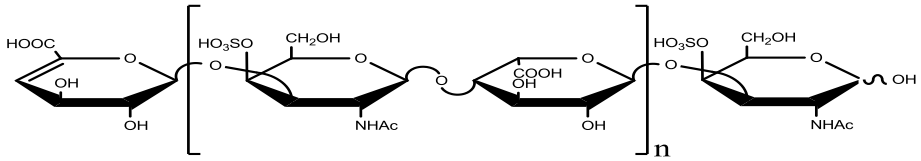

Dermatan sulfate (DS)

Figure 5.1. The general structure for the CSA and DS oligosaccharides studied. The value of n for the molecules analyzed is 1, 2, 3 and 4 for dp4, 6, 8, and 10 respectively.

Mass Spectrometry Analysis

The experiments were carried out using a 9.4 Bruker Apex Ultra Qh-FTICR instrument (Billerica, MA) operating in negative polarity source conditions. Metal capillary (G2427A, Agilent Technologies, Santa Clara, CA) was used to introduce the samples to the MS. The sample concentrations was 0.05-0.1mg/mL in 50:50, MeOH:H_2O and CSA and DS of different length were introduced individually at the rate of 2 uL/min. Between 0.5-1.0 mM NaOH in the spray solution was used to vary the degree of sodiation of the analytes and varying the degree of ionization. Ions of interest were isolated in a mass selective quadrupole using 3 Da isolation window and CID experiments of CSA/DS dp4-dp10 molecular ions with different level of Na^+/H^+ exchange were performed in the collision cell external to the high magnetic field region. The intensity of the precursor ion was maintained above the fragment ions during CID

experiments. The fragment ions were assigned using high resolution accurate mass measurement assisted with glycoworkbench software [42]. Wolff et al annotation [22] derived from Domon and Costello nomenclature [43] was used to show the identified product ions.

PCA Analysis

The statistical method used to visualize the differences between the epimeric compounds spectra is PLS toolbox (Eigenvector Research, Inc., Wenatchee, WA, USA). Five spectra were obtained for each CS and DS oligosaccharide and ion assignment was carried out and the intensity of at least 40 of the assigned fragment ions was used for PCA analysis. Before the PCA analysis, the intensity of the ions was normalized using the base peak of the background spectrum of each respective oligosaccharide chain. PCA analysis matrix was created in an excel spreadsheet with each sample spectrum represented in a row while the intensity of the particular ions was entered in a given column. The data was mean-centered and cross-validated during the PCA analysis.

RESULTS AND DISCUSSION

The only difference between CSA and DS GAGs is the stereochemistry of hexuronic acid residues which plays a key role in their biological functions. Although considerable mass spectrometry work has been done to distinguish CSA and DS stereoisomers using tandem mass spectrometry, most of published work on these biomolecules investigated molecular ions with the number of ionized acidic groups equal to the number of sulfate groups within the chains. These molecular ions are isobaric for different length of the CSA/DS chains due to the symmetric nature of the CSA and DS oligosaccharides with the general formula ΔHexA(GalNAc SO_3^--HexA)nGalNAcSO_3^-)

where n=1,2,3, etc. Generally, these molecular ions produce B and Y glycosidic fragments and few cross-ring fragments thus reducing the extent of structural information that can be gleaned [18]. Use of higher charge state precursors or derivatized CSA/DS molecules eliminate this isobaric nature of these molecules enabling tandem mass spectrometry of mixtures of different chain length of the oligomers. Use of higher charge state precursor ions also increases the number of product ions observed. The diagnostic ability of the ring fragments obtained from glucuronic and iduronic acid residues will be studied here. We investigated CSA/DS chains from degree of polymerization (dp) 4 to 10.

Diagnostic Ion Criteria

Samples were run in triplicates obtained different months apart. The error bars in the graphs represent the standard error of those three measurements. Relative intensity calculations were obtained by dividing the intensity of the diagnostic product ion with the total ion current in the spectrum excluding the precursor. Investigation of the MS/MS products proved that the number of ionized acidic groups in the molecular ions plays a significant role in controlling the diagnostic value of the product ions. Although other precursor ions produced ^{2,4}A and ^{0,2}X uronic acid fragment ions with intensity differences between CSA and DS, the molecular ions that produced all the diagnostic ions had particular characteristics. The charge state was higher than the number of sulfate groups within the chain by one and the molecular ion contained single free acidic hydrogen. The same precursor produced both A and X diagnostic fragment ions.

dp	Molecular ion	$^{2,4}A_n$	Mass	CSA $\frac{IonInt}{TIC}*100$	CSB $\frac{IonInt}{TIC}*100$
4	$[M-3H]^{3-}$ (305.0374)	$^{2,4}A_3$	500.0716	17.05 ± 0.65	4.70 ± 0.17
6	$[M-5H+Na]^{4-}$ (348.7892)	$^{2,4}A_3$		2.02 ±0.06	0.96 ± 0.04
		$[^{2,4}A_5+Na]^{2-}$	490.0571	6.83 ± 0.71	0.32 ± 0.02
8	$[M-7H+2Na]^{5-}$ (375.0399)	$^{2,4}A_3$		1.17 ± 0.03	0.32 ± 0.03
		$[^{2,4}A_5+Na]^{2-}$		0.64 ± 0.04	0.08 ± 0.003
		$^{2,4}A_5+2Na$	1003.1049	0.11 ±0.01	0.0
		$[^{2,4}A_7+2Na]^{3-}$	486.7192	2.06 ± 0.24	0.07 ±0.005
10	$[M-9H+3Na]^{6-}$ (392.5403)	$^{2,4}A_3$		0.66 ± 0.06	0.24 ± 0.01
		$[^{2,4}A_5+Na]^{2-}$		0.17± 0.02	0.0
		$[^{2,4}A_7+2Na]^{3-}$		0.29 ± 0.02	0.0
		$[^{2,4}A_7+3Na]^{2-}$	741.5734	0.26 ± 0.01	0.0
		$[^{2,4}A_9+3Na]^{4-}$	485.0501	0.63 ± 0.10	0.0

Table 5.1. The list of diagnostic molecular ions for each chain length with their masses, $^{2,4}A_n$ diagnostic fragments and their masses and the % abundance of that given ion compared to the total ion abundance. It can be seen from the table that most of the $^{2,4}A$ ions obtained for the dp10 were unique for CSA.

Furthermore, even for the molecular ions with the specific characteristics mentioned above, only ions with a specific charge and sodium level combinations were diagnostic. $^{2,4}A_n$ diagnostic ions had all the acidic groups ionized except one and whenever any of these ions were produced regardless of the precursor ion, they were found to be diagnostic. In most cases there were no such ions in unsodiated molecular ions and their prevalence and diagnostic qualities increased with the number of Na^+ ions present in the molecular ion. Fully ionized precursor ions generally produced fewer fragment ions including the ones that were diagnostic. Using this criterion, the molecular

ions and the $^{2,4}A_n$ fragments identified in the spectra investigated including their masses is shown in Table 5.1.

For the $^{0,2}X_n$ fragments that were found to be diagnostic especially for longer chains, diagnostic ions were either fully ionized or the ones with a single free acidic protons. The ions with a single free proton were also accompanied by another peak resulting from loss of SO_3 that was also diagnostic.

dp4 CSA and DS

CSA/DS tetrasaccharide epimers were the shortest chains that were investigated in this study. They have a total of four acidic groups (2 sulfate and 2 carboxyl groups). In all the chains studied, the non-reducing end hexuronic acid residue is unsaturated due to the double bond between C_4 and C_5 so its C_5 stereochemistry is lost. Due to this, only one hexuronic acid stereochemistry can be determined experimentally for dp4. The precursor ion with the aforementioned diagnostic characteristics is $[M-3H]^{3-}$ and it's unsodiated. The MS/MS spectrum obtained for these two epimers is shown in Figure 5.2. CSA most intense product ions are isobaric C_2/Z_2 followed by the $^{2,4}A_3$ fragment and then Y_1. Considering that C_2 and Z_2 are isobaric and assuming the intensity of the peak is a contribution of both ions, the most intense single ion fragment would be the $^{2,4}A_3$ fragment which is diagnostic. The bonds that are broken to produce them are believed to be more labile for that compound so their intensity is higher than the other ions in the spectrum. Collisional activation of DS dp4 produces ions with abundance $B_2 > Y_3^{2-} > {}^{0,2}X_3^{2-}$. The differences in intensity of the ions resulting from CSA and those of DS should be due to hexuronic acid residue C_5 stereochemistry because that is the only difference between the two chains.

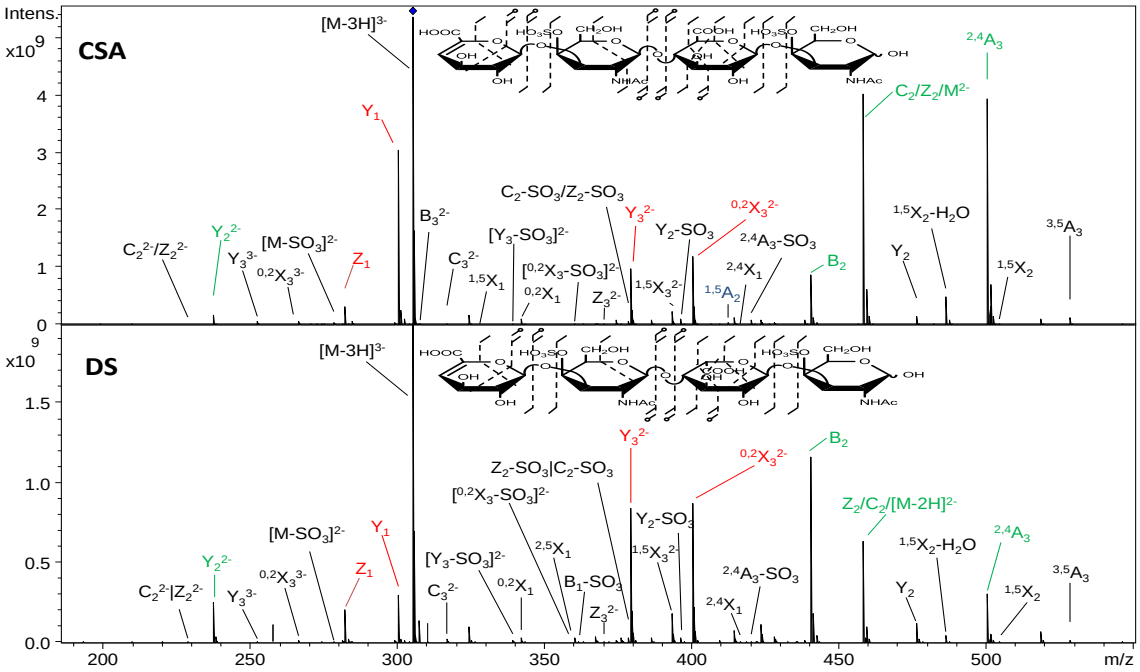

Figure 5.2. The mass spectra for dp4 CSA and DS chains displaying differences in ion abundance and distributions. The ions highlighted in red have been found to be diagnostic for this chain by other researchers. The fragment ions (shown in green) were found in this work and they are highly diagnostic for CSA and DS. Relative abundance of ion pair B_2 and C_2/Z_2 also differ between the two chains.

One of the most interesting ions that will be discussed throughout this study is the intensity of the uronic acid cross-ring fragment $^{2,4}A_3$ which is much more intense in CSA compared to DS for the dp4 chains. This fragment ($^{2,4}A_3$) is one of the ions bearing the diagnostic characteristics for CSA/DS chains studied in this work. Although this ion is not as diagnostic as the $^{2,4}A_n$ fragments for longer chains, the intensity ratio between CSA and DS is 4.6:1 which is pretty high (Table 5.1 and Figure 5.2). During the investigation of unique EDD fragments that distinguish GlcA and IdoA in heparan sulfate tetrasaccharides, it was postulated that having a charged uronic acid bring about the diagnostic $^{0,2}A_3$ within the uronic acid due to radical mechanisms [20]. Although other

researchers have explained the occurrence of $^{2,4}A_n$ to originate from $^{0,2}A_n$ fragments that occur after reducing end ring opening [44, 45], we believe that $^{2,4}A_n$ and $^{0,2}X$ fragments obtained from this study are consistent with mechanism put forward before [46] for metal adducted oligosaccharides. $^{2,4}A$ fragments have also been observed before for other Na^+ adducted oligosaccharides [47]. $^{0,2}X_n$ ions were less diagnostic for both dp4 and dp6.

Some of the other distinguishing ions have been observed in the previous work on doubly deprotonated precursor, $[M-2H]^{2-}$ and they follow a similar pattern for this precursor. For instance Y_1 is more intense in CSA than in DS. Other previously identified diagnostic ions were also present; these include Z_1, Y_3^{2-}, and $^{0,2}X_3^{2-}$ although their intensity differences are not very pronounced [31, 37]. The molecular ion investigated here reveals other ions like B_2 which is much more intense in DS than in CSA. Another useful detail that can be used to compare the two isomers include a pair of ions, in CSA dp 4, B_2 intensity is lower compared to the Z_2/C_2 while in the DS the relative intensity is reverse, i.e., the intensity of the Z_2/C_2 is more intense than B_2 (Figure 5.2). This can be useful in quick identification of contamination without doing quantitation.

The PCA analysis of the intensity of the peaks from both CSA and CSB confirms the observation discussed above (Appendix C). From the score plot, it's apparent that the 1st principal component explains 99.68% of the difference between the two spectra while the 2nd PC explains only 0.29% of the spectra differences. Although the scores for the CSB seems spread out, the PC2 scale is very small compared to the PC1 scale and thus not as far apart as it seems on the scale plot. The loading plot (Appendix C) shows the ions that are most responsible the separation of the ions within the spectra, the ions

discussed above especially the hexuronic acid fragment $^{2,4}A_3$ seen to have a huge contribution for the separation.

Dp6 CSA and DS

The hexasaccharides have two uronic acids whose C_5 stereochemistry can be determined. The molecular ion that is diagnostic is $[M-5H+Na]^{4-}$ (Figure 5.4) and the graph showing differences in ion intensity is shown in Figure 5.3. The fragment ion distribution is a bit similar to what is observed for dp4.

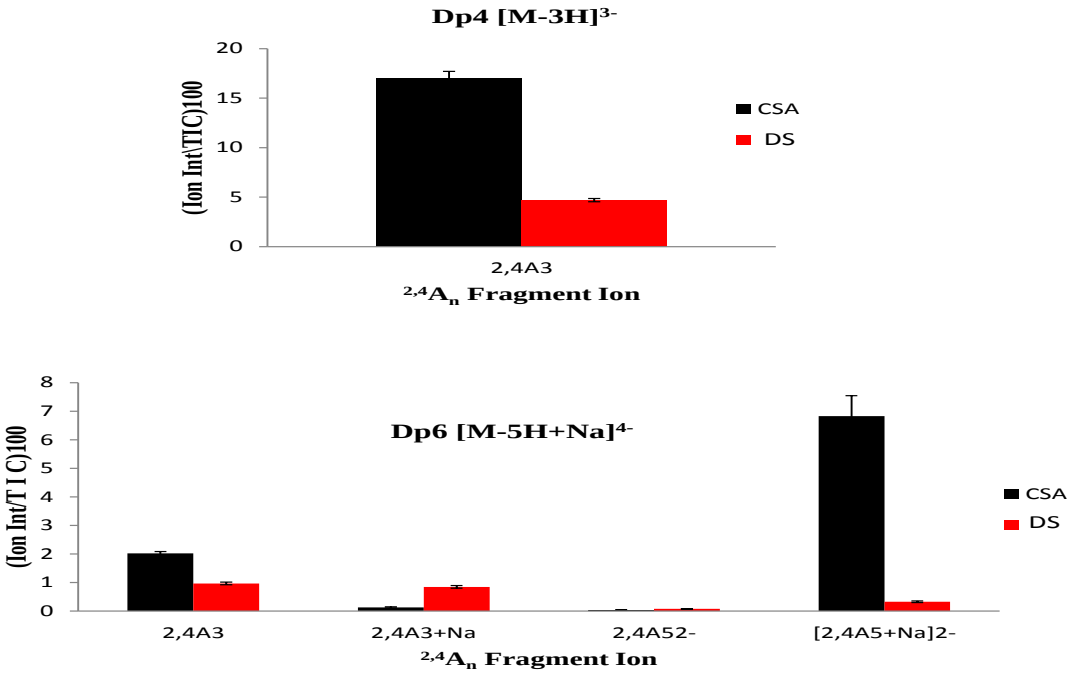

Figure 5.3. The graph shows relative intensity of $^{2,4}A_n$ fragments obtained from dp4 and dp6 CSA and DS with the standard error bar from three time sample runs. Although only a single ion ($^{2,4}A_3$) was diagnostic for the dp4 there are several $^{2,4}A$ ions for dp6 but only $^{2,4}A_3$ and $[^{2,4}A_5+Na]^{2-}$ had the diagnostic qualities discussed in the text. $[^{2,4}A_5+Na]^{2-}$ ion present in uronic acid near the reducing end and is more diagnostic that the $^{2,4}A_3$ in the middle uronic acid.

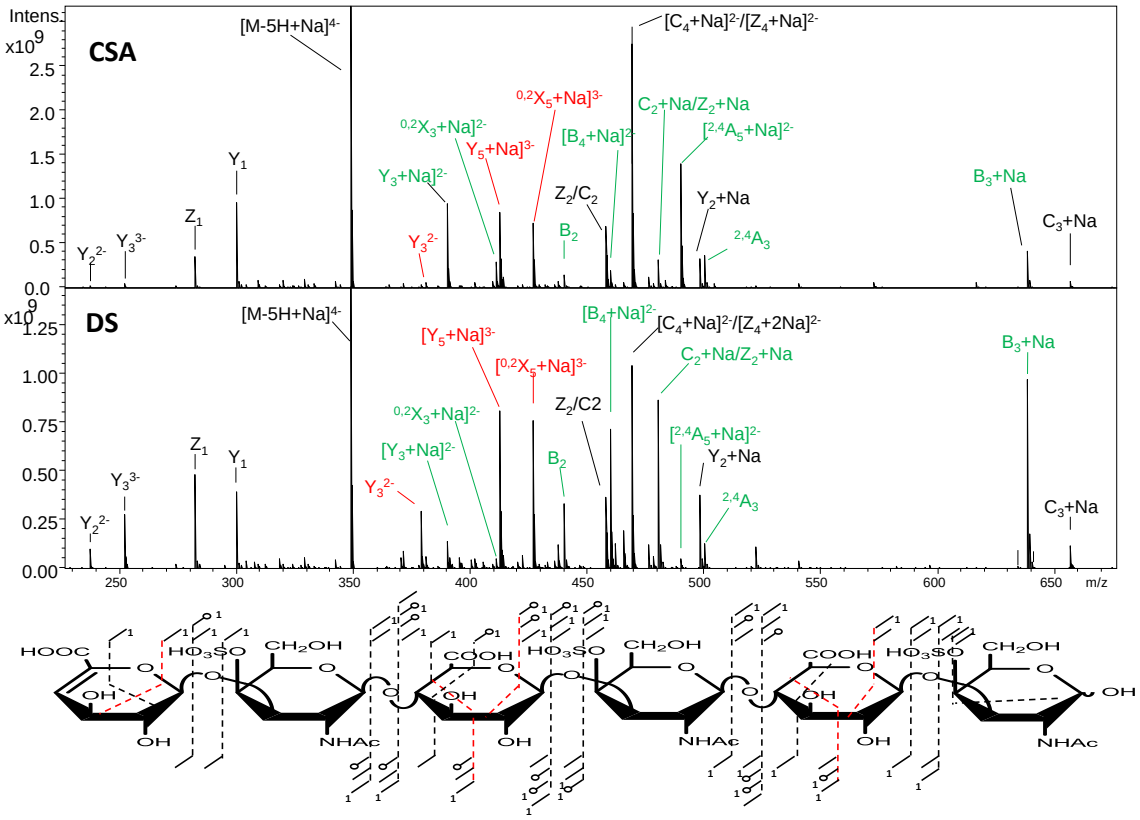

Figure 5.4. Spectra for the CSA/DS dp6 showing ions that differ in intensity between the two chains. Only the ions with intensity differences between the two chains are annotated in the spectra but all the ions found in the spectrum are shown in the structure below the spectra with ^{2,4}A and ^{0,2}X ions appearing in red. The ions that are shown in red in the spectra have been identified before but they don't seem to play a big role in the oligomer differentiation using this precursor except Y_3^{2-}. Ions shown in green especially the $^{2,4}A_n$ fragments with given characteristics are found to be more diagnostic.

The most intense fragment in both spectra is isobaric $[C_4+Na]^{2-}/[Z_4+Na]^{2-}$ ions followed by $[^{2,4}A_5+Na]^{2-}$; a fragment occurring within the hexuronic acid at the reducing end and is diagnostic (Table 5.1 and Figure 5.3, 5.4). For the CSB, notable diagnostic ions include B_3+Na, $[B_4+Na]^{2-}$, B_2, and C_2+Na/Z_2+Na. There are some ions whose

intensity differences were found to be diagnostic before like Y_3^{2-}, $[Y_5+Na]^{3-}$, $[^{0,2}X_5+Na]^{3-}$ [31].

The dp6 diagnostic precursor produces cross-ring fragments in each uronic acid residue that are apparently diagnostic. $[^{2,4}A_5+Na]^{2-}$ with the ratio of the intensity in CSA to CSB being 16.7:1 and cross-ring fragment $^{2,4}A_3$ whose intensity difference ration between CSA and CSB is 1.7:1. Suffice it to say that, the closer the $^{2,4}A_n$ diagnostic ring fragment is to the reducing end, the more diagnostic it is. $[^{0,2}X_5+Na]^{3-}$ ion is also diagnostic for CSA albeit in low intensity relative to the precursor ion (data not shown). Other notable ions which are less diagnostic include B_3+Na, $[B_4+Na]^{2-}$, B_2, and C_2+Na/Z_2+Na for CSB. $^{2,4}A_5^{2-}$ ion does not have diagnostic characteristics so it's not diagnostic. The PCA data for the two dp6 chains revealed the same ions identified in the spectra and the two samples spectral intensities separated within the first principal component but the first two PCs are shown (Appendix C).

Dp8 CSA and DS

The molecular ion $[M-7H+2Na]^{5-}$ produced the diagnostic ions for dp 8 and the ion distribution profile was slightly different from dp4 and 6. This could be due to the length of the chain thus bringing more flexibility which could affect the energy distribution within the molecule during CID. The most intense fragment is the isobaric fragment ions $[Z_6+2Na]^{3-}/[C_6+2Na]^{3-}$. The other most intense fragments are from glycosidic B and Y fragments. Within the spectrum though, there are cross-ring signature ions with diagnostic characteristics in every uronic acid except the non-reducing end residue and the ratio of intensities in between CSA and DS can be found in Table 5.1 and in Figure 5.5. These include ions like $^{2,4}A_3$, $[^{2,4}A_5+Na]^{2-}$, $^{2,4}A_5+2Na$ and $[^{2,4}A_7+2Na]^{3-}$.

Furthermore, as stated earlier, the chart and the table results indicate that the nearer the diagnostic ion is to the reducing end the more diagnostic it is and of course the more sodium level there is in the ion in order to have the diagnostic characteristics. The other $^{2,4}A$ cross-ring fragment ions observed did not show diagnostic qualities. For instance the $^{2,4}A_3$+Na ion is reverse diagnostic in the sense that it's more intense in DS than in CSA, this behavior is observed for this ion in all the chains that it was found. For the $^{0,2}X_n$ fragments, ions that had all the acidic groups ionized were found to be diagnostic except for $^{0,2}X_1$+Na near the reducing end.

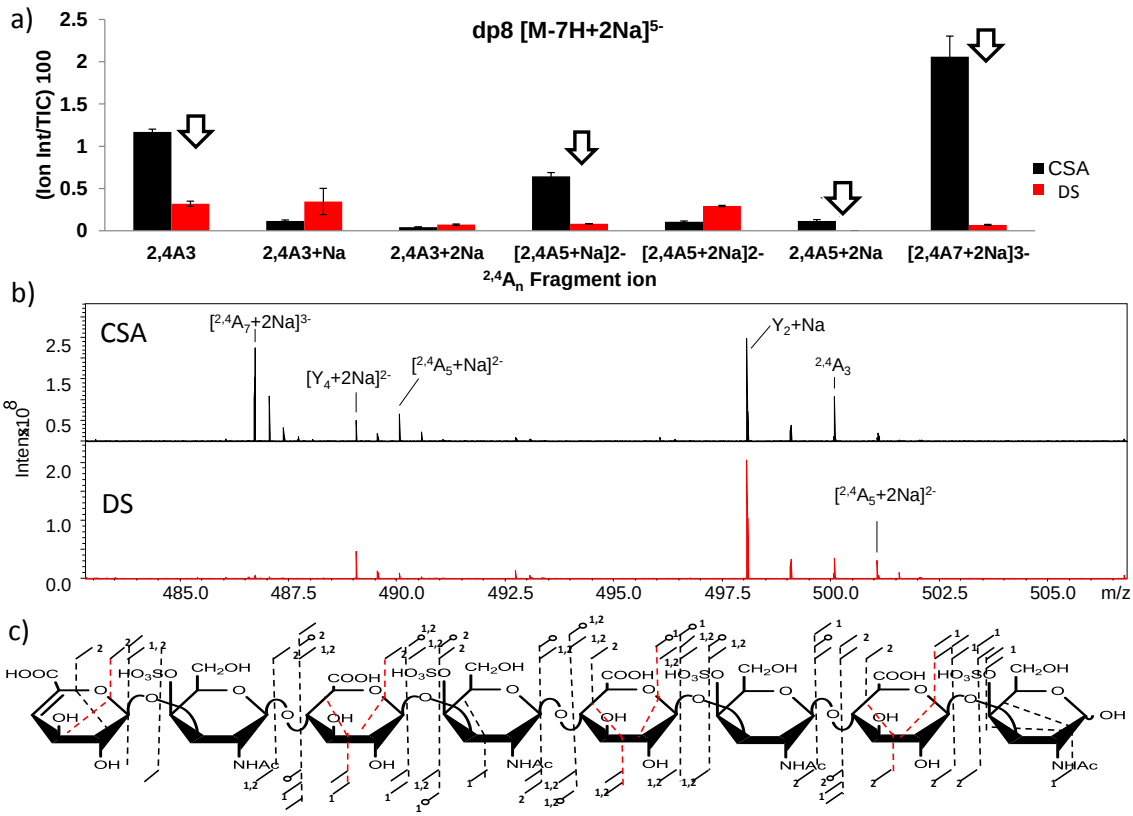

Figure 5.5. A graph of the relative intensities of $^{2,4}A_n$ CID fragments obtained from the two dp8 chains (a). The ions with the arrow on top have the diagnostic qualities discussed in the text. $^{2,4}A_5$+2Na, M/Z 1003.10 was found to be unique but with low intensity. b).

Visual comparison of some of the $^{2,4}A_n$ fragments obtained in CSA and DS with $[^{2,4}A_7 +2Na]^{3-}$ almost exclusively in CSA. c). A structure with the fragment ions obtained from $[M-7H+2Na]^{5-}$ precursor. $^{2,4}A$ and $^{0,2}X$ fragments are shown in red within the structure.

Other $^{0,2}X_n$ ions that were also diagnostic include the ones with only one acidic group unionized and these ions were often found accompanied by another peak as a result of SO_3 loss that were also diagnostic as shown in Figure 5.7. An exception to this observation was the occurrence of non-reducing end fragment $[^{0,2}X_7+3Na]^{3-}$ which is much less diagnostic because the intensities of the two ions almost match one another with the CSB intensity being more that of CSA. This kind of ion $[^{0,2}X_9+3Na]^{5-}$ at the non-reducing end for the dp10 had similar behavior (Appendix C). These two fragments occur at the non-reducing end residue whose C_5 stereochemistry is nonexistent due to its unsaturation. Ions with more than one free acidic group were not found to be diagnostic, for example, $[^{2,4}X_5+Na-SO_3]^{2-}$ ion in Figure 5.7. The PCA loading plot shows the ions that were responsible for the spectral differences within the dp8 CSA/DS spectra including $^{2,4}A_n$ and $^{0,2}X_n$ fragments (Appendix C).

Dp 10 CSA and DS

CSA and DS dp10 were the longest chains analyzed in this work and their diagnostic molecular ions is $[M-9H+3Na]^{6-}$. As observed in dp8, majority of intense fragments are not the ones resulting from cross-ring cleavages but instead B and Y ions. The most intense fragments were $[C_8+3Na]^{4-}/[Z_8+3Na]^{4-}$. This type of ion combination was found in all the chains from dp4 to dp10 and could be due to the combination of different ion intensities.

Although there are plenty of $^{2,4}A_n$ and $^{0,2}X_n$ fragment ions in the hexuronic acid residues of both CSA and DS, there are extremely few ring fragments occurring at the amino sugar for this chain. The annotated structure of dp10 CSA shows only one fragment ion at the reducing end glucosamine residue (Figure 5.6).

Another key observation is that, due to higher charge distributed within the molecule, one would expect to find complementary ions for both $^{2,4}A_n$ and $^{0,2}X_n$ fragments but they are not present in the MS/MS data from this chain, this would imply that these ions might be formed simultaneously following the mechanism discussed earlier in the text [46].

The $^{2,4}A_n$ fragments for the dp 10 are highly diagnostic (Table 5.1 and Figure 5.6). There are specific ions only found in the GlcA residues in CSA and they are not present in IdoA of the DS chains. These ions include, $[^{2,4}A_9+3Na]^{4-}$ present in the GlcA residue next to the reducing end. There were two fully diagnostic ions obtained from GlcA residue (7^{th} residue from non-reducing end) these are $[^{2,4}A_7+3Na]^{2-}$ and $[^{2,4}A_7+2Na]^{3-}$. $[^{2,4}A_5+Na]^{2-}$ is diagnostic for the 5^{th} residue from the non-reducing end. Only $^{2,4}A_3$ fragment is found in both GlcA and IdoA residues and it's more intense in CSA than in DS.

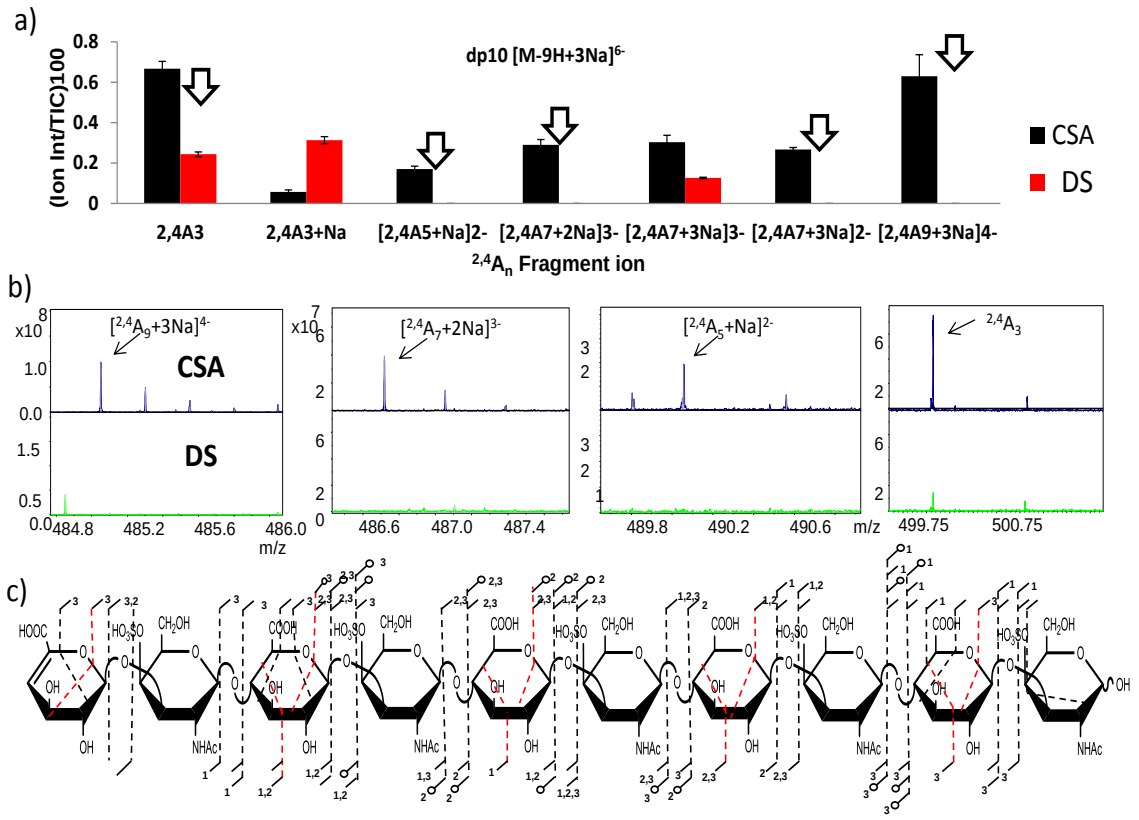

Figure 5.6. a). The graph shows the $^{2,4}A_n$ ions obtained from the dp 10 CSA and DS chains with the ions with the arrow on top having the diagnostic characteristics discussed in the text. There were ions that only appeared in CSA and were absent in DS chains in all the hexuronic acid residues except the one near the non-reducing end. b).The zoom in of some of these particular diagnostic ions is shown below the graph. c). Structure with fragment ions obtained from the diagnostic precursor ion with the $^{2,4}A$ and $^{0,2}X$ fragments shown in red.

$^{2,4}A_n$ fragments have been shown to arise from the C ion by retro-aldo rearrangement of ions in negative mode after the formation of $^{0,2}A_n$ fragment ion [44, 45]. The mechanism that requires an open ring reducing terminal aldehyde and such structures are formed from C-type fragments. But the observations from these experiments show

that the C_5 stereochemistry of the uronic acid of the precursor ions have a profound effect on the diagnostic ions observed and they don't seem to follow the stated mechanisms because the $^{2,4}A$ and $^{0,2}X$ fragments seem to occur simultaneously since there are very few complementary $^{2,4}X$ and $^{0,2}A$ fragments.

$^{0,2}X_n$ fragments with all the acidic groups fully ionized or the ones with one free acidic group are also found to have diagnostic characteristics for this chain (Figure 5.7). As mentioned for the dp8, $[^{0,2}X_9+3Na]^{5-}$ which has one free acidic proton was obtained in high intensity but was found to be less diagnostic. $[^{0,2}X_9+3Na]^{6-}$ ion was found to be fully diagnostic for the dp10 CSA as it was not found in DS. Other fully diagnostic ions include $[^{0,2}X_5+2Na]^{2-}$ and $[^{0,2}X_5+2Na\text{-}SO_3]^{2-}$ found only in GlcA and not present in IdoA. Figure 5.7 shows the $^{0,2}X_n$ ions that were obtained from the diagnostic precursor including the ones that were not found to be diagnostic. Ions like $[^{0,2}X_7+2Na]^{3-}$ and $[^{0,2}X_7+2Na\text{-}SO_3]^{3-}$ with more than one free acidic proton were not diagnostic.

Although $^{2,4}A$ and $^{0,2}X$ of the respective uronic acid display more diagnostic characteristics than the rest of the ions, other ions were found to be diagnostic as well, these includes some of the glycosidic fragments that have been identified in the earlier work by other researchers. We were unable to find common diagnostic characteristics of these ions like the ones identified for the $^{2,4}A_n$ and $^{0,2}X_n$ fragments.

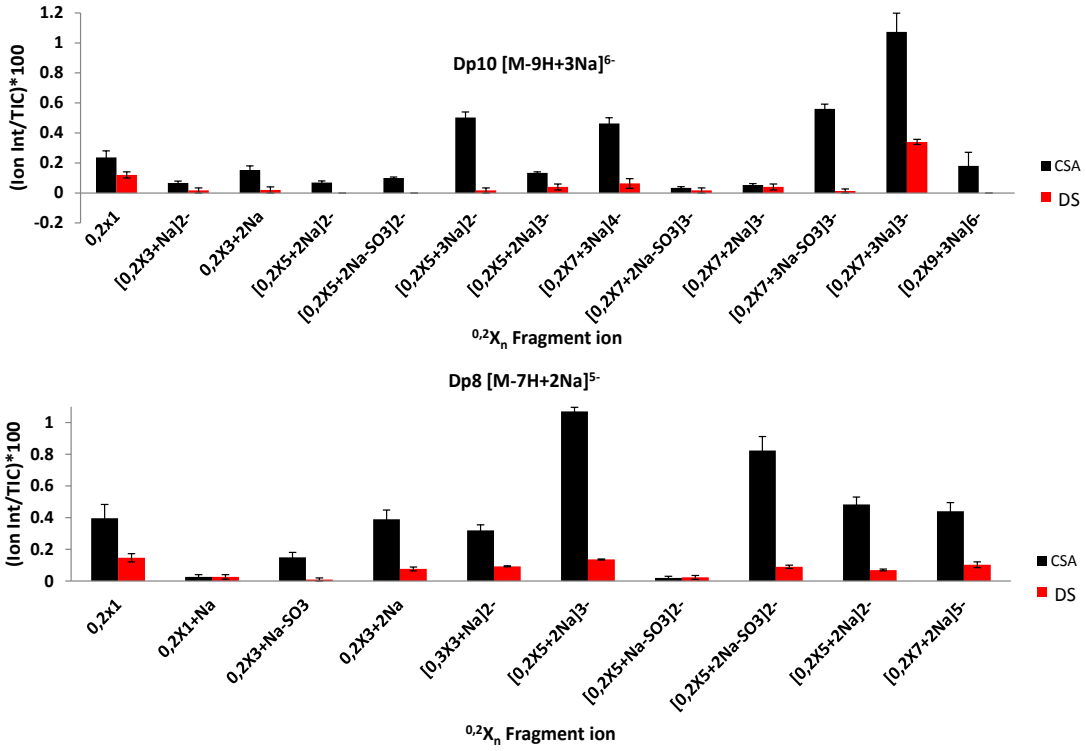

Figure 5.7. Graphs showing the $^{0,2}X$ fragments obtained from dp8 and dp 10 CSA and DS chains. The ions at the non-reducing end that were not diagnostic but of high intensity compared the other $^{0,2}X$ fragments have been removed. The ions with defined characteristics are diagnostic.

When the molecular ion with diagnostic charge state is not sodiated [M-6H] $^{6-}$, $^{2,4}A_n$ ions are present but not entirely diagnostic except for the $^{2,4}A_9$ $^{4-}$ ion which is present only in GlcA and not in IdoA (Appendix C). Both the score and loadings plot PCA data for the diagnostic molecular ions is shown in the Appendix C.

CONCLUSIONS

The work described in this chapter shows that ionizing all acidic groups except one, it is possible obtain stereo-chemical information of chondroitin sulfate glycosaminoglycans using CID. Previous work in our lab has shown that $^{2,4}A$ fragments are rear even in heparin and heparan sulfate oligosaccharides IdoA residues. Addition of small NaOH solution helps in obtaining higher charge states thus eliminating the isobaric nature of molecular ions resulting from different CSA and DS chain length. Ion activation of higher charge state molecular ions leads to the production of large number of cross-ring fragments which can be used to distinguish closely related structures.

$^{2,4}A_n$ and $^{0,2}X_n$ ions were present in all the spectra taken from dp4-dp10 CS but $^{0,2}X_n$ were found to be less diagnostic for dp4 and 6. This is the first indication that unique CID fragments that can distinguish between CSA and DS chains can be obtained. $^{2,4}A$ fragments near the reducing end are more diagnostic than the ones near the non-reducing end. $^{0,2}X_n$ fragments ions at the non-reducing residue produce a mixture of diagnostic and non-diagnostic ions. This residue as lost its C_5 stereochemistry due to its unsaturation so it's not expected to produce diagnostic ions.

REFERENCES

1. Sugahara, K.; Mikami, T.; Uyama, T.; Mizuguchi, S.; Nomura, K. and Kitagawa, H., Recent advances in the structural biology of chondroitin sulfate and dermatan sulfate. *Curr. Opin. Struct. Biol.* **2003**, 13, 612-620.
2. Gandhi, N. S. and Mancera, R. L., The structure of glycosaminoglycans and their interactions with proteins. *Chem. Biol. Drug Des.* **2008**, 72, 455-482.
3. Silbert, J. E. and Sugumaran, G., Biosynthesis of Chondroitin/Dermatan Sulfate. *IUBMB Life.* **2002**, 54, 177-186.
4. Sisu, E.; Flangea, C.; Serb, A. and Zamfir, A. D., Modern developments in mass spectrometry of chondroitin and dermatan sulfate glycosaminoglycans. *Amino Acids.* **2011**, 41, 235-256.
5. Akatsu, C.; Mizumoto, S.; Kaneiwa, T.; Maccarana, M.; Malmstrom, A.; Yamada, S. and Sugahara, K., Dermatan sulfate epimerase 2 is the predominant isozyme in the formation of the chondroitin sulfate/dermatan sulfate hybrid structure in postnatal developing mouse brain. *Glycobiology.* **2011**, 21, 565-574.
6. Shriver, Z.; Liu, D. and Sasisekharan, R., Emerging views of heparan sulfate glycosaminoglycan structure/activity relationships modulating dynamic biological functions. *Trends Cardiovasc. Med.* **2002**, 12, 71-77.
7. Mitsunaga, C.; Mikami, T.; Mizumoto, S.; Fukuda, J. and Sugahara, K., Chondroitin sulfate/dermatan sulfate hybrid chains in the development of cerebellum - Spatiotemporal regulation of the expression of critical disulfated

disaccharides by specific sulfotransferases. *J. Biol. Chem.* **2006**, 281, 18942-18952.

8. Bao, X. F.; Nishimura, S.; Mikami, T.; Yamada, S.; Itoh, N. and Sugahara, K., Chondroitin sulfate/dermatan sulfate hybrid chains from embryonic pig brain, which contain a higher proportion of L-iduronic acid than those from adult pig brain, exhibit neuritogenic and growth factor binding activities. *J. Biol. Chem.* **2004**, 279, 9765-9776.
9. Dundar, M.; Muller, T.; Zhang, Q.; Pan, J.; Steinmann, B.; Vodopiutz, J.; Gruber, R.; Sonoda, T.; Krabichler, B.; Utermann, G.; Baenziger, J. U.; Zhang, L. J. and Janecke, A. R., Loss of Dermatan-4-Sulfotransferase 1 Function Results in Adducted Thumb-Clubfoot Syndrome. *Am. J. Hum. Genet.* **2009**, 85, 873-882.
10. Hou, S.; Maccarana, M.; Min, T. H.; Strate, I. and Pera, E. M., The Secreted Serine Protease xHtrA1 Stimulates Long-Range FGF Signaling in the Early Xenopus Embryo. *Dev. Cell.* **2007**, 13, 226-241.
11. Vicente, C. P.; He, L.; Pavão, M. S. and Tollefsen, D. M., Antithrombotic activity of dermatan sulfate in heparin cofactor II-deficient mice. *Blood.* **2004**, 104, 3965-3970.
12. Plaas, A. H.; West, L. A.; Thonar, E. J.; Karcioglu, Z. A.; Smith, C. J.; Klintworth, G. K. and Hascall, V. C., Altered fine structures of corneal and skeletal keratan sulfate and chondroitin/dermatan sulfate in macular corneal dystrophy. *J. Biol. Chem.* **2001**, 276, 39788-39796.
13. Yamada, S. and Sugahara, K., Potential therapeutic application of chondroitin sulfate/dermatan sulfate. *Curr Drug Discov Technol.* **2008**, 5, 289-301.

14. Sudo, M.; Sato, K.; Chaidedgumjorn, A.; Toyoda, H.; Toida, T. and Imanari, T., 1H Nuclear Magnetic Resonance Spectroscopic Analysis for Determination of Glucuronic and Iduronic Acids in Dermatan Sulfate, Heparin, and Heparan Sulfate. *Anal. Biochem.* **2001**, 297, 42-51.

15. Casu, B. and Torri, G., Structural characterization of low molecular weight heparins. *Semin. Thromb. Hemost.* **1999**, 25 Suppl 3, 17-25.

16. Scott, J. E. and Heatley, F., Detection of secondary structure in glycosaminoglycans via the H n.m.r. signal of the acetamido NH group. *Biochem. J.* **1982**, 207, 139-144.

17. Kailemia, M. J.; Li, L.; Xu, Y.; Liu, J.; Linhardt, R. J. and Amster, I. J., Structurally informative tandem mass spectrometry of highly sulfated natural and chemoenzymatically synthesized heparin and heparan sulfate glycosaminoglycans. *Mol. Cell. Proteomics.* **2013**, 12, 979-990.

18. Bielik, A. M. and Zaia, J., Multistage tandem mass spectrometry of chondroitin sulfate and dermatan sulfate. *Int. J. Mass Spectrom.* **2011**, 305, 131-137.

19. Wolff, J. J.; Amster, I. J.; Chi, L. and Linhardt, R. J., Electron Detachment Dissociation of Glycosaminoglycan Tetrasaccharides. *J. Am. Soc. Mass. Spectrom.* **2007**, 18, 234-244.

20. Wolff, J. J.; Chi, L.; Linhardt, R. J. and Amster, I. J., Distinguishing Glucuronic from Iduronic Acid in Glycosaminoglycan Tetrasaccharides by Using Electron Detachment Dissociation. *Anal. Chem.* **2007**, 79, 2015-2022.

21. Wolff, J. J.; Laremore, T. N.; Busch, A. M.; Linhardt, R. J. and Amster, I. J., Influence of Charge State and Sodium Cationization on the Electron Detachment

Dissociation and Infrared Multiphoton Dissociation of Glycosaminoglycan Oligosaccharides. *J. Am. Soc. Mass. Spectrom.* **2008**, 19, 790-798.

22. Wolff, J. J.; Laremore, T. N.; Busch, A. M.; Linhardt, R. J. and Amster, I. J., Electron Detachment Dissociation of Dermatan Sulfate Oligosaccharides. *J. Am. Soc. Mass. Spectrom.* **2008**, 19, 294-304.

23. Zaia, J.; Li, X.-Q.; Chan, S.-Y. and Costello, C. E., Tandem mass spectrometric strategies for determination of sulfation positions and uronic acid epimerization in chondroitin sulfate oligosaccharides. *J. Am. Soc. Mass. Spectrom.* **2003**, 14, 1270-1281.

24. Zaia, J.; Miller, M. J. C.; Seymour, J. L. and Costello, C. E., The Role of Mobile Protons in Negative Ion CID of Oligosaccharides. *J. Am. Soc. Mass. Spectrom.* **2007**, 18, 952-960.

25. Zamfir, A.; Seidler, D. G.; Kresse, H. and Peter-Katalinić, J., Structural characterization of chondroitin/dermatan sulfate oligosaccharides from bovine aorta by capillary electrophoresis and electrospray ionization quadrupole time-of-flight tandem mass spectrometry. *Rapid Commun. Mass Spectrom.* **2002**, 16, 2015-2024.

26. Zamfir, A.; Seidler, D. G.; Kresse, H. and Peter-Katalinić, J., Structural investigation of chondroitin/dermatan sulfate oligosaccharides from human skin fibroblast decorin. *Glycobiology.* **2003**, 13, 733-742.

27. Zhou, Z.; Ogden, S. and Leary, J. A., Linkage position determination in oligosaccharides: mass spectrometry (MS/MS) study of lithium-cationized carbohydrates. *J. Org. Chem.* **1990**, 55, 5444-5446.

28. Kailemia, M. J.; Li, L.; Ly, M.; Linhardt, R. J. and Amster, I. J., Complete mass spectral characterization of a synthetic ultralow-molecular-weight heparin using collision-induced dissociation. *Anal. Chem.* **2012**, 84, 5475-5478.

29. Wolff, J. J.; Amster, I. J.; Chi, L. and Linhardt, R. J., Electron detachment dissociation of glycosaminoglycan tetrasaccharides. *J. Am. Soc. Mass. Spectrom.* **2007**, 18, 234-244.

30. Wolff, J. J.; Laremore, T. N.; Busch, A. M.; Linhardt, R. J. and Amster, I. J., Influence of charge state and sodium cationization on the electron detachment dissociation and infrared multiphoton dissociation of glycosaminoglycan oligosaccharides. *J. Am. Soc. Mass. Spectrom.* **2008**, 19, 790-798.

31. Zaia, J.; Li, X. Q.; Chan, S. Y. and Costello, C. E., Tandem mass spectrometric strategies for determination of sulfation positions and uronic acid epimerization in chondroitin sulfate oligosaccharides. *J. Am. Soc. Mass. Spectrom.* **2003**, 14, 1270-1281.

32. Zaia, J.; McClellan, J. E. and Costello, C. E., Tandem mass spectrometric determination of the 4S/6S sulfation sequence in chondroitin sulfate oligosaccharides. *Anal. Chem.* **2001**, 73, 6030-6039.

33. Zamfir, A.; Seidler, D. G.; Kresse, H. and Peter-Katalinic, J., Structural investigation of chondroitin/dermatan sulfate oligosaccharides from human skin fibroblast decorin. *Glycobiology.* **2003**, 13, 733-742.

34. Ly, M.; Leach III, F. E.; Laremore, T. N.; Toida, T.; Amster, I. J. and Linhardt, R. J., The proteoglycan bikunin has a defined sequence. *Nat. Chem. Biol.* **2011**, 7, 827-833.

35. Miller, M. J. C.; Costello, C. E.; Malmström, A. and Zaia, J., A tandem mass spectrometric approach to determination of chondroitin/dermatan sulfate oligosaccharide glycoforms. *Glycobiology.* **2006**, 16, 502-513.

36. Hitchcock, A. M.; Costello, C. E. and Zaia, J., Glycoform quantification of chondroitin/dermatan sulfate using a liquid chromatography-tandem mass spectrometry platform. *Biochem.* **2006**, 45, 2350-2361.

37. Leach III, F. E.; Ly, M.; Laremore, T. N.; Wolff, J. J.; Perlow, J.; Linhardt, R. J. and Amster, I. J., Hexuronic Acid Stereochemistry Determination in Chondroitin Sulfate Glycosaminoglycan Oligosaccharides by Electron Detachment Dissociation. *J. Am. Soc. Mass. Spectrom.* **2012**, 23, 1488-1497.

38. Sagi, D.; Peter-Katalinic, J.; Conradt, H. and Nimtz, M., Sequencing of tri- and tetraantennary N-glycans containing sialic acid by negative mode ESI QTOF tandem MS. *J. Am. Soc. Mass. Spectrom.* **2002**, 13, 1138-1148.

39. Vakhrushev, S. Y.; Zamfir, A. and Peter-Katalinic, J., 0,2An cross-ring cleavage as a general diagnostic tool for glycan assignment in glycoconjugate mixtures. *J. Am. Soc. Mass. Spectrom.* **2004**, 15, 1863-1868.

40. Pervin, A.; Gallo, C.; Jandik, K. A.; Han, X.-J. and Linhardt, R. J., Preparation and structural characterization of large heparin-derived oligosaccharides. *Glycobiology.* **1995**, 5, 83-95.

41. Muñoz, E.; Xu, D.; Avci, F.; Kemp, M.; Liu, J. and Linhardt, R. J., Enzymatic synthesis of heparin related polysaccharides on sensor chips: rapid screening of heparin–protein interactions. *Biochem. Biophys. Res. Commun.* **2006**, 339, 597-602.

42. Ceroni, A.; Maass, K.; Geyer, H.; Geyer, R.; Dell, A. and Haslam, S. M., GlycoWorkbench: A Tool for the Computer-Assisted Annotation of Mass Spectra of Glycans†. *J. Proteome Res.* **2008**, 7, 1650-1659.

43. Domon, B. and Costello, C. E., A Systematic Nomenclature for Carbohydrate Fragmentations in Fab-MS MS Spectra of Glycoconjugates. *Glycoconjugate J.* **1988**, 5, 397-409.

44. Carroll, J. A.; Willard, D. and Lebrilla, C. B., Energetics of cross-ring cleavages and their relevance to the linkage determination of oligosaccharides. *Anal. Chim. Acta.* **1995**, 307, 431-447.

45. Saad, O. and Leary, J., Delineating mechanisms of dissociation for isomeric heparin disaccharides using isotope labeling and ion trap tandem mass spectrometry. *J. Am. Soc. Mass. Spectrom.* **2004**, 15, 1274-1286.

46. Lemoine, J.; Fournet, B.; Despeyroux, D.; Jennings, K. R.; Rosenberg, R. and de Hoffmann, E., Collision-induced dissociation of alkali metal cationized and permethylated oligosaccharides: Influence of the collision energy and of the collision gas for the assignment of linkage position. *J. Am. Soc. Mass. Spectrom.* **1993**, 4, 197-203.

47. Orlando, R.; Allen Bush, C. and Fenselau, C., Structural analysis of oligosaccharides by tandem mass spectrometry: Collisional activation of sodium adduct ions. *Biol. Mass Spectrom.* **1990**, 19, 747-754.

CHAPTER 6

HIGH-FIELD ASYMMETRIC-WAVEFORM ION MOBILITY SPECTROMETRY AND ELECTRON DETACHMENT DISSOCIATION OF ISOBARIC MIXTURES OF GLYCOSAMINOGLYCANS*

* Kailemia, M.; Park, M.; Kaplan, D.; Venot, A.; Boons, G.-J.; Li, L.; Linhardt, R.; Amster, I. J. High-Field Asymmetric-Waveform Ion Mobility Spectrometry and Electron Detachment Dissociation of Isobaric Mixtures of Glycosaminoglycans. *J. Am. Soc. Mass Spectrom*. **2014**, 25,258-268. Reprinted here with permission of publisher.

ABSTRACT

High-field asymmetric waveform ion mobility spectrometry (FAIMS) is shown to be capable of resolving isomeric and isobaric glycosaminoglycan negative ions, and to have great utility for the analysis of this class of molecules when combined with Fourier transform ion cyclotron resonance mass spectrometry (FTICR-MS) and tandem mass spectrometry. Electron detachment dissociation (EDD) and other ion activation methods for tandem mass spectrometry can be used to determine the sites of labile sulfate modifications and for assigning the stereochemistry of hexuronic acid residues of GAGs. However, mixtures with overlapping mass-to-charge values present a challenge, as their precursor species cannot be resolved by a mass analyzer prior to ion activation. FAIMS is shown to resolve two types of mass-to-charge overlaps. A mixture of chondroitin sulfate A (CSA) oligomers with 4-10 saccharides units produces ions of a single mass-to-charge by electrospray ionization, as the charge state increases in direct proportion to the degree of polymerization for these sulfated carbohydrates. FAIMS is shown to resolve the overlapping charge. A more challenging type of mass-to-charge overlap occurs for mixtures of diastereomers. FAIMS is shown to separate two sets of epimeric GAG tetramers. For the epimer pairs, the complexity of the separation is reduced when the reducing end is alkylated, suggesting that anomers are also resolved by FAIMS. The resolved components were activated by EDD and the fragment ions were analyzed by FTICR-MS. The resulting tandem mass spectra were able to distinguish the two epimers from each other.

INTRODUCTION

Glycosaminoglycans (GAGs) are a linear, anionic, structurally diverse, and ubiquitous family of polysaccharides composed of a hexuronic acid and a hexosamine repeating disaccharide unit [1-3]. The identity of the monosaccharide residues, the linkage position of glycosidic bonds between the monosaccharides, as well as the degree and location of sulfate modifications distinguish the various classes of GAGs [2, 4]. Research has shown that modifications of the residues, specifically O-sulfation, N-deacetylation/sulfation, or epimerization of uronic acid residues impacts their biological activity. GAGs are present on all animal cell surfaces and in the extracellular matrix (ECM) within which they regulate many cellular and physiological processes [1-5]. They are known to bind and regulate a number of distinct proteins including small secreted proteins (chemokines) [6], small secreted cell signaling proteins (cytokines) [7], growth factors like morphogens [5], enzymes, and adhesion molecules [4], GAGs also modulate cell–cell and cell–extracellular matrix communication, angiogenesis, axonal growth, tumor progression, metastasis, and anti-coagulation [2, 5]. Although numerous functions of GAGs are known, there are only a few function specific sequences whose structures have been fully elucidated [8]. To advance the study of the biological functions of GAGs, sophisticated analytical methods are needed to identify and characterize biologically important motifs within their basic sequences [9]. The structural complexity of GAG molecules, especially heparin and heparan sulfate makes their structural determination more challenging than other biomolecules. The complexity is a consequence of the non-template nature of their biosynthesis, and the vast number of modifications that occur

post-synthesis, including de-acetylation, sulfation and epimerization giving rise to a considerable polydispersity and heterogeneity.

Mass spectrometry (MS) using negative mode electrospray ionization (ESI) is widely used for the structural elucidation of GAGs [10, 11]. In addition to retention of sulfo groups during MS analysis and the production of multiply charged ions, ESI can be coupled with liquid chromatography or capillary electrophoresis separation methods that enhance sensitivity and selectivity of the GAG analysis [12]. In order to obtain detailed information about monosaccharide connectivity and their unique modifications, several tandem mass spectrometry (MS/MS) techniques have been examined and refined for the structural analysis of GAGs, including collision induced dissociation (CID[13-18], electron detachment dissociation (EDD) [19-23], and negative electron transfer dissociation (NETD) [24, 25]. These methods have been effective on relatively small oligomers produced by enzymatic digestion of full-length glycans. Recently, full length chains from a proteoglycan have been characterized by Fourier transform ion cyclotron resonance tandem mass spectrometry (FTICR-MS/MS) [8]. Despite a propensity for decomposition of sulfo modifications via SO_3 loss during MS/MS, careful control of the ion activation conditions lead to glycosidic and cross-ring cleavages which can be used to assign the location of sites of sulfation at both the monosaccharide level and the ring position in GAG oligosaccharides [16, 17, 19, 20, 24-30].

Despite the versatility of mass spectrometry for characterizing GAGs, the complex mixtures produced by enzymatic de-polymerization, and the isomeric nature of the resulting sequences require separation steps before they are introduced to the mass spectrometer [31-34]. Chromatographic separation methods such as normal phase and

reverse phase high performance liquid chromatograph (HPLC), porous graphite carbon liquid chromatograph (PGC-LC) and hydrophilic interaction liquid chromatography (HILIC) have been used for separation of GAGs [32, 33, 35]. Ion exchange methods such as high-performance anion-exchange chromatography (HPAEC) [36] have also been used for GAG separations. However, these present challenges when combined with MS analysis, requiring desalting or removal of ion pairing reagents prior to introduction to the mass spectrometer [37]. Capillary electrophoresis (CE) methods have also been used for separating and characterizing GAGs [31]. The short time for LC or CE peak elution does not match the long analysis times required for high resolution analysis by FTICR-MS, particularly for ion activation by EDD [21].

As an alternative to liquid separations, there has been considerable recent interest in gas-phase separation of ions prior to mass spectrometry analysis, using ion mobility spectrometry (IMS). IMS separates gas phase ions on the basis of their charge state, overall shape and the ionic collision cross-section while under a weak, time-invariant electric field [38, 39] and can achieve separation of structural and positional isomers [39-42]. Previously, others have used a combination of ion mobility, mass spectrometry and proton NMR to characterize iduronic and glucuronic acid containing heparan sulfate hexasaccharides [34], and recently, IMS was used for separation and analysis of positional isomers of heparin octasaccharides [43]. However, the peak width for a component in an IMS separation is on the order of microseconds, which is far too short to be used for FTICR-MS.

High-field asymmetric waveform ion mobility spectrometry (FAIMS), also known as differential mobility spectrometry (DMS), separates gas-phase ions depending

on the differences between their mobility in high and low electric fields, and at atmospheric pressure [44, 45]. It is a particularly attractive choice for coupling to FTICR-MS, as ions are separated spatially rather than temporally [45, 46]. With FAIMS, ions are drawn by the flow of buffer gas into a mobility region consisting of two parallel or coaxial electrodes, located between an atmospheric pressure ion source and the inlet to the mass spectrometer. An asymmetric alternating potential, the peak amplitude of which is called the dispersion voltage (DV), is applied between the electrodes producing an electric field tangential to the direction of gas flow. The mobility of ions differ during the high-field and low-field portion of the waveform, leading to their lateral displacement. A small static voltage called the compensation voltage (CV) is applied to one electrode, to direct ions of a particular differential mobility onto the mass spectrometer inlet. In this fashion, ions that have been separated by FAIMS can be continuously admitted into the mass spectrometer, allowing this separation method to be coupled with slow analysis methods such as FTICR-MS. The FAIMS separation is orthogonal to both chromatographic and mass spectrometric techniques, thereby increasing selectivity and specificity of analysis when combined [45, 47].

ESI-FAIMS-MS has been used to effect gas phase separation and differentiation of anomers, linkage, and position isomers of disaccharides [48], glycopeptides [49] and other biomolecules [50-54]. In addition, FAIMS has been used to selectively introduce different gas phase conformers of ubiquitin ions prior to FTICR-MS analysis, making it possible to resolve and identify different populations of conformers [55]. Here we show the utility of FAIMS as a separation tool coupled to FTICR-MS and FTICR-MS/MS for the analysis of mixtures of glycosaminoglycans. A chondroitin sulfate A mixture of

oligomers of degree of polymerization (dp) 4-10 produces isobaric ions due to the linear relationship between charge and length of the polymer. These cannot be resolved by a mass-to-charge separation, but are resolved by differential mobility spectrometry. A more demanding separation is demonstrated for a mixture of epimeric GAG tetramers, facilitating their MS/MS analysis. The effect of the reducing end anomericity and the behavior of sodiated adducts on the separation are examined. This is the first application of FAIMS separation to GAGs, with subsequent analysis of the separated isobaric molecular ions using EDD.

EXPERIMENTAL

Epimer Synthesis

Heparan sulfate tetrasaccharides epimers (GlcA-GlcNAc6S-IdoA-GlcNAc6S (GI) and GlcA-GlcNAc6S-GlcA- GlcNAc6S (GG)) and GlcA-GlcNAc6S-GlcA-GlcNAc6S-(CH2)5-NH2 (GG2) and GlcA-GlcNAc6S-IdoA-GlcNAc6S-(CH2)5-NH2 (GI2) showed in Scheme 6.1,were synthesized and purified as described in literature [56]. Use of accurate mass measurement and ^{1}H NMR confirmed the structures of the tetra-saccharides.

Preparation of CS GAG Oligosaccharides

Chondroitin sulfate A (CS-A) oligosaccharides were prepared by partial enzymatic depolymerization of bovine trachea chondroitin sulfate A (Celsus Laboratories, Cincinnati, OH) and purified as described in the previous paper [57]. High-field nuclear magnetic resonance (NMR), ESI-MS and PAGE were used to characterize the final isolated individual oligosaccharide fractions [58].

ESI FAIMS

Ions were generated using negative mode ESI. Solutions for both tetra-saccharides were made at a concentration of 0.05 mg/mL in 50:50:0.1 MeOH: H_2O: HCOOH (Sigma, St. Louis, MO, USA) unless otherwise stated. All sample solutions were infused at a rate of 120 μL/h using ESI metal capillary (Agilent Technologies, Santa Clara, CA, #G2427A) tip placed about 2-3 mm from the FAIMS curtain gas cap. Generated ions were passed through Bruker Daltonics planar FAIMS analyzer (Billerica, MA, USA) with electrode gap width of 0.5 mm. The FAIMS device was held in place by a cylindrical peek that facilitates proper interfacing to a 9.4 T Bruker Apex IV QeFTMS (Billerica, MA, USA).

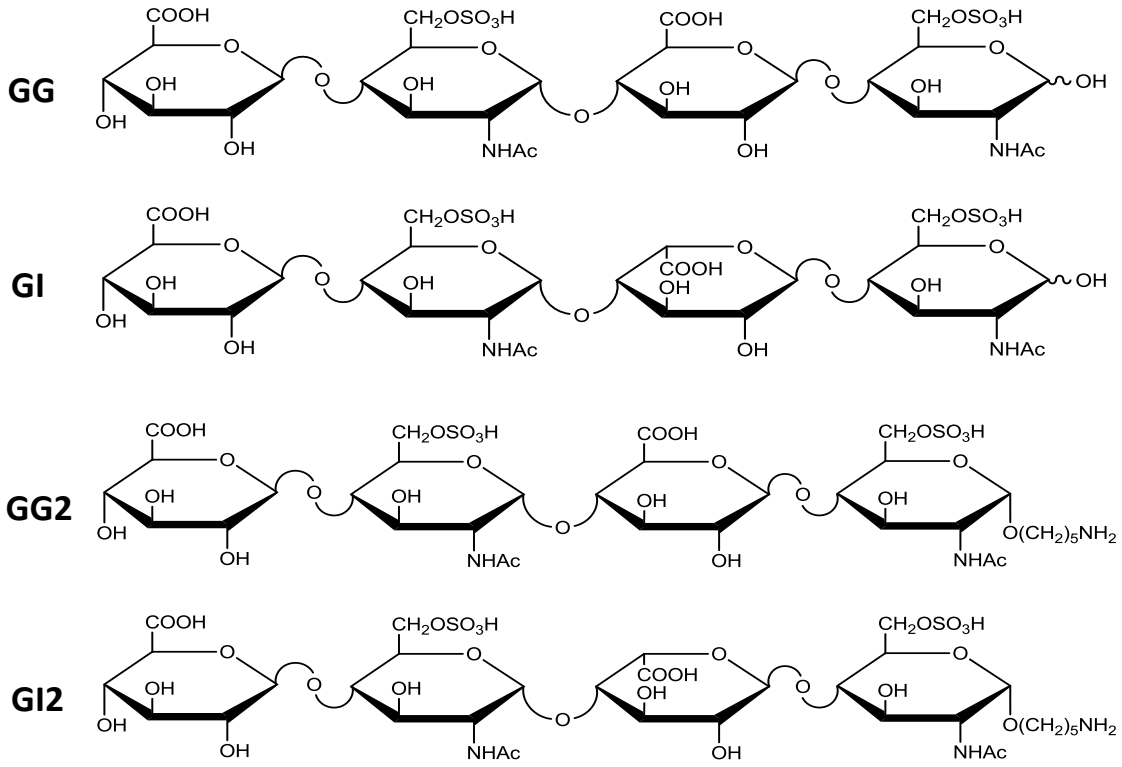

Figure 6.1. Structures for the HS tetra-saccharides used in this study; GG and GI have a free reducing end and they differ only at C5 stereochemistry of the uronic acid residue near the reducing end. GG2 and GI2 epimers have the same sequence like GG and GI but they are alkylated at their reducing end.

Ions were separated in FAIMS using 2.4 MHz bi-sinusoidal waveform between dispersion voltages (DV) 1.50 - 1.95 kV and the carrier gas used was air. No modifiers were added to the carrier gas.

ESI-FAIMS-EDD

The positive CV scan (0-30 V) was carried out (negative CV scan did not yield any ions) and the specific CV at which the ion of interest appears in the MS was noted and subsequently used to selectively and continuously transmit one ion at a time for EDD

experiments. Indirectly heated hollow cathode was used for generating electrons for EDD experiments. Isolation refinement of the precursor was done in the external quadrupole where the ions were accumulated for 1–2.5 s before they enter the FTICR-MS analyzer cell. The isolation/cell fill was repeated up to 3 times. In-cell isolation with a coherent harmonic excitation frequency (CHEF) event was used for further ion selection. The precursor ions were irradiated with electrons for 1 second. For electron irradiation the cathode bias, ECD lens, and cathode heater were set at -19 V, -18.6V, and 1.6A respectively. The 36 acquisitions per mass spectrum were averaged and for each mass spectrum 512 k points were acquired, padded with one zero fill, and apodized using a sinebell window. Background spectra were acquired by leaving all parameters the same but setting the cathode bias to 0 V to ensure that no electrons reached the analyzer cell. All EDD products are reported using the Domon and Costello nomenclature [59].

Principal Component Analysis (PCA)

PLS toolbox (Eigenvector research, inc., Wenatchee, WA) was used for the principal component analysis (PCA). The intensity of 19 assigned fragment ions for each spectrum was used for PCA analysis. These fragment ions were selected based on relative intensity and then normalized using the intensity of the base peak from the background spectra. Each row of the data matrix consists of the mass spectra of each particular epimer sample, while each column contained the normalized peak intensities for the selected fragment ions. During the PCA analysis, the data was mean-centered and cross-validated. For each epimer peak, the spectra were acquired in quintuplicate starting with the same precursor intensity and using the same EDD experimental conditions.

RESULTS AND DISCUSSION

As the MS/MS methods for GAGs have improved, there has been considerable interest in applying these approaches for the analysis of GAGs samples from natural sources, which are often heterogeneous mixtures. Particularly difficult is the characterization of isomeric oligosaccharides, which produce isobaric molecular ions in the MS step and generally identical MS/MS fragmentation patterns. In some cases, a mixture of different length GAGs may produce molecular ions with overlapping mass-to-charge values, resulting from longer oligomers having higher charge states. All these hurdles make complete characterization of GAG mixtures using mass spectrometry difficult. FAIMS separation is orthogonal to mass-to-charge separation in MS and can selectively and continuously transmit an ion of selected differential mobility into the mass spectrometer, thus making it possible to use multiple ion activation methods within a single experiment on an FT-ICR platform. Unlike LC and CE methods, FAIMS has the ability to continuously transmit selected ions, enabling the utilization of a host of ion activation methods for GAGs, some of which require a long activation time (seconds to tens of seconds), and/or significant signal-averaging, such as EDD.

Charge State Separation by ESI-FAIMS

Enzymatic depolymerization of chondroitin sulfate (CS) or dermatan sulfate (DS) yields oligomers of composition ΔHexA(GalNAc SO_3^--HexA)$_n$GalNAcSO_3^-) where n=1,2,3, etc., as shown in the inset of Figure 6.1a. The mass spectrum in Figure 1a exhibits a peak at *m/z* 458.06, which corresponds to group of isobaric molecular ions $[M-mH]^{m-}$ for Δ-unsaturated CS/DS oligosaccharides of various lengths, with m=n+1. Although the spacing of the isotope peaks above m/*z* 458.06 indicates the presence of a mixture of different charge states, it is not possible, using mass-to-charge discrimination,

to isolate a length-selected component for MS/MS analysis by mass filtering. On the other hand, FAIMS is able to separate this mixture of gas phase ions $[M\text{-}mH]^{m-}$ for dp 4, 6, 8 and10 for chondroitin sulfate (CSA) before the MS analysis.

The mixture that produced the data in Figure 1a was composed of oligomers dp4, dp6, dp8 and dp10. The dispersion voltage (DV) used was 1950 V with a compensation voltage (CV) scan from11-20 V, and a step size of 0.2 V. The extracted ion chromatogram (EIC) for ions of m/z 458.06 obtained from this scan is shown in Figure 1(b), which shows the separation of the various oligomers in the mixture. The mass-to-charge separation of the isotope peaks at CV 12.0 V allows us to assign this peak to dp4 $[M\text{-}2H]^{2-}$.

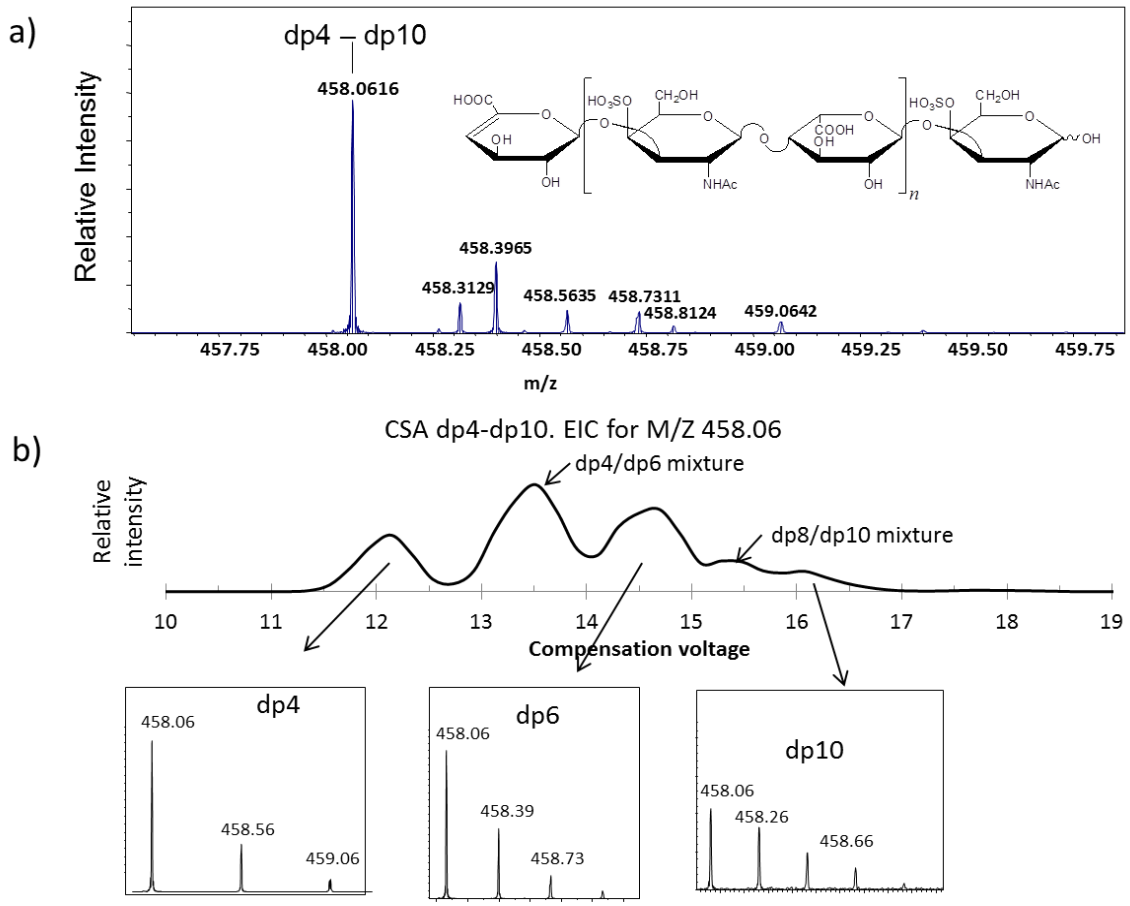

Figure 6.2. MS and the EIC of the mixture of dp4, dp6, dp8 and dp10 of chondroitin sulfate A (CSA). a) The general structure of the dermatan sulfate (DS) and CS oligomers that ionize to produce an overlapping charge states at m/z 458.06 and the mass spectrum of the mixture showing the overlapping isotopic distributions of four different charge states. b) FAIMS MS Extracted ion chromatogram (EIC) for m/z 458.06 with the respective MS spectra at the indicated CV voltages for which various individual ions are transmitted into the FTICR.

The other charge states in the EIC profile are not baseline resolved but at specific CV only a single charge state is transmitted into the MS. The isotope profile at CV 14.5V

shows that only dp6 $[M-3H]^{3-}$ is transmitted at that CV, while dp 10 $[M-5H]^{5-}$ is the sole component passed at a CV of 16.2 V. Interestingly, the number of distinct FAIMS peaks observed is greater than the number of components in the mixture. Some components appear in more than one peak within the CV scan. A mixture of dp4 and dp 6 appear at CV 13.5 V while dp8 $[M-4H]^{4-}$ and dp10 ion appear at CV 15.4 V. Dp4 and dp6 appear as separate EIC peaks and as a mixture; the same is observed for the dp10 that appears as an individual peak and also as a mixture with dp8 peak. This suggests the existence of different stable conformers or anomers from individual molecular ions that are separated within the FAIMS device, with some having a unique differential mobility that distinguishes them from other charge states, while others have similar mobility to other charge states. The extracted ion chromatogram for the second peak in each charge state isotope distributions confirms this conclusion (Figure 6.3).

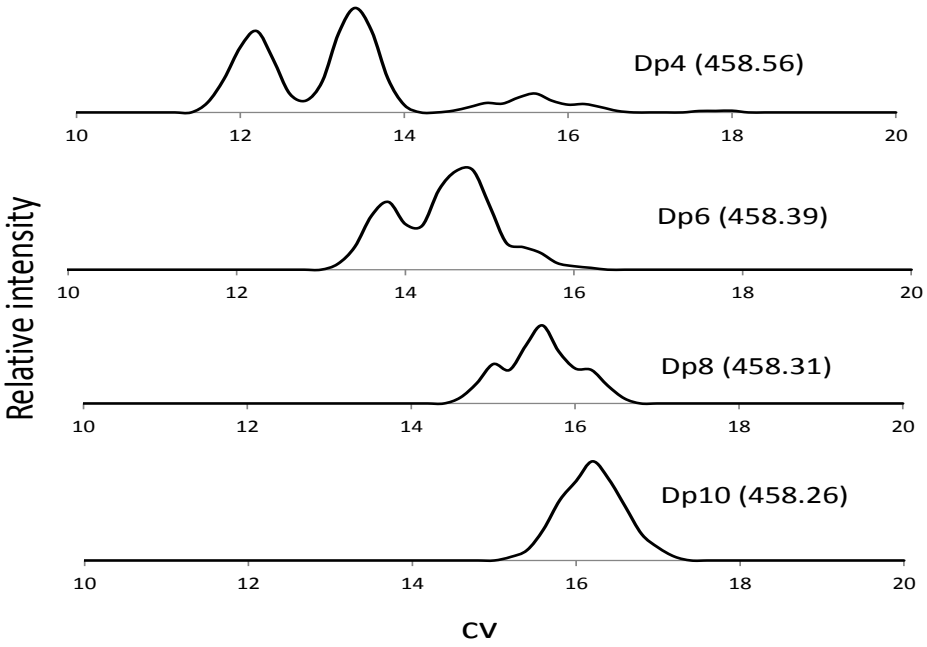

Figure 6.3. Extracted ion chromatograms for the second peak in each charge state isotope distributions for each individual species in the CSA dp4-dp10 mixture. M/Z 458.56 extracted for the dp4 is identical to the third stable isotope for [dp 8] $^{4-}$ so the dp4 peak appearing after the cv 14.2 is assumed to be from dp8 and not from dp4

Epimeric Tetrasaccharides

Even more challenging to analyze is a mixture of diastereomers. The structures of two pairs of synthetically-produced diastereomeric heparan sulfate tetramers, GG, GI, GG2 and GI2, are shown in figure 6.1. The labels denote the type of uronic acid moiety in the first and the third residues, respectively, from the non-reducing end. GG indicates GlcA in the first and third residues from the nonreducing end, while GI has IdoA in the third residue, which differs from glucuronic acid only by the stereochemistry of C5. GG2 and GI2 epimers are alkylated at the reducing end while GG and GI contain a free

reducing end. In solution, the anomeric isomers of the reducing end sugar are in equilibrium with each other for the non-alkylated samples (GG and GI). In contrast, the alkylated samples (GG2 and GI2) have a single conformation of the anomeric carbon established during synthesis. In order to separate and characterize individual sets of epimeric tetramers, a mixture containing 0.05 mg/ml of each epimer was electro-sprayed using normal electrospray at the rate of 120 μL/h. The dispersion voltage within the electrode gap was 1800 V and four spectra were averaged at every 0.2 V. The molecular ions of interest appeared within a CV range of 9-22 V.

Figure 5.4 shows the CV scan obtained for the GG and GI molecular ion $[M-2H]^{2-}$, m/z 467.06. The epimer containing two glucuronic acids (GG) produced only one main peak at CV 16.6 V, while epimer (GI) produced two main distinct peaks with the first and the second peak appearing at CV 15.0 V and 18.5 V respectively. There is also a small peak at CV 13.0 V that appears in both epimers. The assignment of the peaks from the two epimers was confirmed by introducing each individual epimer separately into the ESI-FAIMS-MS.

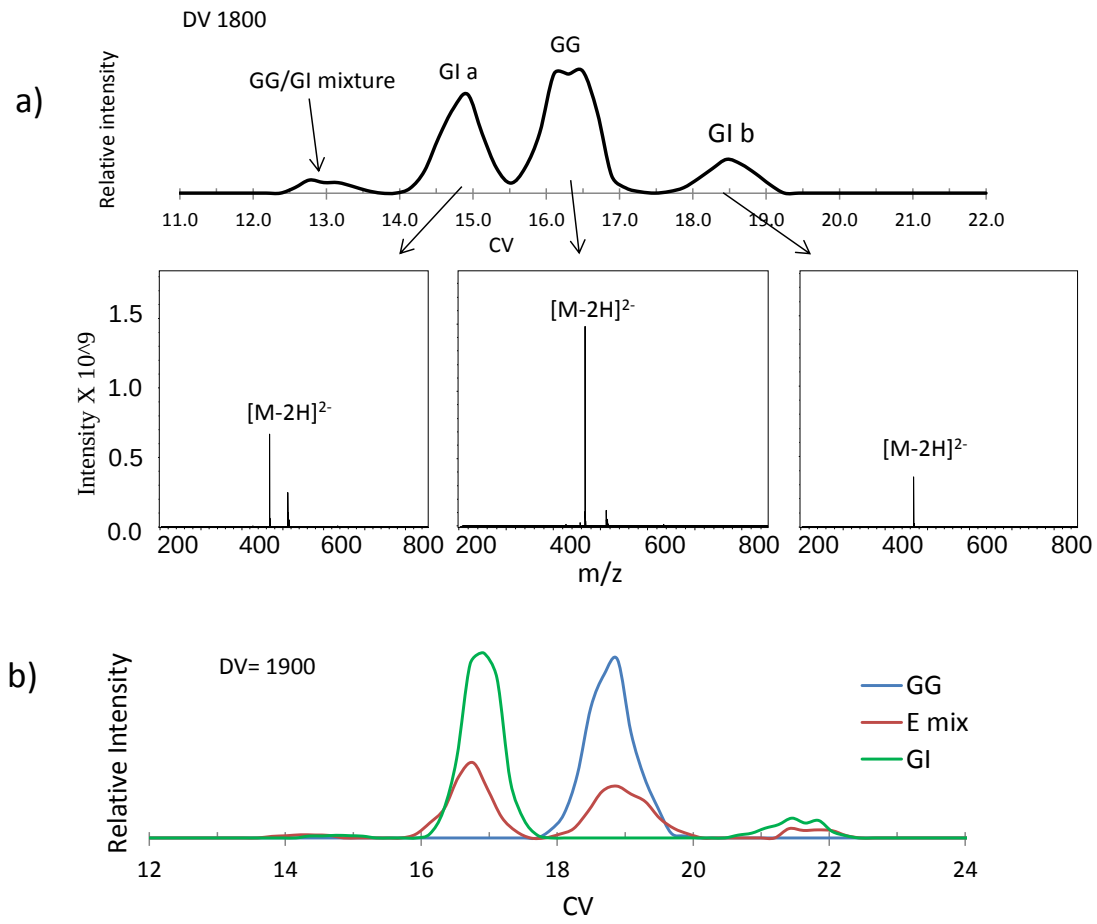

Figure 6.4. EIC for the epimeric mixture $[M-2H]^{2-}$ m/z 467.06. (a) EIC for a mixture of GG and GI epimers with the MS at different peaks showing the separation of ions of the same mass-to-charge. (b) EIC for individual epimers overlayed on the EIC of the mixture. The GG molecular ion appears as a single peak while that of GI appear as two distinct peaks.

The appearance of multiple peaks for the GI epimer suggests a mixture of conformers or anomers. The reducing end sugar undergoes equilibration in solution, and so both anomers are expected in the sample that was analyzed. The presence of the acyclic form of the reducing end sugar could also introduce an additional component to the mixture, although this form is expected to be a minor component in solution. Finally,

a mixture of conformers may also separate by FAIMS. Multiple peaks from a single reducing end monosaccharide residue have been observed in IMS experiments before [40]. Although GG and GI both have equal anomeric and acyclic form possibilities, the flexibility of iduronic acid may be responsible for more peaks being observed in the EIC profile of the GI epimer. The appearance of a single major peak for epimer GG could suggests a single dominant conformer or anomer, although it could also indicate a mixture of unresolved components.

Iduronic acid is known to be more flexible than glucuronic acid, and to exist as a mixture of different chair and skew conformations including $^{4}C_{1}$, $^{1}C_{4}$ and $^{2}S_{0}$ [60, 61]. This explains the appearance of more peaks for GI than GG $[M-2H]^{2-}$ molecular ion, although we cannot discount the possibility that the peaks may consist of unresolved multiple gas phase conformers of the molecule originating from the ESI process. The small peak at 13.0 V could be conformers of both epimers having the same FAIMS behavior.

To explore the origin of the multiple peaks in the CV scan, the two epimers that are alkylated at the reducing end, GG2 and GI2, respectively, were selected for FAIMS-MS analysis. With these samples, the reducing end stereochemistry is locked into the α configuration, thus reducing the complexity of the sample. The CV scan obtained for the molecular ion $[M-2H]^{2-}$ produces only one main peak for each individual epimer as shown in Figure 6.5, suggesting that some of the additional FAIMS peaks obtained for the GG and GI epimers with a free RE resulted from the anomeric α and β isomers.

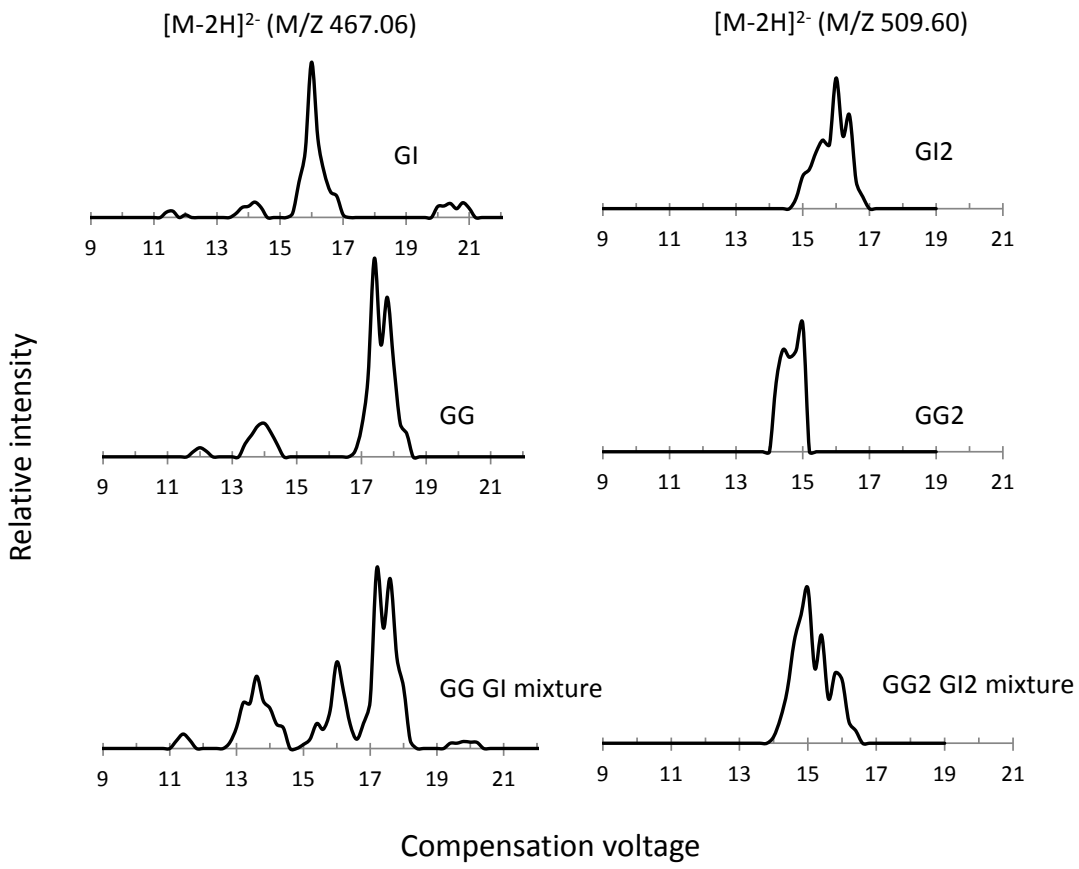

Figure 6.5. Comparison between the GG and GI $[M-2H]^{2-}$ (m/z 467.06) EIC with the corresponding $[M-2H]^{2-}$ (M/Z 509.60) EIC obtained from GG2 and GI2 epimers. Multiple peaks are observed from the epimers with a free reducing end while only one main peak is observed for GG2 and GI2 epimers. In both cases, ions for each epimer can be separately passed into the FTICR for MS/MS analysis.

Investigation of a higher charge state molecular ion $[M-3H]^{3-}$ for both sets of epimers produced similar result where two or more peaks are observed for epimers with free reducing end (GG and GI) and only one peak is observed for each epimer GG2 and GI2 (Figure 6.6).

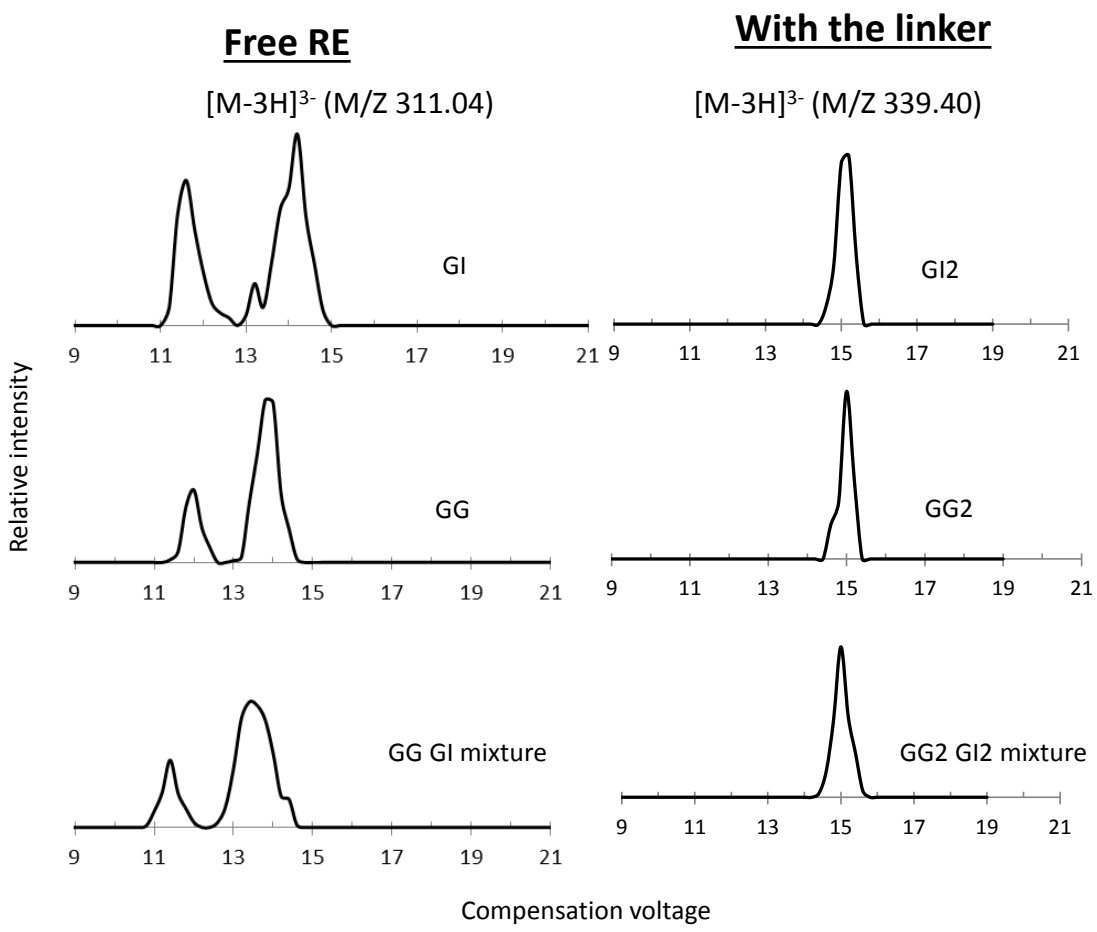

Figure 6.6. Extracted ion chromatograms for the $[M-3H]^{3-}$ for the four epimers showing multiple peaks that are observed for the free reducing ended GG and GI and single peaks from GG2 andGI2 that are alkylated at their reducing end.

Another observation for the $[M-3H]^{3-}$ is that there is less separation in the CV scan between the epimers, suggesting closer similarity in configuration when the molecular ion assumes an extended form due to charge-charge repulsion. Although the components are not baseline separated in their CV scan, GG2 and GI2 for $[M-2H]^{2-}$ (509.60) are well-enough separated to enable selective introduction of an individual epimer ion for MS/MS analysis. Only $[M-2H]^{2-}$ ion for GG2 ion is observed at CV 14.5 while only GI2 is present at CV 16.0 V. The separation of the alkylated GG2 and GI2

epimers is due to differences in the uronic acid C5 stereochemistry, since the reducing end is alkylated, locking in the stereochemistry of C_1 for these samples. The iduronic acid residue is known to be more flexible that the glucuronic acid residue, causing differences in the overall shape of the molecules. Chemical reduction of the reducing end of GG and GI epimers using $NaBH_4$ using the procedure described before [62] also reduced the number of peaks per single species to one, again suggesting that anomeric mixtures produce multiple peaks in the CV scan of the non-reduced samples (data not shown).

We also investigated the effect of Na^+ cationization on the FAIMS MS separation of the four epimers by extracting ion chromatograms of the molecular ions that contain Na^+. All the four epimers generally produced single main peaks indicating that Na^+ alters the shape of the molecules and thus the mobilities within the FAIMS device. Na^+, being larger than the H^+, has been noted to bind multiple oxygen atoms within the GAG molecules which leads to more stable gas phase ion conformations and thus a more defined shape [38]. In this particular case, the presence of Na^+ leads to gas phase configurations with similar differential mobility. There is less separation for the GG and GI epimers compared to GG2 and GI2 sodiated molecular ions as seen in Supplemental Figure 6.7. Having a single peak per component during the analysis will be especially important when dealing with complex mixtures.

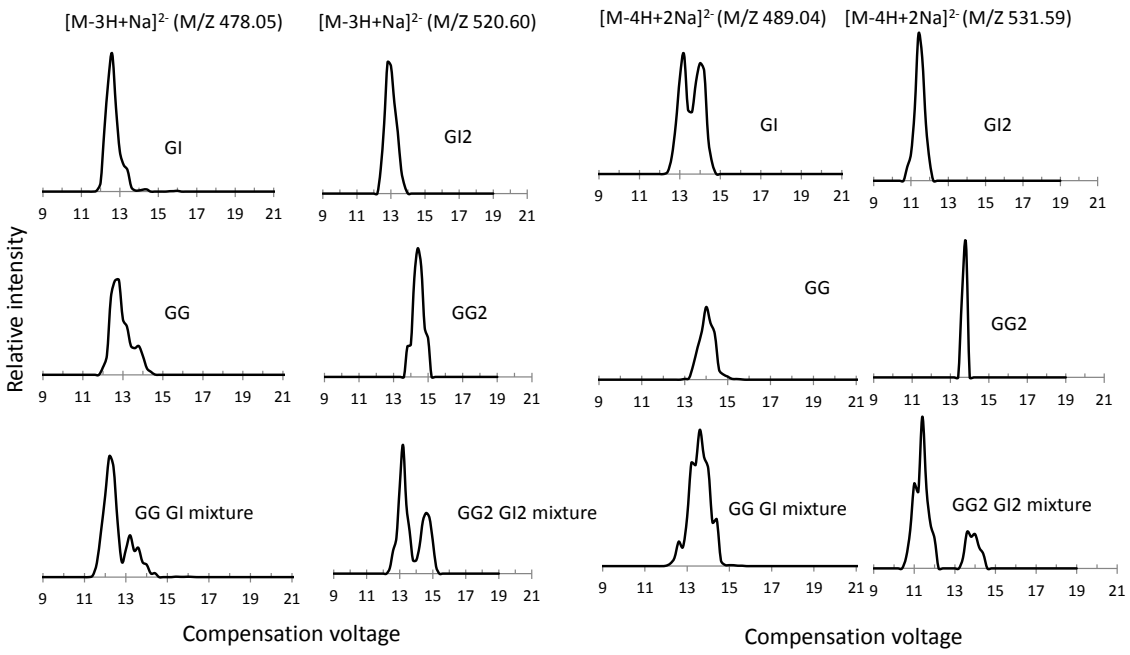

Figure 6.7. EIC of other useful molecular ions $[M-3H+Na]^{2-}$ and $[M-4H+2Na]^{2-}$ for the two sets of epimers. Each epimer produced a single principal peak, thus reducing the complexity of mixture. Sodiated ion of the alkylated GG2 and GI2 show better separation compared to GG and GI epimers.

FAIMS-FTICR-EDD for the Epimers

To explore the potential of applying MS/MS on the separated molecular ions, CV separated GG and GI $[M-2H]^{2-}$ were selected for EDD experiments. From a CV scan, the respective value was obtained for the $[M-2H]^{2-}$ of each epimer, GG and GI. The CV values were used to select a single epimer for the EDD experiments. Although there was a general reduction in signal intensity at high DV, the intensity of the two peaks emanating from the epimer GI differed with the DV voltage applied in a reverse order. The relative intensity of the first peak increased with the increase in the DV voltage, while that of the second peak decreased (Figure 6.8).

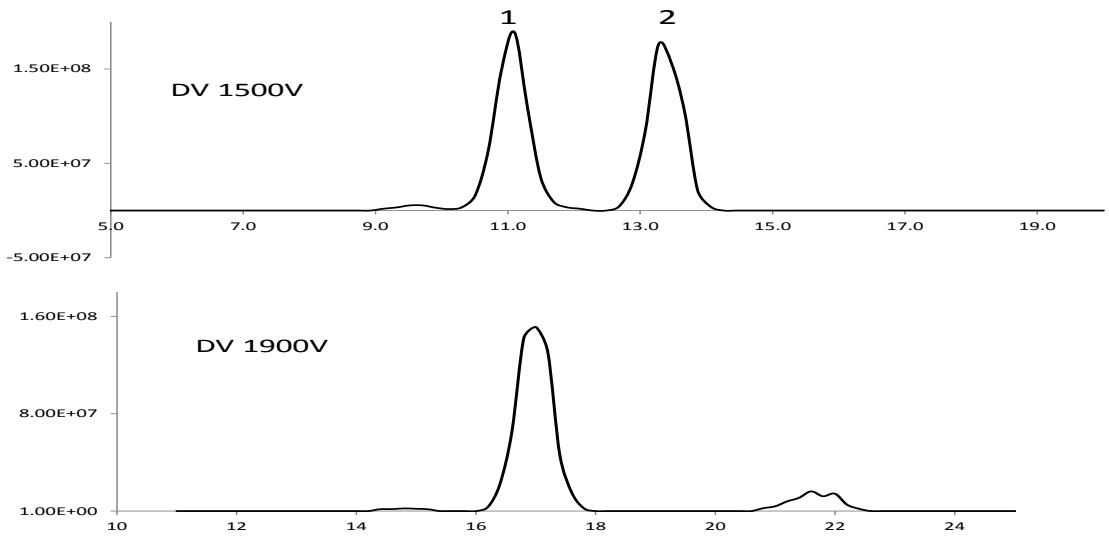

Figure 6.8. Showing the changes in abundance of the two main components of GI epimer with the dispersion voltage. Peak 2 amplitude diminishes with the at high DV 1900 V while peak 2 amplitude slightly increases compared to their amplitude at lower DV of 1500 V.

This behavior is observed for type A and C ions, respectively, with cylindrical FAIMS [45], but there is no focusing effect from inhomogeneous fields with planar FAIMS, so other mechanisms must be responsible, for example heating of the ions by the higher DV producing a change in their conformational equilibrium. DV 1800V was used for the selection and EDD fragmentation and all other experimental conditions were identical and all the experiments were done the same day. The uniformity of the EDD precursor intensity was ensured for all the selected peaks and each experiment was done in quintuplicate. Background spectra were acquired by leaving the other experimental conditions constant but changing the value of the ECD bias to zero to ensure no electrons reaches the analyzer cell.

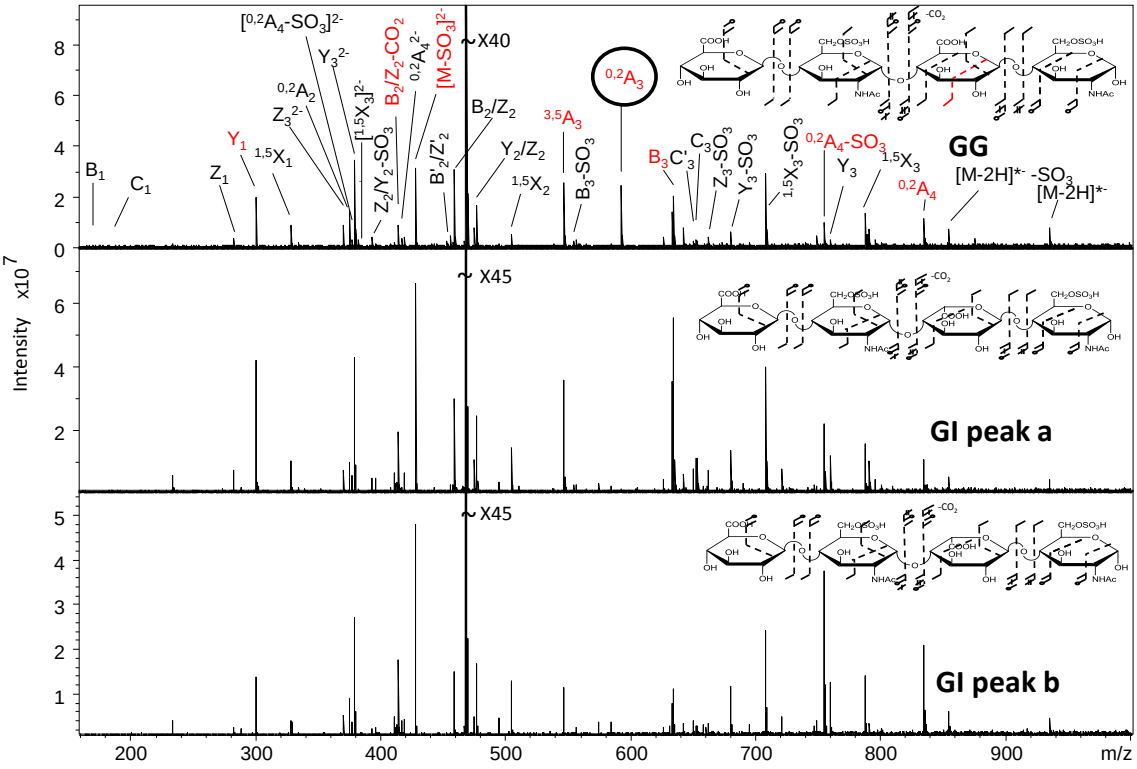

Figure 6.9. EDD spectra for the FAIMS separated GG and GI epimers, $[M-2H]^{2-}$ molecular ions. A single GG peak and two GI peaks (GI peak a and b) were isolated from a mixture and subjected to EDD analysis. $^{0,2}A_3$ peak (encircled) is only contained in the GG spectra. EDD spectra from the two GI (GI a and GI b) peaks have many similarities, displaying similar fragmentation patterns, but with consistently different abundances. PCA identified Ions that differ significantly within the spectra, these ions are colored in red.

EDD spectra obtained from the three peaks are shown in Figure 6.4. EDD fragmentation patterns were similar to those observed in previous studies [19, 20]. The three spectra are rich in both glycosidic and cross-ring cleavages. The majority of peaks were glycosidic bond cleavages, and among the cross-ring fragments, there are more A type cleavages compared to the X type. Most of the assigned ions peaks are observed in

the three spectra except the ion $^{0,2}A_3$ (encircled in Fig 6.9) which is only present in the GG epimer spectra, consistent with earlier findings on the EDD fragmentation of GlcA versus IdoA [20].

Principal Component Analysis of EDD Data

Multivariate analysis (MVA) of complex data has previously been used to distinguish closely related MS spectra [63, 64], and more recently, PCA of the EDD data was used to differentiate four epimeric heparan sulfate tetra-saccharides [65]. To compare the fragment ion intensities for the EDD spectra obtained from the three CV values, principal component analysis was used. The data obtained from principal component analysis indicate that the three spectra differ in terms of the fragment ion intensities. As shown in Figure 6.10a, the first principal component (PC1) distinguishes the two GI peaks in the CV scan, while PC2 distinguishes GG spectra from both GI spectra. The two principal components account for 96 % of the spectral differences.

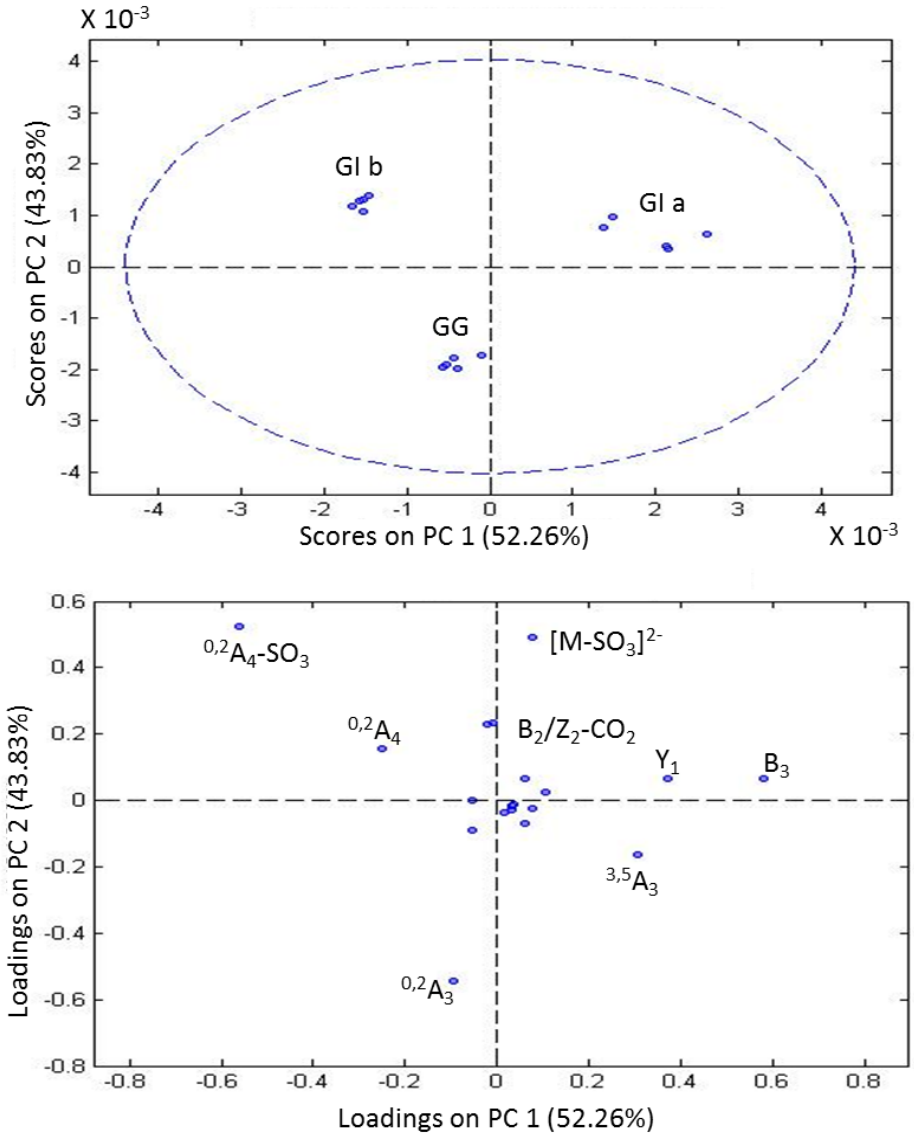

Figure 6.10. PCA results for the EDD spectra obtained from the three $[M-2H]^{2-}$ FAIMS separated EIC peaks. (a) A plot of the first two principal components distinguishes the three sets of spectra obtained, with 95% of the spectral differences accounted for by these two principal components. (b) The loading plot for the first two principal components reveals the ions whose intensities differentiate the three sets of EDD spectra. The further away the ion is from the center of the plot, the more significant it is in distinguishing the three sets of spectra.

A close observation of the loading plot in Figure 5b reveals the fragment ions that differ significantly between the spectra. These includes; $^{0,2}A_4$-SO_3, $^{0,2}A_4$, B_2/Z_2-CO_2, $[M\text{-}SO_3]^{2-}$, B_3, Y_1, $^{3,5}A_3$, and $^{0,2}A_3$ (they are shown in red in Figure 6.9). Some of these ions have been correlated with differences in the EDD behavior of GlcA versus IdoA [20]. The observed differences in the fragmentation intensities of the two GI peaks show that conformational differences have a significant effect on the dissociation behavior of the gas-phase ions.

CONCLUSION

EDD is known to be an important tool for the MS/MS characterization of GAGs, due to its ability to produce spectra with high-information content, including both glycosidic and cross-ring cleavages. The results obtained in this study indicate that by combining FAIMS with FTICR-MS, it is possible to separate isomeric or isobaric GAG gas phase ions which have the same mass-to-charge, and therefore can't be separated by a mass analyzer, including stereoisomers or conformers. Such GAG ions can then be characterized using EDD. The fragmentation patterns from EDD of different gas-phase conformations of GI were similar, but with consistently observed intensity differences, as revealed by PCA analysis. This gas phase separation method can be used as an alternative to solution phase separation methods such as HPLC to resolve GAGs isomer mixtures. The complexity introduced from single components producing multiple FAIMS peaks can be reduced by removing anomeric isomers from the mixture, via alkylating the reducing end or by chemical reduction of the reducing end monosaccharide. A reduction of complexity in the CV scan can also be achieved by using sodium adduction. Sodiated

molecular ions have been found to give very detailed structural information for highly sulfated GAGs [16, 28]. The work provides a step forward towards the characterization of these useful biomolecules from their natural sources.

ACKNOWLEDGMENTS

MJK, LL, RJL, and IJA gratefully acknowledge financial support from the National Institutes of Health, R01-GM038060. MJK, AV, GJB, and IJA gratefully acknowledge financial support from the National Institutes of Health, P41-GM103390. MJK personally acknowledges Dr. Franklin Leach for useful discussions about mass spectrometry analysis of GAGs.

REFERENCES

1. Vynios, D. H.; Karamanos, N. K. and Tsiganos, C. P., Advances in analysis of glycosaminoglycans: its application for the assessment of physiological and pathological states of connective tissues. *J. Chromatogr. B.* **2002**, 781, 21-38.
2. Capila, I. and Linhardt, R. J., Heparin–Protein Interactions. *Angew. Chem. Int. Ed.* **2002**, 41, 390-412.
3. Hardingham, T. and Fosang, A., Proteoglycans: many forms and many functions. *The FASEB Journal.* **1992**, 6, 861-870.
4. Gandhi, N. S. and Mancera, R. L., The Structure of Glycosaminoglycans and their Interactions with Proteins. *Chem. Biol. Drug Des.* **2008**, 72, 455-482.
5. Bernfield, M.; Götte, M.; Park, P. W.; Reizes, O.; Fitzgerald, M. L.; Lincecum, J. and Zako, M., Functions of Cell Surface Heparan Sulfate Proteoglycans. *Annu. Rev. Biochem.* **1999**, 68, 729-777.
6. Lortat-Jacob, H.; Grosdidier, A. and Imberty, A., Structural diversity of heparan sulfate binding domains in chemokines. *Proc. Natl. Acad. Sci. U. S. A.* **2002**, 99, 1229-1234.
7. Gupta, P.; McCarthy, J. and Verfaillie, C., Stromal fibroblast heparan sulfate is required for cytokine-mediated ex vivo maintenance of human long-term culture-initiating cells. *Blood.* **1996**, 87, 3229-3236.

8. Ly, M.; Leach III, F. E.; Laremore, T. N.; Toida, T.; Amster, I. J. and Linhardt, R. J., The proteoglycan bikunin has a defined sequence. *Nat. Chem. Biol.* **2011**, 7, 827-833.

9. Guerrini, M.; Naggi, A.; Guglieri, S.; Santarsiero, R. and Torri, G., Complex glycosaminoglycans: profiling substitution patterns by two-dimensional nuclear magnetic resonance spectroscopy. *Anal. Biochem.* **2005**, 337, 35-47.

10. Oguma, T.; Toyoda, H.; Toida, T. and Imanari, T., Analytical method of chondroitin/dermatan sulfates using high performance liquid chromatography/turbo ionspray ionization mass spectrometry: application to analyses of the tumor tissue sections on glass slides. *Biomed. Chromatogr.* **2001**, 15, 356-362.

11. Zaia, J. and Costello, C. E., Compositional Analysis of Glycosaminoglycans by Electrospray Mass Spectrometry. *Anal. Chem.* **2000**, 73, 233-239.

12. Zhang, Z. and Linhardt, R. J., Sequence Analysis of Native Oligosaccharides Using Negative ESI Tandem MS. *Curr. Anal. Chem.* **2009**, 5, 225-237.

13. Zaia, J.; McClellan, J. E. and Costello, C. E., Tandem Mass Spectrometric Determination of the 4S/6S Sulfation Sequence in Chondroitin Sulfate Oligosaccharides. *Anal. Chem.* **2001**, 73, 6030-6039.

14. Zaia, J.; Li, X.-Q.; Chan, S.-Y. and Costello, C. E., Tandem mass spectrometric strategies for determination of sulfation positions and uronic acid epimerization in chondroitin sulfate oligosaccharides. *J. Am. Soc. Mass Spectrom.* **2003**, 14, 1270-1281.

15. Zaia, J. and Costello, C. E., Tandem Mass Spectrometry of Sulfated Heparin-Like Glycosaminoglycan Oligosaccharides. *Anal. Chem.* **2003**, 75, 2445-2455.

16. Kailemia, M. J.; Li, L.; Ly, M.; Linhardt, R. J. and Amster, I. J., Complete mass spectral characterization of a synthetic ultralow-molecular-weight heparin using collision-induced dissociation. *Anal. Chem.* **2012**, 84, 5475-5478.

17. Saad, O. M. and Leary, J. A., Heparin Sequencing Using Enzymatic Digestion and ESI-MSn with HOST: A Heparin/HS Oligosaccharide Sequencing Tool. *Anal. Chem.* **2005**, 77, 5902-5911.

18. Meissen, J.; Sweeney, M.; Girardi, M.; Lawrence, R.; Esko, J. and Leary, J., Differentiation of 3-O-sulfated heparin disaccharide isomers: Identification of structural aspects of the heparin CCL2 binding motif. *J. Am. Soc. Mass Spectrom.* **2009**, 20, 652-657.

19. Wolff, J. J.; Amster, I. J.; Chi, L. and Linhardt, R. J., Electron Detachment Dissociation of Glycosaminoglycan Tetrasaccharides. *J. Am. Soc. Mass Spectrom.* **2007**, 18, 234-244.

20. Wolff, J. J.; Chi, L.; Linhardt, R. J. and Amster, I. J., Distinguishing Glucuronic from Iduronic Acid in Glycosaminoglycan Tetrasaccharides by Using Electron Detachment Dissociation. *Anal. Chem.* **2007**, 79, 2015-2022.

21. Leach Iii, F. E.; Wolff, J. J.; Laremore, T. N.; Linhardt, R. J. and Amster, I. J., Evaluation of the experimental parameters which control electron detachment dissociation, and their effect on the fragmentation efficiency of glycosaminoglycan carbohydrates. *Int. J. Mass Spectrom.* **2008**, 276, 110-115.

22. Wolff, J. J.; Laremore, T. N.; Busch, A. M.; Linhardt, R. J. and Amster, I. J., Electron Detachment Dissociation of Dermatan Sulfate Oligosaccharides. *J. Am. Soc. Mass Spectrom.* **2008**, 19, 294-304.

23. Leach Iii, F. E.; Xiao, Z.; Laremore, T. N.; Linhardt, R. J. and Amster, I. J., Electron detachment dissociation and infrared multiphoton dissociation of heparin tetrasaccharides. *Int. J. Mass Spectrom.* **2011**, 308, 253-259.

24. Wolff, J. J.; Leach, F. E.; Laremore, T. N.; Kaplan, D. A.; Easterling, M. L.; Linhardt, R. J. and Amster, I. J., Negative Electron Transfer Dissociation of Glycosaminoglycans. *Anal. Chem.* **2010**, 82, 3460-3466.

25. Leach III, F. E.; Wolff, J. J.; Xiao, Z.; Ly, M.; Laremore, T. N.; Arungundram, S.; Al-Mafraji, K.; Venot, A.; Boons, G.-J. and Linhardt, R. J., Negative electron transfer dissociation Fourier transform mass spectrometry of glycosaminoglycan carbohydrates. *Eur. J. Mass Spectrom.* **2011**, 17, 167.

26. Zaia, J.; Miller, M. J. C.; Seymour, J. L. and Costello, C. E., The Role of Mobile Protons in Negative Ion CID of Oligosaccharides. *J. Am. Soc. Mass Spectrom.* **2007**, 18, 952-960.

27. Naggar, E. F.; Costello, C. E. and Zaia, J., Competing fragmentation processes in tandem mass spectra of heparin-like glycosaminoglycans. *J. Am. Soc. Mass Spectrom.* **2004**, 15, 1534-1544.

28. Kailemia, M. J.; Li, L.; Xu, Y.; Liu, J.; Linhardt, R. J. and Amster, I. J., Structurally Informative Tandem Mass Spectrometry of Highly Sulfated Natural and Chemoenzymatically Synthesized Heparin and Heparan Sulfate Glycosaminoglycans. *Mol. Cell. Proteomics.* **2013**, 12, 979-990.

29. Desaire, H. and Leary, J. A., The effects of coordination number and ligand size on the gas phase dissociation and stereochemical differentiation of cobalt-coordinated monosaccharides. *Int. J. Mass Spectrom.* **2001**, 209, 171-184.

30. Wolff, J. J.; Laremore, T. N.; Aslam, H.; Linhardt, R. J. and Amster, I. J., Electron-Induced Dissociation of Glycosaminoglycan Tetrasaccharides. *J. Am. Soc. Mass Spectrom.* **2008**, 19, 1449-1458.

31. Volpi, N.; Maccari, F. and Linhardt, R. J., Capillary electrophoresis of complex natural polysaccharides. *Electrophoresis.* **2008**, 29, 3095-3106.

32. Costell, C.; Contado-Miller, J. and Cipollo, J., A glycomics platform for the analysis of permethylated oligosaccharide alditols. *J. Am. Soc. Mass Spectrom.* **2007**, 18, 1799-1812.

33. Hitchcock, A. M.; Costello, C. E. and Zaia, J., Glycoform quantification of chondroitin/dermatan sulfate using a liquid chromatography-tandem mass spectrometry platform. *Biochemistry (Mosc).* **2006**, 45, 2350-2361.

34. Schenauer, M. R.; Meissen, J. K.; Seo, Y.; Ames, J. B. and Leary, J. A., Heparan Sulfate Separation, Sequencing, and Isomeric Differentiation: Ion Mobility Spectrometry Reveals Specific Iduronic and Glucuronic Acid-Containing Hexasaccharides. *Anal. Chem.* **2009**, 81, 10179-10185.

35. Staples, G. O.; Bowman, M. J.; Costello, C. E.; Hitchcock, A. M.; Lau, J. M.; Leymarie, N.; Miller, C.; Naimy, H.; Shi, X. and Zaia, J., A chip-based amide-HILIC LC/MS platform for glycosaminoglycan glycomics profiling. *Proteomics.* **2009**, 9, 686-695.

36. Bruggink, C.; Wuhrer, M.; Koeleman, C. A. M.; Barreto, V.; Liu, Y.; Pohl, C.; Ingendoh, A.; Hokke, C. H. and Deelder, A. M., Oligosaccharide analysis by capillary-scale high-pH anion-exchange chromatography with on-line ion-trap mass spectrometry. *J. Chromatogr. B.* **2005**, 829, 136-143.

37. Maslen, S.; Sadowski, P.; Adam, A.; Lilley, K. and Stephens, E., Differentiation of Isomeric N-Glycan Structures by Normal-Phase Liquid Chromatography−MALDI-TOF/TOF Tandem Mass Spectrometry. *Anal. Chem.* **2006**, 78, 8491-8498.

38. Jin, L.; Barran, P. E.; Deakin, J. A.; Lyon, M. and Uhrín, D., Conformation of glycosaminoglycans by ion mobility mass spectrometry and molecular modelling. *PCCP.* **2005**, 7, 3464-3471.

39. Fenn, L. S. and McLean, J. A., Structural resolution of carbohydrate positional and structural isomers based on gas-phase ion mobility-mass spectrometry. *PCCP.* **2011**, 13, 2196-2205.

40. Dwivedi, P.; Bendiak, B.; Clowers, B. H. and Hill Jr, H. H., Rapid Resolution of Carbohydrate Isomers by Electrospray Ionization Ambient Pressure Ion Mobility Spectrometry-Time-of-Flight Mass Spectrometry (ESI-APIMS-TOFMS). *J. Am. Soc. Mass Spectrom.* **2007**, 18, 1163-1175.

41. Clowers, B. H.; Dwivedi, P.; Steiner, W. E.; Hill, J. H. H. and Bendiak, B., Separation of Sodiated Isobaric Disaccharides and Trisaccharides Using Electrospray Ionization-Atmospheric Pressure Ion Mobility-Time of Flight Mass Spectrometry. *J. Am. Soc. Mass Spectrom.* **2005**, 16, 660-669.

42. Li, H.; Giles, K.; Bendiak, B.; Kaplan, K.; Siems, W. F. and Hill Jr, H. H., Resolving structural isomers of monosaccharide methyl glycosides using drift tube and traveling wave ion mobility mass spectrometry. *Anal. Chem.* **2012**, 84, 3231-3239.

43. Seo, Y.; Andaya, A. and Leary, J. A., Preparation, separation, and conformational analysis of differentially sulfated heparin octasaccharide isomers using ion mobility mass spectrometry. *Anal. Chem.* **2012**, 84, 2416-2423.

44. Schneider, B. B.; Covey, T. R.; Coy, S. L.; Krylov, E. V. and Nazarov, E. G., Chemical Effects in the Separation Process of a Differential Mobility/Mass Spectrometer System. *Anal. Chem.* **2010**, 82, 1867-1880.

45. Purves, R. W. and Guevremont, R., Electrospray Ionization High-Field Asymmetric Waveform Ion Mobility Spectrometry−Mass Spectrometry. *Anal. Chem.* **1999**, 71, 2346-2357.

46. Barnett, D. A.; Ells, B.; Guevremont, R. and Purves, R. W., Separation of leucine and isoleucine by electrospray ionization-high field asymmetric waveform ion mobility spectrometry-mass spectrometry. *J. Am. Soc. Mass Spectrom.* **1999**, 10, 1279-1284.

47. Guevremont, R. and Purves, R. W., High field asymmetric waveform ion mobility spectrometry-mass spectrometry: an investigation of leucine enkephalin ions produced by electrospray ionization. *J. Am. Soc. Mass Spectrom.* **1999**, 10, 492-501.

48. Gabryelski, W. and Froese, K. L., Rapid and sensitive differentiation of anomers, linkage, and position isomers of disaccharides using High-Field Asymmetric

Waveform Ion Mobility Spectrometry (FAIMS). *J. Am. Soc. Mass Spectrom.* **2003**, 14, 265-277.

49. Creese, A. J. and Cooper, H. J., Separation and identification of isomeric glycopeptides by high field asymmetric waveform ion mobility spectrometry. *Anal. Chem.* **2012**, 84, 2597-2601.

50. Robinson, E. W.; Garcia, D. E.; Leib, R. D. and Williams, E. R., Enhanced Mixture Analysis of Poly(ethylene glycol) Using High-Field Asymmetric Waveform Ion Mobility Spectrometry Combined with Fourier Transform Ion Cyclotron Resonance Mass Spectrometry. *Anal. Chem.* **2006**, 78, 2190-2198.

51. Levin, D. S.; Vouros, P.; Miller, R. A. and Nazarov, E. G., Using a nanoelectrospray-differential mobility spectrometer-mass spectrometer system for the analysis of oligosaccharides with solvent selected control over ESI aggregate ion formation. *J. Am. Soc. Mass Spectrom.* **2007**, 18, 502-511.

52. Kolakowski, B. M. and Mester, Z., Review of applications of high-field asymmetric waveform ion mobility spectrometry (FAIMS) and differential mobility spectrometry (DMS). *Analyst.* **2007**, 132, 842-864.

53. Shvartsburg, A. A.; Bryskiewicz, T.; Purves, R. W.; Tang, K.; Guevremont, R. and Smith, R. D., Field Asymmetric Waveform Ion Mobility Spectrometry Studies of Proteins: Dipole Alignment in Ion Mobility Spectrometry? *J. Phys. Chem. B.* **2006**, 110, 21966-21980.

54. Shvartsburg, A. A.; Creese, A. J.; Smith, R. D. and Cooper, H. J., Separation of Peptide Isomers with Variant Modified Sites by High-Resolution Differential Ion Mobility Spectrometry. *Anal. Chem.* **2010**, 82, 8327-8334.

55. Robinson, E. W. and Williams, E. R., Multidimensional Separations of Ubiquitin Conformers in the Gas Phase: Relating Ion Cross Sections to H/D Exchange Measurements. *J. Am. Soc. Mass Spectrom.* **2005**, 16, 1427-1437.

56. Arungundram, S.; Al-Mafraji, K.; Asong, J.; Leach, F. E.; Amster, I. J.; Venot, A.; Turnbull, J. E. and Boons, G.-J., Modular Synthesis of Heparan Sulfate Oligosaccharides for Structure−Activity Relationship Studies. *J. Am. Chem. Soc.* **2009**, 131, 17394-17405.

57. Leach III, F. E.; Ly, M.; Laremore, T. N.; Wolff, J. J.; Perlow, J.; Linhardt, R. J. and Amster, I. J., Hexuronic Acid Stereochemistry Determination in Chondroitin Sulfate Glycosaminoglycan Oligosaccharides by Electron Detachment Dissociation. *J. Am. Soc. Mass Spectrom.* **2012**, 23, 1488-1497.

58. Muñoz, E.; Xu, D.; Avci, F.; Kemp, M.; Liu, J. and Linhardt, R. J., Enzymatic synthesis of heparin related polysaccharides on sensor chips: Rapid screening of heparin-protein interactions. *Biochem. Biophys. Res. Commun.* **2006**, 339, 597-602.

59. Domon, B. and Costello, C. E., A Systematic Nomenclature for Carbohydrate Fragmentations in Fab-Ms Ms Spectra of Glycoconjugates. *Glycoconjugate J.* **1988**, 5, 397-409.

60. Remko, M. and von der Lieth, C.-W., Gas-Phase and Solution Conformations of the α-L-Iduronic Acid Structural Unit of Heparin. *J. Chem. Inf. Model.* **2006**, 46, 1194-1200.

61. Mulloy, B. and Forster, M. J., Conformation and dynamics of heparin and heparan sulfate. *Glycobiology.* **2000**, 10, 1147-1156.

62. Pomin, V. H.; Sharp, J. S.; Li, X.; Wang, L. and Prestegard, J. H., Characterization of glycosaminoglycans by 15N NMR spectroscopy and in vivo isotopic labeling. *Anal. Chem.* **2010**, 82, 4078-4088.

63. Berman, E. S. F.; Kulp, K. S.; Knize, M. G.; Wu, L.; Nelson, E. J.; Nelson, D. O. and Wu, K. J., Distinguishing Monosaccharide Stereo- and Structural Isomers with TOF-SIMS and Multivariate Statistical Analysis. *Anal. Chem.* **2006**, 78, 6497-6503.

64. Fängmark, I.; Jansson, A. and Nilsson, B., Determination of Linkage Position and Anomeric Configuration in Glucose-Containing Disaccharide Alditols by Multivariate Analysis of Data from Mass Spectrometry. *Anal. Chem.* **1999**, 71, 1105-1110.

65. Oh, H.; Leach, F.; Arungundram, S.; Al-Mafraji, K.; Venot, A.; Boons, G.-J. and Amster, I., Multivariate Analysis of Electron Detachment Dissociation and Infrared Multiphoton Dissociation Mass Spectra of Heparan Sulfate Tetrasaccharides Differing Only in Hexuronic acid Stereochemistry. *J. Am. Soc. Mass Spectrom.* **2011**, 22, 582-590.

CHAPTER 7

CONCLUSIONS

One of the key challenge for complete characterization of sulfated glycosaminoglycans have been loss of SO_3 groups during ion activation thus leading to less structural information especially for the highly sulfated chains. The work described here highlights a way to stabilize the SO_3 groups in these biologically relevant chains and then activating them using collision induced dissociation to get more informative structural information. Ionizing all or all but one acidic group within the highly sulfated chains through charge and Na^+/H^+ exchange strengthens the molecules against the unwanted SO_3 loss during CID. This is believed to occur due to the ability of the Na^+ (unlike hydrogen) to bind with multiple oxygen atoms of both the sulfo groups and the glycosidic bond oxygen thus minimizing fragments resulting from loss of SO_3 and at the same time increasing the more useful ring fragments.

This was first demonstrated using a pentasaccharide heparin like drug Arixtra which has 8 sulfo groups thus more than three sulfates per disaccharide unit. Ionizing 8 acidic groups which is equal to the number of SO_3 groups in the chain helped in getting a few glycosidic fragment ions through collision activation providing very little information about the structure. It is only when all the ionizable groups were deprotonated that we ended having more fragment ions that were found to be useful.

The findings from these experiments prompted us to test other heparin like compounds including chemoenzymatically produced chains. It was found that the method can be useful for long highly sulfated chains and even less sulfated ones. For example a dp8 with 11 sulfate groups from the naturally occurring ones and a dp12 with 10 sulfate groups for the chemoenzymatically produced chains. The compounds with a free reducing end were found to produce very intense cross-ring fragments ^{0,2}A and ^{2,4}A fragments at the reducing end. ^{0,2}A fragment was believed to be due to the reducing end ring opening and retro aldo rearrangements. The ^{0,2}A ion formed can easily form ^{2,4}A fragments through rearrangements within the remaining residue. These observations were corroborated due to lack of these ^{0,2}A and ^{2,4}A fragments in the reducing end of the chains with locked reducing end like Arixtra and the chemoenzmatically produced GAGs.

During this initial work, it was noted that glucuronic acid residue had some fragment ions that were not in the iduronic acid residue. These findings lend us to investigate other kinds of compound including CSA and DS chains. It was noted that only particular molecular ions produced all the diagnostic ions and the diagnostic ions also had a given charge and Na^+ cation characteristics. The molecular ions had a single mobile proton and the ^{2,4}A and ^{0,2}X diagnostic fragments also had their own characteristics. Since these ions were uronic acid C5 stereochemistry specific, their fragmentation mechanism should have some relationship with the glucuronic and iduronic acid characteristics. The shorter the chain the less diagnostic their fragments were so there were no unique fragments for the dp 4 and dp6 CSA and DS. For the longer chains like dp8 and dp 10 there were fragments that were only present in glucuronic acid in CSA but not in iduronic acid counterparts in DS chains.

Another key obstacle to complete characterization of glycosaminoglycans is their presence in multiple isomeric glycoforms. Although liquid chromatography and capillary electrophoresis have been applied to separate oligomers prior MS analysis, some compounds like epimeric ones are hard to separate using these methods. Another key issue with these methods is that they separate in time and thus use of multiple ion activation methods to explore a give elute is limited. In the work described here, epimeric heparan sulfate tetrasaccharides were separated using gas phase field asymmetric-waveform ion mobility (FAIMS). FAIMS separate in space rather than time so it's suitable when you are using more than one ion activation method to activate the precursor ions or when the ion activation method like EDD that requires more time to acquire a spectrum than the LC peak elution duration. This work also indicates that it's possible to separate anomers. Although separation of anomers shows that FAIMS is a separation method with high specificity, multiple peaks obtained from these separations can hinder correct interpretation of the results. The multiplicity of peaks can be reduced by either reducing the reducing end or introducing a derivative that locks the reducing end to one state. The closeness of the spectra obtained from ion activation of isomeric molecular ions can be simplified using PCA analysis and the peaks that differ between the spectra can be obtained.

APPENDICES

APPENDIX A

SUPPLEMENTAL DATA FOR CHAPTER 3

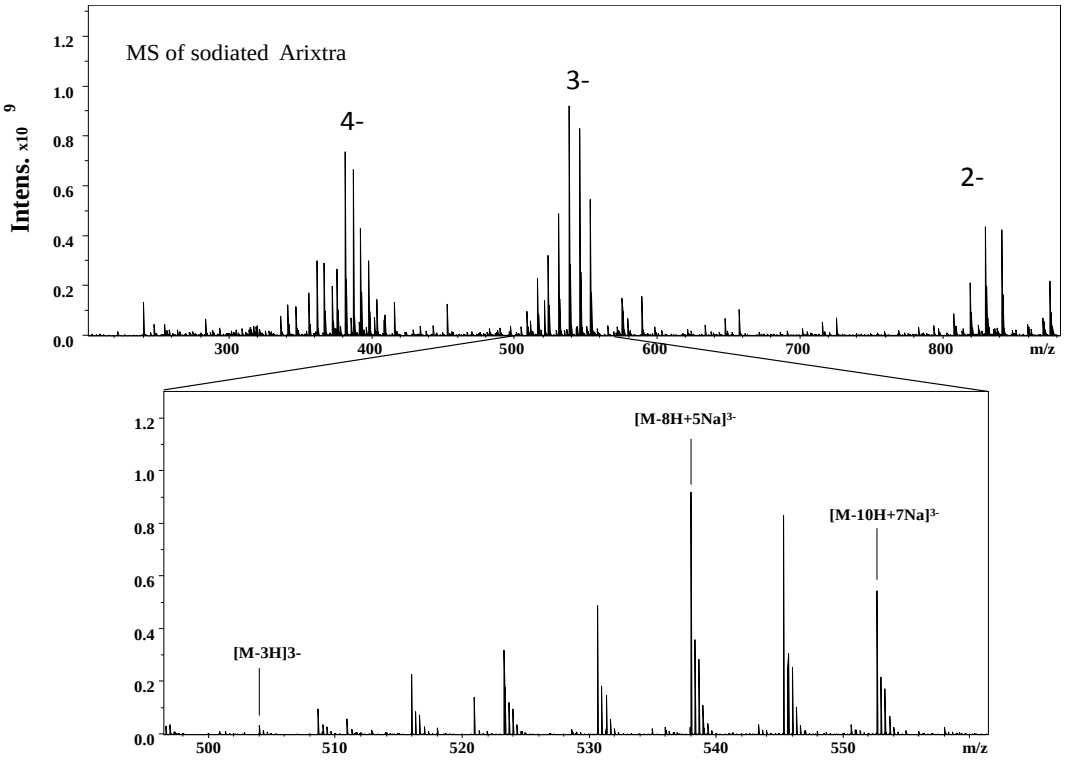

Figure. Mass spectrum of Arixtra in aqueous methanol containing 1mM NaOH.

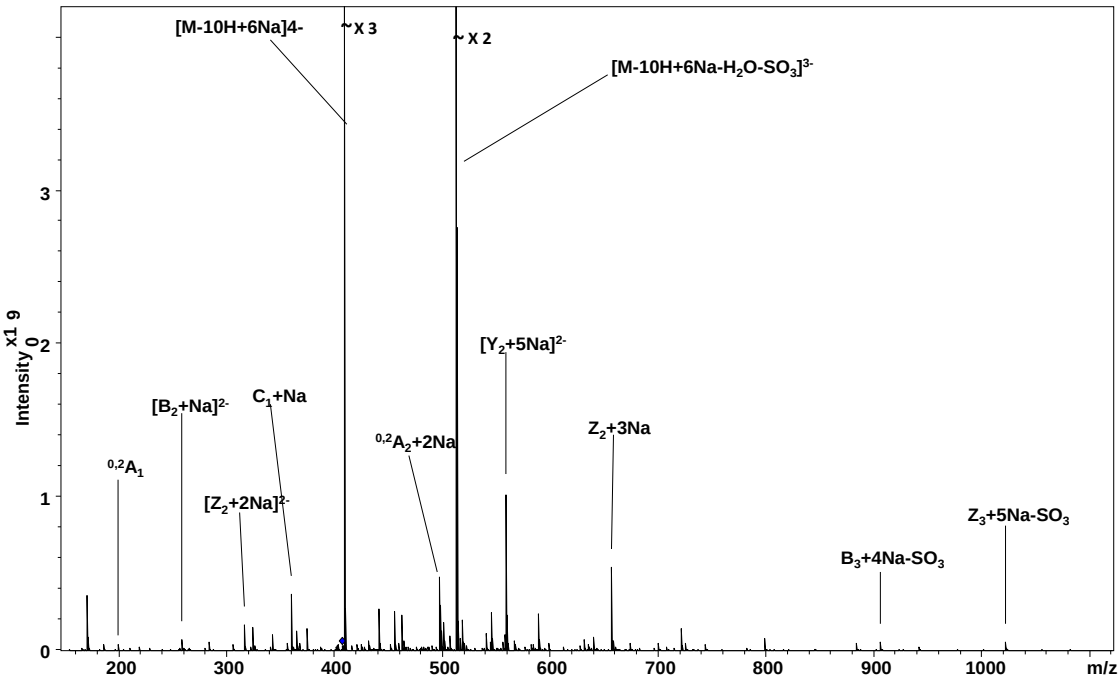

Figure. CID spectra for Arixtra $[M-10H+6Na]^{4-}$

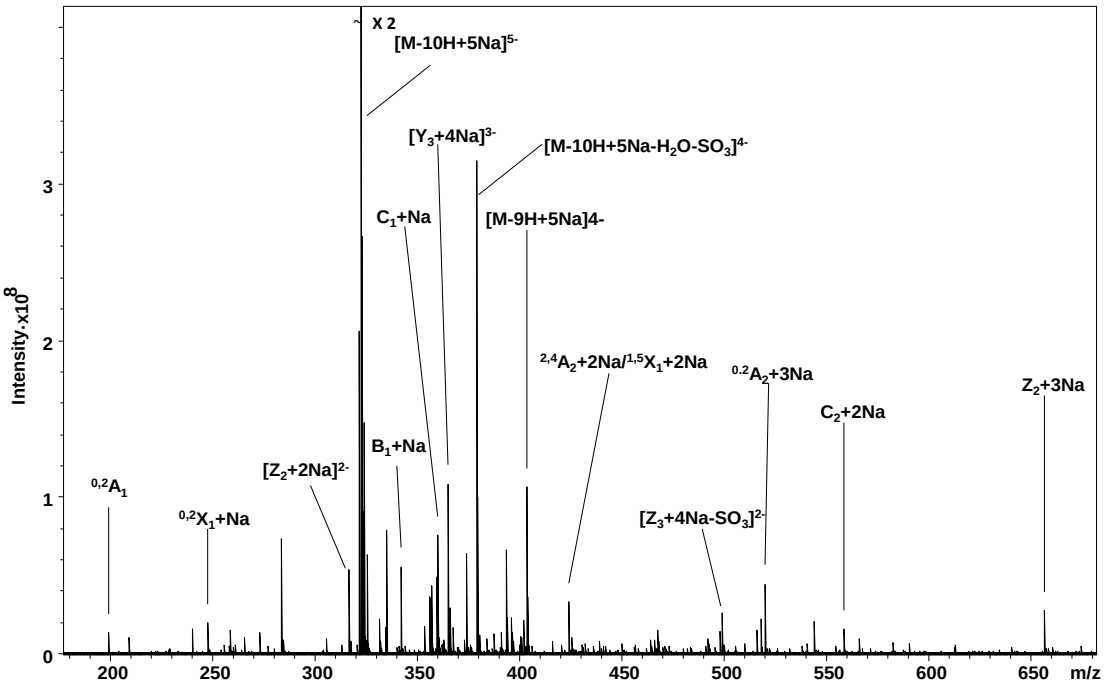

Figure. CID spectra for Arixtra $[M-10H+5Na]^{5-}$

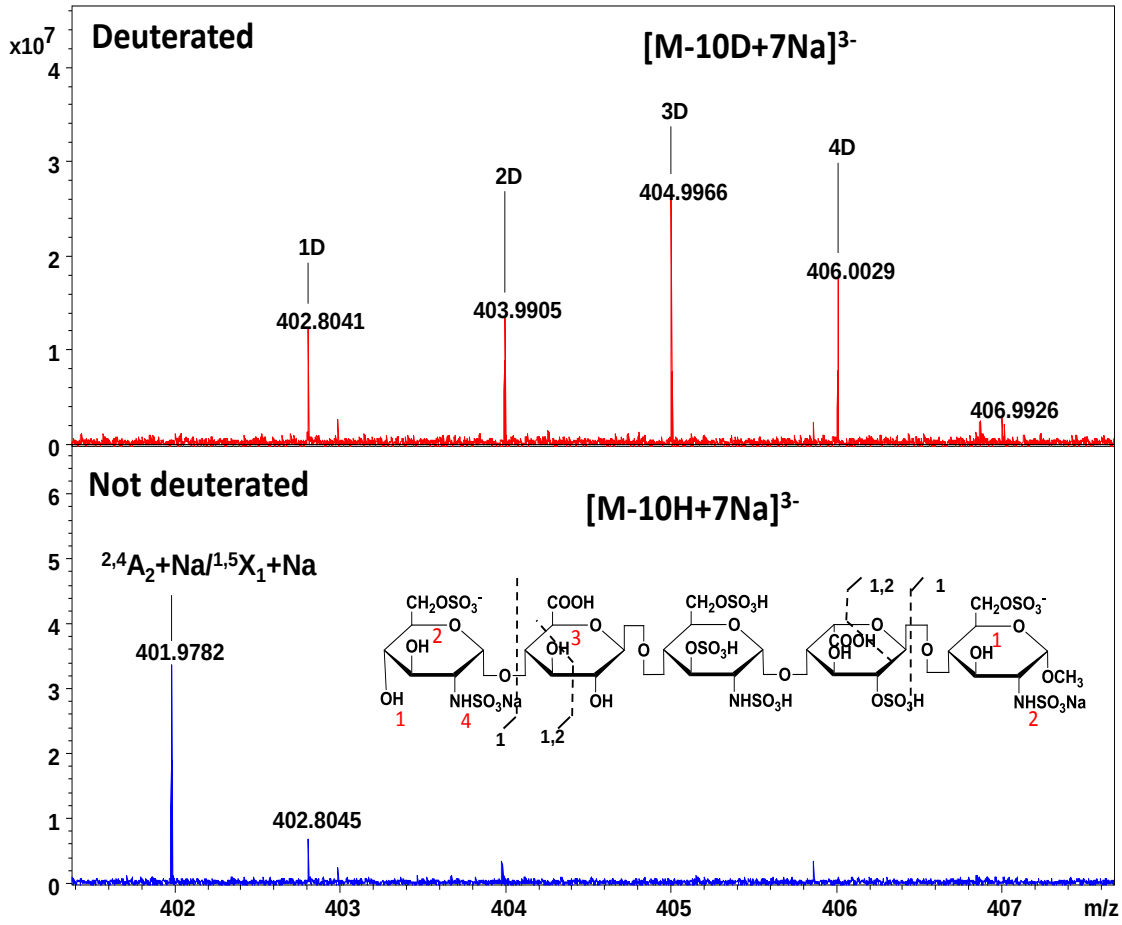

Figure. H/D exchange for 2,4A 2+Na/1,5X1+Na isobaric peaks

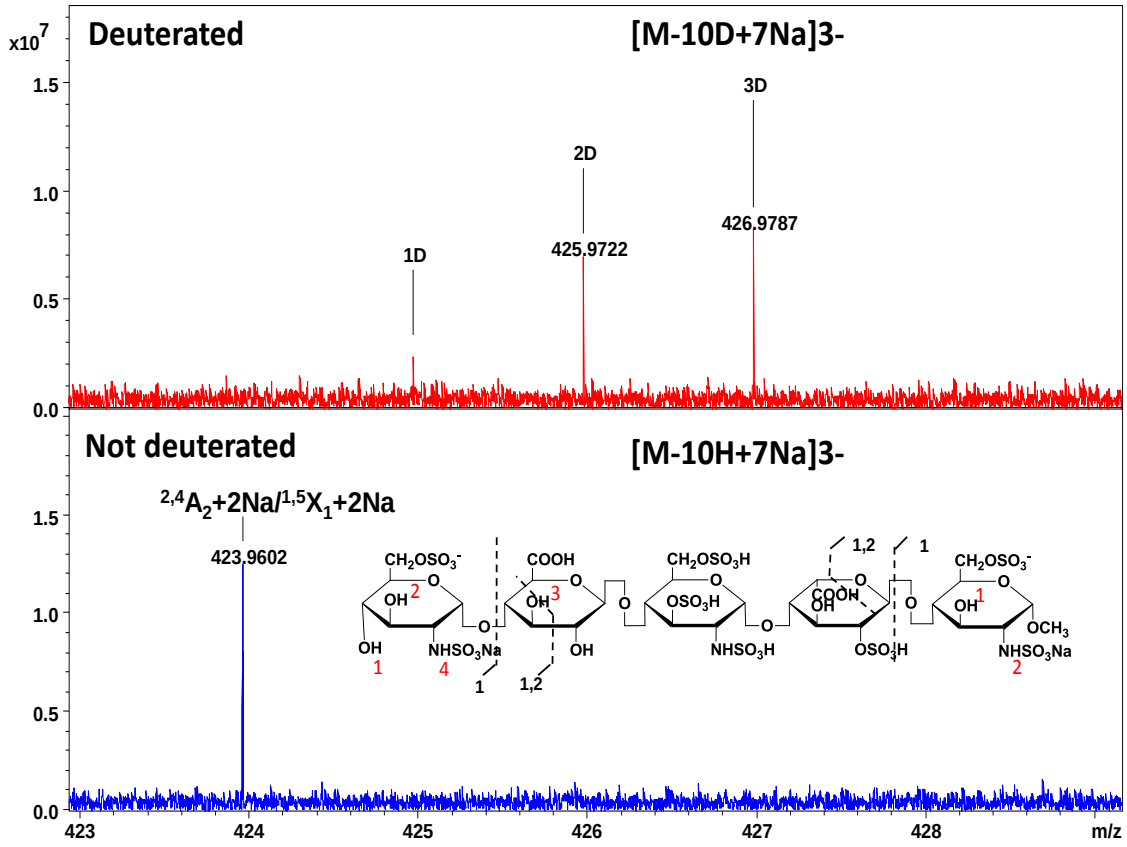

Figure. H/D exchange for 2,4A 2+2Na/1,5X1+2Na Isobaric peaks.

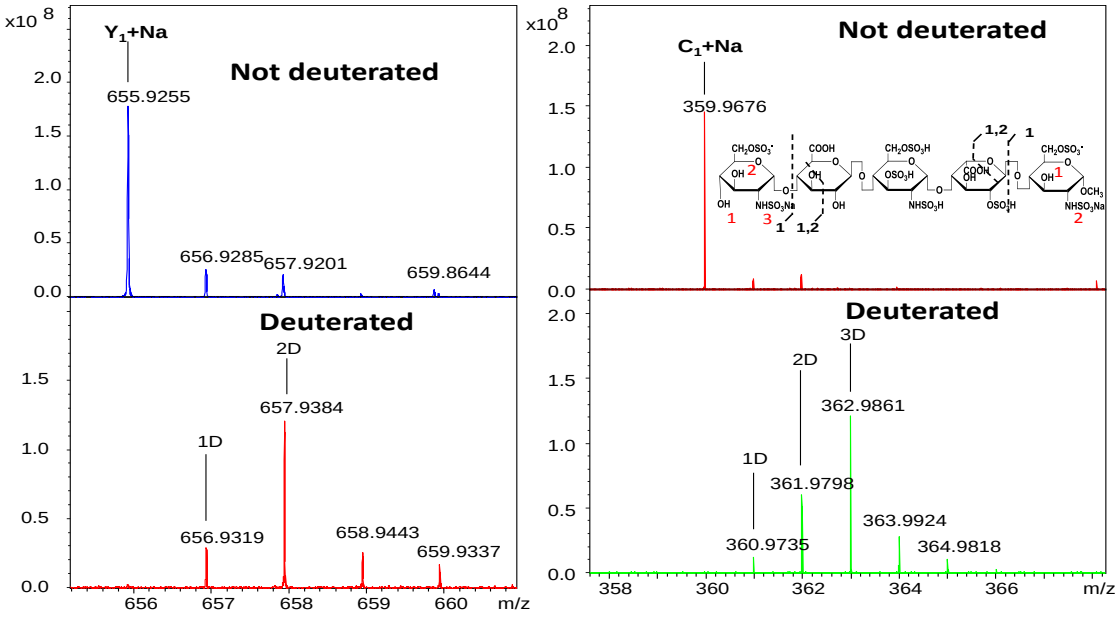

Figure. H/D exchange for Y_1+Na and C_1+Na.

Table. Arixtra $[M-8H+4Na]^{3-}$ peak list.

Mass to charge	Assignment	Intensity	Accuracy PPM
416.0499	B2-SO3	1.28E+07	1.27
438.0318	B2+Na-SO3	3207123	1.32
456.0425	C2+Na-SO3	3255512	0.96
484.6419	[M-8H+5Na-2SO3]3-	7436939	-0.07
496.007	B2	6331788	0.46
496.9553	[Y3+3Na-SO3]2-	6754740	0.67
503.9665	[M-7H+4Na-SO3]3-	1.72E+07	0.63
507.9461	[Y3+4Na-SO3]2-	1.49E+07	1.00
511.2939	[M-8H+5Na-SO3]3-	6.72E+08	0.46
517.9888	[B4+2Na-2SO3]2-	3.85E+08	0.73
517.9888	B2+Na	3.85E+08	0.73
532.0049	Z2+Na-SO3	4300042	-0.04
535.9994	C2+Na	3.40E+07	0.63
537.946	[M-8H+4Na]3-	6.56E+08	0.74
547.9248	[Y3+4Na]2-	5.33E+08	0.38
558.9158	[Y3+5Na]2-	2.16E+07	0.33
635.9413	[Y4+4Na]2-	1.81E+07	-0.38
646.9324	[Y4+5Na]2-	2.57E+07	-0.56

Table. Arixtra [M-10H+7Na] $^{3-}$ peak list.

Mass to charge	Assignment	Intensity	Accuracy PPM
198.9917	0,2A1	1.17E+07	0.44
240.0182	B2-SO3	3339319	0.54
314.0551	0,2X1-2SO3	4666034	0.19
316.4681	[Z2+2Na]2-	4089132	0.25
341.9571	B2+Na	4.16E+07	-0.06
355.9727	Z1+Na	1.04E+07	0.22
359.9676	C1+Na	1.47E+08	0.11
373.9834	Y1+Na	4.05E+07	-0.16
401.9782	2,4A2+Na	3.37E+07	0.02
401.9782	1,5X1+Na	3.37E+07	0.15
415.9939	0,2X1+Na-SO3	9341459	0.02
423.9602	2,4A2+2Na	1.26E+07	-0.10
423.9602	1,5X1+2Na	1.26E+07	0.02
434.0611	C2-SO3	3989453	-0.25
438.0325	B2+Na-SO3	3.34E+07	-0.27
449.9696	[C3+3Na-SO3]2-	3357881	-0.48
451.9553	[B3+4Na-SO3]2-	3058211	-0.49
452.0479	Z2+Na-2SO3	4853705	0.40
456.0429	C2+Na-SO3	5197643	0.09
470.0585	Y2+Na-2SO3	2.33E+07	0.30
491.9336	[B3+4Na]2-	3913651	-0.24
497.9604	0,2A2+2Na	3.16E+07	0.31
500.9387	[C3+4Na]2-	2.21E+07	0.12
507.9465	[Y3+4Na-SO3]2-	2.65E+07	0.22
517.9327	0,2X1+2Na	6.82E+07	-0.08
517.9892	B2+Na	3.44E+07	-0.04
518.9371	[Y3+5Na-SO3]2-	9644630	0.93
539.9145	0,2X1+3Na	4452295	0.20
539.9712	B2+2Na	4.65E+07	-0.13
550.0155	Y2+Na-SO3	3244283	-0.11
552.601	[M-10H+7Na]3-	4.43E+08	0.06
553.9868	Z2+2Na-SO3	2.55E+07	0.05
557.9818	C2+2Na	3.46E+07	-0.20
558.916	[Y3+5Na]2-	7.01E+07	-0.03
569.9073	[Y3+6Na]2-	5498967	-0.60
571.9975	Y2+2Na-SO3	5555067	-0.19
575.9687	Z2+3Na-SO3	6866877	0.14
593.9792	Y2+3Na-SO3	5275453	0.24
648.9177	[Z4+6Na]2-	1.48E+07	0.05

655.9254	Z2+3Na	9.35E+07	0.27
673.9361	Y2+3Na	4.65E+07	0.06
677.9068	Z2+4Na	4353111	1.08
695.9182	Y2+4Na	2.49E+07	-0.16
904.917	B2+4Na-SO3	1.76E+07	0.48
940.9152	Z3+5Na-2SO3	1.14E+07	-0.13
1020.8725	Z3+5Na-SO3	1.31E+07	-0.61

Table. Assignment list for Arixtra $[M-10H+6Na]^{4-}$.

Mass to charge	Assignment	Intensity	Accuracy PPM
198.9917	0,2A1	3.93E+07	0.44
240.0182	B1-SO3	6035774	0.54
247.4717	0,2X1+Na	7040639	0.08
258.4909	[B2+Na]2-	7.56E+07	0.21
265.4988	[Z2+Na-SO3]2-	1.27E+07	0.02
305.4772	[Z2+Na]2-	3.60E+07	0.02
316.4681	[Z2+2Na]2-	1.72E+08	0.25
325.4734	[Y2+2Na]2-	3.02E+07	0.18
341.9572	B1+Na	1.05E+08	-0.35
355.6657	[Y4+2Na-2SO3]3-	1.65E+07	0.23
355.9727	Z1+Na	4.49E+07	0.22
359.9677	C1+Na	3.66E+08	-0.17
363.9389	B1+2Na	8632978	0.36
364.9475	[Y3+4Na]3-	1.25E+08	0.23
373.9833	Y1+Na	1.44E+08	0.11
381.9494	C1+2Na	4304885	0.50
382.3181	[Y4+2Na-SO3]3-	8277558	-0.13
390.9689	[Z4+4Na-SO3]3-	8904675	0.67
401.9783	2,4A2+Na	3.29E+07	-0.23
401.9783	1,5X1+Na	3.29E+07	-0.10
408.7033	[M-10H+6Na]4-	1.04E+10	0.42
415.9939	0,2X1+Na-SO3	3.33E+07	0.02
420.2768	[B4+5Na]3-	2.24E+07	0.11
423.9602	2,4A2+2Na	4.03E+07	-0.10
423.9602	1,5X1+2Na	4.03E+07	0.02
424.9488	[Z4+5Na]3-	2.78E+07	-0.13
426.9666	[1,5A3+3Na-SO3]2-	2.40E+07	0.12
426.9666	[2,4X2+3Na-SO3]2-	2.40E+07	0.18
430.9523	Y4+5Na]3-	6.38E+07	-0.08
438.0323	B2+Na-SO3	1.14E+07	0.18
440.9642	[B3+3Na-SO3]2-	2.71E+08	-0.22
445.9865	[Y3+2Na-2SO3]2-	5963797	-0.54
451.9551	3,5A2+2Na	1.55E+07	-0.06
451.9551	[B3+4Na-SO3]2-	1.55E+07	-0.04
456.043	C2+Na-SO3	1.54E+07	-0.13
491.9335	[B3+4Na]2-	1.19E+07	-0.04
497.9607	0,2A2+2Na	7.48E+07	-0.30
498.9414	[Z3+4Na-SO3]2-	1.27E+08	-0.14
500.9388	[C3+4Na]2-	1.10E+08	-0.08

509.9322	[Z3+5Na-SO3]2-	8882291	0.21
510.6124	[1,5A5+4Na]3-	7186648	-0.73
510.6124	[2,4X4+4Na]3-	7186648	-0.70
511.9298	[C3+5Na]2-	5315593	-0.13
517.9326	0,2X1+2Na	2.00E+08	0.11
517.9892	B2+Na	3.73E+07	-0.04
518.9373	[Y3+5Na-SO3]2-	5.88E+07	0.55
519.9427	0,2A2+3Na	4.52E+07	-0.38
535.9997	C2+Na	1.41E+07	0.07
539.9147	0,2X1+3Na	1.72E+07	-0.17
539.9712	B2+2Na	1.09E+08	-0.13
545.2738	[M-9H+6Na]3-	2.50E+08	-0.15
553.9867	Z2+2Na-SO3	1.68E+07	0.23
557.9816	C2+2Na	1.01E+08	0.16
558.916	[Y2+5Na]2-	1.03E+09	-0.03
569.907	[Y3+6Na]2-	1.94E+07	-0.07
575.9687	Z2+3Na	2.16E+07	0.14
579.9215	[0,2X3+5Na]2-	6305185	-0.40
590.9403	[B4+5Na-SO3]2-	1.55E+07	0.35
597.9485	[Z4+5Na-SO3]2-	4.75E+07	-0.24
641.9103	[B4+6Na]2-	6459701	-0.65
648.9183	[Z4+6Na]2-	1.18E+07	-0.88
655.9256	Z2+3Na	5.44E+08	-0.03
673.936	Y2+3Na	4.63E+07	0.21
677.9071	Z2+4Na	1.10E+07	0.63
695.9184	Y2+4Na	1.39E+07	-0.45
904.9173	B3+4Na-SO3	5.62E+07	0.14
926.8999	B3+5Na-SO3	6337397	-0.56
940.9143	Z4+5Na-2SO3	2.59E+07	0.83
1020.8724	Z3+5Na-SO3	5.90E+07	-0.51

Table. Assignment list for Arixtra $[M-10H+5Na]^{5-}$.

Mass to charge	Assignment	Intensity	Accuracy PPM
168.4893	C12-	1.03E+07	-0.53
175.497	Y12-	1.38E+07	0.34
198.9917	0,2A1	1.19E+08	0.44
207.5215	[B2-SO3]2-	5332529	0.39
214.4829	[3,5A2+Na]2-	6732445	0.13
214.4829	[B3+2Na-SO3]4-	6732445	0.14
240.0183	B1-SO3	7.61E+07	0.12
247.4717	0,2X1+Na	1.67E+08	0.08
247.4999	B22-	2.53E+07	0.32
254.0339	Z1-SO3	2.29E+07	0.51
258.0288	C1-SO3	3.26E+07	0.35
258.4909	[B2+Na]2-	1.47E+08	0.21
265.4987	[Z2+Na-SO3]2-	1.12E+08	0.40
267.4961	[C2+Na]2-	9842431	0.50
267.9634	[Y3+3Na]4-	6207507	-0.07
272.0445	Y1-SO3	5885870	0.33
274.504	[Y2+Na-SO3]2-	7816819	0.31
286.4866	[Y4+2Na-SO3]4-	8897724	0.42
294.0263	Y1+Na-SO3	6956130	0.82
296.9885	[Y3+2Na-2SO3]3-	1.52E+07	-0.28
298.4694	[B4+2Na]4-	1.15E+07	-0.15
303.9648	[B4+3Na]4-	4.00E+07	0.14
305.4771	[Z2+Na]2-	1.43E+08	0.34
309.4603	[B4+4Na]4-	2.82E+07	0.10
313.9621	1,5A1+Na	5331036	0.23
313.9621	2,4X0+Na	5331036	0.39
314.0552	0,2X1-SO3	5631049	-0.13
314.4825	[Y2+Na]2-	5672506	-0.05
316.4681	[Z2+2Na]2-	6.12E+08	0.25
320.2926	[B3+3Na]3-	6.28E+07	-0.06
322.3648	[M-10H+5Na]5-	4.84E+09	0.41
324.4656	[2.4A5+4Na]4-	7737584	0.04
324.4656	[1,5X4+4Na]4-	7737584	0.08
324.9645	[Z3+3Na-SO3]3-	6.84E+07	-0.06
325.4734	[Y2+2Na]2-	1.50E+08	0.18
326.296	[C3+3Na]3-	4.38E+07	0.31
341.9572	B1+Na	5.24E+08	-0.35
349.6621	[Z4+2Na-2SO3]3-	5639632	0.47
355.9727	Z1+Na	2.94E+08	0.22

359.9677	C1+Na	7.28E+08	-0.17
363.939	B1+2Na	2.98E+07	0.08
364.9475	[Y3+4Na]3-	1.58E+09	0.23
373.9833	Y1+Na	6.41E+08	0.11
377.9547	Z1+2Na	1.59E+07	0.08
381.9494	C1+2Na	6853826	0.50
386.2972	[B4+4Na-SO3]3-	6.57E+07	0.16
390.9691	[Z4+4Na-SO3]3-	3.09E+08	0.16
395.9652	Y1+2Na	3.77E+07	0.23
401.9783	2,4A2+Na	2.77E+08	-0.23
401.9783	1,5X1+Na	2.77E+08	-0.10
403.208	[M-9H+5Na]4-	4.61E+08	-0.04
412.9495	[B4+4Na]3-	8644652	0.07
415.9939	0,2X1+Na-SO3	1.02E+08	0.02
416.0504	B2-SO3	4.23E+07	0.07
420.2768	[B4+5Na]3-	1.02E+08	0.11
423.9603	2,4A2+2Na	4.58E+08	-0.33
423.9603	1,5X1+2Na	4.58E+08	-0.21
424.9488	[Z4+5Na]3-	5.88E+07	-0.13
426.9667	[1,5A3+3Na-SO3]2-	1.11E+07	-0.11
426.9667	[2,4X2+3Na-SO3]2-	1.11E+07	-0.06
430.9524	[Y4+5Na]3-	6.13E+07	-0.31
434.0609	C2-SO3	8230418	0.21
437.9577	[1,5A3+4Na-SO3]2-	1.25E+07	-0.17
437.9577	[2,4X2+4Na-SO3]2-	1.25E+07	-0.11
438.0324	B2+Na-SO3	3.30E+07	-0.05
440.9642	[B3+3Na-SO3]2-	1.08E+08	-0.22
447.9721	[Z3+3Na-SO3]2-	4.62E+07	-0.32
449.9695	[C3+3Na-SO3]2-	2.15E+07	-0.26
451.9552	3,5A2+2Na	5.18E+07	-0.28
451.9552	[B3+4Na-SO3]2-	5.18E+07	-0.27
456.0429	C2+Na-SO3	9623320	0.09
456.9922	[1,4A4+4Na-3SO3]2-	8096384	0.72
456.9922	[2,5X3+4Na-3SO3]2-	8096384	0.77
461.9996	3,5X1+Na-SO3	2.36E+07	-0.46
487.9504	[Z3+3Na-SO3]2-	5463174	-0.09
491.9336	[B3+4Na]2-	2.47E+07	-0.24
497.9607	0,2A2+2Na	2.74E+08	-0.30
498.9414	[Z3+4Na-SO3]2-	7.89E+08	-0.14
507.9468	[Y3+4Na-SO3]2-	6182968	-0.37
509.9323	[Z3+5Na-SO3]2-	1.44E+08	0.01
517.9327	0,2X1+2Na	3.21E+08	-0.08

517.9892	B2+Na	6.71E+07	-0.04
519.9426	0,2A2+3Na	8.18E+08	-0.19
537.9462	[M-8H+5Na]3-	6864637	0.37
539.9148	0,2X1+3Na	3.62E+07	-0.35
539.9713	B2+2Na	1.32E+08	-0.31
547.9251	[Y3+4Na]2-	2.56E+07	-0.16
553.9868	Z2+2Na-SO3	7.82E+07	0.05
557.9817	C2+2Na	2.44E+08	-0.02
558.916	[Y3+5Na]2-	3.71E+07	-0.03
561.9531	B2+3Na	2.33E+07	-0.04
575.9689	Z2+3Na-SO3	3.01E+07	-0.21
579.9212	[0,2X3+5Na]2-	3.10E+07	0.12
583.9352	[0,3X3+4Na]2-	1.25E+07	0.65
597.9484	[Z4+5Na-SO3]2-	8.03E+07	-0.08
633.9438	Z2+2Na	7802677	-0.27
655.9257	Z2+3Na	5.50E+08	-0.18
673.9362	Y2+3Na	7.99E+07	-0.09
677.9075	Z2+4Na	5.46E+07	0.04
695.9182	Y2+4Na	5.98E+07	-0.16
904.9179	B3+4Na-SO3	1.20E+07	-0.52
926.8996	B3+5Na-SO3	2.15E+07	-0.24
940.9147	Z3+5Na-2SO3	8135565	0.40
1020.8722	Z3+5Na-SO3	9602360	-0.31

Table. Extra assignment list from Orbitrap HCD MS/MS for Arixtra $[M-10H+7Na]^{3-}$ at low mass range (100-220 Da).

Mass to charge	Assignment	Intensity	Accuracy PPM
137.9863	1,3A1	8000	-2.55
138.9703	0,4A1	47800	-2.64
168.9807	0,3A1	1470	-3.15
203.9961	0,3X0+Na	3020	5.83
219.9910	3,5X0+Na	1420	5.79

APPENDIX B

SUPPLEMENTAL DATA FOR CHAPTER 4

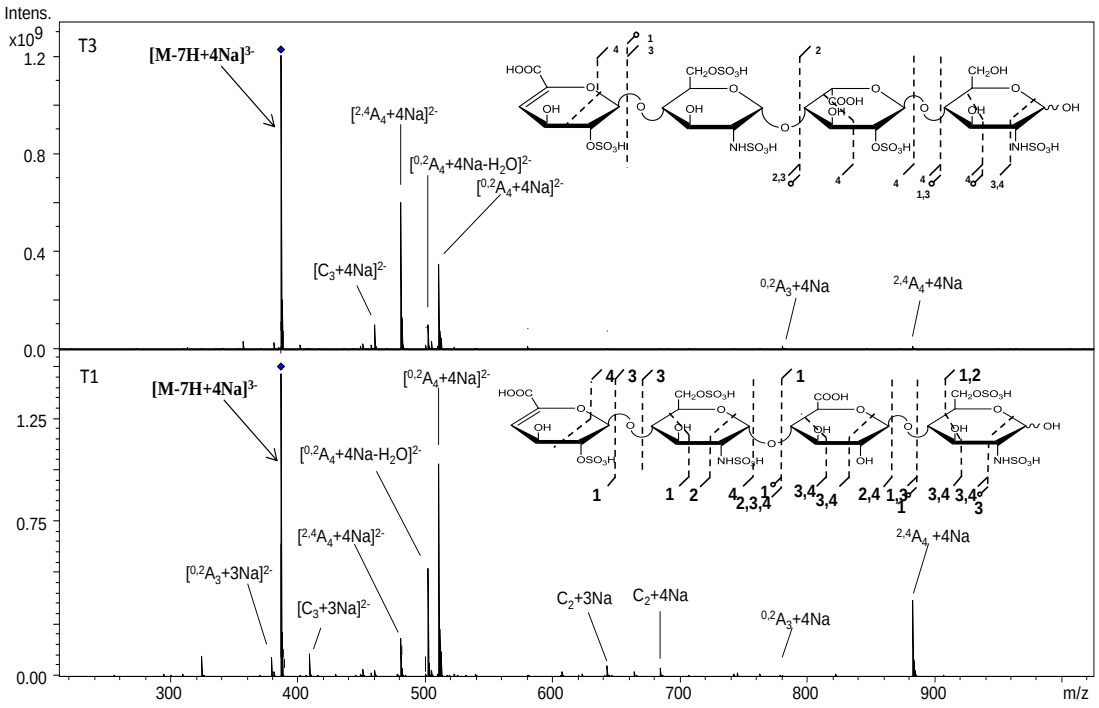

Figure. Comparison for the spectra from two isomeric tetrasaccharides showing that T1 produces more fragment ions than T2

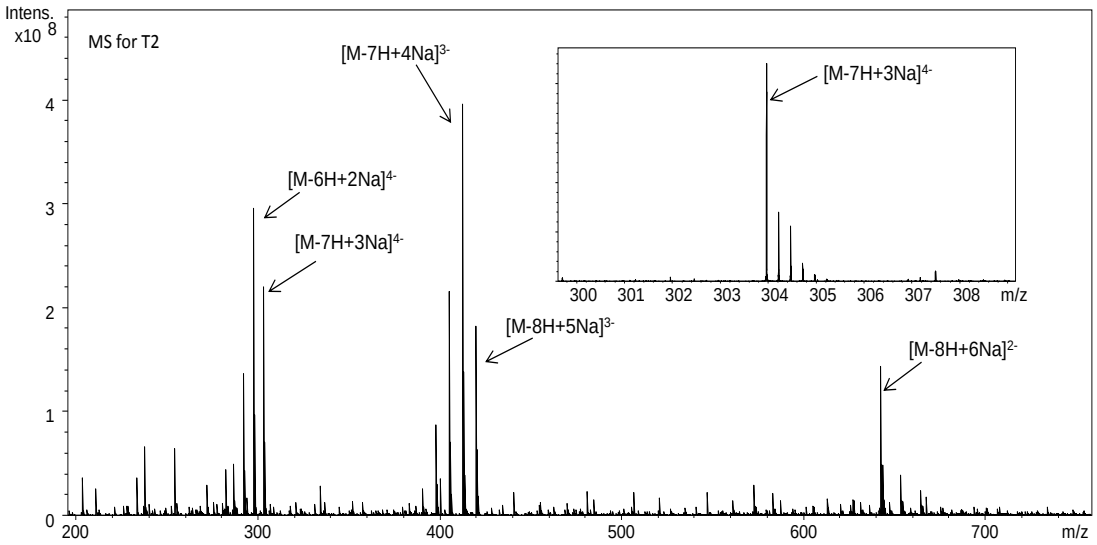

Figure. MS spectrum for T2

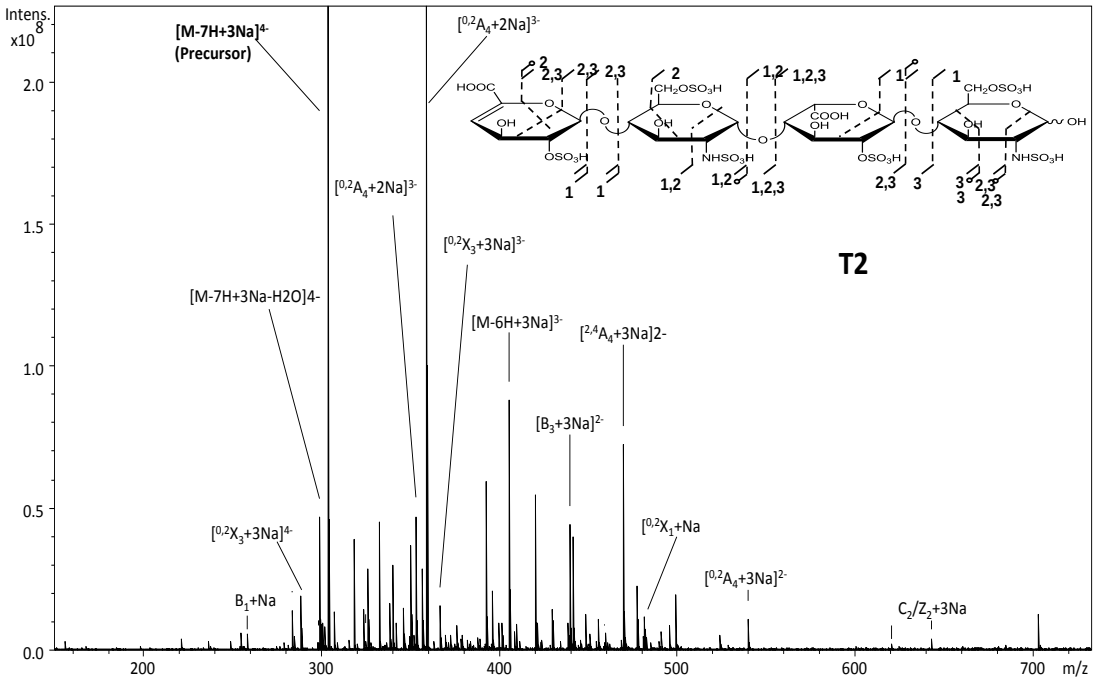

Figure. The CID spectrum of T2 molecular ion $[M-7H+3Na]^{4-}$.

List of annotations obtained from the T2 dp 4 spectra.

Mass to charge	Type	Intensity
168.4892	Y1 2-	1259937
236.971	B1	3218323
238.4947	B2-SO3	1364968
240.0181	Z1-SO3	1052776
249.4857	[B2+Na-SO3]2-	3222343
254.9813	C1	1314598
258.9531	B1+Na	5534002
274.9626	[0,2X3+3Na]4-	1110835
276.9635	C1+Na	1210440
283.9757	[M-7H+3Na-SO3]4-	1.37E+07
285.2973	[B3+2Na]3-	4991964
289.4641	[B2+Na]2-	7670537
298.4691	[C2+Na]2-	2095032
	[Z2+Na]2-	2095032
298.6283	[C3+3Na]3-	2611011
300.4552	[B2+2Na]2-	9162077

301.648	[1,5X3+2Na-SO3]3-	1750779
303.9649	[M-7H+3Na]4-	6.16E+08
307.4747	[Y2+Na]2-	1.36E+07
309.4604	[C2+2Na]2-	2583771
	[Z2+2Na]2-	2583771
318.4657	[Y2+2Na]2-	3.95E+07
318.9686	[Y3+2Na]3-	9017729
325.3115	[0,2A4+2Na-SO3]3-	3197024
326.2963	[Y3+3Na]3-	2.88E+07
328.3007	[1,5X3+2Na]3-	2731378
332.6388	[0,2A4+3Na-SO3]3-	4.54E+07
335.6282	[1,5X3+3Na]3-	1560015
340.2998	[0,2X3+3Na-SO3]3-	3.00E+07
341.9572	Z1+Na	9468056
351.9637	[0,2A4+2Na]3-	5264673
359.291	[0,2A4+3Na]3-	4.70E+08
359.6255	[0,2X3+2Na]3-	1.01E+08
366.952	[0,2X3+3Na]3-	1.54E+07
378.9699	[M-6H+3Na-SO3]3-	5318248
399.4622	[B3+3Na-SO3]2-	9640934
405.6224	[M-6H+3Na]3-	8.82E+07
408.4676	[C3+3Na-SO3]2-	6725738
428.4488	[B3+2Na]2-	1532901
429.4729	[2,4A4+3Na-SO3]2-	1.46E+07
429.9744	[Z3+2Na-SO3]2-	3817753
439.4407	[B3+3Na]2-	4.43E+07
440.9652	[Z3+3Na-SO3]2-	2230471
448.446	[C3+3Na]2-	1.28E+07
448.9473	[2,4X2+2Na]2-	2170754
449.9699	[Y3+3Na-SO3]2-	2298003
458.9524	0,2A2+Na	2754190
469.4514	[2,4A4+3Na]2-	7.26E+07
480.9339	0,2A2+2Na	4900006
481.9359	0,2X2+Na	2556994
499.4617	[0,2A4+3Na-SO3]2-	2380818
539.4404	[0,2A4+3Na]2-	1.08E+07
	[0,2X3+2Na]2-	2464958
619.9271	C2+2Na	2037570
	Z2+2Na	2037570
623.8986	B2+3Na	1459132
641.9104	C2+3Na	3820371
	Z2+3Na	3820371

683.9223 2,4A3+3Na 1791505

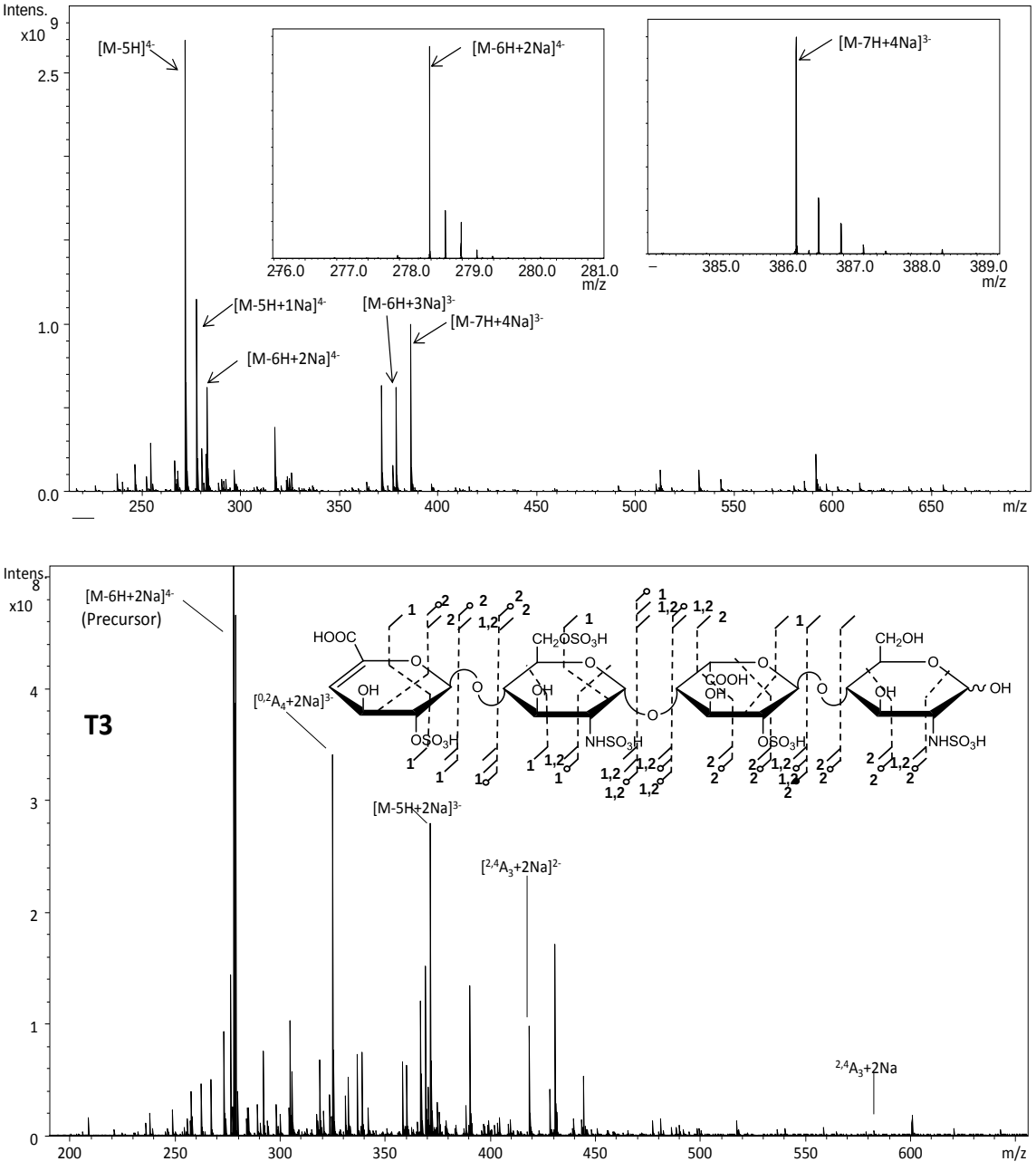

Figure. Mass spectrum and the CID spectrum of T3 molecular ion [M-6H+2Na]4-. The list of annotations obtained from the T3 dp 4 is shown below.

Mass to charge	Type	Intensity
230.9581	1,5A1+Na	3259220
236.9711	B1	1.15E+07

238.4947	[B2-SO3]2-	2.04E+07
240.0184	Z1	7270695
247.5	[C2-SO3]2-	4029798
247.5	Z22-	4029798
249.4775	[0,2X3+2Na]4-	3303252
249.4857	[B2+Na-SO3]2-	2.38E+07
249.9939	[C3-SO3]3-	3000519
251.0097	[Y3-SO3]3-	3673961
254.9816	C1	7814516
256.5053	Y22-	1.56E+07
258.0289	Y1	1.41E+07
258.491	[C2+Na-SO3]2-	4.02E+07
258.491	[Z2+Na]2-	4.02E+07
258.491	[M-6H+2Na-SO3]4-	4.02E+07
258.953	B1+Na	1.80E+07
267.4963	[Y2+Na]2-	5.08E+07
276.9636	C1+Na	8037289
277.97	[B3+Na]3-	5100710
278.4802	[M-6H+2Na]4-	1.64E+09
284.9893	[Y3+Na]3-	2.56E+07
285.2973	[B3+2Na]3-	2.60E+07
286.3134	[Z3+2Na]3-	2470270
289.4642	[B2+Na]2-	2.80E+07
291.3008	[C3+2Na]3-	1.21E+07
291.3317	[0,2A4+Na-SO3]3-	3258351
292.3165	[Y3+2Na]3-	7.73E+07
294.3209	[1,5X+Na]3-	1.34E+07
298.4693	[C2+Na]2-	7760193
298.6591	[0,2A4+2Na-SO3]3-	2.82E+07
300.4551	[B2+2Na]2-	2.02E+07
305.3043	[2,4A4+2Na]3-	1.04E+08
306.3202	[0,2X3+2Na-SO3]3-	5.77E+07
309.4603	[C2+2Na]2-	5441659
317.9841	[0,2A4+Na]3-	1.92E+07
318.3185	0,2X33-	3103711
318.9742	2,4A2+Na	9672884
325.3114	[0,2A4+2Na]3-	3.45E+08
330.4657	[2,4A3+2Na]2-	3780261
332.9724	[0,2X3+2Na]3-	5.34E+07

348.4927	[B3+2Na-2SO3]2-	3405913
357.0137	0,2A2-SO3	3707350
371.6427	[M-5H+2Na]3-	2.80E+08
374.4737	[1,5A3+2Na-SO3]2-	7910904
377.4803	[B3+Na-SO3]2-	3581633
378.5033	[2,4A4+2Na]2-	8437037
378.9953	0,2A2+Na-SO3	1.40E+07
388.4712	[B3+2Na-SO3]2-	2.71E+07
389.9945	[Z3+2Na-SO3]2-	1.03E+07
397.4764	[C3+2Na-SO3]2-	8774894
398.9999	[Y3+2Na-SO3]2-	1.02E+07
401.9786	0,2X1+Na	3323437
412.9973	[1,5X3+2Na-SO3]2-	4531903
414.4519	[1,5A3+2Na]2-	4221979
418.4817	[2,4A4+2Na-SO3]2-	9.90E+07
428.4495	[B3+2Na]2-	4.28E+07
429.973	[Z3+2Na]2-	5525687
438.9784	[Y3+2Na]2-	7109071
456.043	Y2+Na-SO3	4467213
458.4602	[2,4A4+2Na]2-	3872562
458.9523	0,2A2+Na	3475504
480.934	0,2A2+2Na	1.62E+07
488.4703	[0,2A4+2Na]2-	8306916
497.9602	2,4X1+2Na	6793631
499.9785	B2+Na-SO3	4980819
517.9891	C2+Na-SO3	6333176
517.9891	Z2+Na	6333176
517.9891	[M-4H+2Na-SO3]2-	6333176
521.9605	B2+2Na-SO3	3407680
535.9996	Y2+Na	6337390
539.971	C2+2Na-SO3	6448918
539.971	Z2+2Na	6448918
557.9816	Y2+2Na	8275336
563.9944	1,5X2+Na	4322263
581.9813	2,4A3+2Na-SO3	4970396
619.9271	C2+2Na	7270995

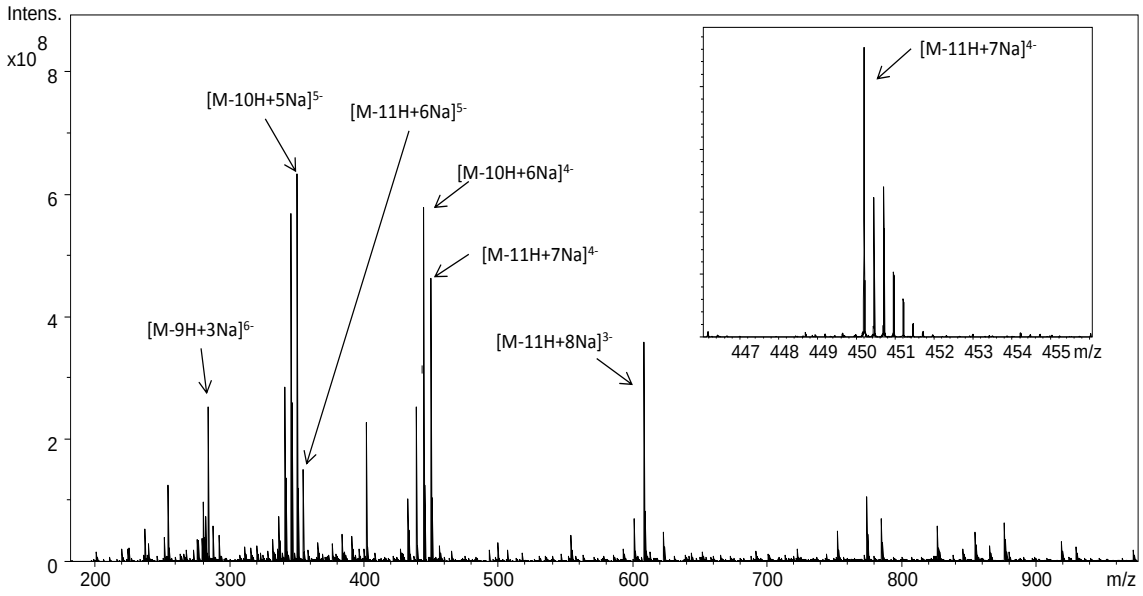

Figure. Mass spectrum of dp6 8S with the inset showing the region around the precursor ion used for MS/MS analysis.

The mass list for dp6 with 8S $[M-11H+7Na]^{4-}$.

Mass to charge	Type	Intensity
258.9529	B1+Na	4984716
299.9464	2,4X0+Na	8195879
309.4603	[C2+2Na]2-	3575464
318.9742	2,4A2+Na	2567656
359.9678	Y1+Na	2026596
424.3164	[C5+2Na-SO3]3-	2431740
449.9692	[Y3+3Na]2-	4499612
450.2004	[M-11H+7Na]4-	8.27E+08
466.2745	[0,2A5+6Na]3-	1.97E+07
480.9342	[0,2A2+2Na	8504308
486.2814	[C5+6Na]3-	1.53E+07
486.6158	[2,4X4+5Na]3-	6915157
500.2852	[2,4A6+6Na]3-	8370949
500.6195	[Z5+5Na]3-	4399340
513.9495	[Y5+6Na]3-	9062216
520.2923	[0,2A6+6Na-SO3]3-	4213206
539.0069	0,3A5-2SO3	3.52E+07
546.9446	[0,2A6+6Na]3-	6140067
547.2786	[0,2X5+5Na]3-	2339933
554.2718	[0,2A6+7Na]3-	2.87E+08

554.6061	[0,2X5+6Na]3-	1.19E+08
555.9384	[3,5X3+5Na]2-	4368569
561.9327	[0,2X5+7Na]3-	2.23E+07
590.9402	[C4+5Na-SO3]2-	7155144
590.9402	[Z4+5Na]2-	7155144
599.9459	[Y4+5Na]2-	3074815
600.6029	[M-10H+7Na]3-	2.87E+07
632.9047	[B4+6Na]2-	3750901
641.9102	C2+3Na	2.87E+07
641.9102	[C4+6Na]2-	2.87E+07
652.9011	[C4+7Na]2-	2560747
659.9368	[0,2A5+6Na-SO3]2-	2879917
662.9153	[2,4A5+6Na]2-	2.50E+07
691.9168	[2,5A5+6Na]2-	1.85E+07
710.906	[0,2A5+7Na]2-	1.38E+07
720.9196	[B5+6Na]2-	3351030
721.9441	[2,4A6+7Na-SO3]2-	9220799
722.4452	[Z5+6Na-SO3]2-	4492063
731.9115	[B5+7Na]2-	1.81E+07
741.4169	[2,4X4+6Na]2-	4562072
761.9219	[2,4A6+7Na]2-	6.05E+08
762.4235	[Z5+6Na]2-	2.59E+08
782.4183	[Y5+7Na]2-	4839473
881.9351	2,4A4+4Na-SO3	2857517
1005.8532	2,4A4+6Na	3275464

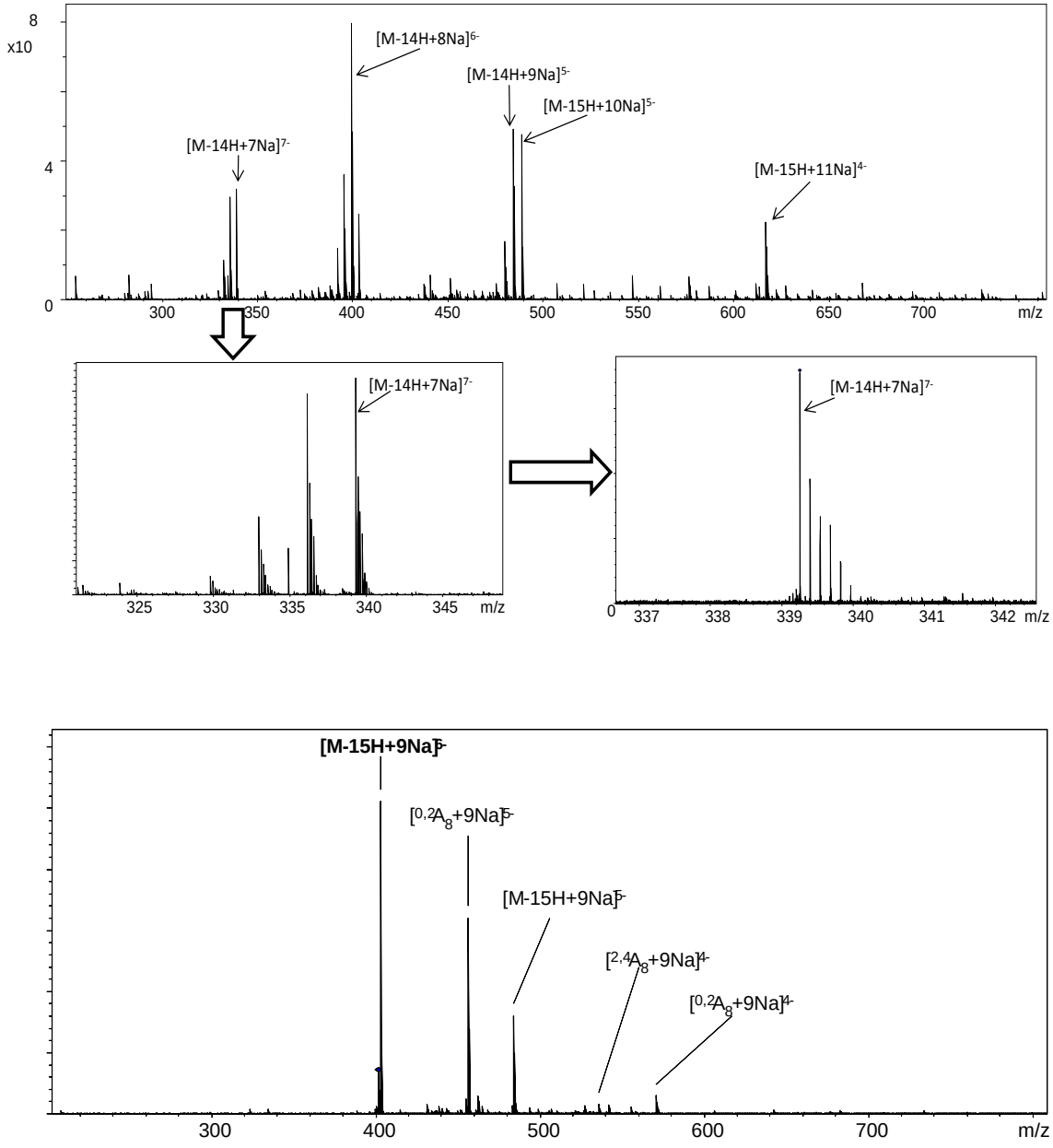

Figure. Mass spectrum of dp8 11S showing molecular ion obtained followed by a list of annotations obtained from the CID of [M-14H+7Na] 7-. Below the MS is the MS/MS spectrum of the fully deprotonated precursor for the same compound showing abundant 0,2 A and 2,4A fragments.

List of fragments for dp8 with 11sulfates

Mass to charge	Type	Intensity
168.4894	Y12-	4479713
249.4858	[B2+Na-SO3]2-	7731088
254.9819	C1	3055304
258.9531	B1	4949704
267.4963	[Y2+Na]2-	4.14E+07
285.2974	[B3+2Na]3-	3051354
288.4784	[Y4+3Na]4-	2.36E+07
289.4641	[B2+Na]2-	5030745
300.4551	[B2+2Na]2-	6410255
304.9578	[B4+4Na]4-	3875564
309.4604	[C2+2Na]2-	6194873
309.4604	[C4+4Na]4-	6194873
309.4604	[C6+6Na]6-	6194873
327.8277	[M-14H+7Na-SO3]7-	1.99E+07
330.3931	0,3A75-	6714473
341.9572	Z1	1.04E+07
351.9604	[B6+6Na-SO3]5-	5.31E+07
356.2967	[Y7+7Na]6-	6374763
359.1646	[Y6+6Na]5-	4.44E+07
359.4678	[0,2A8+7Na-SO3]6-	5564013
359.9676	Y1+Na	6658933
363.5561	[B6+5Na]5-	1.24E+07
367.9518	[B6+6Na]5-	2.86E+07
372.3481	[B6+7Na]5-	1.15E+07
372.794	[0,2A8+7Na]6-	4.53E+07
374.4503	[B5+5Na]4-	7475135
375.9503	[C6+7Na]5-	1.48E+07
378.9954	0,2A2+Na-SO3	6937228
379.7147	[Y5+5Na]4-	4638434
380.2938	[B4+4Na-SO3]3-	5.46E+07
380.6283	[3,5X7+6Na]6-	1.20E+07
382.6334	[M-13H+7Na-SO3]6-	2.72E+07
384.4486	[C5+6Na]4-	3697470
384.9735	[Y4+3Na]3-	1.17E+07
386.2972	[C4+4Na-SO3]3-	6580223
386.2972	[Z4+4Na]3-	6580223
390.3595	[0,2A7+5Na]5-	3741610
391.5631	[B7+7Na-SO3]5-	4.27E+07
392.3007	[Y4+4Na]3-	1.18E+07
395.9597	[M-13H+7Na]6-	3.26E+08
396.9597	[3,5X6+7Na]5-	7334740

397.4764	[C3+2Na-SO3]2-	8759418
399.462	[B3+3Na-SO3]2-	3521621
406.946	[B4+4Na]3-	1.43E+07
407.5544	[B7+7Na]5-	2.31E+08
408.4674	[C3+3Na-SO3]2-	1.59E+07
409.9563	[0,2A6+6Na-SO3]4-	5630415
414.2733	[B4+5Na]3-	2.15E+07
420.2768	[C4+5Na]3-	9463523
429.2187	[Y6+6Na-SO3]4-	4561288
429.9458	[0,2A6+6Na]4-	5439597
435.4412	[0,2A6+7Na]4-	3.80E+07
439.4404	[B3+3Na]2-	8343323
440.2023	[B6+6Na-SO3]4-	1.66E+07
440.964	[Z3+3Na]2-	6018888
445.6978	[B6+7Na-SO3]4-	5.39E+07
447.5542	[0,2A8+7Na]5-	1.95E+07
447.7549	[0,2X7+6Na]5-	1.25E+07
448.4457	[C3+3Na]2-	5634376
449.2075	[Y6+6Na]4-	1.51E+07
449.985	[2,5X3+4Na-2SO3]2-	1.13E+07
450.2004	[C6+7Na-SO3]4-	1.03E+08
450.2004	[Z6+7Na]4-	1.03E+08
452.1508	[0,2X7+7Na]5-	5734230
452.3015	[C5+5Na-2SO3]3-	4155869
460.1911	[B6+6Na]4-	4837501
460.7033	[2,4A7+7Na-SO3]4-	9986845
465.6869	[B6+7Na]4-	1.69E+07
470.1896	[C6+7Na]4-	1.23E+08
475.3531	[M-12H+7Na]5-	7.23E+07
480.6924	[2,4A7+7Na]4-	5500224
480.9341	0,2A2+2Na	5537107
486.2814	[C5+6Na-SO3]3-	2.53E+07
486.6159	[2,4X4+5Na]3-	8505295
489.7059	[B7+7Na-SO3]4-	1.18E+07
506.9302	[B5+6Na]3-	1.80E+07
507.9463	[Z5+6Na]3-	8233310
509.695	[B7+7Na]4-	6.40E+07
512.9336	[C5+6Na]3-	7508546
513.9495	[Y5+6Na]3-	8638295
521.9606	B2+2Na-SO3	6368459
534.2647	[2,4A6+7Na]3-	1.84E+07
554.2717	[0,2A6+7Na-SO3]3-	5.04E+07

554.6063	[0,2X5+6Na]3-	2.20E+07
561.9327	[0,2X5+7Na]3-	1.60E+07
567.9473	[B6+7Na-2SO3]3-	1.30E+07
573.9507	[C6+7Na-2SO3]3-	7736524
573.9507	[Z6+7Na-2SO3]3-	7736524
580.9239	[0,2A6+7Na]3-	3.14E+07
581.9353	[B4+5Na-SO3]2-	4705133
590.9407	[Z4+5Na]2-	6283632
594.5999	[B6+7Na-SO3]3-	6546650
599.9454	[Y4+5Na]2-	6367650
600.6032	[C6+7Na-SO3]3-	1.11E+07
600.6032	[Z6+7Na]3-	1.11E+07
641.9102	C2+3Na	9477174
641.9102	[C4+6Na]2-	9477174
761.9233	[2,4A6+7Na-SO3]2-	3.96E+07

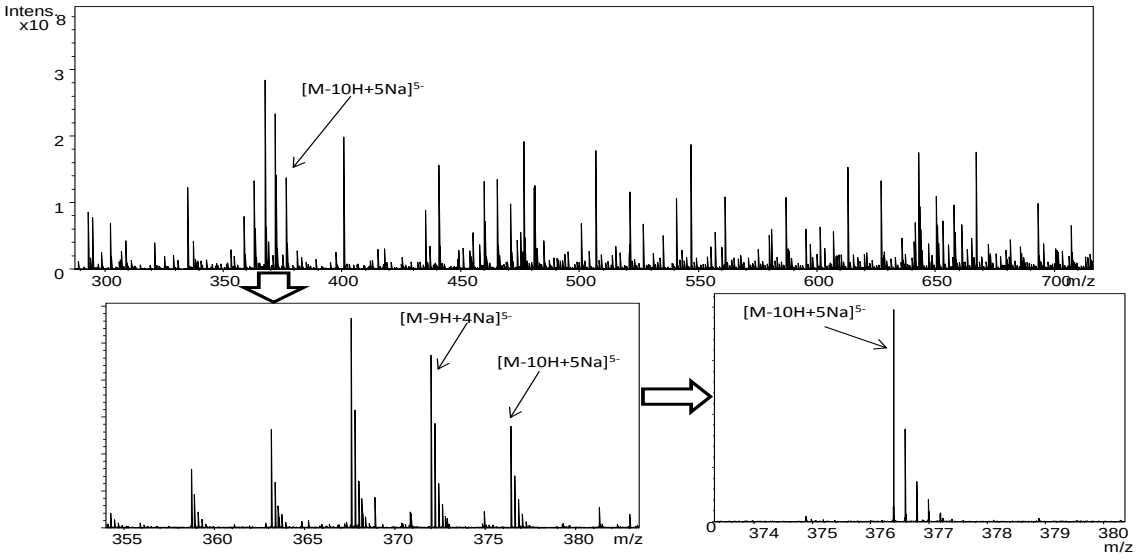

Figure. Mass spectra for dp7 7S with the expanded region around the precursor [M-10H+5Na]$^{5-}$.

List of MS/MS annotations for molecular ion [M-10H+5Na]$^{5-}$.

Mass to charge	Type	Intensity
198.9918	0,2A1	1.53E+07

220.9738	0,2A1+Na	1.05E+07
282.0289	B1	3.79E+07
300.0395	C1	8.67E+07
306.3201	[C3+2Na]3-	9338888
313.3346	[Z4+2Na]3-	4386507
321.0827	Z2	4225431
339.0934	Y2	2.03E+07
340.5252	[Y3+Na]2-	2.59E+07
342.0502	2,4A2	6349648
343.577	[B6+5Na]5-	1.29E+07
349.9736	[0,2A5+4Na]4-	6793217
361.5304	[0,2X3+NaSO3]2-	5138528
364.032	2,4A2+Na	5498661
369.9936	[Z6+4Na-SO3]4-	5850691
376.3906	[M-10H+5Na]5-	3.97E+08
378.1046	B2-SO3	3471737
385.715	[B5+5Na]4-	1.17E+07
390.2176	[C5+5Na]4-	1.36E+08
395.4783	[Z6+5Na]4-	4.91E+07
399.981	[Y6+5Na]4-	7.29E+07
400.3007	[B4+4Na]3-	8445863
400.7202	[2,4A6+5Na]4-	1.22E+07
404.2385	[B6+4Na-SO3]4-	3424950
406.3044	[C4+4Na]3-	2.59E+07
408.2228	[1,4A6+5Na]4-	3977224
409.7338	[B6+5Na-SO3]4-	2.80E+07
411	[0,2X3+2Na]2-	1.08E+07
420.0053	[C3+2Na-SO3]2-	4364660
429.7229	[B6+5Na]4-	1.99E+07
430.527	[Z4+2Na]2-	2.88E+07
434.9834	[2,5A5+4Na-SO3]3-	9203312
434.9834	[Z5+4Na-SO3]3-	9203312
438.0324	[0,2A2+Na	1.52E+07
440.3149	[0,2A5+4Na-SO3]3-	2.70E+07
450.2389	[2,4X6+4Na]4-	8506864
453.9902	[B5+4Na-2SO3]3-	3809926
458.061	B2	7.50E+07
470.5055	[Z4+2Na]2-	8640268
470.74	[M-9H+5Na]4-	2.00E+08
470.9746	[C3+3Na]2-	1.08E+07
474.2944	[0,2A5+5Na]3-	2.09E+08
474.967	[Y5+5Na]3-	2.78E+07

480.0429	B2+Na	7830718
481.4964	[Z4+3Na]2-	8.25E+07
481.9662	[C3+4Na]2-	4006469
487.97	[B5+5Na-SO3]3-	6.13E+07
488.9698	[0,2X5+5Na]3-	9107277
490.5016	[Y4+3Na]2-	1.89E+07
493.9735	[C5+5Na-SO3]3-	4.89E+07
494.9844	[3,5A4+2Na]2-	1.63E+07
498.0535	C2+Na	4.86E+07
498.0535	2,5X2+Na	4.86E+07
500.9879	[Z6+5Na-SO3]3-	4.47E+07
507.9771	[2,4A6+5Na-SO3]3-	5980668
513.9911	[1,4A42-	4256644
517.9887	[0,2A4+2Na]2-	4196043
520.626	[C5+5Na]3-	7747676
527.6403	[Z6+5Na]3-	1.22E+07
533.6437	[Y6+5Na]3-	1.64E+07
539.9711	[0,2A4+4Na]2-	1.47E+07
559.2958	[0,2A6+5Na]3-	1.35E+07
560.9764	[B4+4Na-SO3]2-	2.13E+07
569.9816	[C4+4Na-SO3]2-	9284524
569.9816	[2,5X4+4Na]2-	9284524
590.9872	[2,4A5+4Na-SO3]2-	1.16E+07
600.9554	[B4+4Na]2-	4249928
611.9459	[B4+5Na]2-	3.16E+07
620.9512	[C4+5Na]2-	1.97E+07
627.9897	[M-8H+5Na]3-	7509571
641.9565	[2,4A5+5Na]2-	4.59E+08
671.967	[0,2A5+5NaSO3]2-	2.01E+07
686.0289	2,5A3+2Na-SO3	2.04E+07
686.0289	Z3+2Na	2.04E+07
704.0395	Y3+2Na	1.94E+07
844.9888	B3+3Na-SO3	9680534

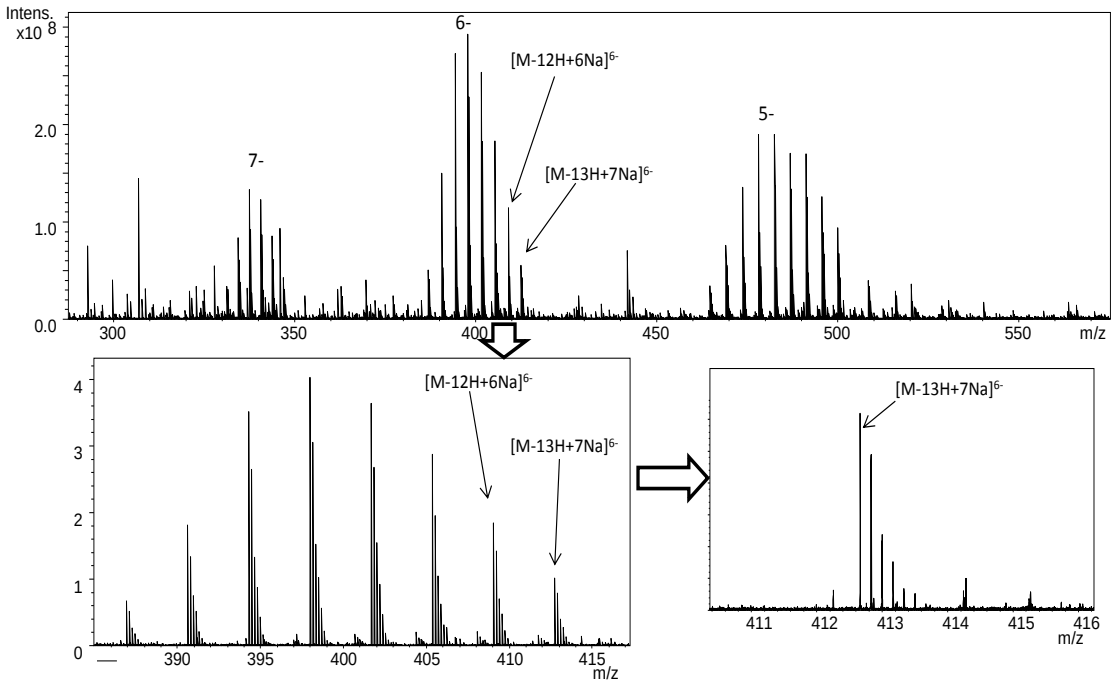

Figure. Mass spectrum of the dp10 8S.

Fragments for decasaccharide with 8 sulfate groups molecular ion $[M-13H+7Na]^{6-}$

Mass to charge	Type	Intensity
267.4953	C2+Na	6597467
339.0932	Y2	6658410
340.5251	[Y3+Na]2-	2.74E+07
346.5071	[B3+Na]2-	7494399
357.4981	[B2+2Na]2-	3783717
377.6668	[0,2A5+4Na-SO3]3-	7488464
384.343	[B5+3Na-SO3]3-	3253578
384.343	[2,4X9+2Na]6-	3253578
385.3205	[B9+7Na]6-	9010882
396.3419	[B5+Na]3-	9853119
397.0062	0,2A2+Na	6.71E+07
398.0097	[M-11H+3Na]6-	8247257
398.786	[0,2A8+6Na]5-	5631168
407.0075	[Y5+3Na]3-	1.62E+07
410.2162	[2,4X9+2Na-SO3]5-	1.75E+07
412.6652	[M-13H+7Na]6-	2.39E+08
427.3795	[B8+7Na]5-	7255480
430.5272	[Z4+2Na]2-	4926796
430.9816	[C8+7Na]5-	7.33E+07
438.0328	B2+Na-SO3	1.67E+07

439.3837	[2,4A9+7Na]5-	9319113
439.5327	[Y4+2Na]2-	7921180
440.2485	[Y7+5Na]4-	2.66E+07
445.3861	[1,4A9+7Na]5-	4702562
446.5945	[B9+7Na-SO3]5-	2.73E+07
456.0434	C2+Na-SO3	9204776
460.1932	[Y9+7Na]5-	1.09E+07
462.5858	B9+7Na]5-	1.24E+07
468.4887	[0,2A4+3Na]2-	1.85E+07
478.7452	[0,2A8+6Na-SO3]4-	1.10E+07
492.3163	[0,2A6+5Na]3-	1.20E+07
495.3995	[M-13H+7Na]5-	8.54E+07
504.23	[0,2A8+7Na]4-	1.83E+08
514.4867	[B8+7Na-SO3]4-	9577850
518.9892	[C8+7Na-SO3]4-	8791279
529.4915	[2,4A9+7Na-SO3]4-	8601026
529.4915	[2,5X9+7Na]4-	8601026
539.9709	[B4+4Na]2-	1.22E+07
539.9709	B2+2Na	1.22E+07
539.9709	[B6+6Na]3-	1.22E+07
545.9744	[C6+6Na]3-	9887771
557.9814	C2+2Na	1.36E+07
559.9779	[2,4A7+6Na]3-	5755043
567.3258	[2,4X7+5Na]3-	1.23E+07
571.9956	[B7+6Na-SO3]3-	1.28E+07
599.9916	2,4A3+2Na	1.19E+07
605.9749	[B7+7Na]3-	6894930
621.9728	2,4A3+3Na	6622705
625.9816	[2,4A8+7Na]3-	1.66E+08
645.9883	[0,2A8+7Na-SO3]3-	7175739
668.9867	[2,4A6+5Na]2-	1.28E+07

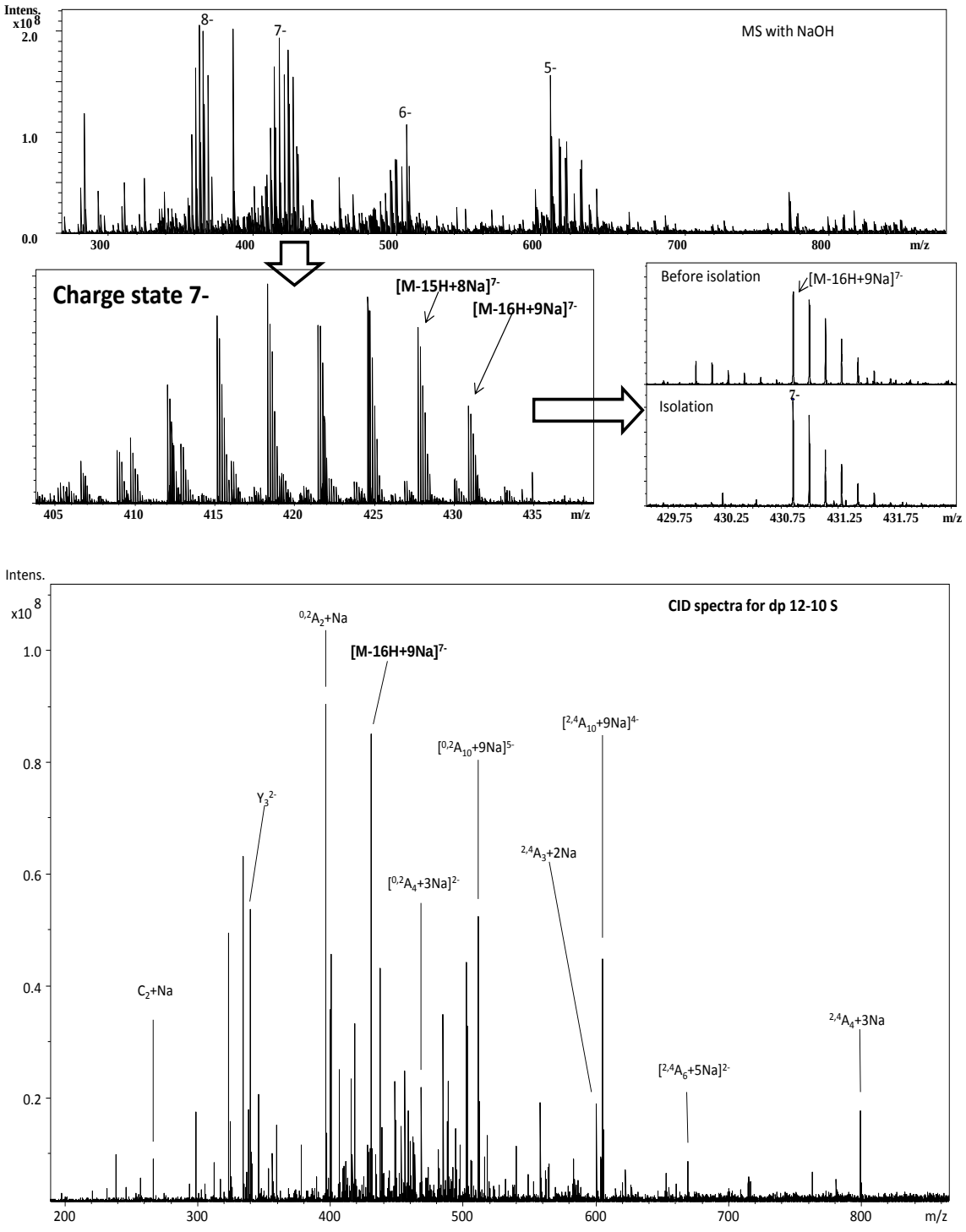

Figure. MS spectrum of dp 12 10S and CID spectrum of molecular ion $[M-16H+9Na]^{7-}$.

Fragments for dodecasaccharide with 10 sulfate groups $[M-16H+9Na]^{7-}$.

Mass to charge	Type	Intensity
247.5	B44-	3943817
247.5	B22-	3943817
258.491	B66-	5750292
258.491	[B2+Na]2-	5750292
258.491	[B6+3Na]6-	5750292
267.4963	[C2+Na]2-	9001010
306.5286	[B3+Na-SO3]2-	4510112
318.3379	[B4+2Na-SO3]3-	5480837
318.3379	[B8+4Na-2SO3]6-	5480837
339.0933	Y2	1.80E+07
340.5252	[Y3+Na]2-	5.44E+07
346.507	[B3+Na]2-	2.06E+07
349.0112	[Y6+3Na]4-	3636408
357.4983	[B3+2Na]2-	4870180
407.0071	[Y5+3Na]3-	2.51E+07
410.995	[B5+3Na]3-	7648838
412.8521	[0,3X11+8Na]7-	4439231
416.0503	B2-SO3	2.34E+07
417.5191	[0,2A4+2Na-SO3]2-	5048231
418.173	[0,2X10+3Na]6-	4545805
430.527	[Z4+2Na]2-	5254437
430.8513	[M-16H+9Na]7-	8.52E+07
430.9946	[1,5X5+5Na]3-	7.45E+07
435.1525	[B10+6Na]6-	4395095
438.0323	[B2+Na-SO3	4.37E+07
439.5321	[Y4+2Na]2-	1.48E+07
440.248	[Y7+5Na]4-	6291112
449.1461	[C10+9Na]6-	2.33E+07
449.8116	[2,5X9+2Na]5-	4271808
456.0428	C2+Na-SO3	2.51E+07
456.1476	[2,4A11+9Na]6-	6428470
458.3366	[0,2A6+4Na-SO3]3-	4813288
460.1927	[Y9+7Na]5-	1.21E+07
462.157	[B11+9H-SO3]6-	1.29E+07
468.4884	[0,2A4+3Na]2-	2.20E+07
473.0116	[Y6+4Na]3-	5582342
475.4829	[B11+9H]6-	4387354
492.3163	[0,2A2+5Na]5-	7486805
498.0071	[C4+3Na-SO3]2-	1.17E+07
502.8277	[M-15H+9Na]6-	4.43E+07

505.9917	[B6+5Na-SO3]3-	8804915
511.3779	[0,2A10+9Na]5-	5.24E+07
531.5874	[2,4A11+9Na-SO3]5-	5348609
531.5874	[2,5X9+9Na]5-	5348609
548.976	[C4+4Na]2-	6255244
557.9815	C2+2Na	1.94E+07
582.9884	[C9+7Na]4-	9100291
599.9922	[2,4A3+2Na	1.89E+07
603.5944	[M-14H+9Na]5-	9608097
604.4801	[2,4A10+9Na]4-	4.56E+07
619.4857	[0,2A10+9Na-SO3]4-	4799855
621.9743	2,4A3+3Na	6994490
668.9889	[2,4A6+5Na]2-	8669320
798.0064	2,4A4+3Na	1.79E+07

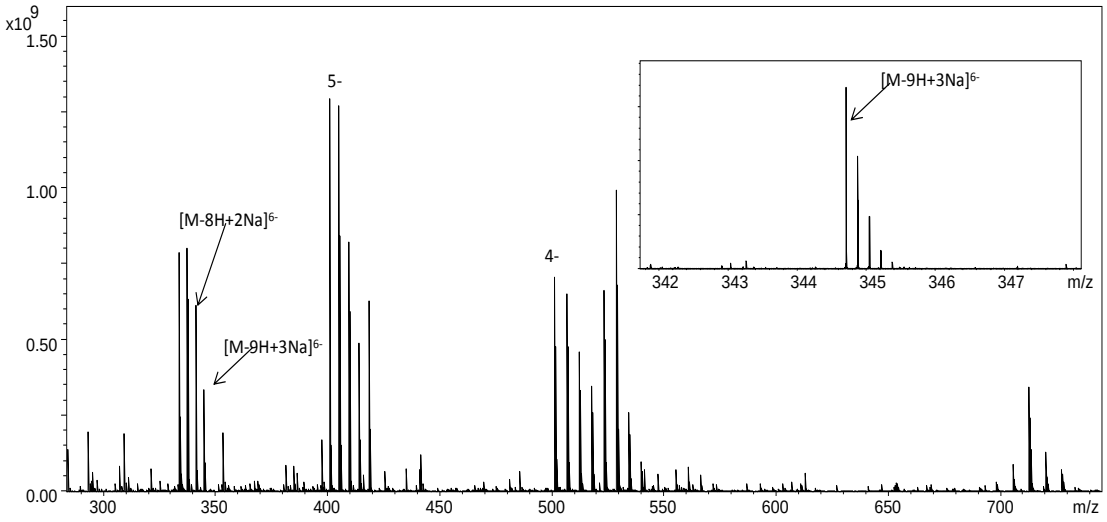

Figure. MS for dp10 4S with insert of the molecular ion selected for the MS/MS analysis.

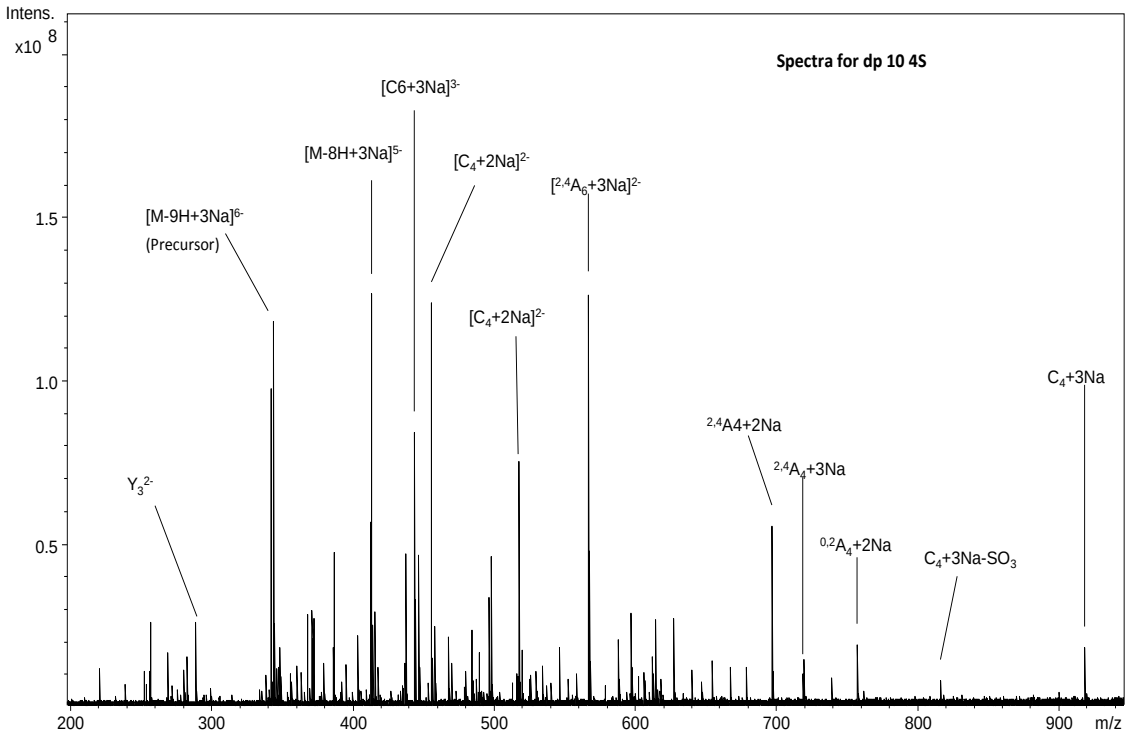

Figure. CID spectrum of molecular ion $[M-9H+3Na]^{6-}$ for dp10 4S.

Fragments from decasaccharide with 4 SO_3 groups molecular ion $[M-9H+3Na]^{6-}$.

Mass to charge	Type	Intensity
257.0279	2,4A2+Na	1.09E+07
289.5558	[Y32-	2.61E+07
295.5376	B32-	3651483
315.5339	[C3+Na]2-	3902235
336.5392	[2,4A4+Na]2-	5108608
339.0482	[Y5+Na]3-	1.01E+07
344.7057	[M-9H+3Na]6-	1.19E+08
347.5304	[2,4A4+2Na]2-	3868584
349.4302	[C8+3Na]5-	1.83E+07
363.7942	[Y7+2Na]4-	1.07E+07
366.5497	[0,2A4+Na]2-	4581149
370.3701	[2,4A6+2Na]3-	5616976
372.2804	[B7+3Na]4-	3829242
378.6419	[Y9+3Na]5-	4393977
381.0344	[B9+3Na]5-	4203768
387.0631	[B4+Na-SO3]2-	7322719
387.2858	[2,4A8+3Na]4-	4.76E+07
413.8482	[M-8H+3Na]5-	1.27E+08

416.0504	B2	2.94E+07
427.0413	[B4+Na]2-	4727769
427.0413	[B8+2Na]4-	4727769
434.0611	C2	5039825
436.0464	[C4+Na]2-	6497746
436.7086	[C6+2Na]3-	5641534
437.0395	[C8+3Na]4-	1.38E+07
438.0323	[B4+2Na]2-	4.75E+07
438.0323	B2+Na	4.75E+07
438.0323	[B6+3Na]3-	4.75E+07
444.0358	[C6+3Na]3-	8.48E+07
447.0376	[C4+2Na]2-	4.69E+07
453.5649	[Y9+3Na-SO3]4-	7521683
456.0429	C2+Na	1.24E+08
458.0393	[2,4A7+3Na]3-	2.51E+07
458.0393	[2,5X6+3Na]3-	2.51E+07
468.043	[2,4A5+2Na]2-	2.18E+07
468.043	[2,5X4+2Na]2-	2.18E+07
473.5539	[Y9+3Na]4-	4870322
479.0338	[2,4A5+3Na]2-	6100571
479.0338	[2,4X4+3Na]2-	6100571
490.0646	[2,4A8+3Na-SO3]3-	1.67E+07
492.7219	[Y7+3Na]3-	4717183
496.7098	[B7+3Na]3-	3.39E+07
498.0535	2,4A3+Na	4.64E+07
498.0535	2,5X2+Na	4.64E+07
516.034	[0,2A5+3Na]2-	1.03E+07
516.0806	[2,4A6+2Na-SO3]2-	8334257
516.7168	[2,4A8+3Na]3-	9277651
517.562	[M-7H+3Na]4-	7.57E+07
520.0355	2,4A3+2Na	1.73E+07
520.0355	2,5X2+2Na	1.73E+07
520.0664	[Y5+2Na]2-	1.09E+07
526.0482	3,5A3+Na	9758418
526.0482	[B5+2Na]2-	9758418
534.1075	B3+Na-SO3	1.26E+07
537.0396	[B5+3Na]2-	6518305
546.0446	[C5+3Na]2-	1.82E+07
552.1182	C3+Na-SO3	8543680
567.0498	[2,4A6+3Na]2-	1.28E+08
594.1283	2,4A3+Na-SO3	4603201
597.0604	[0,2A6+3Na]2-	2.90E+07

602.101	Y3+Na	9616690
614.0644	B3+Na	2.72E+07
616.0179	0,2A3+3Na	5376588
617.5737	[B6+3Na-SO3]2-	8602060
626.5789	[C6+3Na-SO3]2-	2.77E+07
654.0571	C3+2Na	1.42E+07
654.1498	0,2A4+Na-SO3	6480394
666.5575	[C6+3Na]2-	1.23E+07
696.0673	2,4A4+2Na	5.61E+07
718.0492	2,4A4+3Na	1.03E+07
756.0885	0,2A4+2Na	1.95E+07
815.1258	C3+2Na-SO3	8380501
917.0636	C4+3Na	1.86E+07

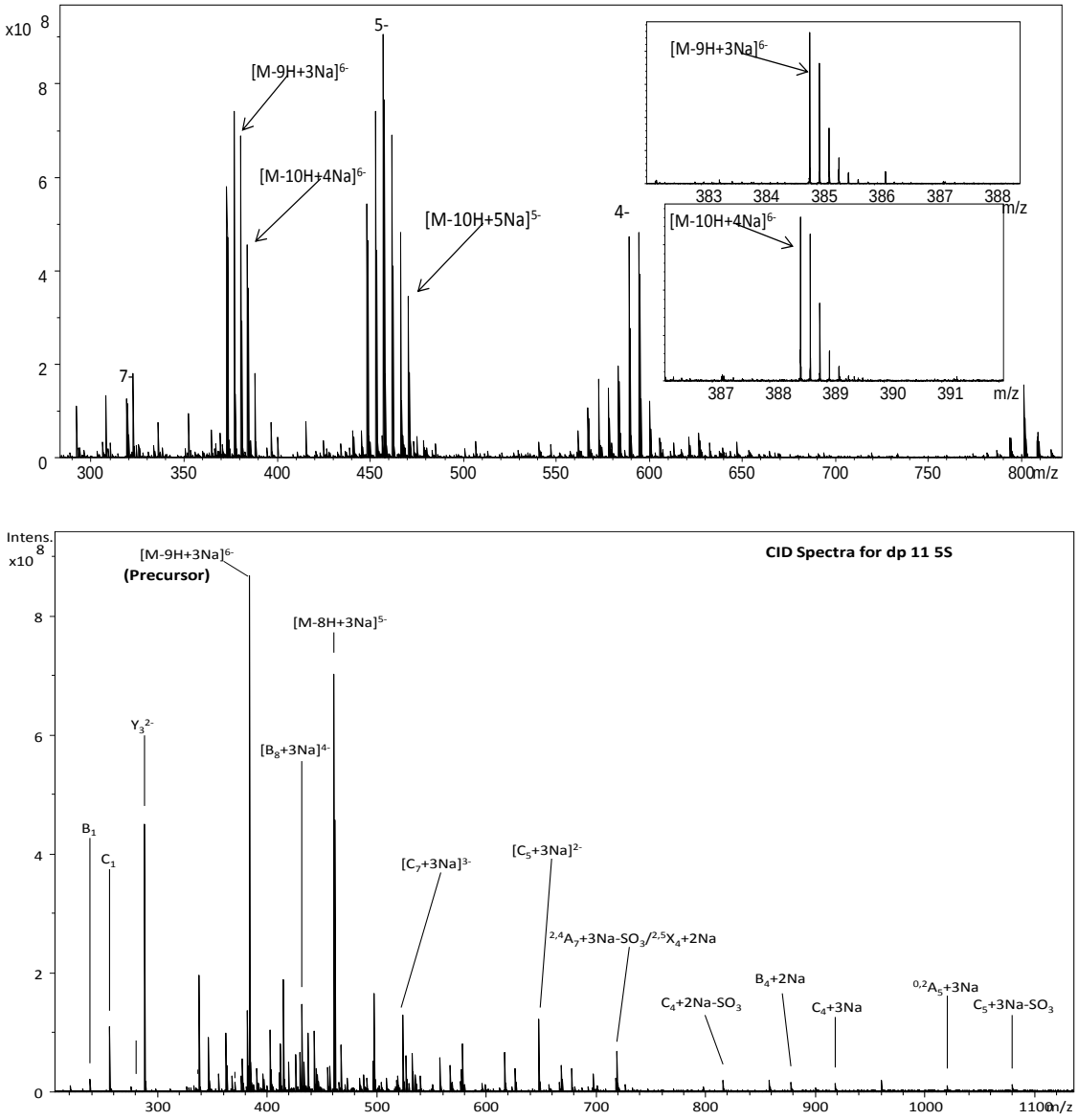

Figure. Mass spectrum for dp 11 5S and CID spectrum of molecular ion [M-9H+3Na] $^{6-}$ followed by a list of annotations obtained from it.

Fragments obtained from undecasaccharide [M-9H+3Na] $^{6-}$ $5SO_3$ groups

Mass to charge	Type	Intensity
240.0184	B1	2.21E+07
258.029	C1	1.11E+08
282.0291	[0,2A7+2Na]5-	4499190
289.5559	Y32-	4.55E+08
300.0394	2,4A2	5142234
328.0345	3,5A2	9738265

328.0345	B32-	9738265
330.0501	1,4A2	6603699
331.7208	Y53-	7163293
337.0397	C32-	4800199
338.0482	[B5+Na-SO3]3-	4045606
339.0255	[B3+Na]2-	1.30E+07
339.0481	[Y5+Na]3-	1.98E+08
339.0933	Y2	5073763
348.0308	[C3+Na]2-	9.25E+07
350.0166	3,5A2+Na	4885117
350.0166	[B3+2Na]2-	4885117
363.7941	[Y7+2Na]4-	1.00E+08
364.7004	[B5+Na]3-	9449790
368.5665	Z42-	5064810
369.036	[2,4A4+Na]2-	2.28E+07
371.5503	[M-9H+3Na-SO3]6-	7785414
372.0278	[B5+2Na]3-	5763001
378.0313	[C5+2Na]3-	2.73E+07
378.6418	[Y9+3Na]5-	5.67E+07
384.8766	[M-9H+3Na]6-	8.70E+08
387.063	[B4+Na-SO3]2-	1.61E+07
388.5628	[Y4+Na]2-	1.21E+07
392.0348	[2,4A6+2Na]3-	4.00E+07
393.0315	[C7+3Na]4-	1.43E+07
397.6353	[C9+3Na]5-	3.10E+07
403.5342	[2,4A8+3Na]4-	1.04E+08
404.0529	[B6+2Na-SO3]3-	1.88E+07
405.0527	[Y6+2Na]3-	3.89E+07
412.5478	[B8+3Na-SO3]4-	3.26E+07
413.2977	[Y8+3Na]4-	8.08E+07
416.0504	B2	1.89E+08
418.0038	0,2A2+2Na	6610985
423.3779	[B6+Na]3-	6911510
424.8434	[B10+2Na]5-	7867478
427.0413	[B4+Na]2-	5.79E+07
427.5532	[2,4A9+3Na-SO3]4-	5545081
427.5532	[2,5X8+3Na-SO3]4-	5545081
429.2394	[B10+3Na]5-	9208185
430.7051	[B6+2Na]3-	6.70E+07
432.5369	[B8+3Na]4-	1.49E+08
434.0608	C2	4817212
437.0394	[C8+3Na]4-	7456715

438.0323	[C4+2Na]2-	9.94E+07
444.0358	[C6+3Na]3-	1.61E+07
447.0377	[C4+2Na]2-	2.33E+07
447.5425	[2,4A9+3Na]4-	1.86E+07
447.5425	[2,5X8+3Na]4-	1.86E+07
456.0429	C2+Na	4.10E+07
458.0393	[2,4A7+3Na]3-	4.38E+07
458.0393	[2,5X6+3Na]3-	4.38E+07
462.0533	[M-8H+3Na]5-	7.12E+08
468.0429	[2,4A5+2Na]2-	7.88E+07
468.0429	[2,5X4+2Na]2-	7.88E+07
473.554	[Y9+3Na]4-	2.28E+07
478.0462	[0,2A7+3Na]4-	5976500
479.0337	[2,4A5+3Na]2-	7160001
479.0337	[2,5X4+3Na]2-	7160001
479.0663	2,5A5+Na	6882898
479.0663	[2,4X4+Na]2-	6882898
485.3945	[Y7+2Na]3-	2.42E+07
487.0626	[0,2A5+Na]2-	5255149
491.722	[B7+3Na-SO3]3-	2.29E+07
497.2958	[C9+3Na]4-	7425811
497.7255	[C7+3Na-SO3]3-	5.14E+07
498.0535	2,4A3+Na	1.67E+08
498.0535	2,5X2+Na	1.67E+08
505.6205	[0,2A6+2Na-SO3]2-	5420371
509.0756	[Y5+Na]2-	2.26E+07
511.729	[2,4A8+3Na-SO3]3-	5764889
518.3744	[B7+3Na]3-	1.04E+07
520.0354	2,4A3+2Na	2.76E+07
520.0354	2,5X2+2Na	2.76E+07
524.3777	[C7+3Na]3-	1.30E+08
527.5719	[C5+2Na-SO3]2-	6.23E+07
530.0821	[0,2X5+Na]2-	1.38E+07
536.0926	0,2A3	9951863
550.3992	[B8+3Na-SO3]3-	5484626
551.3992	[Y8+3Na]3-	1.18E+07
558.0744	[0,2A3+Na	5.85E+07
567.5504	[C5+2Na]2-	4.47E+07
569.5361	[B5+3Na]2-	1.61E+07
577.0515	[B8+3Na]3-	1.83E+07
577.8183	[M-7H+3Na]4-	3.80E+07
578.5412	[C5+3Na]2-	8.20E+07

580.1188	Y3	1.30E+07
596.5682	[0,2A6+3Na-SO3]3-	1.38E+07
597.0596	[2,4A9+3Na]3-	4892592
597.0596	[2,5X8+3Na]3-	4892592
599.101	B3+Na-SO3	1.19E+07
599.5461	[2,4A6+3Na]2-	8101677
602.1011	Y3+Na	5769178
657.552	[B6+3Na]2-	1.19E+07
666.5575	[C6+3Na]2-	1.65E+07
677.5946	[0,2A7+3Na]2-	3.95E+07
679.0581	B3+Na	7228203
687.5625	[2,4A7+3Na]2-	7623786
687.5625	[2,5X6+3Na]2-	7623786
697.0685	C3+Na	3.13E+07
701.0397	B3+2Na	1.12E+07
717.5732	[0,2A7+3Na]2-	2.39E+07
719.0502	C3+2Na	6.83E+07
747.0913	[C7+3Na-SO3]2-	6064588
797.1152	B4+2Na-SO3	8775359
815.1255	C4+2Na-SO3	2.01E+07
857.136	2,4A5+2Na-SO3	2.06E+07
857.136	2,5X4+2Na-SO3	2.06E+07
877.0715	B4+2Na	1.68E+07
917.0643	C4+2Na	1.43E+07
917.1565	0,2A5+2Na-SO3	1.27E+07
959.0751	2,4A5+3Na	2.01E+07
959.0751	2,5X4+3Na	2.01E+07
1019.0959	0,2A5+3Na	1.17E+07
1078.1332	C5+3Na-SO3	1.21E+07

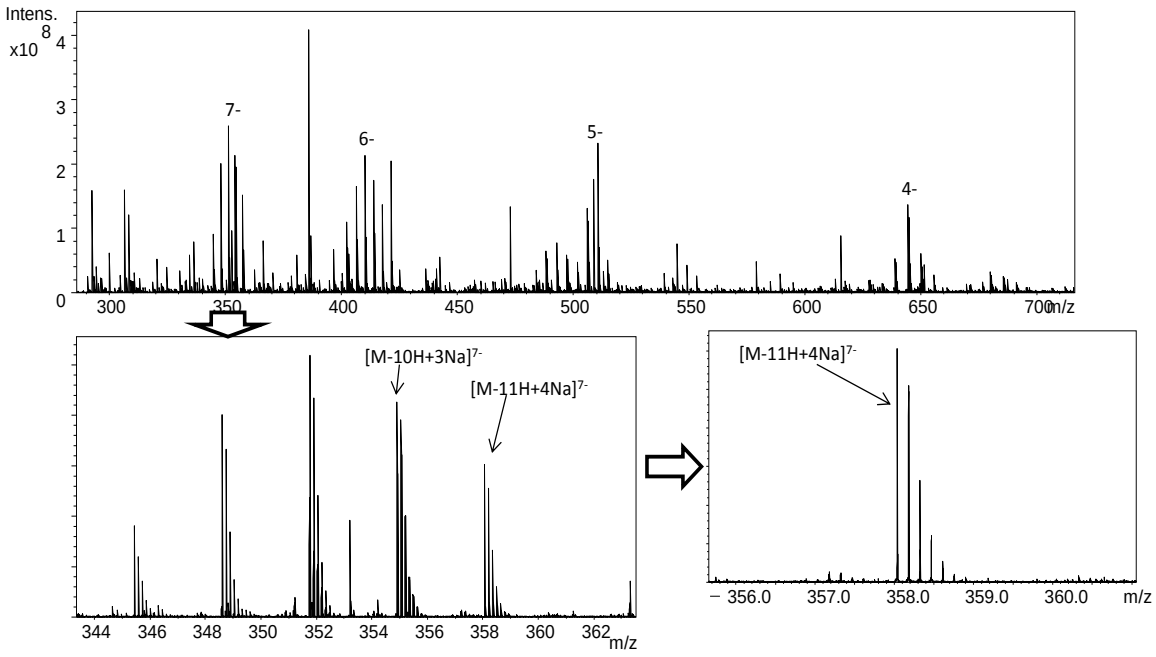

Figure. Mass spectrum for dp12 5S.

The fragments for molecular ion $[M-11H+4Na]^{7-}$ for dp12 with $5SO_3$ groups.

Mass to charge	Assignment	Intensity
257.0279	2,4A2+Na	6117759
289.5558	Y32-	4.40E+07
295.0671	0,2A2	3757211
295.5377	B32-	5569058
300.5468	[Y3+Na]2-	4496709
315.5339	[C3+Na]2-	3203223
331.7208	Y53-	3525633
334.5997	[B11+4Na]7-	2554324
336.5393	[2,4A4+Na]2-	3583175
339.048	[Y5+Na]3-	1.57E+07
339.0932	Y2	2885007
343.0359	[B5+Na]3-	3327863
354.1041	C2-SO3	3425055
358.0379	[M-11H+4Na]7-	1.93E+08
363.794	[B7+2Na]4-	1.17E+07
364.1971	[C10+4Na]6-	2.26E+07
366.5494	[0,2A4+Na]2-	2933018
370.3702	[2,4A5+2Na]3-	3666364
372.2804	[B7+3Na]4-	3709908
373.8301	[2,5A9+4Na]5-	3370863

378.6418	[Y9+3Na]5-	1.68E+07
385.4308	[B9+4Na]5-	3102269
387.0631	[B4+Na-SO3]2-	8670307
387.2858	[2,4A8+3Na]4-	7417169
388.5402	[Y11+4Na]6-	5624570
388.5628	[Y4+Na]2-	4497349
390.5343	[B11+4Na]6-	3236169
397.435	[2,4A10+4Na]5-	4.86E+07
405.0528	[Y6+2Na]3-	3213955
413.2976	[Y8+3Na]4-	2850569
416.0504	B42-	7.35E+07
416.0504	B2	7.35E+07
417.8789	[M-10H+4Na]6-	1.10E+08
418.2446	[Y10+4Na]5-	5595727
427.0413	[B4+Na]2-	9494556
433.6359	[B10+4Na]5-	3038262
434.0608	C2	7232781
436.0466	[C4+Na]2-	6470307
437.2381	[C10+4Na]5-	1.11E+07
438.0324	[B4+2Na]2-	4.37E+07
438.0324	B2+Na	4.37E+07
442.535	[C8+4Na]4-	5.49E+07
444.0359	[C6+3Na]3-	1.66E+07
447.0377	[C4+2Na]2-	3.02E+07
450.4581	[Y11+4Na-SO3]5-	7243021
453.0378	[2,4A9+4Na]4-	2.66E+07
453.0378	[2,5X8+4Na]4-	2.66E+07
456.043	C2+Na	7.46E+07
458.0393	[2,4A7+3Na]3-	1.80E+07
458.0393	[2,5X6+3Na]3-	1.80E+07
462.0511	[B9+4Na-SO3]4-	6545002
466.4497	[Y11+4Na]5-	4618620
468.0429	[2,4A5+2Na]2-	2.20E+07
468.0429	[2,5X4+2Na]2-	2.20E+07
470.0573	[B7+3Na-SO3]3-	4296836
473.5539	[Y9+3Na]4-	4574421
476.5454	[B9+3Na]4-	3497816
477.0564	[2,4A10+4Na-SO3]4-	8810204
479.05	[Y9+4Na]4-	3928217
482.0404	[3,5A5+2Na]2-	2.40E+07
482.0404	[B9+4Na]4-	2.40E+07
486.5431	[C9+4Na]4-	3891252

490.0337	[0,2A7+4Na]3-	3977041
490.0644	[2,4A8+3Na-SO3]3-	5535133
492.7218	[Y7+3Na]3-	6353019
496.7098	[B7+3Na]3-	9785280
497.0455	[2,5A5+2Na]2-	1.29E+07
497.0455	[2,4A10+4Na]4-	1.29E+07
498.0535	2,4A3+Na	4.02E+07
498.0535	2,5X2+Na	4.02E+07
501.6563	[M-9H+4Na]5-	2.95E+07
510.0404	[C7+4Na]3-	8598470
516.0808	[2,4A6+2Na-SO3]2-	3941574
516.7171	[2,4A8+3Na]3-	3119019
520.0355	2,4A3+2Na	1.27E+07
520.0355	2,5X2+2Na	1.27E+07
520.0667	[Y5+2Na]2-	8957274
523.0573	[Y10+4Na]4-	3852742
524.0441	[2,4A8+4Na]3-	8.14E+07
526.0485	3,5A3+Na	8402480
526.0485	[B5+2Na]2-	8402480
534.1077	B3+Na-SO3	8959707
536.724	0,2A8+3Na]3-	3821816
544.0511	0,2A8+4Na]3-	1.55E+07
546.0448	[C5+3Na]2-	4845652
552.1184	C3+Na-SO3	1.06E+07
557.7266	[B8+4Na-SO3]3-	6781295
563.7303	[C8+4Na-SO3]3-	1.29E+07
567.05	[2,4A6+3Na]2-	2.98E+07
577.7339	[2,4A9+4Na-SO3]3-	4136697
577.7339	[2,5X8+4Na-SO3]3-	4136697
590.3827	[C8+4Na]3-	1.37E+07
597.0602	[0,2A6+3Na]2-	6619554
602.1011	Y3+Na	6780777
614.0647	B3+Na	2.46E+07
626.5793	[C6+3Na-SO3]2-	8964937
654.0566	C3+2Na	5567281
654.1501	0,2A4+Na-SO3	5060953
666.5575	[C6+3Na]2-	3688080
677.5485	[C6+4Na]2-	1.54E+07
696.0677	2,4A4+2Na	2.07E+07
698.554	[2,4A7+4Na]2-	1.58E+07
698.554	[2,5X6+4Na]2-	1.58E+07
746.5915	[2,4A8+4Na-SO3]2-	1.61E+07

756.0893	0,2A4+2Na	7224457
756.559	[B7+4Na]2-	5808390
776.6027	[0,2A8+4Na-SO3]2-	5527140
917.0641	C4+3Na	5561024

APPENDIX C

SUPPLEMENTAL DATA FOR CHAPTER 5

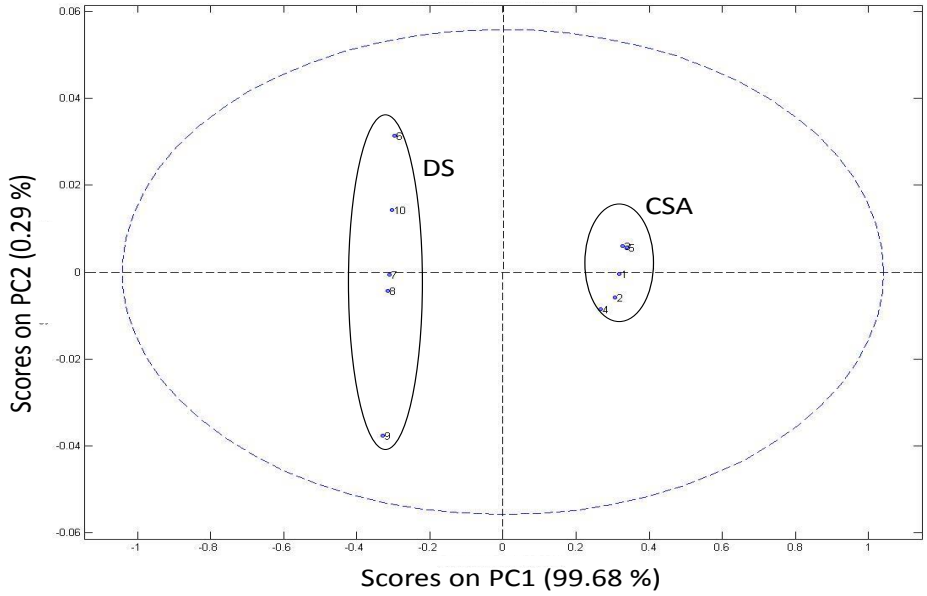

Figure. Score plot of the dp 4 CSA and DS showing that the sample spectra are different as pertains to the intensity of fragment ions.

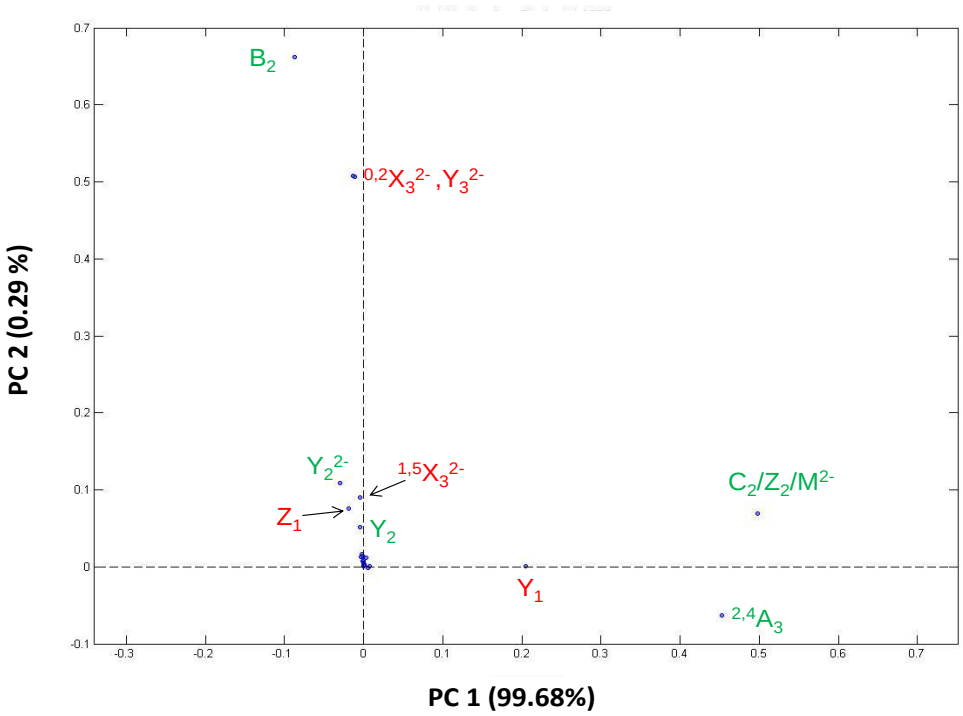

Figure. The loading PCA plot of dp4 CSA and DS showing the ions responsible for the sample separation.

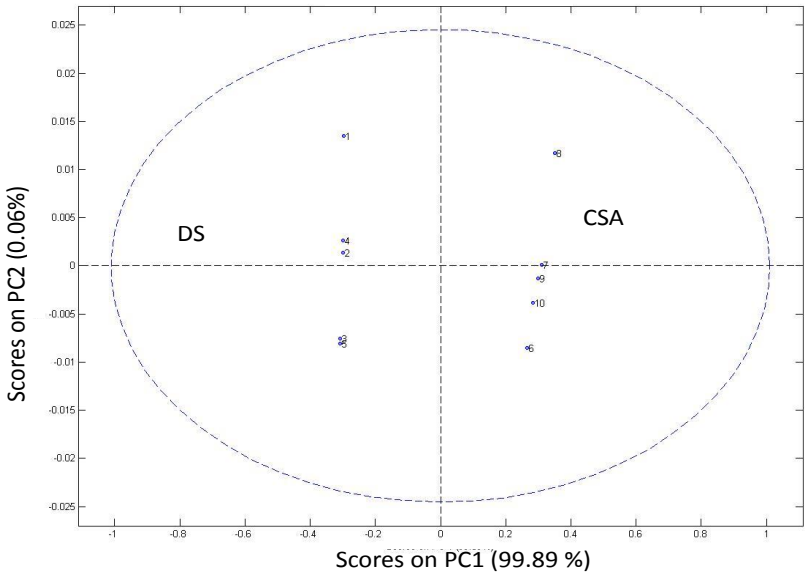

Figure. dp 6 CSA and DS PCA score plot.

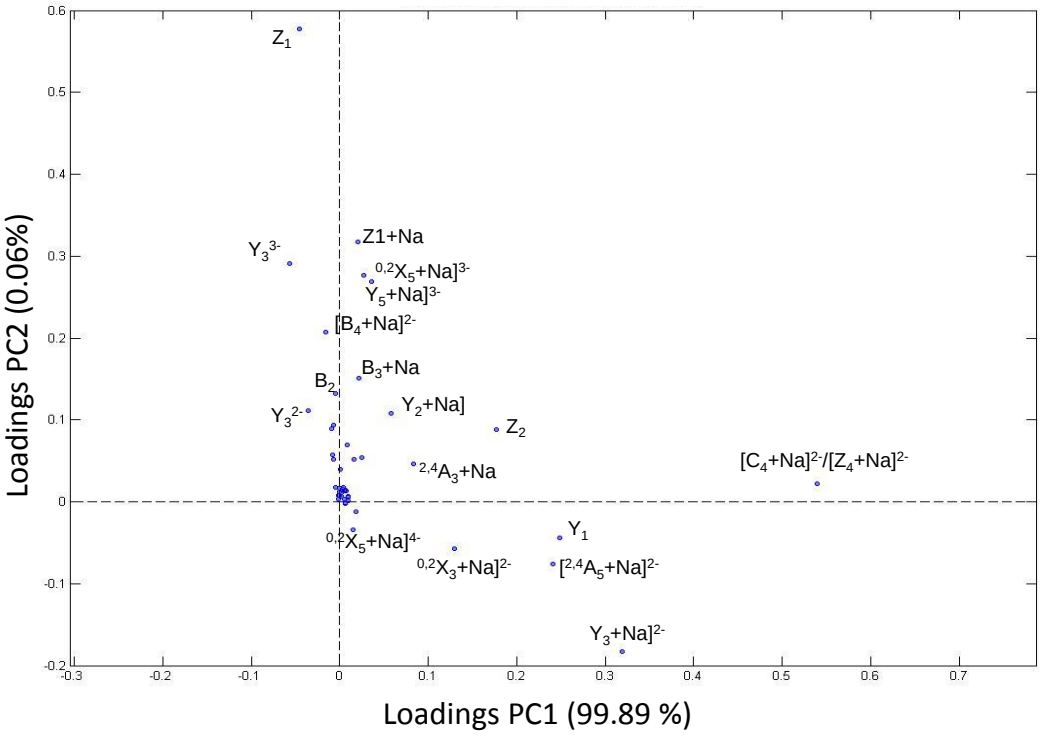

Figure. dp6 CSA and DS loadings plot.

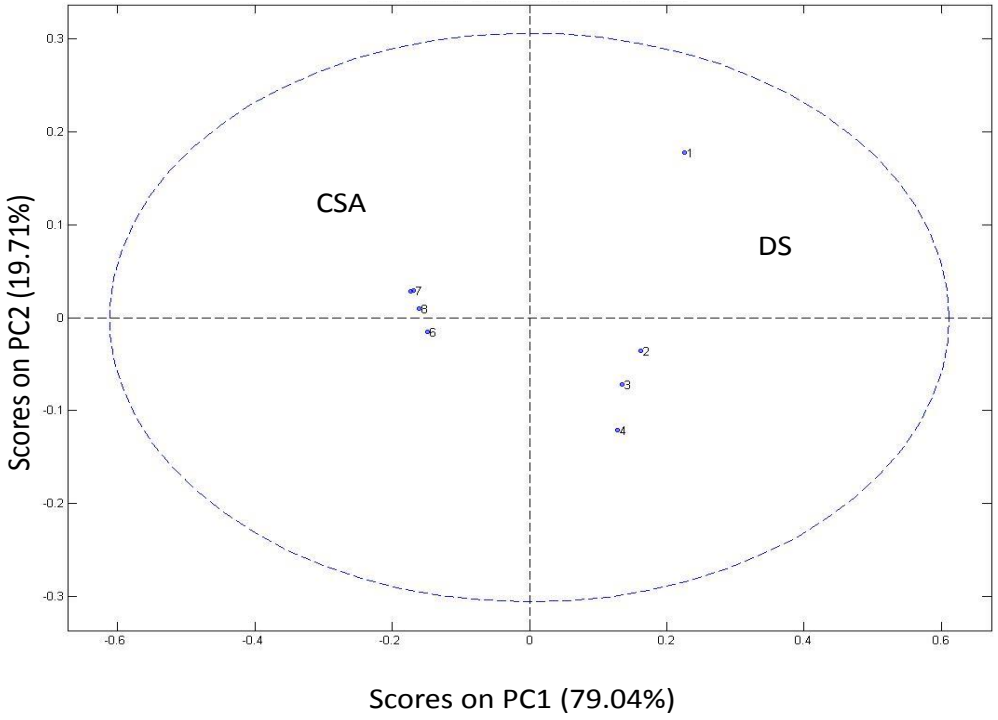

Figure. Score plot for dp8 CSA and DS.

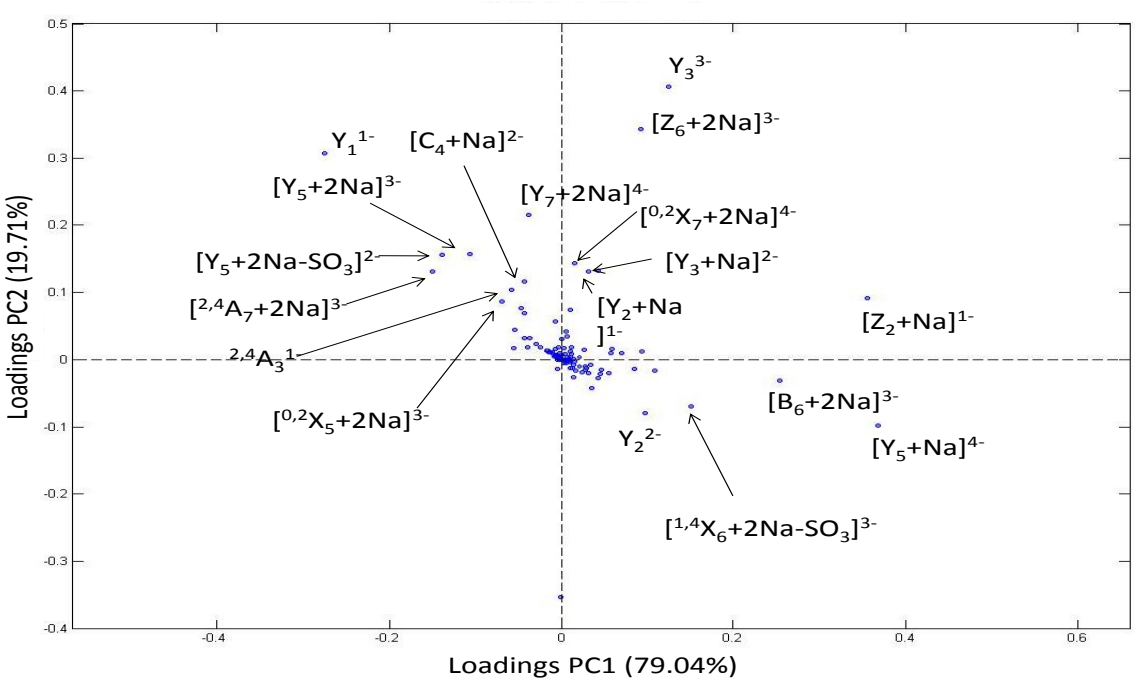

Figure. Loadings plot for dp8 CSA and DS.

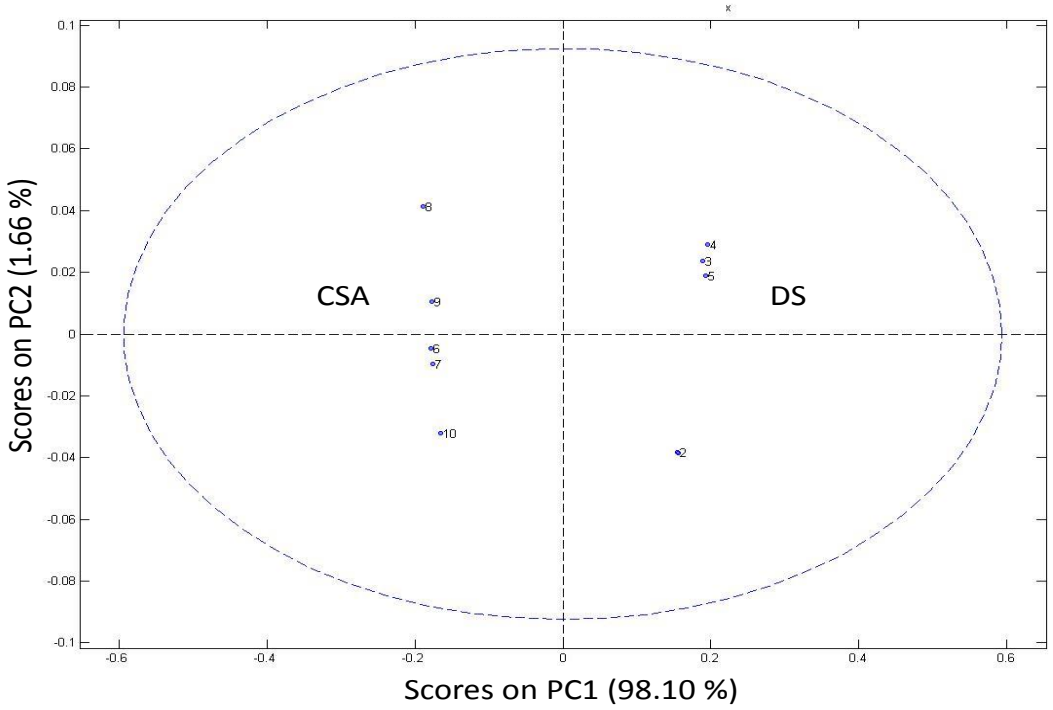

Figure. Score plot for dp10 CSA and DS.

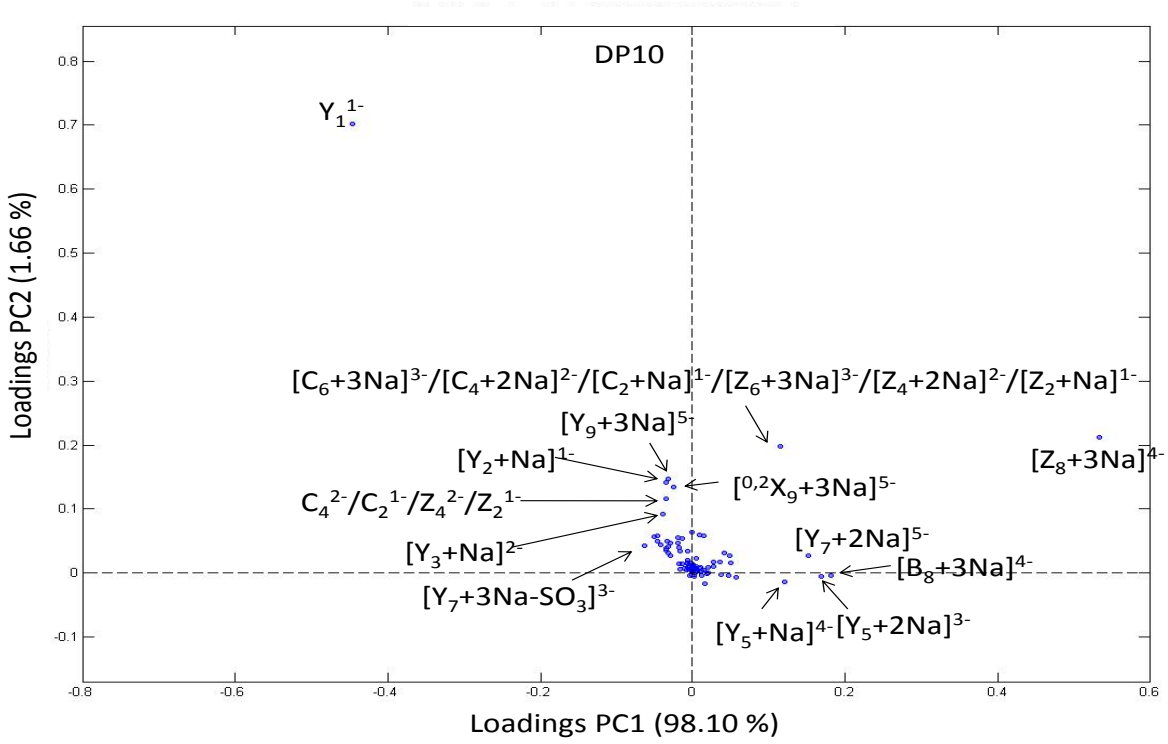

Figure. Loadings plot for dp10 CSA and DS.

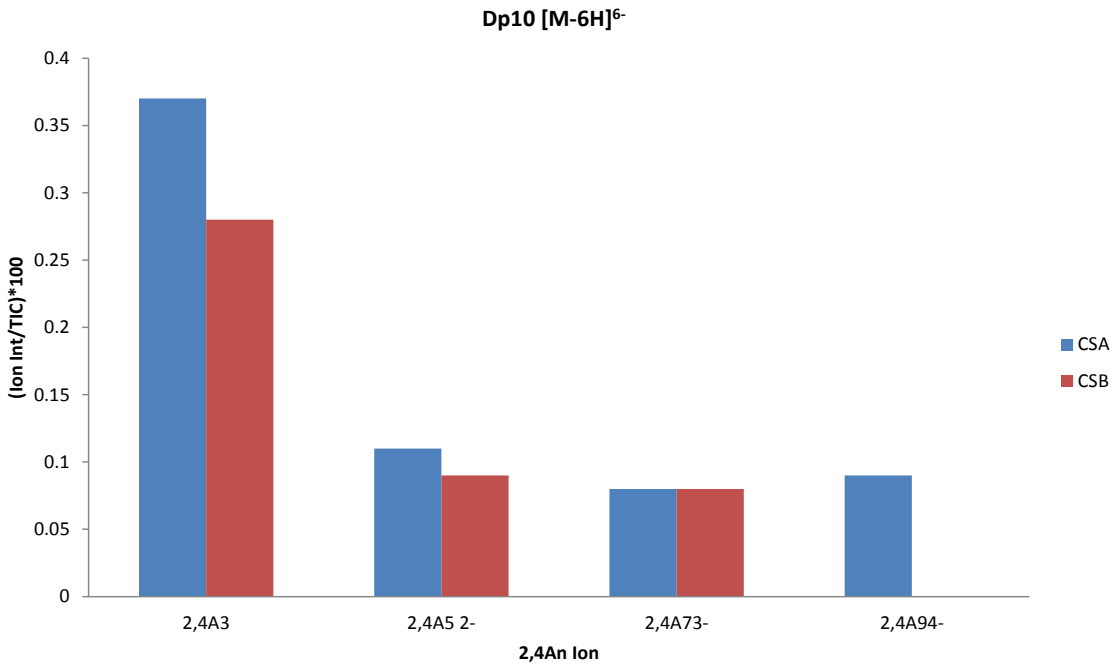

Figure. A plot for the $^{2,4}A_n$ ions obtained from unsodiated molecular ion for dp10 CSA and DS. Only $^{2,4}A_9$ $^{4-}$ was fully diagnostic.